JPRS-JST-89-012

2 JUNE 1989

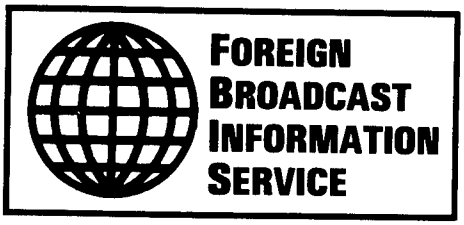

JPRS Report

Science & Technology

Japan

JPRS-JST-89-012

2 JUNE 1989

SCIENCE & TECHNOLOGY

JAPAN

JAPAN-CHINA SUPERCONDUCTORS SYMPOSIUM

40080162 Tokyo JAPAN-CHINA OXIDE HIGH Tc SUPERCONDUCTORS SYMPOSIUM in English 9-12 Apr 89 pp I-IV, 1-159

["Extended abstracts" from talks presented at the Japan-China Oxide High Tc Superconductors Symposium held 9-12 Apr 89 in Tsukuba City; sponsored by the Japan-China Science and Technology Exchange association and Academia Sinica]

CONTENTS

SCIENTIFIC PROGRAM

Monday, April 10

9 : 00— 9 : 15 **OPENING REMARKS**
Ryukiti R. HASIGUTI (The University of Tokyo)
Lin Li (Institute of Physics)
Ryuichi NAKAGAWA (National Research Institute for Metals)

SESSION I Opening Lectures I 9 : 15—10 : 25

9 : 15— 9 : 50 HIGH TEMPERATURE SUPERCONDUCTORS AND ITS APPLICATION
Shoji TANAKA (Tokai University)

9 : 50—10 : 25 SOME RECENT DEVELOPMENT ON THE STUDIES OF HIGH Tc OXIDE SUPERCONDUCTORS IN CHINA
Lin LI (Institute of Physics)

10 : 25—10 : 45 Coffee Break

SESSION II Opening Lectures II 10 : 45—11 : 55

10 : 45—11 : 20 ACTIVITIES ON CONDUCTOR FABRICATION OF HIGH-Tc OXIDE SUPERCONDUCTORS IN JAPAN
Kyoji TACHIKAWA (Tokai University)

11 : 20—11 : 55 OUTLINE OF THE RESEARCH ON HIGH Tc SUPERCONDUCTORS IN THE INSTITUTE OF PHYSICS, CHINESE ACADEMY OF SCIENCES
Zhao Zhong Xian (Institute of Physics)

11 : 55—13 : 00 Lunch

SESSION III Electron Microscopy 13 : 00—14 : 15

13 : 00—13 : 25 THE CRYSTAL STRUCTURE OF HIGH-Tc Bi BASED SUPERCONDUCTORS EXAMINED BY HIGH-RESOLUTION ELECTRON MICROSCOPY
Shigeo HORIUCHI (National Institute for Research in Inorganic Materials)

13 : 25—13 : 50 TRANSMISSION ELECTRON MICROSCOPY STUDY ON HIGH Tc SUPERCONDUCTORS
Li Fang-hua (Institute of Physics)

13 : 50—14 : 15 MODULATED STRUCTURES OF Tl-Ba-Ca-Cu-O SUPERCONDUCTOR OXIDES
Sumio IIJIMA (NEC Corporation)

SESSION Ⅳ Electronic Properties 14 : 20—15 : 35

14 : 20—14 : 45 HIGH-TEMPERATURE SUPERCONDUCTIVITY PRODUCED BY ELECTRON-DOPING IN COPPER OXIDE COMPOUNDS
Yoshinori TOKURA (University of Tokyo)

14 : 45—15 : 10 SPECIFIC HEAT ANOMALY NEAR Tc IN OXIDE SUPERCONDUCTORS
CHEN Zhaojia (University of Science and Technology of China)

15 : 10—15 : 35 TRANSPORT STUDIES OF METALLIC LANTHANUM CUPRATES
Yasuhiro IYE (University of Tokyo)

15 : 35—15 : 55 Coffee Break

SESSION Ⅴ Elastic Properties 15 : 55—17 : 10

15 : 55—16 : 20 THE BEHAVIOR OF OXYGEN AND ITS DEFFECTS IN YBCO
XIE Leiming (Shanghai Institute of Metallurgy)

16 : 20—16 : 45 ULTRASONIC AND TRANSPORT STUDIES OF HIGT Tc SUPER-CONDUCTORS
Shoichi MASE (Kyushu University)

16 : 45—17 : 10 STRUCTURAL INSTABILITY IN Bi-Sr-Ca-Cu-O AND Tl-Ca-Ba-Cu-O SYSTEMS
Yening WANG (Nanjing University)

18 : 00—20 : 00 WELCOME RECEPTION

Tuesday, April 11

SESSION Ⅵ Synthesis Ⅰ 9 : 00—10 : 15

9 : 00— 9 : 25 Bi-BASED HIGH TEMPERATURE SUPERCONDUCTING SYSTEM
Hiroshi MAEDA (National Research Institute for Metals)

9 : 25— 9 : 50 PREPARATION AND PROPERTIES OF THE HIGH Tc $Bi_{(2-x)}Pb_xSr_2Ca_2Cu_3O_y$ SUPERCONDUCTORS
LIN Wei (Changsha Research Institute of Mining & Metallurgy)

9 : 50—10 : 15 CHEMICAL AND STRUCTURAL ASPECTS OF THE Bi, Pb-Sr-Ca-Cu-O SYSTEM
Mikio TAKANO (Kyoto University)

10 : 15—10 : 35 Coffee Break

SESSION Ⅶ Synthesis Ⅱ 10 : 35—11 : 50

10 : 35—11 : 00 THE CRYSTAL STRUCTURES OF THE SUPERCONDUCTING PHASES IN THE Tl-Ba-Ca-Cu-O SYSTEM
Jing-kui LIANG (Institute of Physics)

11 : 00—11 : 25 SYNTHESIS AND SUPERCONDUCTIVITY OF $Tl_mBa_2Ca_{n-1}Cu_nO_{2n+3}$ COMPOUNDS
Hideo IHARA (Electrotechnical Laboratory)

11 : 25—11 : 50 SINGLE CRYSTAL GROWTH AND CHARACTERIZATION OF $Bi_2Sr_2CaCu_2O_8$
YAN Yifeng (Institute of Physics)

11 : 50—13 : 00 Lunch

SESSION Ⅷ Thin Films 13 : 00—15 : 05

13 : 00—13 : 25 IN-SITU GROWTH OF YBCO SINGLE-CRYSTAL FILMS AT LOW TEMPERATURE
Yoshichika BANDO (Kyoto University)

13 : 25—13 : 50 GROWTH OF HIGH Tc SUPERCONDUCTING THIN FILMS BY MBE
Junming ZHOU (Instiute of Physics)

13 : 50— 4 : 15 SYNTHESIS AND CHARACTERIZATION OF ARTIFICIALLY LAYERED Bi-Sr-Ca-Cu OXIDE FILMS
Keiichi OGAWA (National Research Institute for Metals)

14 : 15—14 : 40 PREPARATION OF YBaCuO THIN FILMS BY MAGNETRON SPUTTERING WITH IN-SITU PLASMA OXIDATION
LI Yuan (Nanjing University)

14 : 40—15 : 05 HIGH Jc SUPERCONDUCTING THIN FILM
Hideo ITOZAKI (Sumitomo Electric Industries Ltd.)

15 : 05—15 : 25 Coffee Break

SESSION IX Devices 15 : 25—16 : 40

15 : 25—15 : 50 THE PRESENT SITUATION AND PROBLEM OF HIGH Tc SQUIDS
Ushio KAWABE (Hitachi Ltd.)

15 : 50—16 : 15 INVESTIGATION OF YBaCuO THIN FILMS AND DEVICES
Shi-guang WANG (Peking University)

16 : 15—16 : 40 FABRICATION AND PATTERNING OF Bi(Pb)SrCaCuO THIN FILMS
Ienari IGUCHI (University of Tsukuba)

SESSION X Wires and Magnetic Shielding 16 : 45—18 : 25

16 : 45—17 : 10 MAGNETIC PROPERTIES OF THE HIGH Tc SUPERCONDUCTORS
Yuan-Dong DAI (Peking University)

17 : 10—17 : 35 PRACTICAL PROPERTIES AND WIRE FABRICATION PROCESSES OF HIGH-Tc OXIDE SUPERCONDUCTORS
Kazumasa TOGANO (National Research Institute for Metals)

17 : 35—18 : 00 $YBa_2Cu_3O_y$ SUPERCONDUCTORS PREPARED WITH DIFFERENT PROCESSES AND THEIR CHARACTERISTICS
WU Xiaozu (Northwest Institute for Non-ferrous Metal Research)

18 : 00—18 : 25 THE MAGNETIC SHIELDING PRORERTIES OF AN YBCO SUPERCONDUCTING CYLINDRICAL TUBE WITH ONE END CLOSED
Y. J. Qian (Fudan University)

18 : 25—18 : 35 **CLOSING REMARKS**

Li Fang-hua (Institute of Physics)
Keiichi OGAWA (National Research Institute for Metals)

HIGH TEMPERATURE SUPERCONDUCTORS AND ITS APPLICATION

Shoji TANAKA
Department of Physics, Tokai University, Hiratsuka, Kanagawa 259-12

Since the discovery of high temperature superconductivity in 1986, the research in this field has been developed explosively. The critical temperature reached 125 K in Tl-based oxide material and higher critical temperature will be observed in some oxide materials in near future. The study of physical properties of these oxide materials has been developed by tremendously many researchers in these one and a half year and it was found that these materials are very peculiar in nature, which slid state physicists have never seen in the long history of solid state physics. This means that it must be necessary to introduce a new concept in solid state physics, which leads to a new theory of high temperature superconductivity.

On the other hand, it becomes clear that these oxide materials have many difficulties, which must be overcome before reaching real applications. It is believed that we must introduce the fruits of modern semiconductor technology in order to solve these difficulties. As to applications, many possibilities are discussed as is shown in the following table, expecially in the field of electronics.

The application of high-Tc superconductors to electronic devices will give rise new attentions. The superconductivity gap in high-Tc superconductors must be quite large compared with conventional low-Tc superconductors. The gap is given by $2\Delta=3.5$ kTc according to an accepted phenomenological theory. Even though the exact values of the gap in high-Tc superconductors have not been determined yet, it seems that real 2Δ is larger than 3.5 kTc. Therefore, if we obtain critical temperature of 300 K, the gap 2Δ may reach 0.1 eV. This value is nearly the same as the band gap of InSb.

Thus, it is hoped that the hybridized devices composed of semiconductors and superconductors may be of great interest in near future. These devices must have high speed and very small power consumption like Josephson devices.

APPLICATIONS

(1) Transportations
- Mag. Lev. Trains
- Electromagnetic Ships
- Spacecraft
- Electric Car

(2) Electricity
- Storage of Electricity
- Transmission Lines
- Superconducting Generator and Motor

(3) Electronics
- Superconducting Wiring in LSI
- One Wafer Computer
- Josephson Devices
- SQUID Devices
  - Infrared Sensor
  - Magnetic Sensor
- Superconducting Transistors
  - MOS Type
  - Bipolar Type
- MRI

SOME RECENT DEVELOPMENT ON THE STUDIES OF HIGH T_c OXIDE SUPERCONDUCTORS IN CHINA.

Lin Li*
*Institute of Physics, Chinese Academy of Sciences, Beijing.

INTRODUCTION

Since the initial report by Bednorz and Muller[1] on the possible high T_c superconductivity in Ba-La-Cu-O system has generated an enormous amount of activity in the research for new oxide superconducting materials. It is now quite easy to synthesis superconductors with zero-resistance temperature higher than 90 K after the breakthrough made independently by Chu et al[2] and Zhao et al[3] in Y-Ba-Cu-O system.

At the beginning of 1988, non-rare earth high T_c oxide superconductors[4,5] were discovered. In China Bi and Tl oxide superconductors were prepared shortly after their discoveries. In this talk, I shall select some of the recent important works carried out in China, and describe them a little more in detail.

Y-Ba-Cu-O SYSTEM

Although the powder sintered Y-Ba-Cu-O superconductor show a high superconducting transition temperature ($\geq$ 90 K), its critical current is, in general, lower than $10^2 - 10^3 A/cm^2$ because of the effects such as the weak links between grain boundaries and the porosity in the material. In order to overcome this problem, many scientists are trying to find new techniques to produce the Y-Ba-Cu-O superconductor. J. S. Zhang et al[6] of the Institute of Metal research, Chinese Academy of Sciences, Shengyang, in collaboration wtih Shuang-Liao Institute of Silicate, Jilin, have applied the new laser floating zone melting technique to the Y-Ba-Cu-O compounds. The crystals grown along a certain direction during solidification and can be changed into superconductors with certain texture and T_c greater than 90 K following suitable heat treatments. Their results also show that the superconducting $YBa_2Cu_3O_{7-y}$ (or 123) phase melts incongruently around 1010°C with a melting range of about 300°C, which limit the possibility of the growth of 123 phase directly from the melt. To overcome this difficulty, they have tried to grow 123 phase by using the eutectic or peritectic reaction which deviates from the 123 stoichiometry and take place at temperatures below the melting point of the 123 phase. Oriented structure composed of the tetragonal 123 phase preferentially arranged in a matrix can be obtained directly from the melt. After a suitable heat treatment,they can be converted into superconductors with T_c around 85 K.

C. L. Ji et al[7] of Northeast University of Technology, Shengyang, used a directed reaction process based on physico-chemical principles which has been designed for producing single phase 90 K zero resistance temperature superconducting compound

$YBa_2Cu_3O_{7-y}$. The reliability of the process has been well proved by the stability and reproducibility of results in resistance and A. C. magnetic susceptibility measurements of seven samples taken randomly from three batches of products. X-ray diffraction, SEM and TEM examination have identified the product is single phase polycrystalline material of orthorhombic structure with lattice parameters a=3.89 Å, b=3.82 Å and c= 11.65 Å. Many micro-twinned defects were observed under the TEM along [110] axes. A physico-chemical method was used to determine the nonstoichiometric fraction.

M. L. Zhou et al[8] of Central South University of Technology have studied the $YBa_2Cu_3O_{7-y}$ powders for making wires; small amount of Ag (3%wt.) powder was added to the $YBa_2Cu_3O_{7-y}$ powder and mixed with plasticine. Diameter size of approximately 0.7 mm could be obtained through extrusion. The wires have good flexibility and could be wound into a coil. They have obtained this kind of wire 0.7 m in length with T_c=93 K and J_c(77 K)=450 A/cm^2.

Although many techniques have been tried to synthesis bulk $YBa_2Cu_3O_{7-y}$ material to obtain high critical current, however it is still not successful. Compared with the bulk sample, a dramatic example is the very much higher critical current densities observed in thin films of these materials. At the Institute of Physics, we have been pursuing several routes to the synthesis of thin fillms of the oxide superconductors. These include e-beam evaporation, magnetron sputtering, ion beam sputtering and molecular beam epitaxy. Up to date, the best films of $YBa_2Cu_3O_{7-y}$ are obtained by sputtering[9]

High quality $YBa_2Cu_3O_{7-y}$ thin films were prepared by both rf magnetron sputtering and ion beam sputtering from the solid state reacted Y-Ba-Cu-O powder target. The substrate was (100) $SrTiO_3$. The chemical composition of the films were analysed by inductively coupled plasma atomic emission spectroscopy and x-ray fluorescence spectroscopy. X-ray diffraction technique was used to determine the structure of the films. Resistivity measurements were used to determine the superconducting properties; Tc and Jc(0) at 77K. The results are listed in Table 1.

Table 1. The physical parameters of the $YBa_2Cu_3O_{7-y}$ thin films.

Sample No.	T_D(°C)	Orientation	$\rho_{300K}/\rho_{Tconset}$	$T_{R=0}$(K)	J_c at 77 K (A/cm^2)
S-408	400	a>>c	2.0	87	1.4×10^4
S-414	400	a>>c	2.5	88	2.5×10^5
S-541	400	c>>a	3.1	90	1.3×10^4
IB-108	425	a∼c	2.8	90	4.5×10^4
IB-114	425	a∼c	3.0	90	3.6×10^4

In our experience, the most important factors governing the

quality of the films are; the need to obtain precise stoichiometry of the "123" line compound, the need to avoid, or at least minimize, interdiffusion and chemical reaction between the film and the substrate, and the need for epitaxial growth to ensure highly-oriented films (it is best to have the c axis normal to the plane of the film). Failure to meet these conditions tends to lead to films that have sharp superconducting onset transition temperatures but long resistive tails extending to very much lower temperatures. The critical current density of such materials is also invariably low. Such behavior is characteristic of granular superconductors.

Bi-Sr-Ca-Cu-O SYSTM

The $BiSrCaCu_2O_y$ with T_c above 80 K was studied by electron diffraction and high resolution electron microscopy[10]. It has been determined that the crystal structure is one-dimensional incommensurate. The direction of the modulation is almost parallel to the b axis of the average structure. The unit cell parameters are a=5.39 Å, b=5.41 Å and c=30 Å. The periodicity of modulation is 25.3Å.

The single crystals[11] $Bi_2Sr_2CaCu_2O_y$ with T_c=85 K were grown by self-flux method. The crystals, with the typical dimensions of 10 mm are stable in the atmosphere and can be easily cleaved after immersed in alcohol. A series of experiments have been done by using such crystals.

The resistivity of superconducting single crystal possesses a quasi-two dimensional anisotropy characteristic with a typical metallic behavior in the a-b planes and a "semiconducting-like" temperature dependence in the c-direction. The resistivity characteristic along c-axis can be fitted with A/T+BT formula above 110 K.

Several reciprocal layered photos of the crystals were recorded by x-ray precession camera[12]. About one thousand reflections in total have been observed. After careful examination, an average structure with space group of Pnnn and a real structure with the superspace group of P^{Pnnn}_{11T} or P^{Pnnn}_{1S1} have been found for this one-dimensional modulated incommensurate material. As well as a basic structure with the space group of Pmmm is deduced from the experimental data.

Tl-Ba-Ca-Cu-O SYSTEM

Two superconducting phases with T_c at 120 K and 90 K in the Tl-Ba-Ca-Cu oxide system identified soon after the Tl oxide superconductor had been discovered[13]. The 120 K superconductor was found to have a composition very close to $Tl_2Ba_2Ca_2Cu_3O_y$ possessing a tetragonal structure with a=5.47 Å and c=36.07 Å and the 90 K superconductor was determined to be the $Tl_2Ba_2Ca_1Cu_2O_y$ compound with a tetragonal structure with a=5.462 Å c=30.06 Å

respectively by x-ray powder diffraction based on near single phase superconducting materials. These phases have been also identified by convergent beam electron diffraction in the multi-phase compounds of $TlBaCaCu_2O_y$ with T_c of 114 K[14]. These phases are tetragonal, with point group 4/mmm. It has been found that c=36.1 Å and c=29.7 Å phases form coherent intergrowths by high resolution electron microscopy. Both ordered and disordered intergrowths have been observed.

Two new phases $TlBa_2CaCu_2O_y$ and $TlBa_2CuO_y$ have been identified in the multiphase compounds of $TlBaCaCuO_y$ with a superconducting temperature of 72.5 K[15,16]. Both phases are weakly modulated incommensuratly in the (100) and (010) directions, their basic structure are tetragonal, with space group P4/mmm and lattice parameters of a=3.87 Å, c=12.9 Å. and a=3.87 Å, c=9.9 Å.. These two phases and the recently reported $TlBa_2Ca_2Cu_3O_y$ are members of a new structural series $TlBa_2Ca_{n-1}Cu_nO_y$.

ACKNOWLEGMENTS

I would like to thank Professors Q.Z. Yang, Z. X. Zhao and Q. Z. Yang for providing the valuable informations. Most of the works are sponsered by the National Center for Research and Development on Superconductivity.

REFERENCES

(1) J. A. Bednoze and K. A. Müller Z. Phys. B. Condensed Matter, 64 (1986) 189.
(2) M. K. Wu, R. J. Ashburn, C. J. Toring, P. H. Hor, R. L. Meng, L. Gao Z. J. Huang, Y. Q. Wang and P. W. Chu, Phys. Rev. Lett. 58 (1987) 908.
(3) Z. X. Zhao, L. Q. Chen, Q. S. Yang, Y. Z. Huang, G. H. Chen, R. M. Tang, G, R. Liu, C. G. Cui, L. Chen, L. Z. Wamg, S. Q. Guo, S. L. Li and J. Q. Bi Kexue Tongbao, 32(10) (1987) 661.
(4) C. Michel,M. Hervieu, M. M. Borel, A. Grandin, F. Deslandes, J. Provost and B. Raveau, Z. Phys. B 68 (1987)412.
(5) Z. Z. Shen and A. H. Herman., Nature, 332, (1988) 138.
(6) H. S. Zhang, X. P. Jiang, J. G. Huang, Y. Yu, M., Jiang, Y. L. Ge, G. W. Qiao, Z. Q. Hu, Y. H. Zhao, Y. J. Wang, submitted to International Cryogenic Material conference (1988).
(7) C. L. Ji, C. M. Cui, K. H. Wan, S. L. Liu, G. Y. Zeng, G. F. Zhang, C. F. Qian, W. M. Bian, Z. G. Fan and Q. Xue. Preprint.
(8) M. L. Zhou, Z. F. Wang, J. R. Wang, T. Y. Zuo. Preprint.
(9) J. Gao, Y. Z. Zhang, B. R. Zhao, P. Out, C. W. Yuan and L. Li, to be published in Appl. Phys Lett. (1988).
(10) D. Y. Yang, J. Q. Li, F. H. Li, Y. Q. Zhao, L. Q. Chen, Y. Z. Hyang, Z. Y. Ran and Z, X, Zhao, Supercon. Sci. and Tech. 1 (1988) 100.
(11) Y. F. Yan et al. Modern Phys. Letts, B2 (1988)
(12) X. Chu, Z. H. Mai, Y. F. Yan, J. H. Wang, D. N. Zhen, C. Z. Li, Q. S. Yang and Z, X, Zhao, to be published in Modern. Phys. Letts.

B 1988).
(13) Z. H. Mai, C. G. Cui, S. S. Xie, D. Y. Dai, X. Chu, Y. L. Zhang, G. C. Che, S. C. Li, J. L. Zhang, W. X. Huang and X. R. Cheng, Supercon. Sci. Tech. (1988) 1.
(14) K. K. Fung, Y. L. Zhang, S. S. Xie and Y. Q. Zhou, to be published in Phys. Rev. B (1988).
(15) J. Q. Huang, J. K. Liang, Y. L. Zhang, S. S. Xie, X. R. Chen and Z. X. Zhao, to be published in Modern Phys. Letts. B (1988).
(16) Y. Liu, Y. L. Zhang, J. K. Liang and K. K. Fung, to be published in J. Phys. C (1988).

ACTIVITIES ON CONDUCTUOR FABRICATION OF HIGH-Tc OXIDE SUPERCONDUCTORS IN JAPAN

K. Tachikawa
Faculty of Engineering, Tokai University
Hiratsuka, Kanagawa 259-12, Japan

1. INTRODUCTION

The development of conductor fabrication process is now the key for the application of high-Tc oxides in wide areas of technology. In this article some of the activites in Japan on the development of different processes which have good potentiality for producing wire or tape of high-Tc oxide superconductors are reviewed.

High-Tc oxide superconductors have similar hard and brittle natures of conventional intermetallic compound such as Nb_3Sn and V_3Ga. These intermetallic compounds have been successfuly fabricated into wires and tapes for practical use. Thus, the application of techniques elaborated the fabrication of intermetallic compound superconductors, such as powder process using metal sheath, diffsion process, solidification process and coating process has been attempted for the processing of high-Tc oxide superconductors.

2. POWDER PROCESS WITH METAL SHEATH

A few companies in Japan developed Ag-sheathed high-Tc oxide tapes through a powder process. Hitachi fabricated a YBCO ($YBa_2Cu_3O_x$) tape of 60 μm in thickness which showed a critical current density Jc (77K,0T) of 3300A/cm^2. Recently, a TBCCO ($Tl_2Ba_2Ca_2Cu_3O_x$) tape with a Jc of ~1×10^4 A/cm^2 has been prepared[1]. Fig. 1 shows the Jc versus thickness of YBCO and TBCCO tapes. The Jc of tapes rapidly increases with the reduction in thickness probably due to the densification and the crystal alignment of the oxide. The TBCCO tape shows Jc more than one order larger than that of YBCO tape at 0.1 Tesla.

Sumitomo Electric Ind. fabricated BPSCCO ($Bi_{1.6}Pb_{0.4}Sr_2Ca_2Cu_3O_x$) tape with a Jc (77K,0T) of ~1×10^4A/cm^2 ; the tape still keeps a Jc of 2850A/cm^2 at 0.1 Tesla[2]. The BSCCO tape shows a large Jc even if the tape thickness exceeds 100 μm, providing a much larger critical current than that of YBCO tape. Meanwhile, a fabrication of multifilamentary BPSCCO tape with 1330 cores has been performed at National Research Institute for Metals (NRIM)[3].

3. POWDER PROCESS WITH ORGANIC BINDER

In the powder process using organic binder developed at Nagoya Institute of Technology, precursors of Y, Ba and Cu nitrates were mixed with organic polymar (e.g., polyvinylalcohol) to give it desirable flow characteristic. The viscous solution is then extruded as a filament into air and coiled on the winding drum. The filament is dried and subjected to a heat treatment to remove volatile components and produce the high-Tc oxide with the appropriate phase and grain size[4].

Flexible thin tapes of BPSCCO have also produced by a combined process of doctor blade, cold rolling and sintering at NRIM [5]. A Tc of 107K and a Jc (77K,0T) of 1850 A/cm^2 have been obtained in the tape, which have been singnificantry improved by the cold rolling and subsequent sintering.

4. DIFFUSION PROCESS

Tokai University and Fujikura found that a dense and uniform YBCO layer is easily formed by the diffusion reaction between a high melting point Y_2BaCuO_5 phase and a low melting point $Ba_3Cu_5O_8$ phase[6]. Fig. 2 shows a composition profile of YBCO layer formed on a Y_2BaCuO_5 substrate. About 50 μm thick YBCO layer is formed in a relatively short reaction time of 6hrs at 930℃, which shows a Jc (77K,0T) of about 2000A/cm^2. A prolonged

diffusion heat treatment causes a grain growth and a degradation in Jc in YBCO.

5. Solidification Process

Nippon Steel Co. has prepared a YBCO sample with almost no grain boundary along a-b direction by a solidification process[7]. Fig. 3 shows a Jc versus magnetic field curve of the specimen. The result of magnetization measurement implies that the specimen shows no weak-link behavior and the corresponding Jc exceeds $10^4 A/cm^2$ at 77K and 1 Tesla. A YBCO disc which shows a strong levitation effect has been perpared by the solidification process at Nippon Steel Co..

6. THICK FILM COATING PROCESS

A low pressure plasma spraying technique developed by a collaboration research between Tokai University and NKK Co. facilitated a coating of thick YBCO film[8]. A Ni alloy like Nimonic is the most suitable substrate for the coating. A typical plasma current is 800A. Superconducting tubes with thick YBCO layer to be useful for power transmission, cavity and magnetic shielding have been prepared by this process. A Jc (77K,0T) of $1400 A/cm^2$ has been obtained in the thick YBCO film after a post annealing. Fig. 4 schematically illustrates the principle of this process. A thick BSCCO filme with a Tc of 104K has been also prepared by a low pressure plasma spraying.

Jc's so far obtained in high-Tc oxide conductors are still not sufficient for practical applications. Studies on microstructual features and progress in fabrication process will yield appreciable improvements in Jc of high-Tc oxides in the near future.

REFERENCES

1. M. Okada, R. Nishiwaki, T. Kamo, T. Matsumoto, K. Aihara, S. Matsuda and M. Seido, Jpn. J. Appl. Physics, 27 , L2345 (1988).
2. H. Mukai, N. Shibuta, T. Hikata, K. Sato, M. Nagata and H. Hitotsuyanagi, to be published in Proc. Osaka Univ. Int. Symp. on New Developments in Applied Superconductivity (Osaka,1988).
3. H. Sekine, K. Ogawa, K. Inoue, H. Maeda and K. Numata, to be published in Jpn. J. Appl. Physics.
4. T. Goto, Jpn. J. Appl. Physics, 27, L680 (1988).
5. K. Togano, H. Kumakura, H. Maeda, E. Yanagisawa, N. Irisawa, J. Shinomiya and T. Morimoto, Jpn. J. Appl. Physics, 28, No 1 (1988).
6. K. Tachikawa, N. Sadakata, M. Sugimoto and O. Kohno, Jpn. J. Appl. Physics, 27, L1501 (1988).
7. M. Murakami, M. Morita, K. Miyamoto and S. Matsuda, to be published in Proc. Osaka Univ. Int. Symp. on New Developments in Applied Superconductivity, (Osaka,1988).
8. K. Tachikawa, I. Watanabe, S. Kosuge, M. Kabasawa, T. Suzuki, Y. Matsuda, and Y .Shinbo, Appl. Phys. Letter, 52, 1011 (1988).

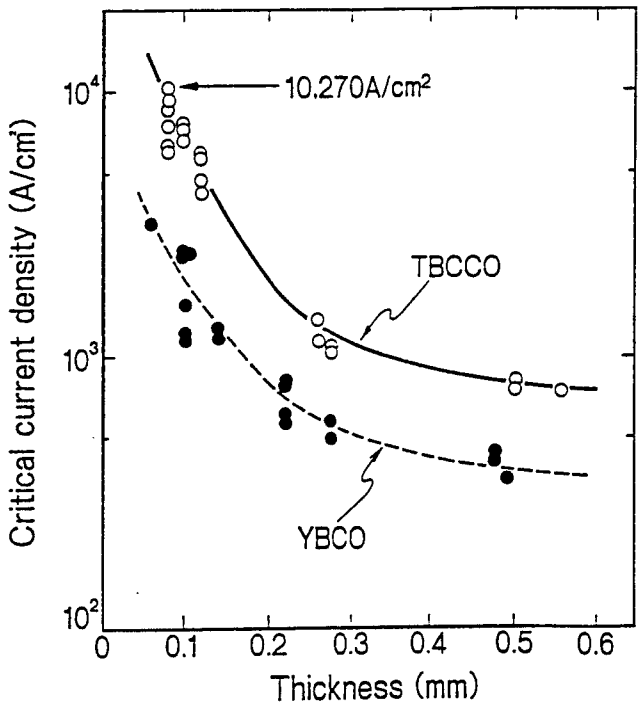

Fig. 1 Jc versus thickness of TBCCO and YBCO tapes prepared by a Ag-sheathed powder process.

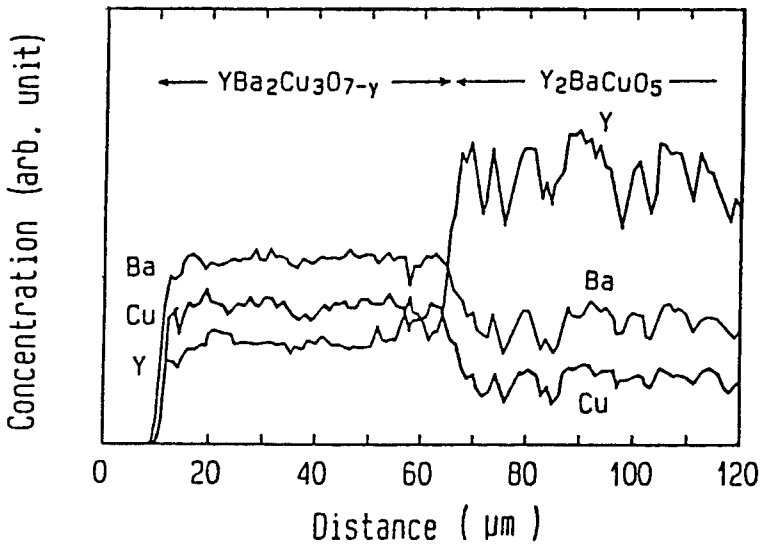

Fig. 2 Concentration profile of YBCO diffusion layer formed on a Y_2BaCuO_5 substrate. The specimen was heat treated at 930°C for 6hrs.

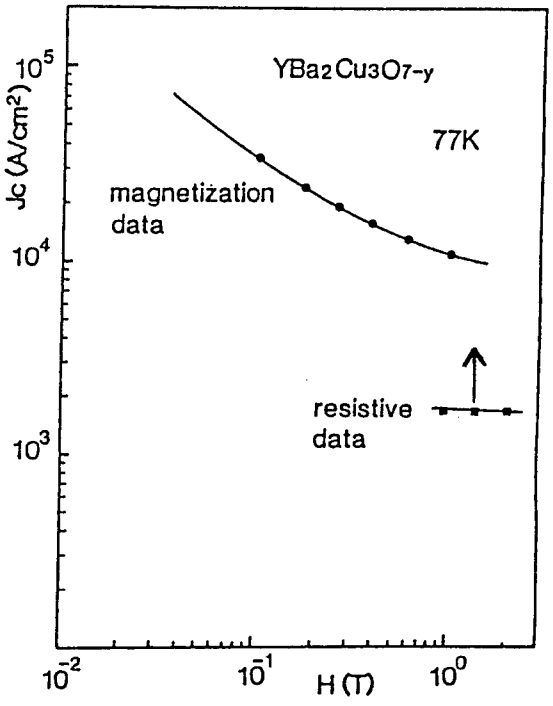

Fig. 3 A Jc versus applied magnetic field curve of YBCO sample prepared by a solidification process.

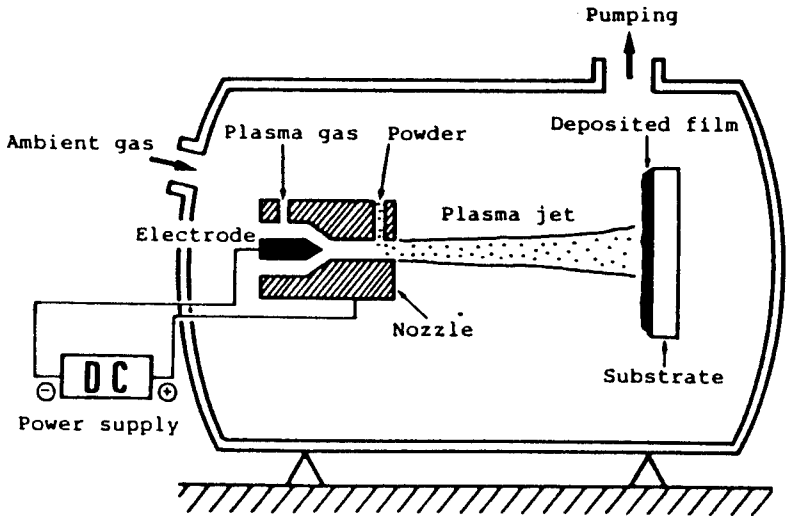

Fig. 4 Schematic drawing of low pressure plasma spraying apparatus.

OUTLINE OF THE RESEARCH ON HIGH Tc SUPERCONDUCTORS IN THE INSTITUTE OF PHYSICS CHINESE ACADEMY OF SCIENCES

Z. X. Zhao
Institute of Physics, Chinese Academy of Sciences
P.O. Box 603, Beijing 100080, P. R. of China

1 BRIEF INTRODUCTION OF THE RESEARCH ON SUPERCONDUCTIVITY

The Institute of Physics is a first research unit to research on superconductivity, because she is the first unit in China to achieve the He liquefaction with a self-design and manufacture liquefier in 1959.

In 1976 just after the "cultural revolution", some scientists in the institute tried to choose a long term project. According to the investigations on academic papers, they found out there were possibilities to push the superconducting transition temperature higher. The reasons were instability of lattice related to Tc. A15 compound Nb_3Ge with Tc of 23K above liquid hydrogen and new mechanism predicting much higher Tc. Since 1976, a great number of works have been done on experimental and theoretical work. Six national conferences on this subject were held every two years. The research on conventional materials and metastable phase were emphasized. In 1979, the project become one of key projects of condensed matter physics of national nature sciences program.

In September of 1986 after Bednorz and Müller's work, the effect of itinerant electrons on the Cu^{2+} and Cu^{3+} have been noticed. This effect makes a alternative Jahn-Teller effect which could lead strong instability of the lattice without structure phase transition and high Tc. We grasped the chance and focused our research on La-Ba-Cu-O system.

In December 1986 we obtained the onset of superconducting transition at 48.6K with ΔTc of 10K for Sr-La-Cu-O system and at 46.3K with ΔTc of 7K for Ba-La-Cu-O system. Both of them are multi-phase materials.

Resistance dropping dramatically to zero at around 70K in several samples had been observed in multi-phase Ba-La-Cu-O, but it was more unstable and the results were not reproducible in successive test. We believed that the materials with high Tc superconductivity around 70K exist in a metastable state [1].

The quenching was failure. According to our and C. W. Chu's results, which showed Tc onset of 52K at that time,the high pressure was ineffective for pushing Tc to 70K.

In early days, the starting materials, which were made in China in 1956, were not of high purity, for example, the chemical pure La_2O_3 with impurity of other rare earth elements. Two-dimensional characteristics of layered perovskite leads us to suggest that keeping the framework of the structure with Ba or La and using some elements with smaller atomic radii to replace some of Ba or La, then a system more close to two-dimensional and with longer period of superstructure could be obtained. As mentioned above,Bednorz and Müller formula $Ba(Sr)_{0.5}La_{4.5}Cu_5O_{5(3-y)}$ is not optimal to obtain single phase K_2NiF_4 ,but in multi-phase it is possible to find new metastable phase,which might have even higher Tc superconductivity. We insisted on research on multi- phase materials and on the way to prepare the samples with doping and substitution. we had tried with several rare earth elements, such as Sc, Y, Yb, Dy, Ho.... The first sample with Tc of 93K was found in $Ba_{0.5}Y_{4.5}Cu_5O_{5(3-y)}$ at the noon on Feb. 19. At 2:00 the early morning on Feb. 20 the results were completely confirmed.

On Feb. 21 our paper was accepted by Kexue Tongbao (Science Bulletin) [2]. On Feb. 23 we obtained duplicated samples. On Feb. 24 the Academia Sinica announced our results of superconductivity above LN_2 temperature in Y-Ba-Cu-O at a news conference, which appeared on Xinhua Wire Service and People's Daily on Feb. 25.

Since then, a family of Ln-Ba-Cu-O superconductors (Ln means rare earth elements) has been formed [3].

2 CHARACTERIZATION IN STRUCTURE AND CHEMISTRY

All of the present high Tc superconducting oxides are derived from perovskite structure. According to the coordination of Cu, there are three types: 4,5 and 6 coordination. It seems to be that the lower coordination favors in critical temperature of superconducting oxides. Up to now, no simple empirical rule with self-consistency for description of the relation between structure and transition temperature has been verified.

The Cu-O chains exist only in YBCO family with 123 structure. In others, no Cu-O chains has been observed up to now. The corrugation of Cu-O plane may play very important role. For the characterization in physics, the perfect sample is the most important. For the justification of a sample in quality, the relation of ordering of atoms, composition and structure in fineness must be considered. The distortion in structure closely relates to chemical composition. The observations of this relationship with physical properties have become starting point for physical models.

For the La-Ba-Cu-O system, the relation between 112 and 123 structure has been observed [4]. There exist a solid solution region, some La ions in 112 structure occupy the position of Ba in 123 structure. These leads to the change of oxygen and structure in fineness. The lower contents of La, the higher Tc. A series single phase sample of La-Ba-Cu-O could give more information.

In 1988, new superconductivity oxides have been found out, i.e. Bi and Tl compounds [5,6,7]. It shows more complex but very interesting relation between composition and structure. For Tl- Ba-Ca-Cu-O system the structures of 2201, 2212, 2223, 1212, 1223 and 1234 have been found and show superconductivity [8]. For Bi- Sr-Ca-Cu-O system,2201,2212 and 2223 structure have also been found [9].

Incommensurate structure with wave length 25.3 Åalong b axis has been identified both for 2212 (Tc=86K) and 2223 (Tc=110K) phases of Bi-Sr-Ca-Cu-O system [10]. Recently, the anti-phase boundary has been found in 2212 Bi-oxides [11].

Growth of single crystals for $Bi_2Sr_2CaCu_2O_y$, with Tc of 86K, is not difficult [12], but it is difficult to rule out the disordering of atom. Lacking of perfect single crystal, no neutron diffraction work for the identification of the positions of atoms at present, so the structures including the right occupation of atoms have not been identified completely. Basing on the samples we could obtain, except the relation between compositions, structure and superconductivity, some characterization in physics could be obtained also.

3 CHARACTERIZATION IN PHYSICS

3.1 Macroscopic Quantum Phenomena

Persistent current experiment shows the upper limit of the resistivity is smaller than 10^{-18} ohm·cm [13]. The Meissner effect and Josephson effect [14] have been observed in most of oxides superconductors. Comparing with the conventional superconductivity and G-L theory, no doubt, the superconductivity in the new oxides shows the macroscopic quantum phenomena.

Energy gap has been observed by tunneling experiment [15]. Even the data from the different groups are scattering but the existence of superconducting energy gap means the cooper-type pairing. The thermo-electric power and Hall effect experiments for most kind of oxides superconductors show the carrier is hole- like in sign [16]. So the pairing of holes should be the basic characteristics of high Tc superconducting oxides, even the mechanism for the pairing is not clear up to now.

3.2 Type II Superconductors

Critical magnetic field measurements show that all of the high Tc superconducting oxides are type II superconductors. According to the equations given by G-L theory, some parameters can be estimated even the data from different groups are a little

different because of the samples. The angular dependence of the critical field Hc_2 for both YBCO and $Bi_2Sr_2CaCu_2O_y$ have been observed. The wide transition from the flux creep and inhomogeneity of samples leads some difficulties for obtaining accurate data.

3.3 Strong Superconductivity Fluctuation

Small ΔCp, the specific heat jump at Tc, has been observed for most superconducting oxides. Considering the very short coherence length $\xi(0)$ and small ΔCp, the Landau-Ginzberg criterion will be 8-9 order of magnitude larger than that of conventional superconductors. The strong fluctuation must exist near the superconducting phase transition. So the mean field calculation can not give accurate results near phase transition.

3.4 Some Physical Parameters

Some physical parameters have been measured for thermal, optical and magnetic properties. The data will be published soon.

The measurements of the anisotropic resistivity on the single crystals of $Bi_2Sr_2CaCu_2O_y$, show the$(A/T) + BT$ relation for the resistivity along the c axis and metallic behaviors on a-b plane [17].

Thermopower and Hall effect measurements show hole-like in sign for $Bi_2Sr_2CaCu_2O_y$ and the carrier density is about 2.9×10^{21} cm^{-3} at 270K and 2.2×10^{21} cm^{-3} at 100K [18,19].

3.5 Energy Gap

For the single crystal of $Bi_2Sr_2CaCu_2O_y$ with Tc of 85K, the point contact measurement on the a-b plane was carried out [20].The data fixed by strong coupling theory show that the energy gap $\Delta(0)$ equals 18 meV and $2\Delta(0)/K_BTc \simeq 5$. The experiment with junction on single crystal $Bi_2Sr_2CaCu_2O_y$ has be done.

First of all is to get perfect sample especially some single crystals and films. It is key problem for the characterization in structure, chemistry and physics.

4 FURTHER RESEARCH

Three aspects will be emphasized in the institute:

a) Searching for new material. It is possible and may find some new which suit for commercial purpose and higher Tc.

b) Growing single crystals with good enough quality for the characterization in physics. This is very important for the understanding of origin of superconducting oxides.

c) Solving some key problems for application. for example, flux creep, flux motion and pinning.

ACKNOWLEDGMENTS

I am indebted to my colleagues for their efforts and effective co-operations and Prof. G. Z. Yang for the encouragements.

REFERENCES

[1] Zhao Zhongxian, Chen Liquan, Cui Changgeng, Huang Yuzhen, Liu Jinxiang, Chen Genghua, Li Shanlin, Guo Shuquan and He Yeye, *Kexue Tongbao* (in English edition), Vol.32, No.8 (1987) 522.

[2] Zhao Zhongxian, Chen Liquan, Yang Qiansheng, Huang Yuzhen, Chen Genghua, Tang Ruming, Liu Guirong, Cui Changgeng, Chen Lie, Wang Lianzhong, Guo Shuquan, Li Shanlin, and Bi Jiangqing, *Kexue Tongbao* (in English edition), Vol.32 No.10 (1987) 661.

[3] Zhao Zhongxian, Chen Liquan, Yang Qiansheng, Huang Yuzhen, Chen Genghua, Tang Ruming, Liu Guirong, Ni Yongming, Cui Changgeng, Chen Lie, Wang Lianzhong, Guo Shuquan, Li Shanlin, Bi Jianqing and Wang Changqing, *Kexue Tongbao* (in English edition), Vol.33 No.16 (1987) 1098.

[4] C. Dong, J.K. Liang, G.C. Che, S.S. Xie, Z.X. Zhao, Q.S. Yang, Y.M. Ni and G.R. Liu, *Inter. J.Modern Phys.* B, 1 (1987) 323.

[5] Z.X. Zhao, L.Q. Chen, Y.Z. Huang, Z.L. Xiao, Y.M. Ni,D.N. Zheng, J.Q. Bi, S.L. Jia, L.Z. Wang, J.H. Wang, Z.Y. Ran, D.H. Sheng, R.J. Xue, J.R. Chen and G.H. Chen, *Kexue Tongbao*, Vol.33 No.11 (1988) 817.

[6] Y.L. Zhang, G.C. Che, J.K. Liang, X.R. Chen, Q.S. Yang, D.N. Zheng, J.H. Wang, J.Q. Huang, S.L. Jia, Y.M. Ni, Z.X. Zhao, D.H. Shen and S.S. Xie, *Supercond. Sci. Technol.*, 1 (2) (1988) 92.

[7] Z.X. Zhao, L.Q. Chen, Z.H. Mai, Y.Z. Huang, Z.L. Xiao, X. Chu, D.N. Zheng, S.L. Jia, J.H. Wang, G.H. Chen, Y.M. Ni, J.Q. Bi, Q.S. Yang, D.H. Shen and L.Z. Wang, *Modern Phys. Lett.* B, 2 (1988) 479.

[8] J.K. Liang, S.S. Xie, G.C. Che, J.Q. Huang, Y.L. Zhang and Z.X. Zhao, *Modern Phys. Lett.* B, 2 (1988) 483.

[9] X. Chu, Z.H. Mai, Y.F. Yan, J.H. Wang, D.N. Zheng, C.L. Li, Q.S. Yang and Z.X. Zhao, *Mod. Phys. Lett.* B, 2 (1988) 981.

[10] D.Y. Yang, J.Q. Li, F.H. Li, Y.Q. Zhou, L.Q. Chen, Y.Z. Huang, Z.Y. Ran and Z.X. Zhao,*Supercond. Sci. Technol.*,1 (1988) 100; J.Q. Li, D.Y. Yang, F.H. Li, Z.Y. Ran and Z.X. Zhao, *Modern Phys. Lett.* B, 2 (1988) 1085.

[11] K.K. Fung, R.L. Withers, Y.F. Yan and Z.X. Zhao, preprint.

[12] Y.F. Yan, C.Z. Li, J.H. Wang, Y.C. Chang, Q.S. Yang, D.S. Hou, X. Chu, Z.H. Mai, H.Y. Zhang, D.N. Zheng, Y.M. Ni, S.L. Jia, D.H. Shen and Z.X. Zhao, *Modern Phys. Lett.* B, 2 (1988)571.

[13] W.J. Yeh, L. Chen, F.Z. Xu, B.K. Bi and P.R. Yang, *Inter. J. Modern Phys.* B, 1 (1987) 421.

[14] L. Chen, W.J. Yeh, F.Z. Xu, B.K. Bi and P.R. Yang, *Inter. J. Modern Phys.* B, 1 (1987) 575.

[15] H.J. Tao, Y.F. Chen, L. Lu, Q.S. Yang , *Chinese Phys. Lett.* 4 (11) (1987) 483.

[16] J.D. Hettinger, A.G. Swanson, J.S. Brooks, Y.P. Ma and Z.X. Zhao, *Inter. J. Modern Phys.* B, 1 (1987) 247; H.M. Duan, L. Lu, X.M. Wang, S.Y. Lin and D.L. Zhang, *Solid State Commun.*, 64 (1987) 489.

[17] Wang Jihong, Chen Genhua, Cui Xi, Yang Yifeng, Zheng Dongning, Mai Zhenghong, Yang Qianshen and Zhao Zhongxiao, *Supercond. Sci. Technol.*, 1 (1988) 27.

[18] G.H. Chen, J.H. Wang, D.N. Zheng, Y.F. Yan, S.L. Jia, Q.S. Yang, Y.M. Ni and Z.X. Zhao, *Modern Phys. Lett.* B, in the press.

[19] Y. Lu, Y.F. Yan, H.M. Duan, L. Lu and L. Li, *Phys. Rev.* B, 38 (1988).

[20] S.P. Zhao, H.J. Tao, Y.F. Chen, Y.F. Yan and Q.S. Yang, *Solid State Commun.*, 67 (1988) 1179.

THE CRYSTAL STRUCTURE OF HIGH-Tc Bi-BASED SUPERCONDUCTORS EXAMINED BY HIGH-RESOLUTION ELECTRON MICROSCOPY

Shigeo HORIUCHI*, Hiroshi MAEDA**, Yoshiaki TANAKA**, Kaoru SHODA***
and Yoshio MATSUI*
*National Institute for Research in Inorganic Materials, Tsukuba, Ibaraki 305
**National Research Institute for Metals, Tsukuba, Ibaraki 305
***Ube Industries Ltd, Ube, Yamaguchi 755

1. INTRODUCTION

It is important to analyze the crystal structure of materials, from the viewpoint not only of the interpretation on the origin of the physical and chemical properties but also of finding the guideline for exploring further new materials. We have examined and noticed that the crystal structure of the high-Tc Bi-based superconductors, found at National Research Institute for Metals[1], shows two outstanding characteristics, 1) very large lattice bending and 2) structural modulation, as compared to the previous high-Tc $YBa_2Cu_3O_x$. Because of these the conventional x-ray or neutron diffraction method are not so useful for the Bi-based superconducting materials and, therefore, we have tried to analyze the crystal structure mainly by means of high-resolution transmission electron microscopy (HRTEM).

2. EXPERIMENTAL

24, 30 and 37 Å phases, whose critical temperature Tc are 20, 80 and 105 K respectively, were obtained by different heating processes. Powder x-ray diffraction and electrical resistivity were measured. Small blocks of the crystals were crushed in an agate mortar and fine fragments created were mounted on the microgrids, which were set and observed in the electron microscopes of JEM4000EX, JEM2000EX or H-900 type.

3. RESULTS AND DISCUSSION

Fig.1(a) shows a lattice image of 30 Å phase. Although the resolution is not so high, we can notice two outstanding features of the crystal, i.e. the (020) crystal lattice planes are prominently bended and, moreover, dark island-like areas are formed [2]. The lattice bending reaches about 20 % at maximum. Fig.1(b) is a corresponding diffraction pattern. The array of the weak spots indicates the formation of a superstructure. They appear at non-integral positions so that it must be of incommensurate-type.

From the standpoint of the image formation we have considered that the dark areas are due to the concentration of Bi atoms and we have named these as Bi-concentrated bands [2,3]. This has been proved true later [4].

Fig.2 is anothor image, which has been taken after rotating the crystal by 45° about the c axis [3]. The photograph was obtained by making a simple image processing in order to decrease the background noise, i.e. the original negative film was printed 5 times on sliding by unit length. It is clear that the crystal is composed of the layered structure being stacked in the c direction and the array of the darkest spots are due to Bi atoms, i.e. the fundamental structure is similar to that of so-called Aurivillius-type [5]. The parts sandwiched by the Bi-O sheets has the perovskite-like structure. This has been coincident with the results by x-ray powder diffraction [6,7] as well as by other HRTEM observation [8-11].

Fig.3 is an HRTEM image, where electrons are incident along the same direction as that in Fig.1. The resolution is now so high that we

can specify not only the positions but also the species of each atom of the structure, based on the computer simulation of image intensity. The calculated image, which well fits to the real one, is represented in the micrograph with the same magnification. The structure model used for the calculation is shown in Fig.4 [4]. Some important conclusions obtained are: 1) A part of Bi atoms in the Bi-deficient bands are replaced by Sr. 2) In the perovskite-like layers metal planes are stacked in the sequence of Sr-Cu-Ca-Cu-Sr. 3) A part of Sr are substituted by Bi. 4) In the Ca planes some are replaced by Sr. 5) The positions of oxygens can be speculated based on the crystal symmetry (S.G.Amma) and the atomic distance. It may be said that CuO_4 piramids are formed.

The 37 Å phase grows from the 30Å one. The growth process can be seen in the SEM images of Fig.5 [12]. The crystals are both plate-like and the 37Å ones are larger than the 30Å ones.

Another structural interest of these superconductors is the intergrowth of layers with different thickness [13-15]. Any specimens intended for getting the 37 Å phase have always showed the intergrowth for the system Bi-Sr-Ca-Cu-O. Fig.6 is an example of such intergrowth. The figure written in the micrograph means the number of the Cu-O planes in the perovskite-like layers. For the 37 Å phase the figure is expected to be 3, but it is often 2 or 4 as seen in the micrograph.

The incommensurate-type structural modulation is found in all of the Bi-based superconductors [2,16,17]. The modulation waves are differernt for each crystal in the wave length and direction. The origin of them are not clear yet but the geometical explanation is possible for the 30 Å phase. In Fig.7 the small frameworks represent the supercell, which are constructed by aligning 5 subcells in the $\underline{b}$ direction. Smaller cells with the size of 4 subcells are locally inserted. The location of the latter is not regular but appear statistically with the frequency of about 1/5.

The diffraction spots at non-integral positions are described based on a four-dimensional space, being denoted by the vector, $h\underline{a}^*+(k+m/s)\underline{b}^*+l\underline{c}^*$, where h,k,l and m are integers [6]. $\underline{c}^*/s$ means the wave length of the structural modulation. In Fig.1(b) the diffraction spots are indexed with these four integers. The value s is measured to be 4.75 in the figure.

The 30 Å phase has been examined by the low-temperature electron microscopy, where the specimen is kept under 10 K [18]. An example of HRTEM image is shown in Fig.8. The results show that the crystal structure with the modulation along the $\underline{b}$ axis is not substantially changed on the transition to the superconducting state.

Acknowledgement: The authors would like to express their thanks to Drs.H.Nozaki,M.Onoda,A.Yamamoto,E.Takayama-Muromachi,A.Ono,S.Takekawa, F.Izumi,F.P.Okamura of NIRIM for valuable discussion and Drs.H.Daimon, F.Sakai,K.Uchida for continuous support.

REFERENCES

[1]H.Maeda,Y.Tanaka,M.Fukutomi and T.Asano:Jpn.J.Appl.Phys.27(1988)L209.
[2]Y.Matsui,H.Maeda,Y.Tanaka and S.Horiuchi:Jpn.J.Appl.Phys.27(1988)L361.
[3]Y.Matsui,H.Maeda,Y.Tanaka and S.Horiuchi:Jpn.J.Appl.Phys.27(1988)L372.
[4]S.Horiuchi,H.Maeda,Y.Tanaka and Y.Matsui:Jpn.J.Appl.Phys.27(1988)L1172.
[5]B.Aurivillius: Ark.Kem.1(1949)463.
[6]M.Onoda,A.Yamamoto,E.Takayama-Muromachi and S.Takekawa:Jpn.J.Appl. Phys.27(1988)L587.
[7]T.Kajitani,K.Kusaba,M.Kikuchi,N.Kobayashi,Y.Shono,T.B.Williams and M.Hirabayashi:Jpn.J.Appl.Phys.27(1988)L587.
[8]Y.Bando,T.Kijima,Y.Kitami,J.Tanaka,F.Izumi and M.Yokoyama: Jpn.J.Appl.Phys.27(1988)L358.
[9]D.Shindo,K.Hiraga,M.Hirabayashi,M.Kikuchi and Y.Shono: Jpn.J.Appl.Phys. 27(1988)L1018.

[10]Y.Hirotsu,O.Tomioka,T.Ohkubo,N.Yamamoto,Y.Nakamura,S.Nagakura,T.Komatsu and K.Matsushita: Jpn.J.Appl.Phys.27(1988)L1869.
[11]H.W.Zandbergen,W.A.Goen,F.C.Mijhoff,G.vanTendeloo and S.Amelinckx: Physica C.156(1988)325.
[12]S.Horiuchi,K.Shoda et al.:to be published.
[13]Y.Matsui,H.Maeda,Y.Tanaka,E.Takayama-Muromachi,S.Takekawa and S.Horiuchi: Jpn.J.Appl.Phys.27(1988)L827.
[14]Y.Matsui,S.Takekawa,H.Nozaki,A.Umezono,E.Takayama-Muromachi and S.Horiuchi: Jpn.J.Appl.Phys.27(1088)L1241.
[15]S.Ikeda,H.Ichinose,T.Kimura,T.Matsumoto,H.Maeda,Y.Ishida and K.Ogawa: Jpn.J.Appl.Phys.27(1988)L999.
[16]Y.Matsui,S.Takekawa,S.Horiuchi and A.Umezono:Jpn.J.Appl.Phys. 27(1988)L1873.
[17]S.Ikeda,K.Aota,T.Hatano and K.Ogawa:Jpn.J.Appl.Phys.27(1988)L2040.
[18]S.Horiuchi,K.Shoda,M.Iwatsuki,Y.Harada and Y.Matsui: to be published.

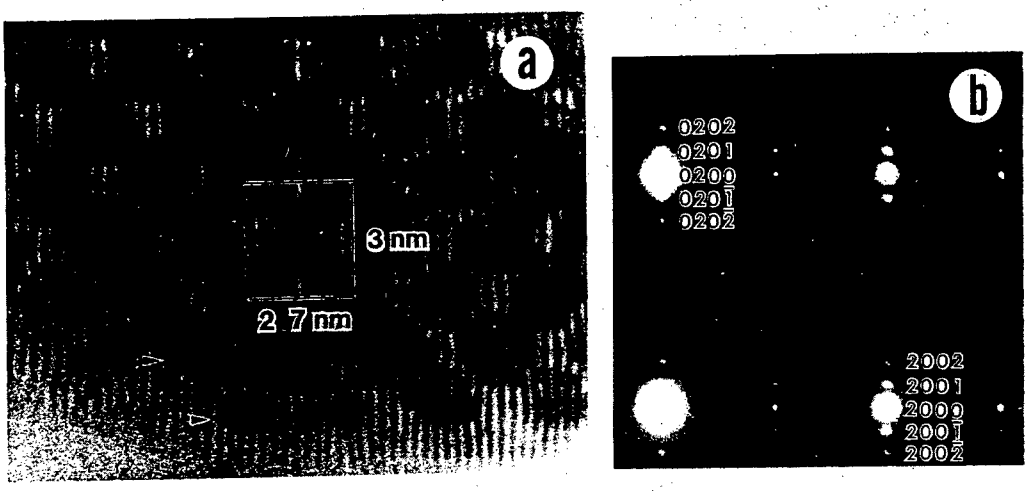

Fig.1 (a) A lattice image of $Bi_2(Sr,Ca)_3Cu_2O_x$, taken by the incident beam parallel to the a axis. (b) A diffraction pattern, teken with the incident beam parallel to the c direction.

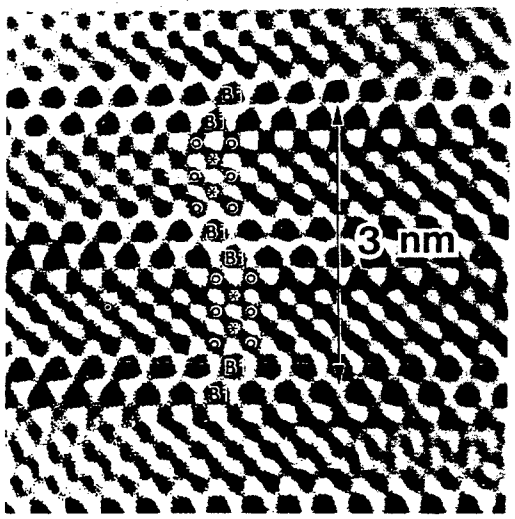

Fig.2 A HRTEM structure image of $Bi_2(Sr,Ca)_3Cu_2O_x$, teken by the incident beam parallel to the a+b direction.

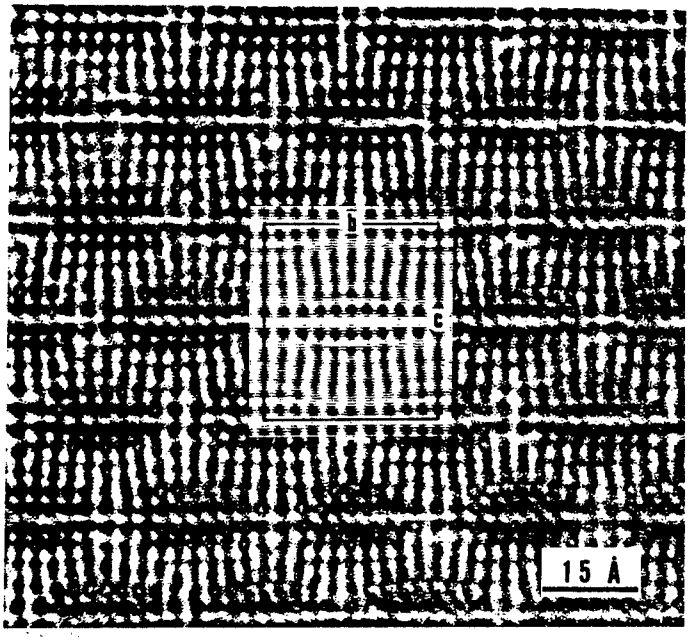

Fig.3 A HRTEM structure image of $Bi_2(Sr,Ca)_3Cu_2O_x$, taken by the incident beam parallel to the a axis. The image inserted is the calculated one.

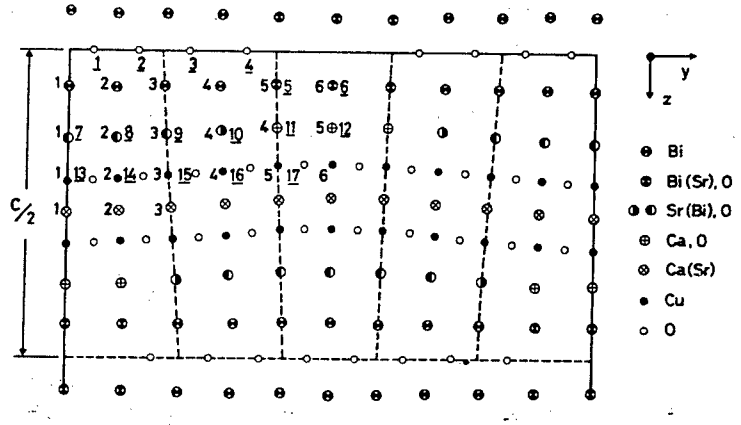

Fig.4 The structure model induced from the HRTEM image in Fig.3.

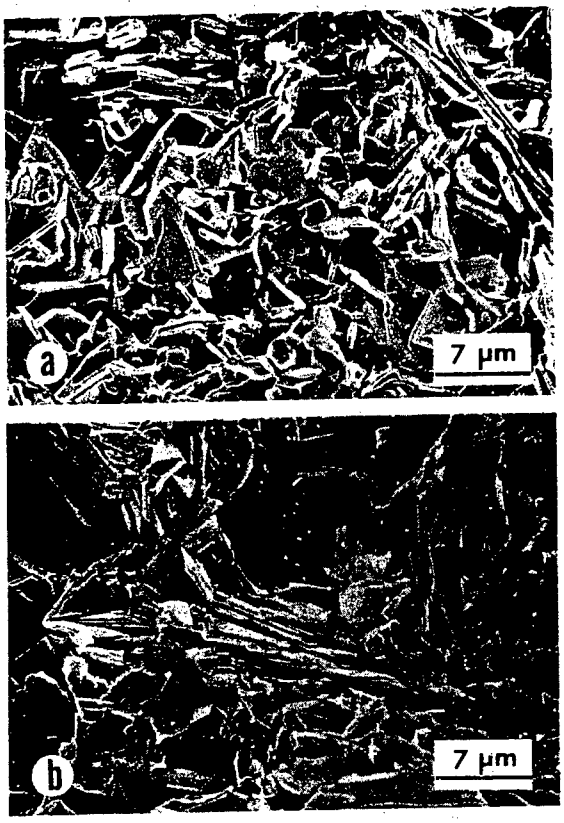

Fig.5 SEM images showing the stages of crystal growth from the 30 to 37 A phases. The specimens were heated finally at 870°C for 12 hr (a) and at 875°C for 12 hr (b).

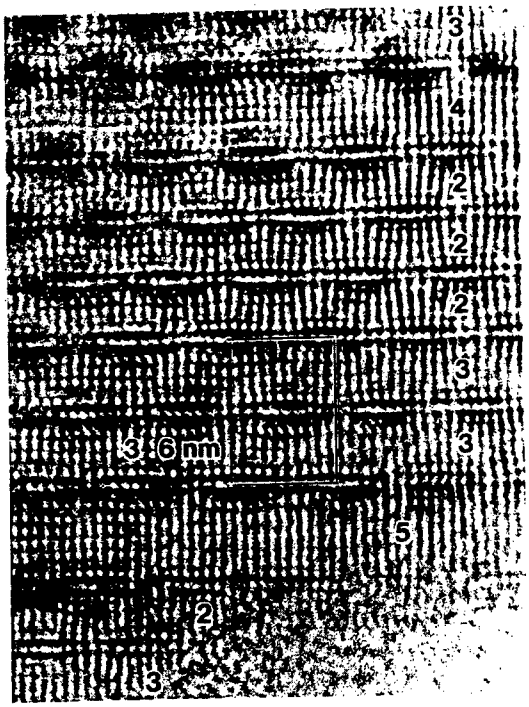

Fig.6 A HRTEM image of $Bi_2(Sr,Ca)_4Cu_3O_y$, showing the frequent occurrence of intergrowth.

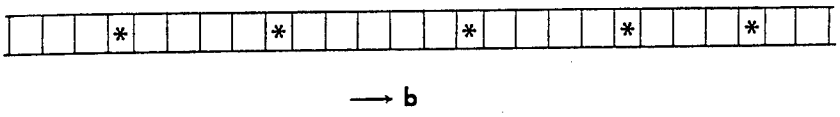

Fig.7 A model for the formation of the structural modulation. Smaller supercells marked by stars are statistically distributed among the larger, major supercells.

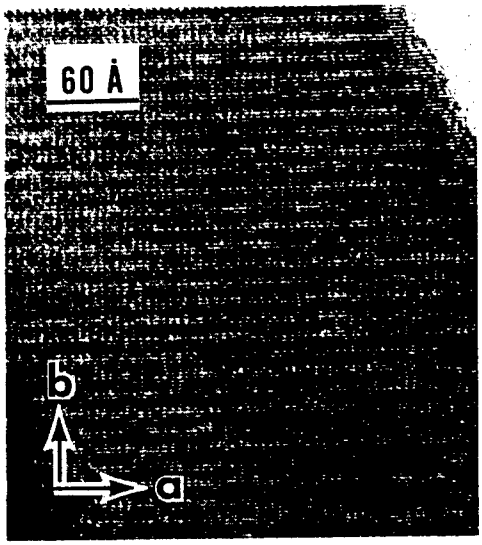

Fig.8 A HRTEM image of $Bi_2(Sr,Ca)_3Cu_2O_x$. taken at the temperature below 10 K. The electrons are incident parallel to the c axis.

TRANSMISSION ELECTRON MICROSCOPY STUDY ON HIGH Tc SUPERCONDUCTORS

Li Fang-hua

CCAST(World Laboratory), P.O.Box 8730, Beijing, China
and
Institute of Physics, Academia Sinica, Beijing 100080, China*
*mailing address

1. INTRODUCTION

Since the discovery of the new superconductor in La-Ba-Cu-O system[1] electron microscopy has revealed its power in studying crystal structures and defects of superconducting oxides. In the early stage of the research on high Tc superconductors most of the samples contain two or more phases. This makes difficult to obtain purely the structure information of high Tc superconducting phase by X-ray diffraction analysis. Even for the single phase samples it is an important task to study the local structure inside grains and the grain boundary which may affect strongly the superconductive behavior. In the present paper the results about crystal structures and defects of several superconducting oxides obtained in the electron microscope laboratory at the Institute of Physics, the Chinese Academy of Sciences are reviewed.

2. EXPERIMENTAL

Samples for electron microscope observation were prepared by grinding powdery oxides in an agate mortar or by ion milling thin slices cut from bulk materials of oxides. Most of the samples are observed under a JEM-200CX high resolution electron microscope. The composition of some samples is determined with a H-800 analytical electron microscope. The high resolution electron microscope images are simulated by the multislice method.

3. RESULTS AND DISCUSSION

90 degrees domains in $LaBaCu_2O_{5-x}$ [2,3]

It is well known that the compound in La-Ba-Cu-O system with the crystal structure of K_2NiF_4 type declared a new kind of superconductors. Later another superconducting phase which may occupy a wide range of composition and possesses a triple perovskite like superstructure was discovered in this system [4]. The difficulty in correctly determining the unit cell by X-ray diffraction is come from the existence of 90 degrees micro domains as shown in the lattice image (Fig.1a). The size

of domains are about tens to hundreds angstrom. Fig.1b and 1c are high resolution images taken from a single domain and from two domains superimposed each other with an angle of 90 degrees respectively. Although it is possible to determine the unit cell of this phase by electron microscopy independently, a combination of X-ray diffraction and high resolution electron microscopy (HREM) makes the task much straightforward.

(110) twins and grain boundary in $YBa_2Cu_3O_{7-x}$ [3,5]

There are always plenty of (110) twins in this phase. The electron micrograph (Fig.2) shows the twin planes running horizontally. Fig.2b shows the twin boundaries in a higher resolution. The bending of lattice fringes near the twin boundary can be interpreted as migration of atoms. The crystals are generally perfect as shown in Fig.2c where a small piece of enlarged photo from the thin region together with the superimposed structure model is given in the bottom right, but heavily defected region can also be found (Fig.2d). The grain boundaries are of different width and of different type. In Fig.2d the boundary of two grains oriented each other in an angle of about 30 degrees is very narrow. Fig.2e shows a boundary of about 10nm in width and the boundary consists of amorphous substance, but in some small regions lattice fringes along one direction or even two directions can be seen. Sometimes boundaries of crack typed can be found (Fig.2a). It is no doubt that the critical current density of the superconducting oxides would depend on the quality of grain boundaries.

Defects in $NdBa_2Cu_3O_{7-x}$ and validity of HREM in demostrating oxygen columns

The sample with Tc equal to 85K is heavily defected as shown in the lattice image projected along the a-axis (Fig.3a), although some perfect regions can also be found (Fig.3b). Fig.3c is the lattice image projected along the c-axis. The difference in image contrast from place to place are due to the different thickness and different defocus. Fig.3d shows the good agreements of the simulated images (right) with the observed images (left) enlarged from regions A, B, C and D. The crystal thickness is 2.33nm for region A and is 3.49nm for regions B, C and D. The underfocus values are 115nm, 165nm, 180nm and 190nm for regions A, B, C and D respectively. It is obvious that only under some peculiar imaging condition it is possible to distinguish occupied by the oxygen column from the vacant one.

One dimensional incommensurate modulated structure and intergrowth of Bi-Sr-Ca-Cu-O compounds [6,7]

Three superconducting phases have been observed by lattice imaging technique. All of them have a one dimensional

incommensurate modulated structure and belong to the orthorhombic system. Their average structures have two common unit cell parameters a=0.541nm and b=0.543nm. The periods along direction c are different for the three phases. The lattice period along direction c of compound $Bi_2Sr_2Ca_2Cu_3O_x$ or the so called 2223 phase with Tc=110K is c_1=3.68nm, and of compound $Bi_2Sr_2CaCu_2O_y$ or the so called 2221 phase with Tc=86K is c_2=3.07nm. The difference between c_1 and c_2 is 0.61nm which equals the thickness of one Cu-O layer and one Ca layer. The third compound with Tc<60K is the so called 2201 phase and has the lattice parameter c_3=2.46nm. The three phases are frequently intergrown coherently one another. The electron diffraction pattern of [100] zone shows that the modulation direction of the one dimensional incommensurate structure is parallel to direction [011] rather than [010].

Intergrowth of Tl-Ba-Ca-Cu-O compounds

The intergrowth of two superconducting phases with Tc equal to 120K and 90K or the so called 2223 phase and 2212 phase seems inevitable. Both of them belong to the tetragonal system with the common unit cell a=0.385nm. The lattice periods along direction c are 3.58nm and 2.94nm for 2223 and 2212 phase respectively. The lattice image projected along the a-axis is shown in Fig.4 where the white bands corresponds to Cu-O and Ca layers.

Substitution of Th for Y and of Er for Tl

It has been found by analytical electron microscopy that Th can partially substitute for Y in $YBa_2Cu_3O_{7-x}$ to obtain $(Th,Y)Ba_2Cu_3O_{7-x}$ which remains a superconductor with Tc around the temperature of liquid nitrogen[8]. The Er can also partially substitute for Tl in Tl-Ba-Ca-Cu-O compounds.

REFERENCES

[1] J.C.Bednorz and K.A.Muller, Z.Phys., B64 (1986) 189.
[2] S.S.Xie et al., Phys.Rew.B, 36 (1987) 2311.
[3] F.H.Li, H.J.Fan, X.J.Wu and J.G.Zhao, Modern Physics B, 1 (1987) 319.
[4] G.C.Che et al., Scientia Sinica, 31 A (1988) 1079.
[5] W.Liu et al., unpublished
[6] D.Y.Yang et al., Supercond.Sci.Technol., 1 (1988) 100.
[7] J.Q.Li et al., Modern Physics Lett. B2 (1988) 1085.
[8] J.G.Zhao et al., Modern Physics lett., B2 (1988) 651.

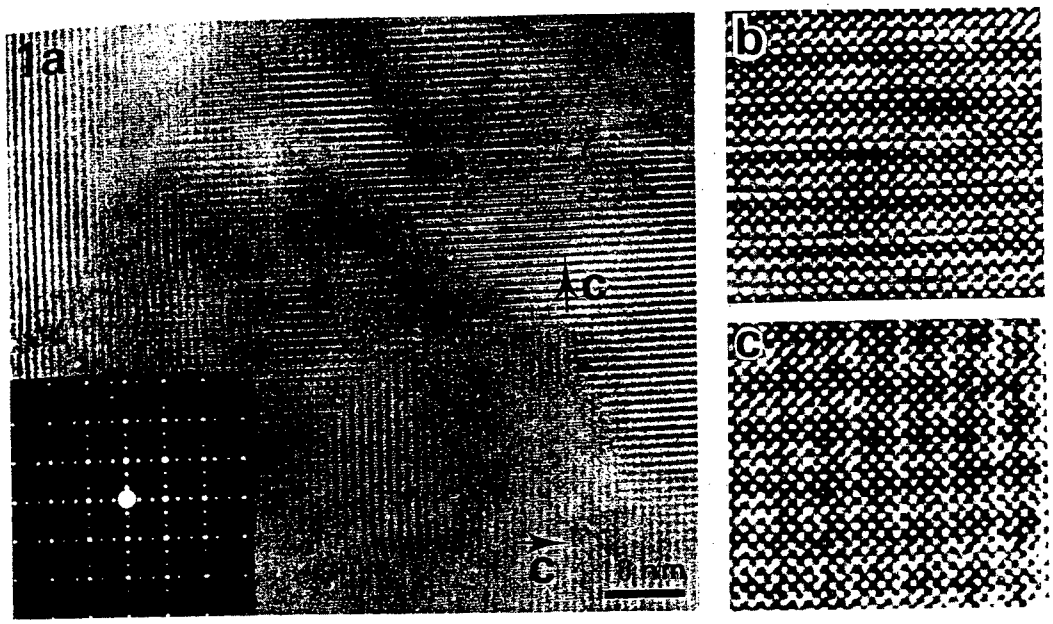
1a
c
c
5 nm

b

c

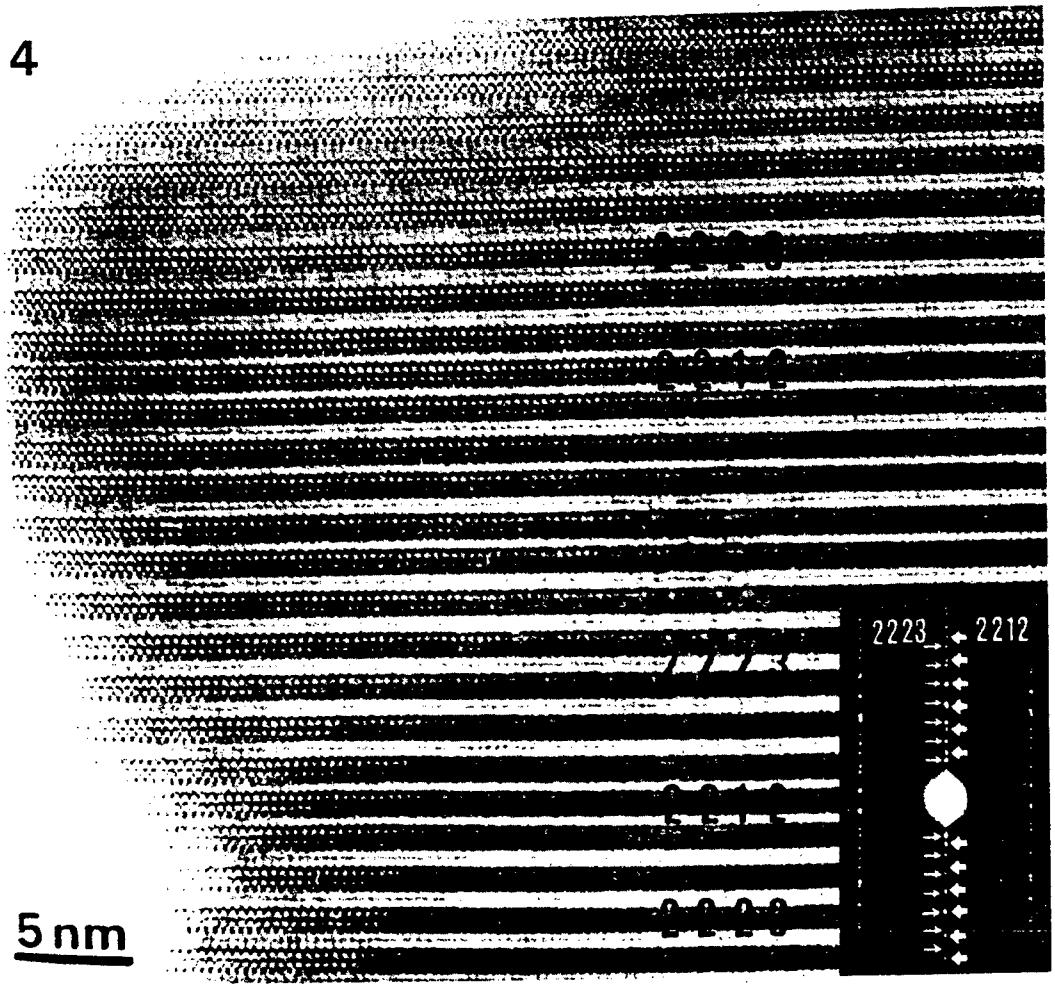
4
2223
2212
5nm

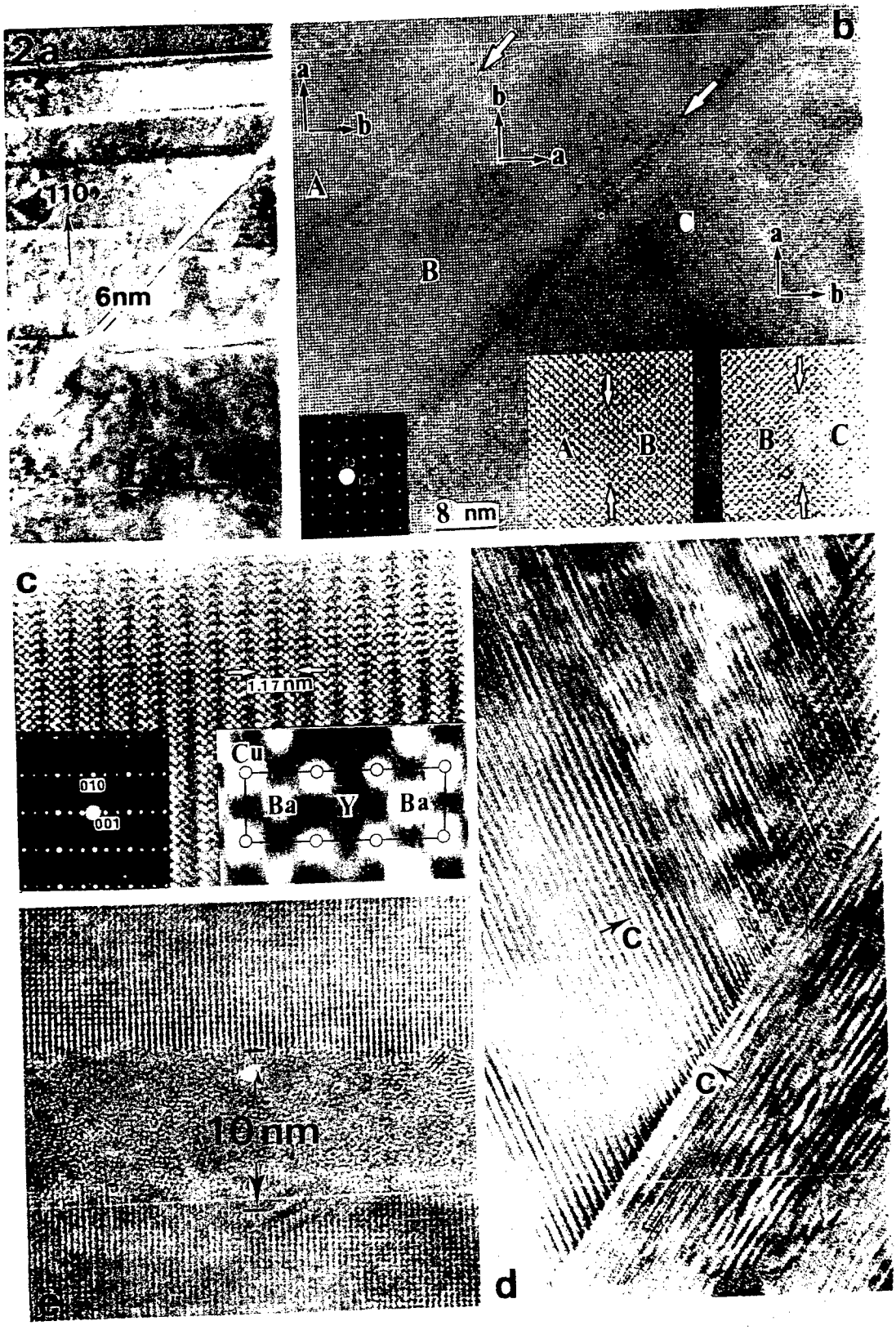
2a
110
6nm
b
a
b
A
B
a
b
8 nm
A
B
B
C
c
1.17 nm
010
001
Cu
Ba
Y
Ba
10nm
d
C
C

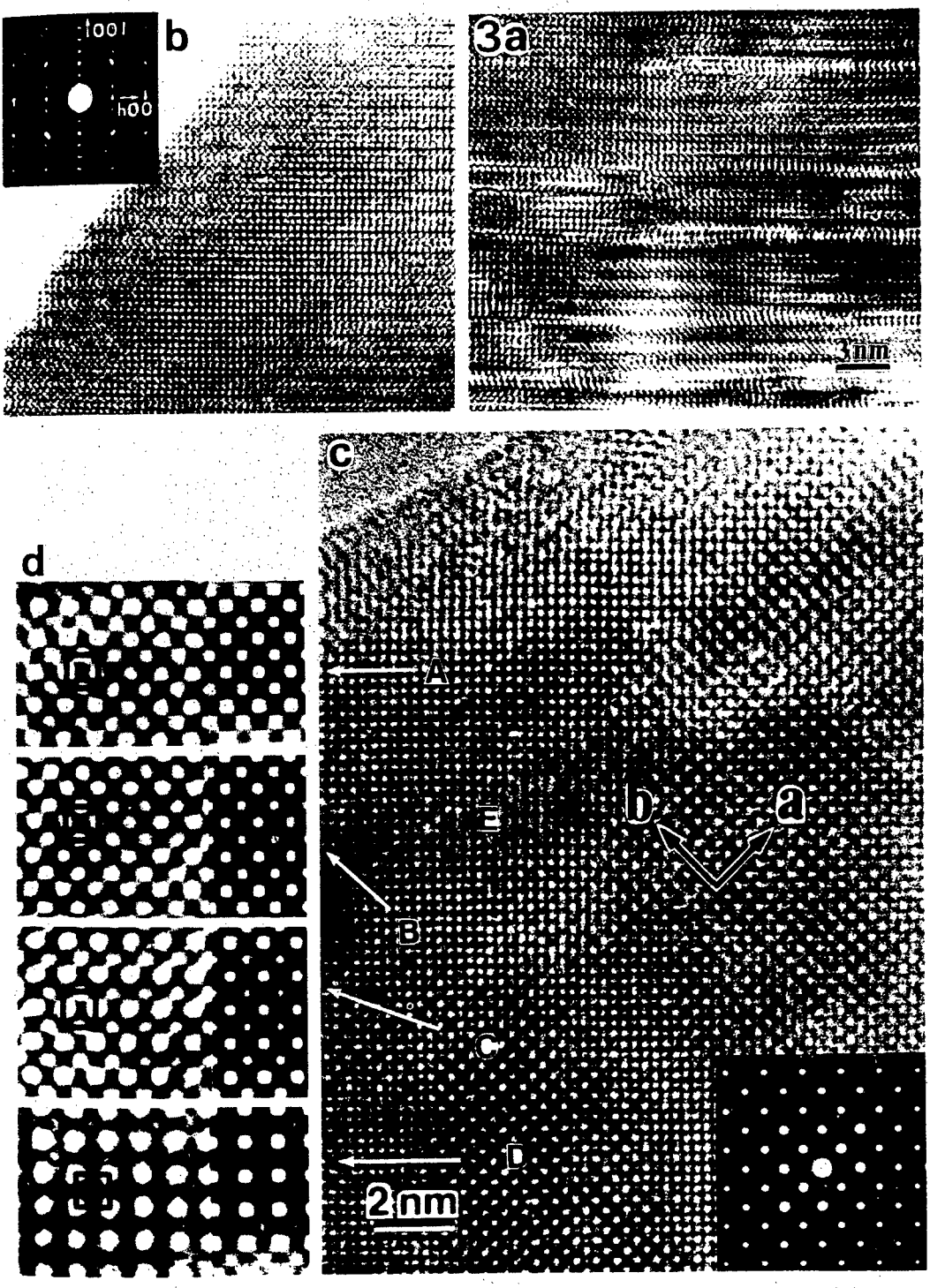
b
001
$\bar{h}00$
3a
3nm
C
d
A
B
C
D
a
b
2nm

MODULATED STRUCTURES OF Tl-Ba-Ca-Cu-O SUPERCONDUCTOR OXIDES

Sumio Iijima
NEC Corporation, Fundamental Research Laboratories
4-1-1, Miyazaki, Miyamae-ku, Kawasaki 213

1. INTRODUCTION

The TBCCO oxides form a homologous series of compounds whose chemical formulae are expressed by $Tl_mBa_2Ca_{n-1}Cu_nO_{2n+6+x}$, which is denoted as (m,2,n-1,n). Among them common phases are the 2212 and 2223, and their Tc values are around 105 and 120K, respectively [1]. The 2201 phase, however, showed a wide range of variations in Tc values between nonsuperconductor and 80K [2,3,4]. This phase is particularly of interest because it contains no Ca atoms at all. Therefore, ambiguity in Ca ion substitution for other metal ions in the Ca containing structures can be avoided. X-ray crystal structures for the 2201 crystals, which were prepared by sintering the raw powder materials at a temperature of around 870°C, are reported to be either tetragonal or orthorhombic. Hewat and co-workers [5] reported that superconductive 2201 crystals were tetragonal, while non-superconductive ones were orthorhombic. Shimakawa et al.[6], however, found that the superconductivity of the 2201 phase occurred equally in both tetragonal and orthorhombic crystals. According to the electron microscope observation of the TBCCO oxides, these crystals contained superlattice modulation [2]. We have been looking for a possible correlation between the lattice modulation and variation in the Tc values.

In the present report, we show some microstructures on TBCCO oxide crystals revealed by an electron microscope. In particular, high resolution electron microscope images of TBCCO, "ordered intergrowth phases", solid state reaction between the 2212 and 2223 phases, superlattice modulations in the 2201 phase and Y-doped 2212 phases are presented.

2. SPECIMENS AND OBSERVATION

TBCCO oxides examined in the present experiment were prepared by the conventional sintering of the powdered materials. For specimen 2201, powder materials, Tl_2O_3, BaO and CuO, with a 2:2:1 mixture ratio were pressed into pellet forms. Then they were heated at temperature between 800 and 905 C for 3hrs, in an oxygen atmosphere. After heating, the pellets were slowly cooled in the oven, or some of them were quenched. Y-doped 2212 samples were prepared by adding CaO and Y_2O_3 powder materials to those for the 2201 at a sintering temperature of 890°C for 1hr. For electron microscope observation, crushed specimen flakes were collected on the microscope specimen grid in the usual preparation method. Specimen observations were conducted by an ABT-002B electron microscope operated at 200keV.

3. "ORDERED-INTERGROWTH" PHASES

Figure 1 shows an "optimum focus" electron micrograph taken from a disordered region of the TBCCO crystal in the [110] orientation. Large and dark blobs are interpreted in terms of Tl and Ba atom positions, and the small blobs are those of Cu and Ca atoms. The micrograph contains three different structures, 2201, 2212 and 2223 structures which are intergrown intimately. The numbers shown in the image indicate the locations and the numbers of the CuO_2 slabs.

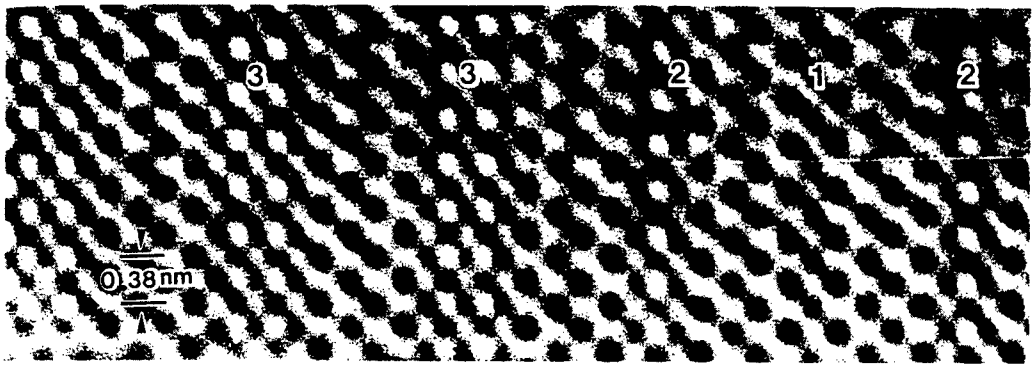

Fig. 1. A high resolution electron micrograph of a TBCCO crystal.

Among intergrowth structures of the TBCCO oxides, we found occasionally regular arrangements consisting of more than two structures in a homologous series of the compounds. We call them "ordered-intergrowths" [7]. An example for such ordered intergrowths is described by a unitcell [2212 + 2223 + 2223] which is regularly stacked in the c-axis direction. Its c-axis length becomes a summation of the three unitcells, namely, 10.06nm. Similarly, we found another ordered-intergrowth which is expressed as [2212 + 2223]. The occurrences of the ordered-intergrowth structures mentioned above suggest a family of ordered-intergrowth structures which are represented by combination of some of the homologous series of the compound. Examples for the compounds with double TlO slabs are illustrated in Fig. 2. The variations in ordered-intergrowths can be diversified by taking a single TlO slab, or a stacking unit as a c/2 axis length.

From a superconductivity point of view, it is of interest in knowing how the Tc values for the ordered-intergrowths are affected by being a sandwiched intergrowth structure. If a separation between neighboring superconducting CuO_2 layers is large enough to avoid interference, two-dimensional superconductive layers can be obtained.

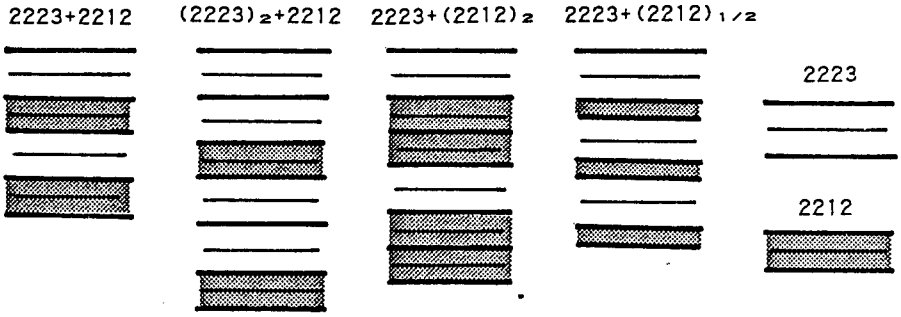

Fig. 2. Some examples for "ordered-intergrowth" phases.

4. SOLID-STATE REACTION

A mechanism for the solid state reaction is important for growing single phase TBCCO oxides. During the heat treatment, removal of the intergrown

2212 phase from the dominant 2223 phase, or vice versa, for instance, is a crucial problem for sintering process. The most common phase boundary between these two phases is on (001) planes which are parallel to the BaO-TlO-TlO-BaO slabs. To eliminate the 2212 structure by moving the boundary, it should move along a direction perpendicular to the (001) plane. Such a solid-state reaction obviously will involve the rearrangement of whole atoms on the boundary, and will take considerable energy. Another type of the phase boundary lying on a (110) was occasionally observed as indicated by the arrow in Fig. 3 [8]. In this case, a 2212-2223 reaction can be achieved by moving the boundary parallel to the (001) plane.

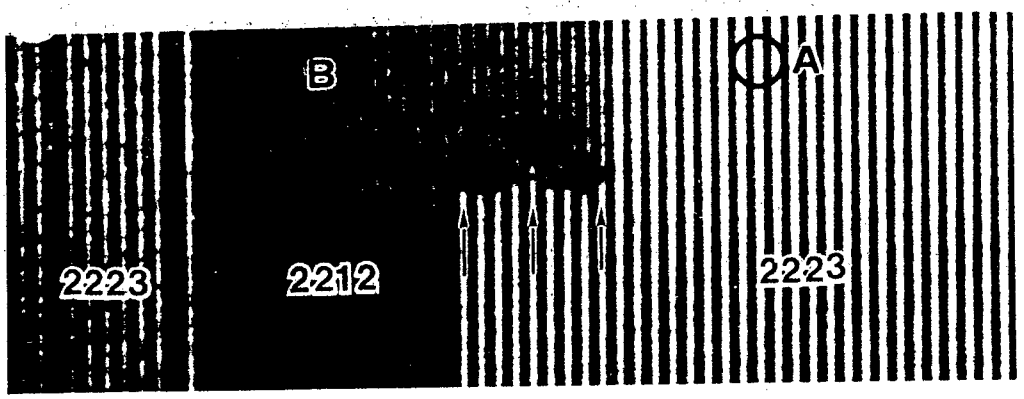

Fig. 3. A phase boundary between the 2212 and 2223 phases.

It was found that the (110) boundary widths between the 2212 and 2223 phases are often characterized by a 4:5 ratio for the number of c/2 axis length along the boundary. This relation can be explained by the fact that every fifth BaO-TlO-TlO-BaO slab in the 2212 phase corresponds to that in the 2223 phase within a 2.9% lattice mismatching ratio. Every fifth BaO-TlO-TlO-Ba slab, therefore, can be preserved unchanged across the boundary. When a (110) boundary width does not meet with the condition of the 4:5 ratio, the boundary displayed strain contrast around it. Such boundaries will have much higher free energy than those with a 4:5 lattice matching boundary, so that the boundaries can be removed easily during the heat treatment of the specimen. Since the 2212 and 2223 phases are different in composition, the above-mentioned reaction will progress presumably with material transport through the boundaries from specimen surfaces.

5. SUPERLATTICE MODULATION IN 2201 OXIDES

In contrast with the 2212 and 2223 compounds, the 2201 compounds showed a wide range of Tc values. Recently, the Tc value variation was found to be strongly affected by oxygen content. Furthermore, crystal symmetries of the compounds, namely, orthorhombic and tetragonal, are not directly related to the superconductivities [6]. The orthorhombic structures appeared at preparation temperatures below 840°C, while the tetragonal ones are obtained above 840°C. Another finding was a correlation between Tc and the c-axis length, where a Tc value increases linearly, independently with crystal symmetry, with an increase in the c-axis length. A similar behavior was observed on Y-doped 2212 compounds [9].

The nonsuperconductive 2201 compounds with tetragonal symmetry show diffuse ring patterns appearing around the fundamental diffraction spots. They suggest the occurrence of some kinds of lattice defects which are usually not taken into account the superconductivities. Since these defects will be correlated to the compositional changes as was reported by Hewat et al.[5], characterization of the defects is needed. The maximum diffuse ring intensities are observed when the crystal was tilted about [010] axis. Similar ring patterns are observed commonly on the TBCCO oxides [10].

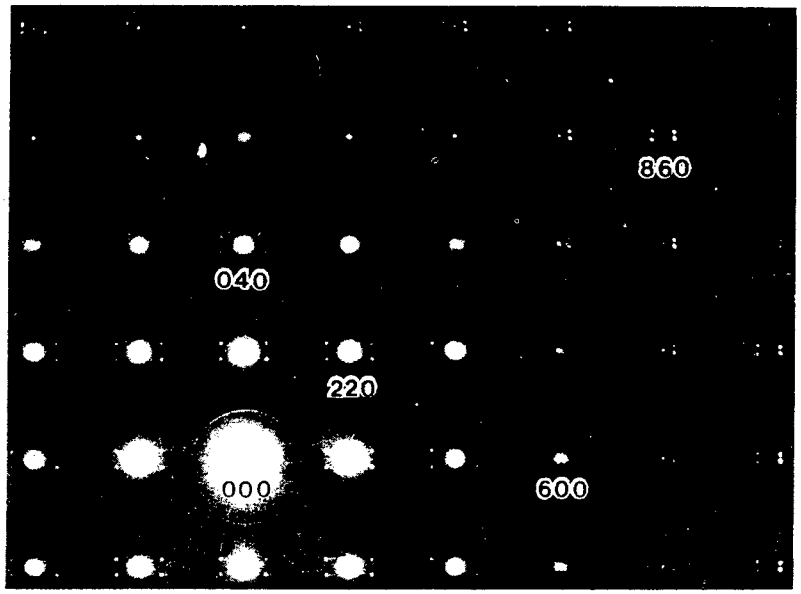

Fig. 4. The [001] axis ED pattern from 2201 crystal.

Another [001] zone axis ED pattern(Fig. 4) shows two sets of satellite spots but no second order spots. Their reflection vectors are approximately $+[3/14, +1/14, 0]$. The details of satellite spot appearances are explained nicely in terms of the Ewald sphere effect. A reciprocal lattice section perpendicular to the [-1,3,0] direction showed the strongest satellite spot intensities, and its corresponding electron micrograph shows bright and dark alternating bands. They are due to the twins on the (110) which are caused by a superlattice.

The satellite spots appears also on four sets of {310} planes. The spots appearing around the (220) and (860), which are fundamental reflections, are shown in Figs. 5a and 5b, respectively. They are compared with those patterns accompanied by two sets of satellite spots as shown in Figs. 5c and 5d. The diffuse ring pattern is also included (Fig. 5e). Three dimensional distribution of the satellite spots is illustrated in Fig. 5f. The superlattice vectors are found to be $Q = +[3/14, +1/14, +1]$. A (001)* plane projection of the superlattice vector is coincident with the radius of the diffuse scattering rings (Fig. 5e) as illustrated by a hatched ring in Fig. 5f.

From the similarity to the satellite spot geometry, the diffuse ring patterns can be interpreted by an imperfect ordering of the superlattice, and also a small size of the superlattice domains occurring equally on the {310} planes. The domains giving rise to the satellite spots are in order of several nm in size. On the correlation between the superstructure and superconductivity, those crystals which do not show strong superlattice modulations tend to have a higher Tc value.

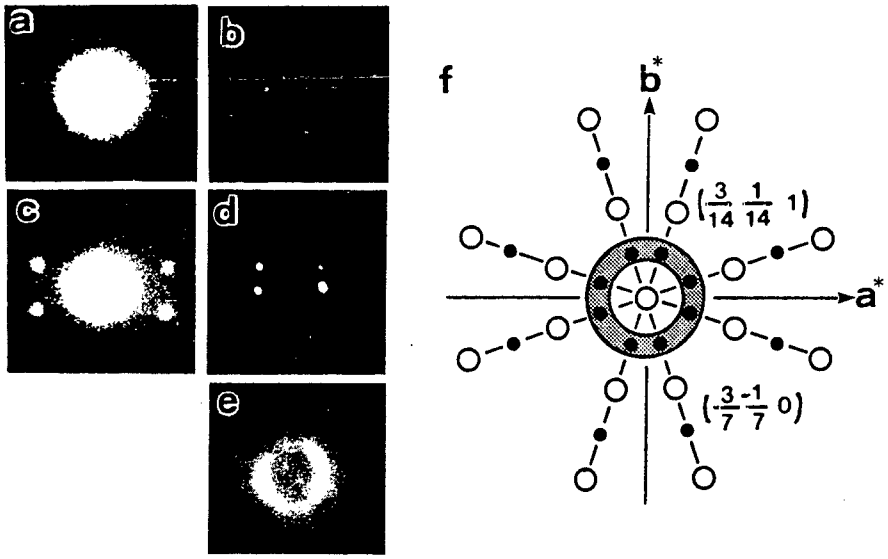

Fig. 5. Some superlattice reflections from the 2201 crystal.

6. LATTICE MODULATION IN Y-DOPED 2212 OXIDES

As substituting Ca atoms for Y atoms, Tc values of 2212 compounds decrease: 100K for the 10% Y-substitution, 70K for 30% and nonsuperconductor for 50%. The crystals shows diffuse ring appearances dependent on an amount of Y dopants. Those compounds with the 10% and 30% Y-substitution show continuous diffuse ring patterns whose diameters are quite similar to one shown in Fig. 6e, while the one with 50% substitution shows spotty ring patterns. Their intensity maxima appear at four positions with reciprocal lattice vectors $=[+0.32\ 0\ +1]$ and $[0\ +0.32\ +1]$(Fig.6a), which are different from those for the superlattice in the 2201 compounds. Figure 6b represents an electron micrograph of the 50% Y-substitution crystal in the [010] orientation. Dark blobs appear approximately in a face-centered arrangement. They are formed in the CuO_2-Ca-CuO_2 slabs. It means that Y atoms go to the Ca atom positions in forming a superlattice.

7. CONCLUSION

Usefulness of electron optical methods for characterization of the local structures of high Tc oxides was emphasized. The "Ordered-intergrowth" structures were observed, and their structural variations are proposed. Stabilities of the (110) phase boundaries between the 2212 and 2223 TBCCO phases were discussed in terms of an atomic structure of the boundary. Lattice modulations in the 2201 compounds prepared under various crystal growth conditions were examined, and their geometries were determined. The modulations don't seem to affect the variation of observed Tc values. For the Y-doped 2212 compounds, two kinds of the lattice modulations were found: one is similar to those observed for the 2201, and is presumably caused by Tl and O vacancies taking place in the TlO slabs as was suggested by Hewat et al.[11]. Another is due to substitution of Ca atoms for Y atoms, and has a strong correlation with Tc value variations.

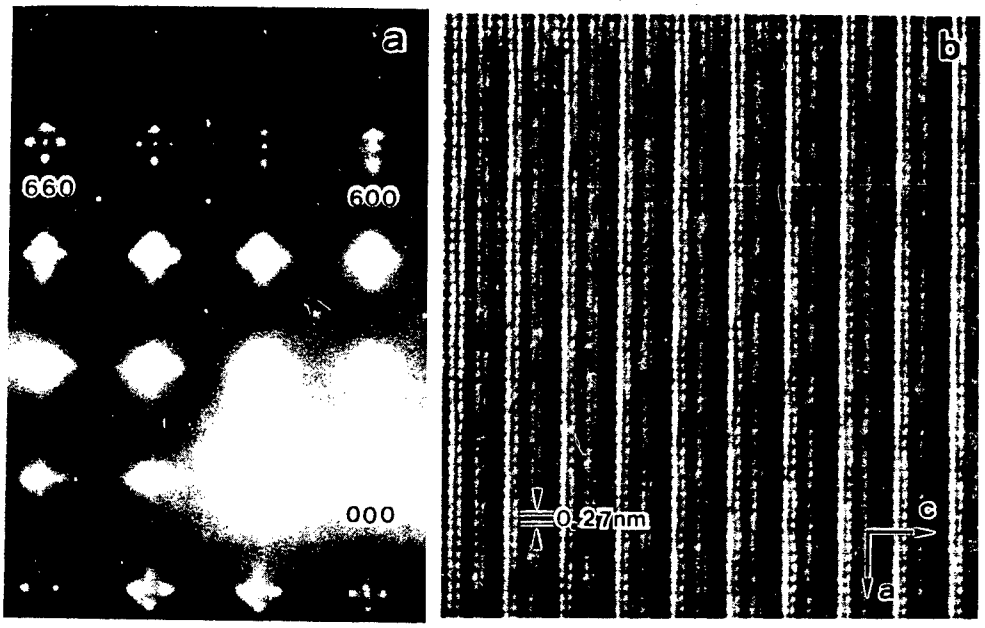

Fig. 6. A slight-off-angle [001] ED pattern (a), and a [010] HREM image of 50% Y-doped 2212 crystal (b).

The author would like to thank his co-workers, Y.Kubo, T.Ichihashi, Y.Shimakawa and T.Manako, for collaboration on the high Tc oxide research project.

REFERENCES

1. Z.Z.Sheng and A.M.Hermann: Nature 332, 136(1986).
2. S.Iijima, T.Ichihashi, Y.Shimakawa, T.Manako and Y.Kubo: Jpn.J.Appl.Phys. 27, L1061(1988).
3. R.Beyers, S.S.Parkin, V.Y.Lee, A.L.Nazzal, R.Savoy, G.Gorman, T.C.Huang, and A.La Placa: Appl.Phys.Phys.Lett. 53, 432(1988).
4. C.C.Torardi, M.A.Subramanian, J.C.Calabrese, J.Gopalakrishnan, K.J.Morrissey, T.R.Askew, R.B.Flippen, V.Chowdhry, and A.W.Sleight: Science 240, 631(1988).
5. E.A.Hewat, P.Bordet, J.J.Capponi, C.Chaillout, J.Chenavas, M.Godinho, A.W.Hewat, J.L.Hodeau and M.Marezio: Physica C, 156, 375(1988).
6. Y.Shimakawa, Y.Kubo, T.Manako, T.Satoh, S.Iijima, T.Ichihashi and H.Igarashi: submitted to Physics C.
7. S.Iijima, T.Ichihashi and Y.Kubo: Jpn.J.Appl.Phys. 27, L1054(1988).
8. S.Iijima, T.Ichihashi and Y.Kubo: Jpn.J.Appl.Phys. 27, L1168(1988).
9. T.Manako, Y.Shimakawa and Y.Kubo: private communication.
10. J.D.Fitz Gerald, R.L.Withers, J.G.Thompson, L.R.Wallenberg, J.S. Anderson, and B.G.Hyde: Phys.Rev.Lett. 60, 2797(1988).
11. A.W.Hewat, P.Bordet, J.J.Capponi, C.Chaillout, J.Chenavas, M.Godinho, E.A.Hewat, J.L.Hodeau and M.Marezio: Physica C, 156, 369(1988).

HIGH-TEMPERATURE SUPERCONDUCTIVITY PRODUCED BY ELECTRON-DOPING IN COPPER OXIDE COMPOUNDS

Yoshinori TOKURA*, Hidenori TAKAGI+ and Shinichi UCHIDA+

*Department of Physics and +Engineering Research Institute, University of Tokyo, Bunkyo-ku, Tokyo 113, Japan

Since the discovery of high temperature superconductivity (High T_c) in cuprate compounds by Bedonorz and Muller [1], unprecedently extensive studies have been carried out to elucidate what is required for High T_c. There have been several families of High T_c cuprates so far discovered, all of which have a common feature: they possess the two-dimensional (2D) sheets of Cu-O pyramids or octahedra which are doped with holes. Here, we report the discovery of new electron-(not hole-)doped superconducting cuprates[2]. The new superconductors are Ce^{4+}-doped compounds, $Ln_{2-x}Ce_xCuO_{4-y}$, where Ln=Pr, Nd and Sm. The compounds have the Nd_2CuO_4 structure [3], or the so-called T'-phase structure, as shown in Fig.1(a), which is composed of 2D sheets of Cu-O squares. This structure has no apical oxygen, in contrast to those of so far known superconducting single-layer cuprates; the T-phase structure with Cu-O octahedra (Fig.1(b)) as observed in $La_{2-x}Sr_xCuO_4$ [1,3] (with T_c=40K) and the T*-phase structure with Cu-O pyramids (Fig.1(c)) in $Nd_{2-x-z}Ce_xSr_zCuO_4$ (T_c=30K)[4,5].

Materials were synthesized from mixture of rare-earth metal oxides (CeO_2, Pr_6O_{11}, Nd_2O_3, Sm_2O_3) and CuO. Mixed powder was first calcined at 950°C for 10 hours in air, then pressed into pellets, and finally sintered at 1150°C for 12 hours in air. The samples were quenched to room temperature in air. To produce superconductivity, procedures of annealing the Ce-doped samples under reducing condition were necessary. The samples

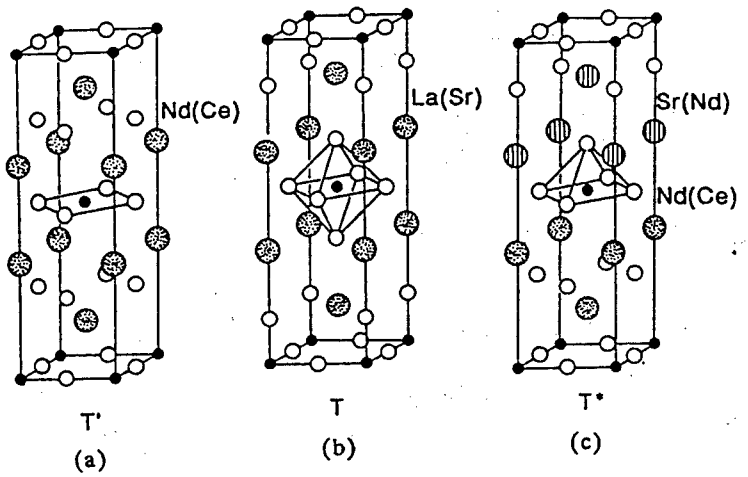

Fig.1: Crystal structures of (a) $Nd_{2-x}Ce_xCuO_4$ (T'-phase), (b) $La_{2-x}Sr_xCuO_4$ (T-phase) and (c) $Nd_{2-x-z}Ce_xSr_zCuO_4$ (T*-phase).

were annealed at 1000°C for 10 hours in a stream of Ar/O_2 gas mixture with the partial O_2 pressure of 10^{-4}atm and quenched to room temperature in the same atmosphere. Figure 2 shows the temperature-dependence of resistivity in $Nd_{2-x}Ce_xCuO_{4-y}$. Although the undoped compound Nd_2CuO_4 is a typical semiconductor, the doping of Ce^{4+} ions makes the sample more conducting [5]. Remarkable decrease in resistivity was also observed in the undoped sample which was quenched from 1150 C in air down to room temperature to make the sample oxygen deficient (y~0.04). These observations clearly show that the doped Ce^{4+} ions and/or oxygen deficiencies introduce mobile electrons into the compounds. According to the recent investigation [5], the T'-phase Nd-based cuprate cannot be doped with holes, whereas the T*-phase compound $Nd_{2-x-z}Ce_xSr_zCuO_4$ (shown in Fig.1(c)) can be doped with holes, but not with electrons, like in the case of the T-phase structure (shown in Fig.1(b)).

Fairly low resistivity ($<10^{-2}$ohmcm) in $Nd_{2-x}Ce_xCuO_{4-y}$ was observed at the Ce-concentration of 0.15, where the sample shows semi-metallic, but not superconducting behavior. (As shown in Fig.2, the x=0.15 sample shows a resistivity drop around 9K, which indicates superconductivity in tiny portion of the sample.) The bulk superconductivity in the same sample (x=0.15) was achieved by the reducing procedure described above. The resistivity as well as the magnetization showed an onset of the superconductivity at around 24K. The concentration (q) of introduced electrons per [Cu-O] unit, or the effective Cu valence (2-q), was estimated by an iodometric titration technique [6], taking into consideration the reductive reaction of Ce^{4+} into Ce^{3+} during the

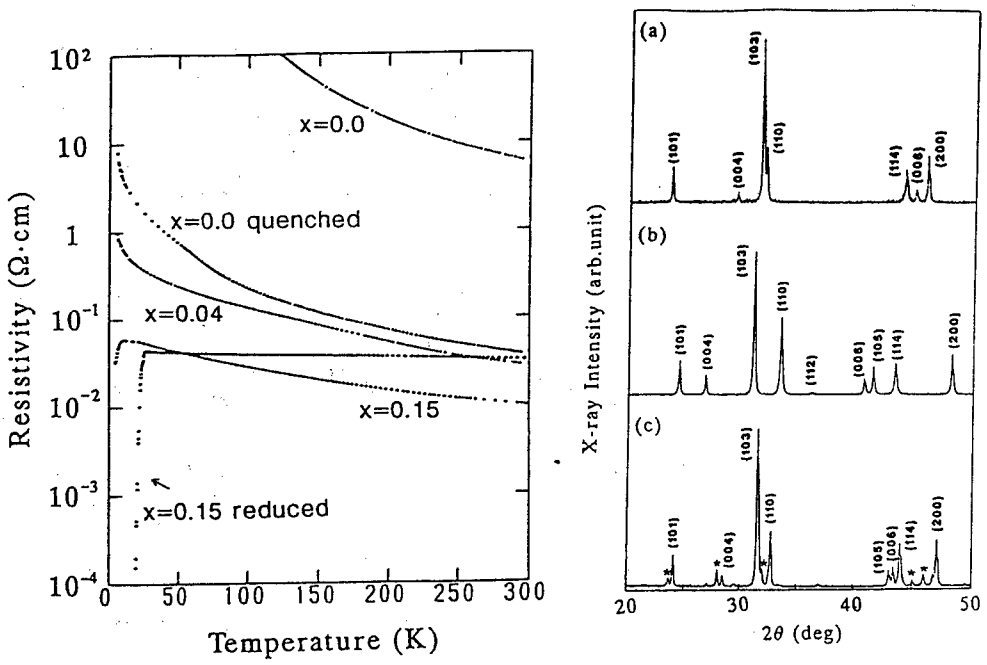

Fig.2: Temperature-dependence of resistivity in $Nd_{2-x}Ce_xCuO_{4-y}$.

Fig.3: Powder X-ray diffraction patterns of (a) $Nd_{1.85}Ce_{0.15}CuO_{4-y}$ (T'-phase), (b) $La_{1.85}Sr_{0.15}CuO_4$ (T-phase) and (c) $Nd_{1.4}Ce_{0.2}Sr_{0.4}CuO_{4-y}$ (T*-phase). Asterisks (*) indicate the peaks due to the secondary phase.

titration process. The x=0.15 sample shown in Fig.2 has the q-value of 0.20 before the reducing procedure, whereas after that the value of q in the supercondcuting sample is increased up to 0.28, which corresponds to the increased oxygen vacancies with y~0.07. Therefore, the increase of electrons beyond a certain value of density (q~0.20) seems to give rise to electron-superconductivity.

Electron-type carriers in the new superconducting compound were also confirmed by measurements of the Hall coefficient. The sample $Nd_{1.85}Ce_{0.15}CuO_{3.93}$ with T_c of 24K shows the negative Hall coefficient; R_H=-6.5x10^{-4}cm^3/C at 300K and -2.3x10^{-3}cm^3/C at 80K. This observation is in sharp contrast with the cases of other hole-superconducting cuprates so far known, in which positive Hall coefficients are always observed.

The X-ray diffraction pattern for this superconducting sample $Nd_{1.85}Ce_{0.15}CuO_{3.93}$ is shown in Fig.3(a), in comparison with those of the hole-superconducting T-phase $La_{1.85}Sr_{0.15}CuO_4$ (b) and T*-phase $Nd_{1.4}Ce_{0.2}Sr_{0.4}CuO_4$ (c) (see also Fig.1). The diffraction pattern (a) of $Nd_{1.85}Ce_{0.15}CuO_{3.93}$ is essentially identical with that of the T'-phase Ce-undoped compound, Nd_2CuO_4, and all diffraction peaks discernible in the pattern (a) can be indexed with the lattice constants of the typical tetragonal T'-phase structure [3]; a=3.95A and c=12.07A in the Ce-doped superconducting sample abd a=3.93A, c=12.11A in the Ce-undoped T'-phase compound. The CuO_4 square in the T'-phase is appreciably expanded and its c axis is shrinked, as compared with the lattice parpameters of the T- and T*-phase structures associated with apical oxygens; a=3.78A, c=13.2A in the T-phase (b) and a=3.85A, c=12.5A in T*-phase (c).

It should be emphasized that the electron-superconductivity is not restricted to the Nd-based compounds. Also in other T'-phase compounds of Pr- and Sm-based cuprates, the Ce-doping and subsequent reducing procedure, which are necessary for increasing the electon concentration beyond 0.20, could give rise to superconductivity of 20K-range. We show in Fig.4 the Meissner effects in three different samples, $Ln_{1.85}Ce_{0.15}CuO_{4-y}$ (Ln=Pr,Nd and Sm), which were measured by a SQUID magnetometer with applied field of 10 Oe (field-cooled). Substantial

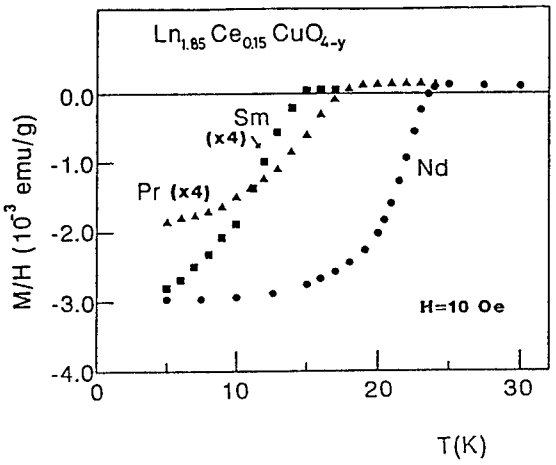

Fig.4: Meissner signals in T'-phase $Ln_{2-x}Ce_xCuO_{4-y}$ (Ln=Pr, Nd and Sm).

amount of Meissner signal was observed in a series of compounds. In particular, the large signal in $Nd_{1.85}Ce_{0.15}CuO_{3.93}$ - more than 25% of the ideal value - guarantees the bulk nature of superconductivity with T_c=24K. The observed T_c is comparably high with those in the hole-superdonducting single-layer cuprates ; T_c=28K in the T^*-phase with Cu-O pyramids and T_c=40K in the T-phase with Cu-O octahedra.

It is worth noting here that the compound $Pr_{1.85}Ce_{0.15}CuO_{4-y}$ shown in Fig.4 is the first example of Pr-based cuprate superconductors. In hole-sustaining systems, the Pr-based cuprates, for example the T^*-phase compound $Pr_{2-x-y}Ce_xSr_zCuO_{4-y}$ [5], and the so-called 1-2-3 compound $PrB_2Cu_3O_7$ [7], show neither metallic nor superconducting behavior. This has been attributed to the partial trapping of doped holes by Pr ions, or equivalently to the mixed valent nature of Pr^{+v} ions (3<v<4). The appearance of superconductivity in $Pr_{2-x}Ce_xCuO_{4-y}$ may be another evidence for the electron-nature of superconducting carriers in this T'-phase compound, because Pr^{3+} cannot be further reduced.

In conclusion, we demonstrate for the first time that electron-doping into CuO_2 sheets with no apical oxygen gives rise to superconductivity with T_c up to 24K. We believe that this discovery provides a crucial test of theories for High T_c and hopefully gives a new important clue to the mystery of High T_c.

We would like to thank Messers H.Matsubara and H.Watabe for their assistance in experiments. This work was partly supported by a grant-in-aid for special distinguished research from the Ministry of Education, Science and Culture of Japan.

REFERENCES

[1] Bedonorz,J.G. and Muller,K.A. Z.Phys. **B64**,189-194 (1986).
[2] Tokura,Y., Takagi,H. and Uchida,S. Nature (Jan.26 1989).
[3] Muller-Buschbaum,H. Angew.Chem.Int.Ed.Engl. **16**,674-687(1977).
[4] Sawa,H. et.al. Nature (in press).
[5] Tokura,Y. et.al. submitted to Phys.Rev.B.
[6] Nazzal,A.I. et.al. Physica, **153-156C**,1367-1368 (1988).
[7] Kambe,S., Kishio,K., Ooba,N., Sugii,N., Kitazawa,K., and Fueki,K. Jpn.J.Appl.Phys.Suppl. 11-14 (1988).

SPECIFIC HEAT ANOMALY NEAR Tc IN OXIDE SUPERCONDUCTORS

CHEN Zhaojia, WANG Keqing
Physics Department, University of Science and Technology of China

1.INTRODUCTION

Since high Tc oxide superconductor was discovered, more than 10(papers have been published about specific heat measurements. Because of the complicacy of ceramic structure for this kind of superconductors, the results reported are sample dependent. Nevertheless, specific heat measurements are still very important for investigation of this new material.

Besides measuring wide temperature range specific heat, we pay more attention to the specific heat anomaly in samples of different compounds, which might give us valuable informations.

2. EXPERIMENTAL

The experiments are performed by a differential calorimeter which can precisely measure the specific heat difference between two samples. For measuring the specific heat anomaly in a superconducting sample, we take a non-superconducting sample as reference sample. Let the two samples have same mass, we could assume that their lattice specific heats are equal. Therefore the specific heat difference is attributed to the transition in the superconducting sample.

This differential calorimeter has quite high sensitivity, it can measure the specific heat anomaly ΔC as little as 0.05% of total specific heat at Tc. Sample with weight of 300 mg is enough for our measurement.

3. Some interesting problems

A lot of samples have been measured so far including YBCO, BCSCO, TCBCO et al. We found some interesting problems in our experimental results.

(1) Two transitions near Tc

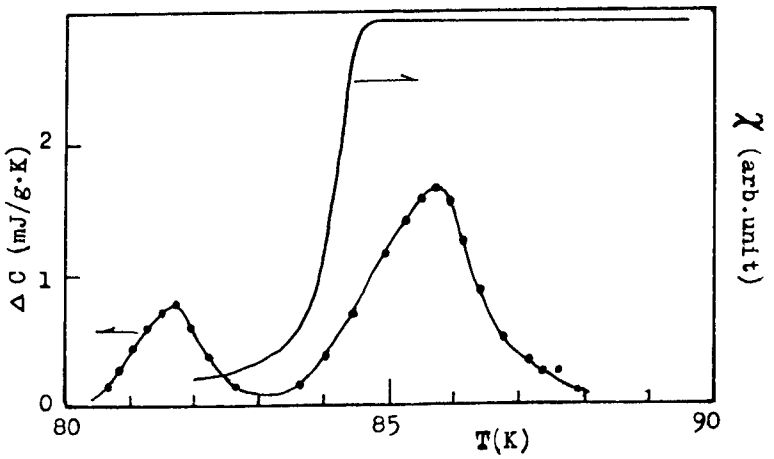

Fig.1. Specific heat anomaly near Tc in $GdBa_2Cu_3O_{7-y}$ crystal with its susceptibility curve

Recently the specific heat of $GdBa_2Cu_3O_{7-y}$ single crystal of 300 mg was measured between 80K-150K. Two well resolved specific heat peaks appeared at 81.7K and 85.2K, see Fig.1. Similar phenomena were reported by several authors. They also observed two transitions at Tc in YBCO both single crystal and single phase samples by specific heat measurements[1,2,3]. There are different explanations for the two transitions. First,it may arising from inhomogeneities in the sample. Second, two transitions are corresponding two superconducting phases. Third, among these two transitions the higher temperature one is related to structrue transition. Our experimental results support the last explanation.

A.C.susceptibility χ -T measurement has performed for the same crystal sample after specific heat experiment. There is only one sharp drop in susceptibility at 84 K, which is corresponding the lower temperature transition. It is clearly that there is only one superconducting transition near Tc.Fig.1 also shows the susceptibility curve.

Quite a few experiments in published papers have proved for oxide superconductors that there are structure change and related anomalous properties appearing befor superconducting transition, including cell parameters of orthorhombic YBCO [4] or Bismuth based superconductor [5], ultrasonic velocity [6], thermal expansion of $GdBa_2Cu_3O_{7-y}$ [7], internal friction [8], positron annihilation [9] et al. According to the above phenomena, we suggest some kind of relation between superconductivity and micro-structure change existing in oxide superconductors.

(2) Cusp or hump shape for the specific heat anomaly curves

In the earlier stage the typical specific heat-temperature curve near Tc for YBCO samples has hump shape, see Fig.2. As sample preparation techniques have improved, the specific heat anomaly at Tc have become increasingly sharper.

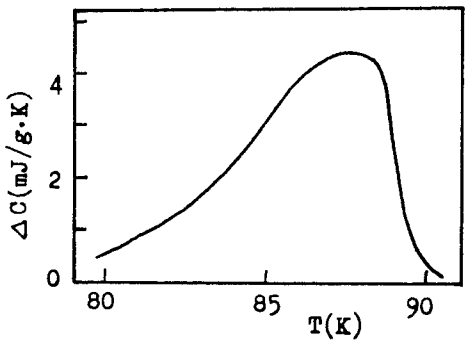

Fig.2. The specific heat anomaly Δ C-T near Tc for one of our earlier YBCO (123) samples

We noticed that for BCSCO system, the Pb doped sample has always cusp shape specific heat anomaly, although the value Δ C is usualy much smaller than that of YBCO samples. see Fig.3.

Hump shape anomaly means inhomogeneties in the sample, different parts of a sample may have different Oxygen concentration which causes superconducting Tc spreading over a temperature range. Therefore we could think the cusp shape Δ C for BCSCO may be explained that Oxygen concentration is not sensitive for this system, which is easier to get homogeneious in the sence of superconductivity.

(3) Compare Δ C(Tc) with a.c. χ -T and R-T curves near Tc

To determine the superconducting transition in a sample,several kinds of measurements can be applied. They give different informations for the same sample.

Zero resistance shows that superconducting path has formed in a sample, some times there are only filaments which connect to each other though two ends of the sample. That is why R-T measurement can not distinguish between bulk and filamentary superconcuctivity.

A.C.susceptibility measurement could show more than one superconducting phases, which appear at differnt temperitures, but it may only be shielding effect by a part of superconducting phase existing in the measured sample.

Specific heat measurement reveals real bulk superconductivity, it might in some sense be better than meissner effect experiment.

Two Pb doped BCSCO samples was investigated. Sample A was prepared by solid state reaction followed by furnace cooling, its nominal composition was $Bi_{1.6}Pb_{0.4}Sr_2Ca_2Cu_3O_y$. Sample B was made by cast-annealing mathod, the composition was $Bi_{1.7}Pb_{0.3}Sr_2Ca_2Cu_{4.5}O_y$.

Fig.3a and 3b show the Δ C, γ-T and R-T results near Tc for sample A and sample B respectively. The R-T curves for these two samples are same, they have equal zero resistance temperature of 107 K. The γ-T curve of sample A shows two drops at 107K and 102K, it is similar to that of sample B. Both of R-T and γ-T measurements can not tell the difference between sample A and B. But Δ C-T for the two samples are quite different. For

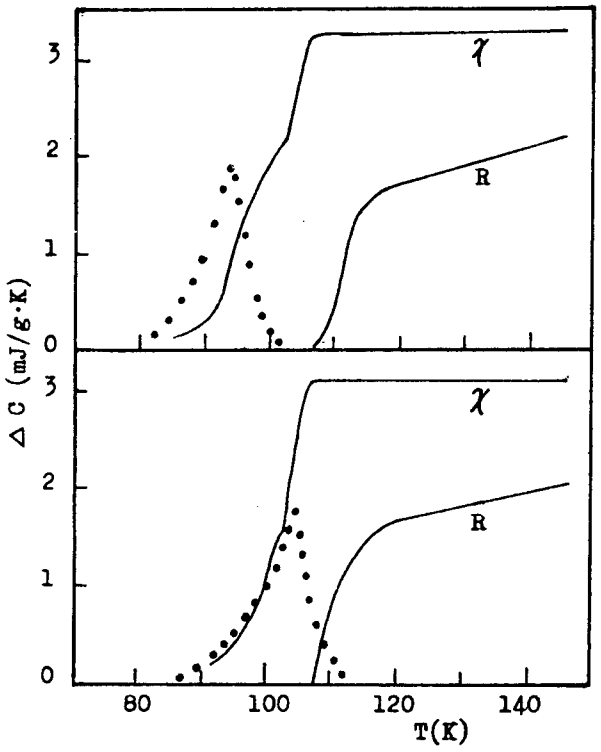

a. $Bi_{1.6}Pb_{0.4}Sr_2Ca_2Cu_3O_y$ made by solid state reaction

b. $Bi_{1.7}Pb_{0.3}Sr_2Ca_2Cu_{4.5}O_y$ made by cast-annealing method

Fig.3. The specific heat experimental resulta with γ-T, R-T curves for Pb doped Bismuth based samples.

sample A, ΔC begins to appear at the temperature just below 107K, the biggest anomaly is at 92K. In contrast with it, sample B has the specific heat anomaly peak at 103K, much higher than 92K. It is clear that the cast-annealed sample has bulk superconductivity at much higher temperature than solid state reaction sample although their zero resistence temperature are exactly same. The dH_{c2}/dT near Tc and magnetization curve have been measured for cast sample B in our laboratory, It shows bigger dH_{c2}/dT value and stronger pinning force than other samples by solid state reaction. Furthermore the mass density of cast sample is about 20% bigger, perhaps the cast-annealing method has good prospect for high critical current superconcuctor.

REFERENCES

1. R.A.Butera, Physical Review B, 37 (1988) 5909
2. M.Ishikawa, Y.Nakazawa, T.Takabatake, A.Kishi, R.Kato,and A.Maesono, Solid State Communications, 66 (1988) 201
3. T.C.Choy, Hong-Xing He and M.P.Das, submitted to Physical Revew Lett.
4. Yin Hua-ging, Gao Yi-mei, Du Jia-ji, Appl.Phys.Lett. (1988)
5. S.L.Yuan, W.Y.Guan, Z.J.Chen, Y.L.Huagn, Y.B.Jia, J.Q.Zheng,B.Zhu, W.Wang and G.G.Zheng, to appear in Physica C
6. D.J.Bishop, A.P.Ramirez, P.L.Gammel, B.Batlogge, E.A.Rietman, R.J.Cava, and A.J.Mills, Phys.Rev.B 36(1987) 2048
7. K.Kadowaki, F.E.Kayzel and J.J.M.Franse, Physica C153-155(1988) 1028
8. Du Jia-ju, Jiang jian-yi, Wang Xiang, Yin Hua-qing, ACTA PHYSICA SINICA, 37 (1988)1559
9. Zhu Jing-sheng,Song Jian-xian,Wang Jun,Yang Zhong-jin, Zhang Yu-heng, C.W.Lung, J.Phys.C, 21 (1988) L128

TRANSPORT STUDIES OF METALLIC LANTHANUM CUPRATES

Yasuhiro IYE
Institute for Solid State Physics, University of Tokyo,
7-22-1 Roppongi, Minato-ku, Tokyo 106, Japan

1. INTRODUCTION

Despite the worldwide intensive research efforts towards its elucidation, the basic mechanism for the high temperature superconductivity in copper oxide systems has so far eluded our grasp. Given the difficulty encountered in a frontal attack on the high T_c materials, it seems a good strategy to try approaches from different angles. One useful method is to apply high pressure and see how it affects the electronic state and superconductivity of a particular material. Another is to study the electronic properties of materials with closely related structures in an attempt to extract common features. We focus in this paper on the La-Sr-Cu-O systems which occur in a variety of chemical compositions and crystal structures, some of which are high termperature superconductors and others are normal metals.

2. PRESSURE STUDY ON $(La_{1-x}Sr_x)_2CuO_4$

It has been known from the early stage of high T_c research that pressure causes an unusually large enhancement of T_c in $(La_{1-x}Sr_x)_2CuO_4$. [1, 2] Also established is the fact that T_c of $(La_{1-x}Sr_x)_2CuO_4$ has a maximum as a function of the strontium content x. [3, 4] As x is increased from zero, an insulator-to-metal transition sets in at $x\sim0.025$ and a finite T_c appears there. The value of T_c increases with x and attains a maximum of ~40 K at $x\sim0.08$ and then decreases as x is further increased, until it vanishes at $x\sim0.15$. It has been argued that the electronic state in the high T_c range of x is dominated by electron correlation, while that in the higher x region is more like an ordinary Fermi liquid. In order to gain more insight into this issue, we have carried out a systematic study of pressure effect on carrier concentration and T_c in $(La_{1-x}Sr_x)_2CuO_4$. Of our particular interest is the comparison between the two regions of x, in one of which T_c increases with carrier concentration, while it decreases in the other.

Figure 1 shows the pressure dependence of the Hall coefficient R_H of five samples of $(La_{1-x}Sr_x)_2CuO_4$. It is seen that the Hall coefficient shows virtually no change up to the highest pressure of the present work. The figure on the right side demonstrates an excellent agreement of the present data of R_H as a function of x, with those reported by Takagi et al. [4] [A small systematic upward deviation of our data from Takagi et al.'s is due to difference in temperature between our (60K) and their (80K) experiments.]

Figure 2 illustrates change in the resistively observed superconducting transition with pressure. It is commonly observed that the onset point defined as shown in the figure increases most dramatically with pressure. The pressure dependence of the midpoint is similar but smaller in magnitude. The pressure dependence of the zero resistance point is found to vary even qualitatively from sample to sample, and is probably governed by the intergrain coupling rather than more intrinsic properties. We therefore plot in Fig. 3 the onset T_c as a function of pressure. The pressure independence of the Hall coefficient shown in Fig. 1 rules out a change in the carrier concentration as an origin of this pressure induced enhancement of T_c.

A remarkable feature apparent in Fig. 3 is that the pressure coefficient dT_c/dp is almost the same for all the five samples. This means that the relative pressure coefficient $d\log T_c/dp$ (or more fundamental quantity — $d\log T_c/d\log V$) is smaller for a higher T_c material. Such trend is generally observed among the high T_c oxides[5,6]. What we note here is that two compounds (for example x=0.06 and 0.10) having the same T_c have very similar pressure coefficients (dT_c/dp or $d\log T_c/dp$). This presents a test discriminating among theoretical models for the mechanism of high temperature superconductivity. In particular, an attempt to explain the shape of the T_c vs x curve in terms of a competition between two completely different causes, would encounter a rather serious difficulty.

In connection with the proposed magnetic mechanism for the high temperature superconductivity, it would be of great interest to investigate the pressure dependence of the exchange coupling J, by studying, for example, the two-magnon scattering under pressure, and to correlate it with the pressure dependence of T_c. We point out here that the compressibilities of $(La_{1-x}Sr_x)_2CuO_4$ and $YBa_2Cu_3O_{7-\delta}$ are quite comparable.[7] If the exchange coupling J is a smooth function of the interatomic distance in the present range of interest, it seems rather difficult to explain the widely different pressure dependence of T_c among the high T_c oxides, notably between $(La_{1-x}Sr_x)_2CuO_4$ and $YBa_2Cu_3O_{7-\delta}$. For a theoretical model for the mechanism of high temperature superconductivity to be valid, it should successfully explain the general trend of the pressure dependence of T_c.

3. HIGH T_c OXIDES VIEWED AS INTERCALATED SYSTEMS

Figure 4 illustrates basic structures of layered perovskites, which are composed of corner-sharing CuO_6 octahedrons, and occur in a series of structures with different number of CuO layers, n, forming the unit. The n=1 structure is the K_2NiF_4 type, n=2 corresponds to the $Sr_3Ti_2O_7$ structure and n=∞ to the cubic perovskite $LaCuO_3$. The chemical formulae for the ideal structures illustrated in Fig. 4 are $A_{n+1}B_nO_{3n+1}$, where B is copper.

The crystal structures of all the high T_c cuprates known to date can be viewed as derivatives of these basic structures. Let us see this by taking the double-CuO-layer (n=2) compounds as an example. Figure 5 illustrates the derivation of the high T_c double CuO layer structure from the basic $La_3Cu_2O_7$ structure. The "basic layer unit" of the high T_c cuprates is constructed in the following way:

(1)Replace the La ions in the middle plane by smaller Y (or Ca) ions.
(2)Remove oxygen ions from the middle plane, and thereby change the CuO_6 octahedrons into CuO_5 pyramids.
(3)Replace the La ions in the outer planes by Ba (or Sr) ions.

The layered material thus created is composed of the Ba(Sr)O-CuO_2-Y(Ca)-CuO_2-Ba(Sr)O basic units.

The high T_c materials can then be viewed as "intercalation compounds" based on the hypothetical "host materials" constructed above. Figure 5 summarizes the currently known double-CuO-layer high T_c materials viewed in this way. The intercalate layers are, CuO chain layer (for $YBa_2Cu_3O_{7-\delta}$), Bi_2O_2 double layer ($Bi_2Sr_2CaCu_2O_{8+y}$), TlO single layer ($TlBa_2CaCu_2O_{7+y}$), Tl_2O_2 double layer ($Tl_2Ba_2CaCu_2O_{8+y}$), and PbO-Cu-PbO layer ($Pb_2Sr_2YCu_3O_{8+y}$). Similar schemes can be also drawn for the single copper layer compounds [$(La_{1-x}Sr_x)_2CuO_4$, $Bi_2Sr_2CuO_{6+y}$, $Tl_2Ba_2CuO_{6+y}$, and $TlBa_2CuO_{5+y}$], and for the triple copper layer compounds [$Bi_2Sr_2Ca_2Cu_3O_{10+y}$, $Tl_2Ba_2Ca_2Cu_3O_{10+y}$, and

$TlBa_2Ca_2Cu_3O_{9+y}$]. It is noteworthy that the T_c's are in the range of 10-60 K for the singel-CuO-layer compounds, 70-100 K for the double layer compounds, and 100-125 K for the triple layer compounds. Such systematics suggests that the "host layers" are principaly responsible for the high temperature superconductivity. The primary role of the "intercalate layers" may be to supply carriers to the "host layers" by charge transfer without introducing disorder into the current carrying "host layers".

4. NON-SUPERCONDUCTING LANTHANUM CUPRATES

In the above context, it is interesting to study $La_2SrCu_2O_6$ (and $La_2CaCu_2O_6$) having double CuO layers but no "intercalate layers". The leftmost figure of Fig. 6 shows the structure of $La_2SrCu_2O_6$. Another class of materials of interest are the three dimensional compounds derived from the cubic perovskite structure. The middle and the rightmost figures of Fig. 6 are the structures of $La_4BaCu_5O_{13-y}$ and $La_{8-x}Sr_xCu_8O_{20-y}$. The former compound had been studied by Raveau's group[8] even before the Bednorz and Mueller's discovery of high temperature superconductivity in the $(La_{1-x}Ba_x)_2CuO_4$ system. The latter system was identified more recently by Michel et al.[9] and by Torrance et al.[10]

Figure 7 shows the temperature dependences of the resistivity and the Hall coefficient of $La_{1.9}Ca_{1.1}Cu_2O_{6+y}$ and $La_{1.9}Sr_{1.1}Cu_2O_{6+y}$. The Hall coefficient is positive for these compounds. The carrier density strongly depends on y. In the case of $La_{1.9}Ca_{1.1}Cu_2O_{6+y}$, it is difficult to increase the oxygen content much higher than 6. The hole density is thus generally low. For the sample of Fig. 7, $n_h \sim 5 \times 10^{20} cm^{-3}$. The temperature dependence of the resistivity of this sample is fitted to a variable range hopping type formula.

In the case of $La_{1.9}Sr_{1.1}Cu_2O_{6+y}$, the oxygen content can be made substantially higher than 6 by low temperature annealing. For the sample shown in Fig. 7, chemical analysis gives $y \sim 0.25$. The carrier concentration derived form the Hall coefficient is $n_h \sim 1.6 \times 10^{22}$ cm^{-3}. This is considerably larger than the chemically estimated hole concentration $n^h \sim 4 \times 10^{21}$ cm^{-3} and suggests that more than one type of carriers contribute to transport. The resistivity behavior is more metallic than $La_2CaCu_2O_6$, but shows a behavior at low temperatures which can be interpreted as the weak localization effect. Magnetoresistance measurements at low temperature have revealed the negative magnetoresistance effect characteristic of a weakly localized system. Superconductivity is not found at temperatures higher than 0.3 K.

As seen above, the transport properties of $La_2CaCu_2O_6$ and $La_2SrCu_2O_6$ are strongly influenced by inherent disorder. Since these compounds have no "intercalate layers", oxygen atoms have to be doped in the Sr (or Ca) plane. Consequently, creation of charge carrier inevitably introduces disorder in the conducting layers. Whether this is the only reason for the absence of high temperature superconductivity in these compounds is not clear. But it is certainly a detrimental factor.

Figure 8 shows the temperature dependence of the resistivities of a series of $La_{8-x}Sr_xCu_8O_{20-y}$ samples with different x. The broad anomalies seen in the resistivity curves for x=1.47 and 1.60 is accompanied by change in the carrier density as estimated from the Hall coefficient. It is probably associated with a certain type of Fermi surface instability such as spin density wave. Its exact nature, however, is to be elcuidated by further studies. Unlike the high T_c materials, the sign of the Hall coefficient is negative. The resis-

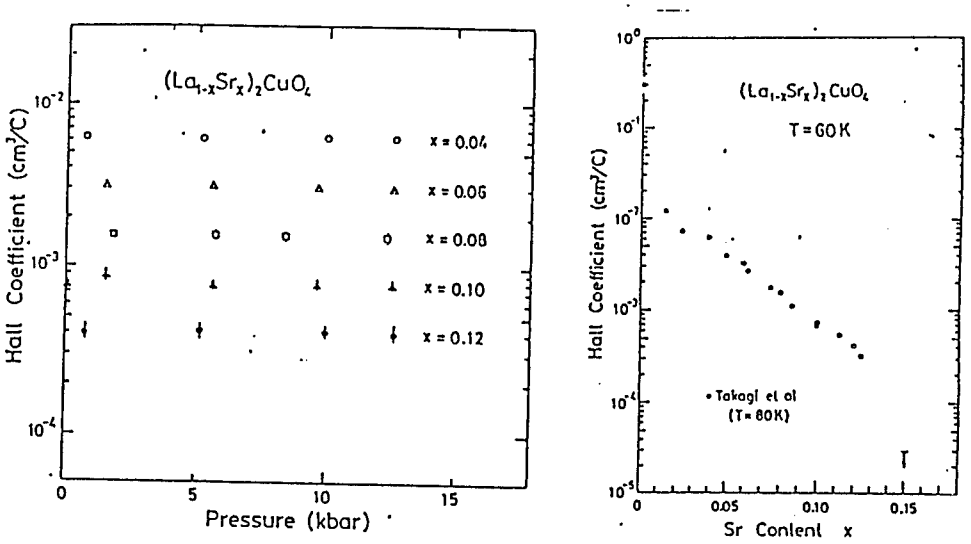

Fig. 1 The pressure dependence of the Hall coefficient for $(La_{1-x}Sr_x)_2CuO_4$ samples with different x. The figure on the right shows the Hall coefficient as a function of x, in comparison with the data of Takagi et al. [4]

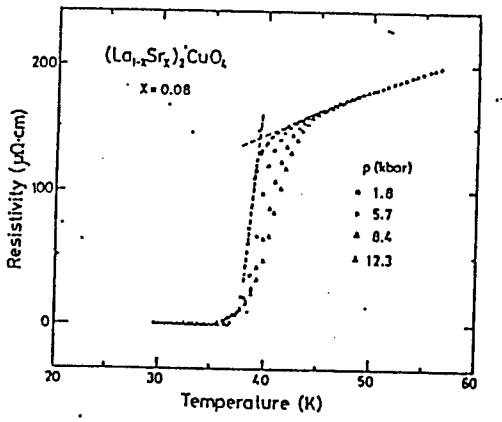

Fig. 2 Pressure dependece of the resistively observed superconducting transition in $(La_{1-x}Sr_x)_2CuO_4$ (x=0.08): The definition of the T_c (onset) is indicated in the figure.

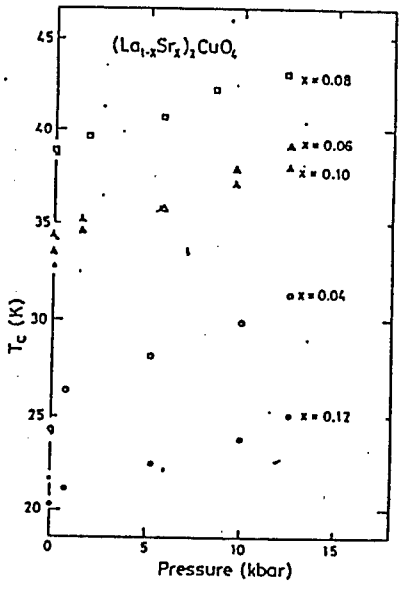

Fig. 3 Pressure dependence of T_c (onset) for $(La_{1-x}Sr_x)_2CuO_4$. Note that the pressure dependence is similar for all samples.

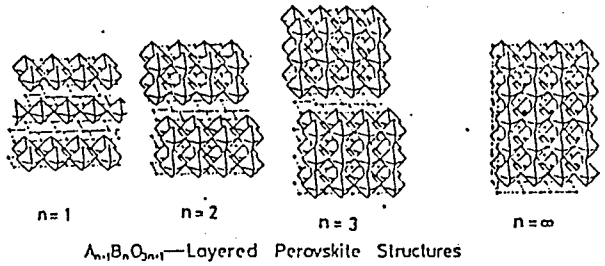

Fig. 4 Structures of layered perovskites, $A_{n+1}B_nO_{3n+1}$.

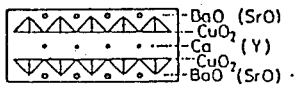

Fig. 5 Structures of the double-CuO-layer high T_c oxides viewed as intercalated systems.

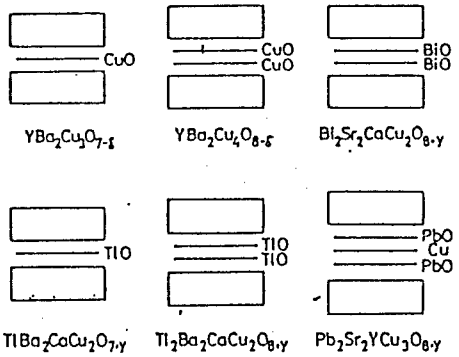

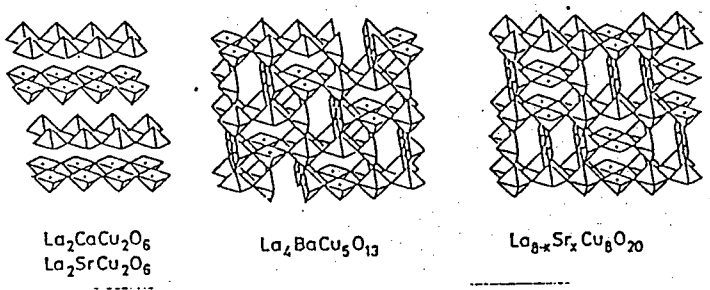

Fig. 6 Crystal structures of $La_2SrCu_2O_6$, $La_4BaCu_5O_{13-y}$ and $La_{8-x}Sr_xCu_8O_{20-y}$.

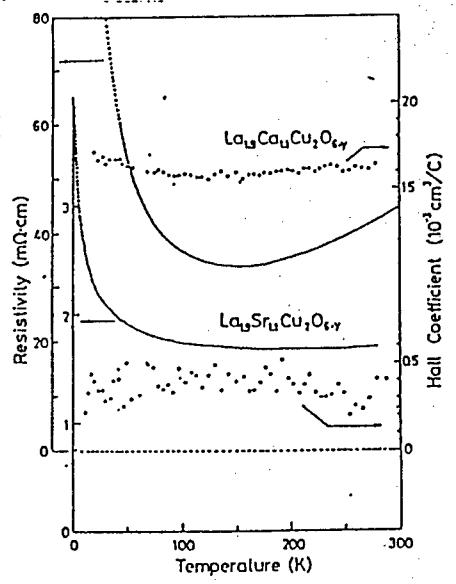

Fig. 7 Resistivity and Hall coefficient of $La_{1.9}Ca_{1.1}Cu_2O_{6+y}$ and $La_{1.9}Sr_{1.1}Cu_2O_{6+y}$.

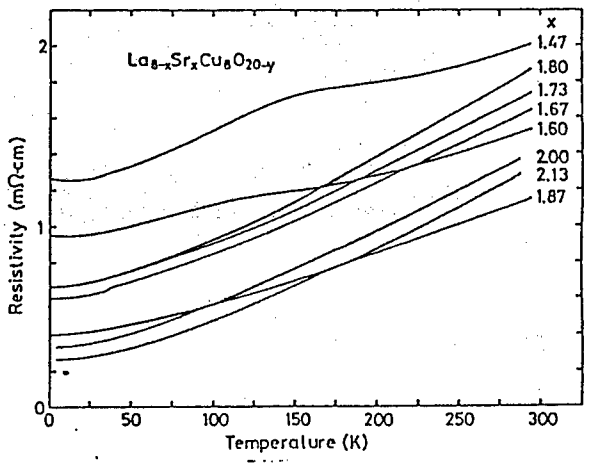

Fig. 8 Resistivities of $La_{8-x}Sr_xCu_8O_{20-y}$ with different values of x.

tivity shows a temperature dependence which look very much like an ordinary metal. The negative Hall coefficient and normal metallic resistivity behavior are also seen in the $La_4BaCu_5O_{13-y}$ system.

The absence of high temperature superconductivity in $La_4BaCu_5O_{13-y}$ or $La_{8-x}Sr_xCu_8O_{20-y}$ may be attributed to their "normal metallic" character. These compounds may be classified in a group similar to $(La_{1-x}Sr_x)_2CuO_4$ with $x > 0.15$, which have "too many carriers" for high temperature superconductivity. Whether the three dimensional nature is relevant to the absence of superconductivity in these compounds should be addressed in future studies.

Acknowledgements

Samples of $(La_{1-x}Sr_x)_2CuO_4$ used in the pressure experiment were kindly supplied by N. Okazaki and K. Kitazawa. This work is supported by Grant-in-Aid for Scientific Research on Priority Areas "Mechanism of Superconductivity", from the Ministry of Education, Science and Culture, Japan.

REFERENCES

[1] C. W. Chu, P. H. Hor, R. L. Meng, L. Gao, Z. J. Huang and Y. Q. Wang, Phys. Rev. Lett. 58 (1987) 405.
[2] S. Yomo, C. Murayama, H. Takahashi, N. Mori, K. Kishio, K. Kitazawa and K. Fueki, Jpn. J. Appl. Phys. 26 (1987) L603.
[3] J. B. Torrance, Y. Tokura, A. I. Nazzal, A. Bezinge, T. C. Huang and S. S. P. Parkin, Phys. Rev. Lett. 61 (1988) 1127.
[4] H. Takagi, Y. Tokura and S. Uchida, to apper in "Mechanisms of High-Temperature Superconductivity", ed. by H. Kamimura and A. Oshiyama (Springer, 1989).
[5] R. Griessen, Phys. Rev. B36 (1987) 5284.
[6] C. Murayama, N. Mori and S. Yomo, preprint.
[7] H. Takahashi, C. Murayama, S. Yomo, N. Mori, W. Utsumi and T. Yagi, Jpn. J. Appl. Phys. 26 (1987) Suppl 26-3, p. 1109.
[8] C. Michel and B. Raveau, Rev. Chim. Miner. 21 (1984) 407.
[9] C. Michel, L. Er-Rakho, M. Hervieu, J. Pennetier, and B. Raveau, J. Solid State Chem. 68 (1987) 143.; C. Michel, L. Er-Rakho, and B. Raveau, J. Phys. Chem. Solids 49 (1988) 451.
[10] J. B. Torrance , Y. Tokura, A. Nazzal, and S. S. P. Parkin, Phys. Rev. Lett. 60 (1988) 542.

THE BEHAVIOR OF OXYGEN AND ITS DEFECTS IN YBCO

XIE Leiming and WU Suhui
Shanghai Institute of Metallurgy, Academia Sinica
Shanghai 200050, China

1. INTRODUCTION

Since the discovery of high T_c oxide superconductors many efforts have been made to understand the role the oxygen and/or its defects may play in the superconductivity and to control their behavior during fabrication. Apart from their similarities between high T_c oxides, the orthorombic $YBa_2Cu_3O_x$ phase has an odd CuO_3 chain. It is well known that by quenching from various temperature oxygen content of $YBa_2Cu_3O_x$ can be change accordingly. It is also recognized that most of the oxygen is coming in or out from the chain, and it can cause orthorhombic to tetragonal phase transition and makes the superconductor a semiconductor. By annealing in oxygen or air the process can be reversed.

In this report we shall review some of the investigations done in our high T_c group, concerning oxygen and its defects in the above mention material.

2. EXPERIMENTAL

The $YBa_2Cu_3O_x$ samples were prepared by conventional powder-sintering techniques. Powder with atomic ratio of Y:Ba:Cu=1:2:3 was prepared by co-deposition of nitrate solution. It was calcined at 850°C and compressed into 50×5×2 mm bar specimens. Sintering was done at 930°C for 18 hrs followed by furnace cooling. Specimens were annealed in air at different temperature (T_A) ranging from 400 to 940°C for 10 hrs, then water quenched under the protection of a quartz sheath.

Standard four-probe method was used to measure the temperature dependence of the resistivity.

Internal friction (IF) was measured at 1 Hz. on an automatic inverted torsional pendulum of Ke type.

KBr pellet method and a Fourier-transform IR Spectrometer was used for the infrared measurements. It covers the range of $4900cm^{-1}\sim400cm^{-1}$. For spectrum lower than $400cm^{-1}$ a Perkin-Elmer 577 grating IR spectrophotometer was also used.

The weight measurements were carried out on a NETZSCH simultaneous thermogravimetry between room temperature and 800°C.

3. RESULTS AND DISCUSSIONS

(1) Internal Friction Spectroscopy has a very sensitive response to external periodic stress acting on microscopic defects in solids. These defects are on an atomic levels, such as point defects of substitutes, vacancies and interstitials and line defects as dislocations. If a point defect has elastic dipole moments, oriented in a certain direction, and an external stress try to force the dipole to point to a different direc-

tion, then thermal excitation will cause the dipole to overcome a barrier and relax to the new direction. At a definite temperature this relaxation rate resonate with the external stress period. And this will give a peak in the IF spectrum. The peak temperature together with the peak height which is proportional to the number of defects is two quantities characterizing the process.

T.G. Chen et al [1] and X.M. Xie et al [2] studied the $YBa_2Cu_3O_x$ compound by the IF method. They found an IF peak at 204°C and the height of the peak increases rapidly with increasing annealing and quenching temperature, at the same time the peak temperature is also shifted a little bit towards the high temperature side. Fig.1a shows a typical IF curve measured from a specimen annealed at and quenched from 400°C. Fig.1b shows the maximum peak height of the 204°C IF peak vs. quench temperature. The activation energy of this peak is determined by the frequency response of the peak temperature displacement [3] and was found to be 1.026eV.

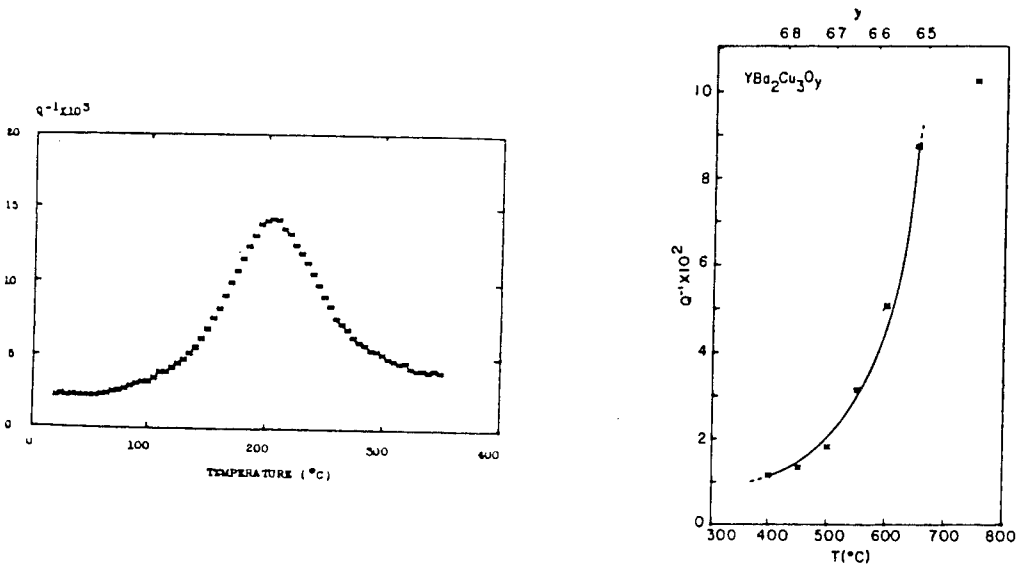

Fig.1 (a) Internal friction curve quench from 400°C.
(b) Max. height of IF peak vs. quench temperature.

The sample producing this IF curve (Fig.1a) has oxygen content y≈6.8 [2], XRD analysis shows that it is an orthorhombic phase. Annealed and quenched at successively higher temperature, y decreases and XRD shows orthorhombic to tetragonal phase transition [4]. IF measured in this sequence give a successively higher peaks. That is to say less oxygen content higher the peak. Why? Chen et al [5] based on the distribution of oxygen atoms and its vacancies in the $YBa_2Cu_3O_y$ structure observed by neutron diffraction [4], suggest that the peak is caused by the oxygen atoms in the CuO_3 chain lying between the two Ba layers lining in the b-axes of the orthorhombic phase jumping from O1 (B site) to O5 (A site) and vice versa, shown in [5]. In order to answer the question why above, they proposed that not all B site oxygen ions can jump into the neighboring A site, only when there are additional B site vacancies along <110> near the A site the B site oxygen ion is allowed to jump into that particular A site. Fig.2 shows schematically the configurations picked out from the Cu-O plan

between the two Ba layers. The A site is at the center of each configuration. (1) to (6) indicate that A sites are vacant and (7) to (12) A sites are occupied. But in (7), (8) and (10) A sites have a rather higher potential compared with other A sites, so around IF measuring temperature they can be regard as forbidden sites. And this higher potential for occupation is a consequence of some degrees of covalent nature exist in the Cu-O bonds.

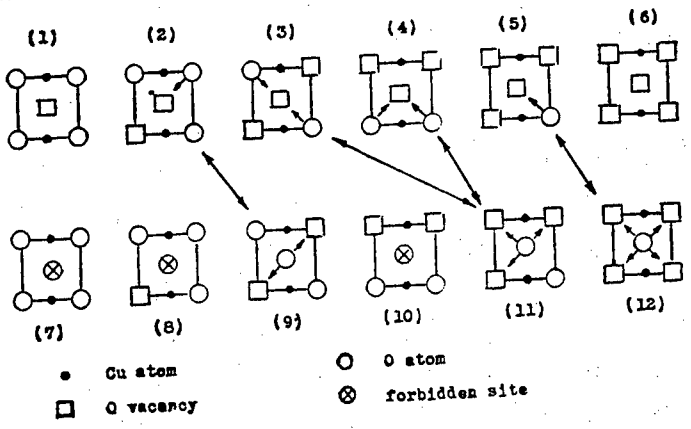

Fig.2 Possible configurations in the Cu-O plan between two Ba layers.

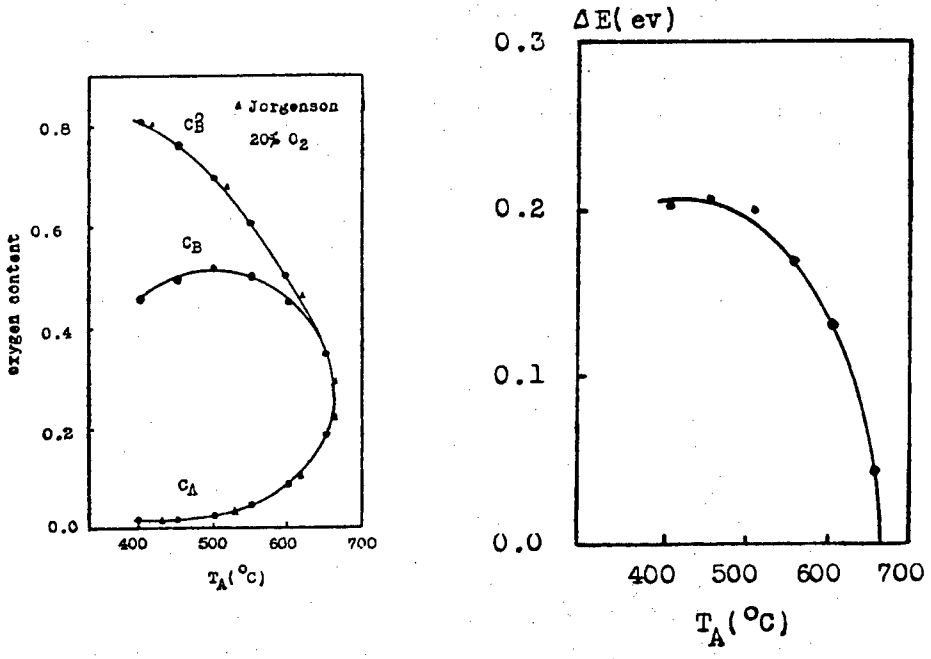

Fig.3 (a) Oxygen site occupation vs. quenching temperature.
(b) The potential difference between B and A sites vs. quenching temperature.

By using statistical mechanics Chen et al [5] derived C_A and C_B as a function of y, the oxygen content, which in turn related to the quenching temperature. Here C_A is the density of A site occupation and C_B is the B site density of those oxygen ions which are capable of jumping. C_B^o is the

total B site occupation density. Fig.3a shows the variations of these density versus quenching temperature, and it also shows that the occupation data agree very good with that of Jorgenson's [4]. The potential difference ΔE between B site and A site at different oxygen content, or quenching temperature T_A, can be derived from $\Delta E=kT_A\ln(C_B/C_A)$. This is shown in Fig.3b. It has a character of order parameter indicating the transformation from tetragonal to orthorhombic phase.

The diffusion coefficient of oxygen in the orthorhombic phase can be expressed as $D=1.80\times10^{-4}\exp(-1.23eV/kT)(cm^2/s)$ in the temperature range from 400 to 550°C. The result shows that the oxygen diffusion rate in this phase is very slow. The apparent high diffusivity is caused by the porosity in the bulk material.

(2) Infrared absorption spectroscopy has been used to investigate annealing and quenching behavior of oxygen in YBCO system [6,7,8]. Fig.4 shows the absorption spectrum of a series quenching temperature. T.S.Shi et al [7] noticed that there were three absorption peaks which could be clearly identified. P_1 around 620 to 640cm^{-1}, P_2 590cm^{-1} and P_3 550~580cm^{-1}. Coincidence of their frequencies (≈600cm^{-1}) with the known Cu-O stretching vibration mode (609cm^{-1}) [9] implies that they originate from the stretching vibration of Cu-O bonds in $YBa_2Cu_3O_x$. They assigned these peaks, after group theoretical consideration, to three crystallographic nonequivalent oxygen ions in the unit cell: P_1 was assigned to the asymmetrical vibration of the Cu-O bond in the one-dimensional Cu-O chain along the b-axis, and P_2 to the asymmetrical vibration of the Cu-O bond in the two-dimensional puckered Cu-O network between Y and Ba layers. In order to explain some features in the spectrums, P_1 and P_2 were characterized as resonance mode induced by oxygen vacancies which may change the force constant of the Cu-O bond next to it. P_3 was assigned to the

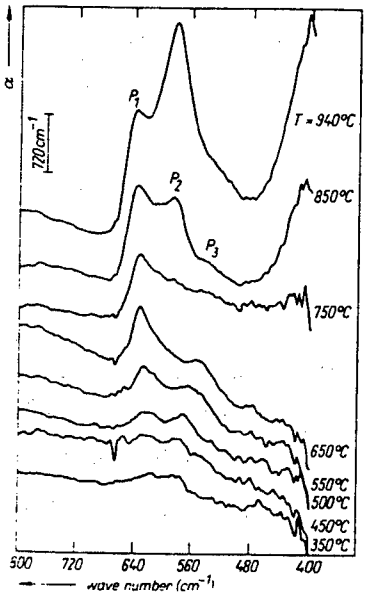

Fig.4 The IR spectra of $YBa_2Cu_3O_x$ air-annealed at various temperatures for 10h, followed by rapid cooling in ice water.

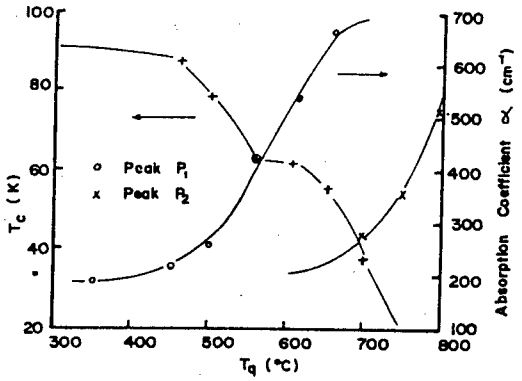

Fig.5 Variation of the peak intensities and T_c with quenching temperature (oxygen content).

asymmetrical vibration of the Cu-O bond, perpendicular to the one-dimensional chain along the C-axis. Since this bond is very stable against heat treatment the peak should be also stable during annealing and quenching, and it was actually the case.

J.M. Chen et al [10] had made a detail observation on P_1, and found that it really consists of two peaks, which are identified as P_1' and P_1''. P_1' is assigned to the vibration of A site oxygen ions in a more or less localized mode and P_1'' to the vibration of B site oxygen ions in a resonance mode as before.

Y.G. Zhao et al [11] noticed that the frequencies of P_1 and P_3 shift monotonically with change of oxygen content y in $YBa_2Cu_3O_y$ and suggested that this could be used to estimate the oxygen content in YBCO powder during fabrication processes.

Since P_1 and P_2 had been related to the oxygen vacancies in the 1D chain and 2D network respectively and there must be some relation exist between the superconductivity of the crystal and the perfection of the chain and network. Zhao et al [12] claimed that there should have direct relationship between the intensity of P_1 and P_2 with the behavior of the superconductivity. By showing Fig.5, Zhao argued that when the chain and the network are perfect the crystal has $T_c \geq 90K$, when P_1 rises, indicating the destruction of the chain, T_c drop to 60K which is maintained by the 2D network, and when P_3 begin to rise indicating the destruction of the 2D network, the substance becomes nonsuperconducting.

4. CONCLUSIONS

Internal friction technique and infrared absorption spectroscopy have been used to study the oxygen and its defects in the YBCO system, and it was proved that both of these method can be applied to other oxide superconducting materials, e.g. Bi-Sr-Ca-Cu system [13].

REFERENCES

[1] T.G. Chen, J.H. Zhang, J. Huang, Y. Chen, M.J. Yang, X.M. Xie, T.W. Li and L.M. Xie, Chinese Phys. Letters. 5, 185 (1988).

[2] X.M. Xie, T.G. Chen and J. Huang, Phys. Stat. Sol. (a) to be published.

[3] A.S. Nowick and B.S. Berry, Anelastic Relaxation in Crystalline Solid (Acad. Press, New York and London) 1972.

[4] J.D. Jorgenson, M.A. Beno, D.G. Grace, I.K. Schuller, C.U. Segre, K. Zhang and M.S. Kleefisch, Phys. Rev. B36, 3608 (1987).

[5] T.G. Chen, X.M. Xie, Y. Chen and L.M. Xie, Proc. 2nd Nat. Conf. High-T_c Superconductors. April 1988, Bao Ji (China) p.196.

[6] M. Stavola, D.M. Krol, W. Weber, S.A. Sunshine, A. Jayaraman, G.A. Kourouklis, R.J. Cava, and F.A. Rietman, Phys. REv. B36, 850 (1987).

[7] T.S. Shi, Y.G. Zhao, P.X. Cai, H.F. Gu, and L.M. Xie, Phys. Stat. Sol. (b) 148, 715 (1988).

[8] J.M. Chen, P.X. Cai, Y.G. Zhao, M.W. Qi, G.R. Bai, and L.M. Xie, Chinese Phys. Lett. 4, 537 (1987).

[9] M.O'Keeffe, J. Chem. Phys. 39, 1789 (1963).

[10] J.M. Chen, Y.G. Zhao, X.A. zhao, and L.M. Xie, Chin. J. Infrared Res. (to be published).
[11] Y.G. Zhao, T.S. Shi, W.F. Gu, P.X. Cai, Y.X. Fu, and L.M. Xie, Chin. J. Infrared Res. 7A, 315 (1988).
[12] Y.G. Zhao, L.M. Xie, J.M. Chen, T.S. Shi, L. Wang, and Y. Peng, Solid State Communications, 68, 847 (1988).
[13] Y.G. Zhao, L.M. Xie, E.Y. Zhou, T.S. Shi, M.Y. Wu, and S.H. Hu, Solid State Communications. (to be published).

ULTRASONIC AND TRANSPORT STUDIES OF HIGH T_c SUPERCONDUCTORS

Shoichi MASE and Yuuji HORIE
Department of Physics, Kyushu University, Fukuoka 812, Japan

1. INTRODUCTION

Since Bednorz and Müller [1] found the oxide superconductor $(La_{1-x}Ba_x)_2CuO_4$ with the superconducting transition temperature $T_c \sim 30$ K, a great deal of studies has been made for understanding high T_c superconductors. The isotope effect [2], $T_c \propto M^{-\alpha}$, shows that $\alpha \lesssim 0.22$ for $BaPb_{1-x}Bi_xO_3$ (BPBO: $T_c \sim 14$ K for $x \sim 0.25$), $\alpha \sim 0.17$ for $(La_{1-x}Sr_x)_2CuO_4$ (LSCO: $T_c \sim 40$ K for $x \sim 0.07$) and $\alpha \sim 0$-0.05 for $YBa_2Cu_3O_{7-\delta}$ (YBCO: $T_c \lesssim 92$ K for $\delta \sim 0.1$). Thus it is found that the T_c being higher, the electron-phonon interaction seems to become less important. Based on this fact and other magnetic properties near the metal-insulator transition region of these oxide superconductors, a quite new non-phonon mechanism of high T_c superconductivity named as the RVB model was proposed by Anderson [3]. However, the origin of the high T_c superconductivity is still not yet settled. The crystal structures of both LSCO and YBCO have the characteristic that some of a-b planes are covered with the networks of coplanar CuO_2. On the other hand, for the former the conventional BCS mechanism must be partly operative, while for the latter it is not so. Therefore, it may be worthwhile to make a comparative study of the oxides superconductors, LSCO and YBCO.

2. EXPERIMENTAL

2.1 Anomalies in Sound Velocity

(a) Theoretical consideration

Let us denote the discontinuities in the compressibility, the volume expansion coefficient and the heat capacity as $\Delta\kappa$, $\Delta\beta$ and ΔC_p, respectively. Ehrenfest gave important results:

$$\Delta\kappa = (1/VT_c)(dT_c/dp)^2\Delta C_p, \tag{1}$$

$$\Delta\beta = (1/VT_c)(dT_c/dp)\Delta C_p . \tag{2}$$

Equation (1) is rewritten in terms of the discontinuity in the sound velocity $V_s(T)$. The sound velocity is given by

$$V_s = (B/\rho)^{1/2}, \tag{3}$$

where B is the bulk modulus and ρ is the mass density of the lattice. Using the relation $\Delta\kappa = -\Delta B/B^2$, the discontinuity in $V_s(T)$ from V_{s+} at $T > T_c$ to V_{s-} at $T < T_c$ is written as

$$(V_{s-}^2 - V_{s+}^2)/V_{s+}^2 = -(B\Delta C_p/VT_c)(\partial T_c/\partial P)^2 . \tag{4}$$

We will examine what magnitude is expected in the change in $V_s(T)$ caused from the superconducting transition. Putting into eq. (4) the following values of the elastic constant B deduced from V_s, the specific heat jump $\Delta C_p/VT_c$ [4] and the pressure derivative of T_c, $\partial T_c/\partial P$ [5], for $YBa_2Cu_3O_{7-\delta}$

$$B = 1.36 \times 10^{12}\ \mathrm{dyn/cm^2},\quad \Delta C_p/VT_c \sim 15\ \mathrm{mJ/(mole\ Cu \cdot K^2)},$$

$$\partial T_c/\partial P \sim 0.07\ \mathrm{K/kbar}, \qquad (5)$$

we obtain the discontinuity in the sound velocity ΔV_s at $T = T_c$:

$$(V_{s-} - V_{s+})/V_{s+} \sim -1.8 \times 10^{-5}\ . \qquad (6)$$

In the evaluation of B the following values were used: $\rho = 6.7\ \mathrm{gr/cm^3}$ and $V_s = 4.5 \times 10^5$ cm/sec. The magnitude in eq. (6) is very small, but it is of a detectable magnitude using a mechanical resonance method. On the other hand, putting the experimental results in eq. (5) for $YBa_2Cu_3O_{7-\delta}$ into eq. (4), we obtain

$$\Delta\beta \simeq 3 \times 10^{-7}\quad (\mathrm{K^{-1}}). \qquad (7)$$

As for the linear expansion coefficient δ we put $\beta = 3\delta$.

(b) Experimental results

Samples measured were made by the sintering method. According to eq. (4), the discontinuity in V_s is related with ΔC_p, and ΔC_p itself is usually considered to be caused from conduction carriers. On the other hand, the conduction carriers should be affected by applying magnetic fields, as will be manifested in the lowering of T_c with increasing field. In order to check this point, the a.c. susceptibility of the sample was simultaneously measured by a pick up coil wound on the sample. Therefore, the superconducting transition temperature T_c of the conduction system is clearly picked up. Here T_c was defined as the point of 1 % decrease of the a.c. susceptibility against the whole change of that from 4 K to $\sim$ 100 K, since the transition becomes blunt by applying magnetic field but we must keep the same standard for determination of T_c.

In Fig. 1 we show a typical result showing an existence of an anomaly in V_s versus T curve [6]. Regarding this curve as a type of discontinuity in the V_s versus T curve, we extrapolate the upper and lower curves against T_c, we obtain $\Delta V_s/V_s \sim -5 \times 10^{-4}$. This magnitude of $-\Delta V_s/V_s$ is the largest one among the results for many tested samples. The magnitudes of $-\Delta V_s/V_s$ is distributed from $\sim 2 \times 10^{-5}$ to $\sim 5 \times 10^{-4}$, but concentrate to the vicinity of

$$\Delta V_s/V_s \sim -8 \times 10^{-5}. \qquad (8)$$

This is about 4.4 times larger than that in eq. (6). It is to be noted that in most cases the superconductivity starts from a little lower temperature than the onset temperature of the velocity anomaly. Similar but less clear results were also observed by other investigators [7-12]. The important point to be noted is that this discontinuity type anomaly is independent of applied magnetic fields up to 10 T. On the other hand, the simmultaneouly measured a.c. susceptibility clearly shows the lowering of T_c (T_c = 92 K at H = 0 to $T_c \sim 88$ K at H = 10 T).

For $(La_{1-x}Sr_x)_2CuO_4$ too, a rather similar type of the anomaly in the $V_s(T)$ versus T curve near T_c was observed. However, in this case the magnitude of the discontinuity decreases with increasing the applied magnetic field as shown in Fig. 2.

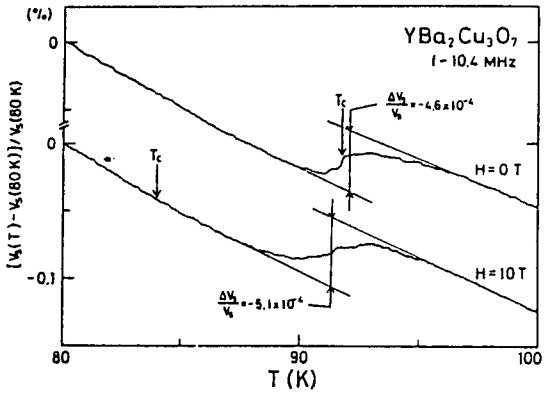

Fig. 1. Anomaly in the V_s versus T curve near T_c for YBCO under H = 0 and H = 10 T.

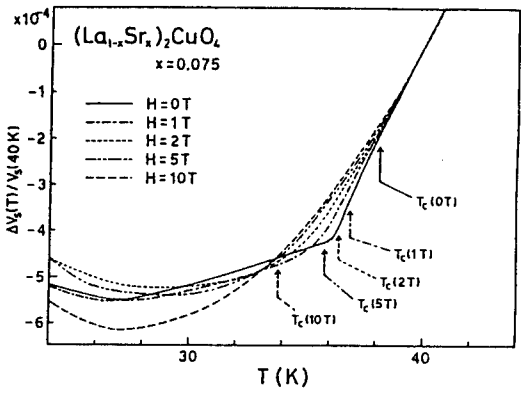

Fig. 2. Anomaly in the V_s versus T curve near T_c for LSCO under H = 0 to H = 10 T.

Measurements of the expansion coefficient in the vicinity of T_c were also made for a sample belonging to the same family as the one used in those of $\Delta V_s/V_s$ mentioned above. The change of the sample length was evaluated by measuring the change of the electrical capacitance between two disks of electrodes which involve a cylindrical sample. The distance of the two electrodes are fixed by a quartz tube whose expansion coefficient is much smaller than the present sample. The a.c. susceptibility of the sample was also measured so as to check the superconducting transition temperature. The result is shown in Fig. 3. The experimental result of the field dependence of the anomaly in $\delta(T)$ also shows the field independence of the position of the anomaly.

Similarly to the case of $\Delta V_s/V_s$, extrapolating the $\delta(T)$ versus T curve above and below T_c, we obtained a discontinuity

$$\Delta\delta \simeq 8 \times 10^{-8} \qquad (9)$$

at the middle of the plateau. The experimental value is the same order of magnitude as the thermodynamical expectation, eq. (7). Kadowaki et al. [13] also observed a similar anomaly.

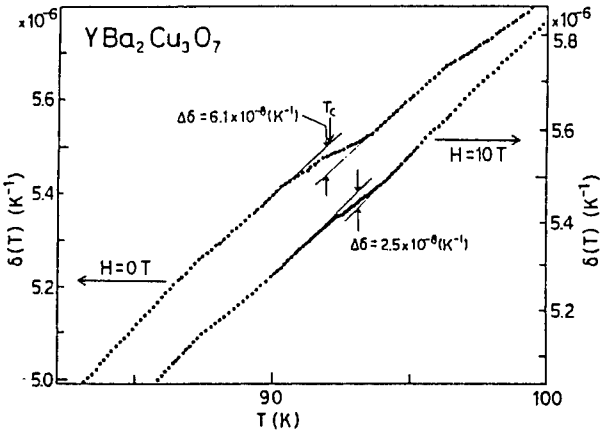

Fig. 3. Anomaly in the δ versus T curves near T_c for YBCO under H = 0 and H = 10 T.

2.2 Hall coefficient

The behavior of the conduction carriers in the normal state give us very useful complementary information on considering the mechanism of superconductivity. In Fig. 4 we show the temperature dependence of the carrier density n(T) as a function of T [14]. This curve was derived from the Hall coefficient for a thin film of YBCO made by a sputtering method. The c-axis is completely oriented perpendicularly to the plane of the substrate, but the a- and b-axes are randomly distributed. Clearly n(T) is written as

$$n(T) = n(0)[a + bT], \tag{10}$$

where a and b are constants. The temperature dependence of n(T) is different from an investigator to another, but it seems that in an ideal case the first term a in the bracket tends tc zero [15].

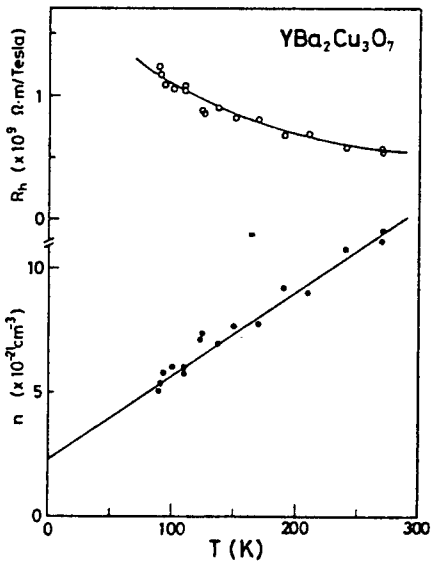

Fig. 4. Temperature dependence of the carrier density in YBCO.

3. DISCUSSIONS

3.1 Temperature dependence of carrier density above T_c for YBCO

Figure 4 clearly shows that the carriers do not obey the Fermi statistics, but rather does the Bose statistics. Considering a two dimensional system for Bose particles the carrier density is written as

$$n(T) \simeq (2\pi m^* k_B T)/h^2 \langle d \rangle, \tag{11}$$

where $\langle d \rangle$ is an average distance between Cu-O layers or between layer and chain. Inserting the experimental values of $n(T) \sim 2 \times 10^{21}$ cm^{-3} at $T = 92$ K ($T \geq T_c$) [15], which is a little smaller than ours, and $\langle d \rangle \sim 3$ A, we obtain $m^*/m \sim 30$ for the effective mass m^*. The large value of the effective mass is consistent with a theoretical model of strongly correted system: according to Oguri and Maekawa [16] m^* is inversely proportional to the exchange paramerter J which is one order of magnitude smaller than the transfer integral t in the Hubbard model.

Inserting eq. (10) into the Drude formula for the resistivity ρ

$$\rho = m^*/n(T)e^2\tau, \tag{12}$$

and using the experimental fact that $\rho \propto T$, we obtain

$$1/\tau = AT + BT^2 \tag{13}$$

for the relaxation time τ. Here, $A \propto a$ and $B \propto b$. The first term may be related with the scattering of holons with some impurities including grain boundaries in a-b planes, while the second term may be related with the holon-spinon scattering. The T^2 dependence of $1/\tau$ for the holon-spinon scattering is also theoretically obtained under some condition in ref. [16]. Thus, the characters of the conduction carriers are well fitted to the holons in the RVB model.

3.2 Interpretation of $-\Delta V_s/V_s$ at T_c for YBCO

As was shown in the previous section, the experimental curve showing the anomaly in the V_s versus T curve is independent of applied magnetic fields in the case of YBCO, and the experimental results of $-\Delta V_s/V_s$ are often one order of magnitude larger than the thermodynamical expectation, eq. (6). These facts may be reasonably understood by interpreting the real situation of the present phenomenon. On the basis of Anderson's theory, we suppose that both the specific heat jump ΔC_p and the present discontinuity $\Delta V_s/V_s$ are caused by immobile valence electrons. In terms of Anderson's concept, these are caused from the spinon system. Namely, the magnetic system falls into a short-range coherent state at $T_c^{(R)}$ which is only a little above or just the same as the superconducting transition temperature $T_c^{(h)}$. Since the exchange interaction energy concerned with the magnetic short-range ordering may be one order of magnitude larger than the Zeeman energy at $H \sim 10$ T, the applied fields hardly affect the anomaly in the V_s versus T curve.

If this assumption is true, the position of the specific heat jump $\Delta C_p/V$ associated with the spinons should also be independent of H. In truth, Fisher et al. [17] found that the observed temperature range of $\Delta C_p/V$ is nearly independent of H up to $H \sim 7$ T. Since the coherence length of the carries in the high T_c superconductor, $YBa_2Cu_3O_{7-\delta}$, is estimated to be $5 \sim 30$ Å from the measurements of the upper critical field H_{c2} [18], even a short-range ordering in the magnetic system may give rise to a crucial effect on the conduction carrier system. Thus,

the conduction carrier system immediately falls into the superconducting state through some attractive force. Since, however, it is pointed out that the attractive force between holons is too weak to result in $T_c \sim 90$ K [19], probably some additional attractive interaction must be invoked. For example, the coherent state in the magnetic system might enhance the electron-phonon interaction through a shift of the singularity in the density of states to the most favorable point at $T_c^{(R)}$ to increase the carrier density of states: otherwise the electron-phonon interaction yields a much lower T_c. In other words, two different but closely correlated types of phase transitions, $T_c^{(R)}$ and $T_c^{(h)}$, simultaneously or successively occur. Then, in the evaluation of the $\Delta V_s/V_s$, we should use $(\partial T_c^{(R)}/\partial p)$ in eq.(4). We anticipate that in order to get the result of eq.(8), $(\partial T_c^{(R)}/\partial p)$ may be $3 \sim 5$ times of $(\partial T_c^{(h)}/\partial p)$.

4. CONCLUSION

In the present paper we have shown the following two points. First, the temperature dependences of the carrier density and the relaxation time in the normal state in YBCO are well understood in terms of the RVB model. Secondly, the field independence of the discontinuity of the sound velocity around T_c in YBCO is also the most reasonably explained in terms of the same model. On the other hand, the field dependence of $-\Delta V_s/V_s$ in LSCO suggests that in this material the spinon system is less stable against the magnetic field. This relatively unstable RVB state in LSCO may be replaced to some extent by a manifestation of the BCS nature in consistency with the larger isotope effect in LSCO than YBCO.

REFERENCES

[1] J. D. Bednorz and K. A. Muller: Z. Phys. B 64 (1986) 189.
[2] B. Batlogg et al.: Phys. Rev. Lett. 58 (1987) 2333; B. Batlogg et al.: Phys. Rev. 35 (1987) 5340.
[3] P. W. Anderson: Science 235 (1987) 1196; P. W. Anderson et al.: Phys. Rev. Lett. 58 (1987) 2790; P. W. Anderson et al.: Physica C153-155 (1988) 527.
[4] S. E. Inderhees et al.: Phys. Rev. B36 (1987) 2401.
[5] J. E. Schirber et al.: Phys. Rev. B35 (1987) 8709.
[6] Y. Horie and S. Mase: Solid State Commn. 66 (1989).
[7] D. J. Bishop et al., Phys. Rev. B36 (1987) 2408.
[8] C. Duran et al.: Solid State Commn. 65 (1988) 957.
[9] S. Bhattacharya et al.: Phys. Rev. B37 (1988) 5901.
[10] S. E. Brown, A. Migliori and Z. Fisk: Solid State Commun. 65 (1988) 483.
[11] V. Müller et al.: Physica 148 B, (1987) 296.
[12] M. Suzuki et al.: Physica C153-155, (1988) 266.
[13] K. Kadowaki et al.: Physica C153-155, (1988) 1028.
[14] T. Yasuda et al.: Jpn. J. Appl. Phys. 27 (1988) L1910.
[15] H. L. Stormer et al.: Phys. Rev. 38 B (1988) 2472.
[16] A. Oguri and S. Maekawa: Physica C, submitted.
[17] R. A. Fisher et al.: Physica C153-155 (1988) 1092.
[18] Y. Hidaka et al.: Physica 148 B (1987) 329.
[19] J. R. Schrieffer et al.: Physica C153-155 (1988) 21.

STRUCTURAL INSTABILITY IN Bi-Sr-Ca-Cu-O AND Tl-Ca-Ba-Cu-O SYSTEMS

Huimin SHEN, Xiaohua CHEN, Yening WANG
Department of Physics, Nanjing University, Nanjing, P.R.CHINA

1.INTRODUCTION

The search for the mechanism responsible for superconductivity in the high Tc oxide superconductors has led to a research on anomalies in physical properties which may be related to the superconducting transition. Since elastic properties are indicative of the interatomic binding forces and also of the phonon-electron interaction, and especially, they are sensitive to a subtle change of lattice structure which may not be detected by electron microscope and other equipments, a number of elasticity studies on high Tc oxide superconductors $YBa_2 Cu_3 Ox$ (hereafter referred to YBCO) have been made.[1,2,3,4,5,6] These results show that there exist anomalies in the temperature range from room temperature to Tc , and the anomaly at 15-30K above Tc is closely relative to superconducting transition.[3][4] Other properties, such as lattice parameters, [7,8] specific heat, [9] acoustic emission, [10] and Debye-Waller factor, [11] also show anomalies at the temperatures mentioned above. In view of conventional high Tc A-15 alloys, those of which exhibit the highest Tc, also exhibit a tendency toward lattice instability above Tc [12], it was considered that the lattice instability near and above Tc favor the superconducting transition followed.[13]

Bi-Sr-Ca-Cu-O and Tl-Ca-Ba-Cu-O systems, the same as YBCO, are of multi-layer distorted perovskite. Whether or not the structure instabilities above Tc take place in two systems similar to that in YBCO is an important problem to understand the mechanism of superconductivity of high Tc oxide superconductors.

2.EXPERIMENTS AND RESULTS

X-ray polycrystalline diffraction data have been recorded on Rigaku D/max-RA rotating anode diffractometer. The data were amended by the (111) line of Si to eliminate the errors introduced by contraction or expansion of heat conduction pole. Resistivity was measured by four probe configuration. Marx three components oscillator method was used for measuring the internal friction and Young's modulus at the frequency of about 100KHz. The stress-strain curves were measured by a Mi44-type micromachine. The all measurements were carried out on heating at rates range from 0.5 to 1.5 K/min.

(1) Bi-Sr-Ca-Cu-O system

The specimens with nominal composition 1112 ($BiSrCaCu_2$ Ox) were prepared by standard powder metallurgical method from high purity Bi_2O_3 $SrCO_3$, $CaCO_3$ and CuO. These specimens are classified into two main types depending on procedures.For the first one (sample-1), the sintered temperature of which is about 865-880°C, the resistivity sharply drops near 107K, and reaches zero near 90K as shown in inset of fig.1a. For the second one (sample-2), the sintered temperature of which is about 810 °C, the resistivity reaches zero at 83K as shown in inset of fig.2. It is generally considered that there exist two superconductive phases with Tc ≈ 84K and Tc ≈ 107K respectively in Bi-Sr-Ca-Cu-O system, [14] these two phases often coexist in a specimen [14]. In our specimens, although the resistivity characteristic seem to indicate single phase, the two superconductive phases may still coexist in sample-1 and sample-2, but it could be said that the higher temperature phase (Tc about 107K) predominates in sample-1 and the lower temperature phase (Tc about 83K) does in sample-2.

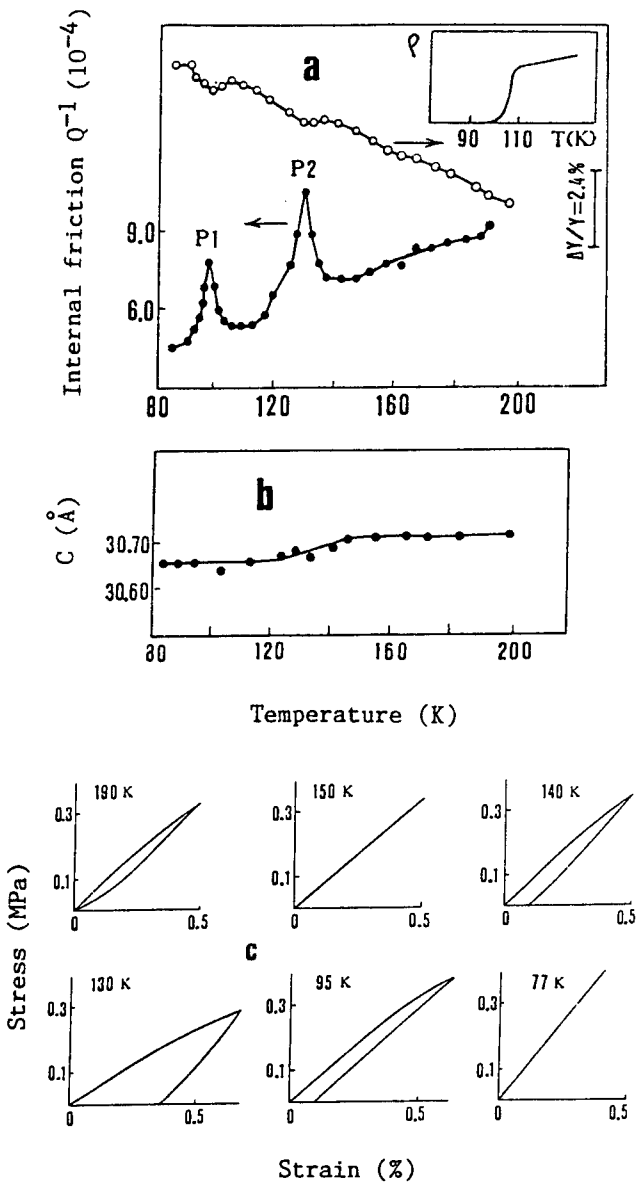

Fig.1 Internal friction Q^{-1} and relative change of Young's modulus $\Delta Y/Y$ (a), lattice parameter c (b) and stress-strain curves (c) as functions of temperature for sample -1. The inset of fig.1(a) is a curve of resistivity (arbitrary unit) vs. temperature.

Fig.1a shows internal friction Q^{-1} as well as relative change of Young's modulus $\Delta Y/Y$ as a function of temperature for sample-1. There exhibit two internal friction peaks P1

(around T_{P1} =95K) and P2 (around T_{P2}=130K), associated with minima of Young's modulus. The values of T_{P1} and T_{P2} vary somewhat from sample to sample and from thermal cycling to cycling. Obvious thermal hysteresis effect was found. The peak P2 is higher than peak P1 in height. In view of the fact that the higher temperature phase predominates in this sample, it could be considered that the P1 and P2 are related to the superconducting transition at about 83K and 110K respectively. The further evidence for this suggestion can be found in fig.2, The curve of Q^{-1} vs. temperature for sample-2 shows that the height of P1 is greater than that of P2, which coincides with the fact that the lower temperature superconductive phase (Tc=83K) predominates in this sample.

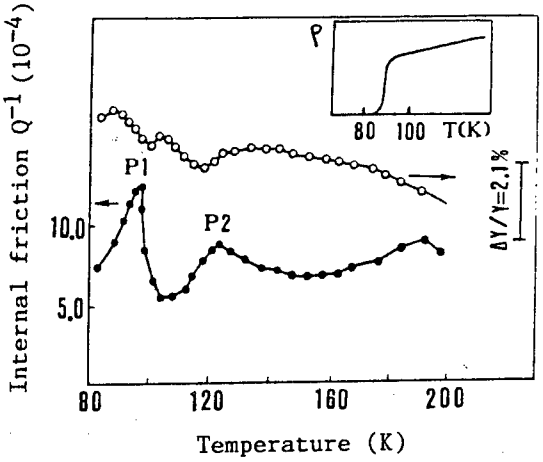

Fig.2 Internal friction Q^{-1} and relative change of Young's modulus ΔY/Y as functions of temperature for sample-2. The inset is the curve of resistivity (arbitrary unit) versus temperature.

X-ray diffraction measurements on sample-1 reveal that the lattice parameter c has a step change at about 130K, but the jump near 95K is not clearly seen for the reason of precision of diffractometer (shown in fig.1b). The general feature of other diffraction lines is similar to this line (00$\underline{10}$). The full width at half maximum (FWHM) around temperatures where lattice parameters jump appears to increase slightly, which is indication of coexistence of two phases with slight different lattice parametners, just similar to that in YBCO [1].

Together, these results demonstrate that phase transition-like structural instability precedes the both known superconducting transition. The symmetry of daughter phase is the same as that of parent phase, but lattice parameters differ a little from each other. This transition is of first order, because of the coexistence of two phases around Tp and thermal hysteresis effect of internal friction peaks. Stress induced movement of phase interfaces results in the internal friction peaks [15].

The mobility of the phase interfaces in sample-1 has been further confirmed by tensile test from room temperature to LN temperature. As shown in fig.1c, obvious ferroelastic loop appears near 130K, less obvious one around 95K, corresponding to the Q^{-1} peak temperatures. The origin of ferroelasticity is due to the stress induced displacement of interfaces between two phases with slight different lattice parameters

can not be recovered after the release of applied stress, because of the lower elastic recovery force, i.e. elastic softening or lattice instability appears near these temperatures.

(2) Tl-Ca-Ba-Cu-O system

The specimens were prepared by standard powder metallurgical method from high purity Tl_2O_3 , CaO , BaO and CuO according to appropriate ratio. The x-ray diffraction pattern at room temperature shows that 2223 phase ($Tl_2Ca_2Ba_2Cu_3O_{10+\alpha}$) is dominant in the specimen. Correspondingly, the resistance drops to zero at 115K within the experimental limit of $10^{-7}\Omega$ as shown in the inset of fig.3(a). Fig.3(a) also shows that an internal friction peak and modulus ($\propto fr^2$) minimum appear near 135K, about 20K higher than Tc. The x-ray diffraction data corrected by Si (111) line as a function of temperature show that the structure symmetry has no change in the range from 200K to 77K but the lattice parameters jump near 135K as shown in fig.3(b). These anomalies near 135K disappear for the specimen which does not undergo a superconducting transition above LN_2 temperature. With the same analysis as in the case of Bi-Sr-Ca-Cu-O, the lattice instability must be closely related to the superconducting transition at 115K.

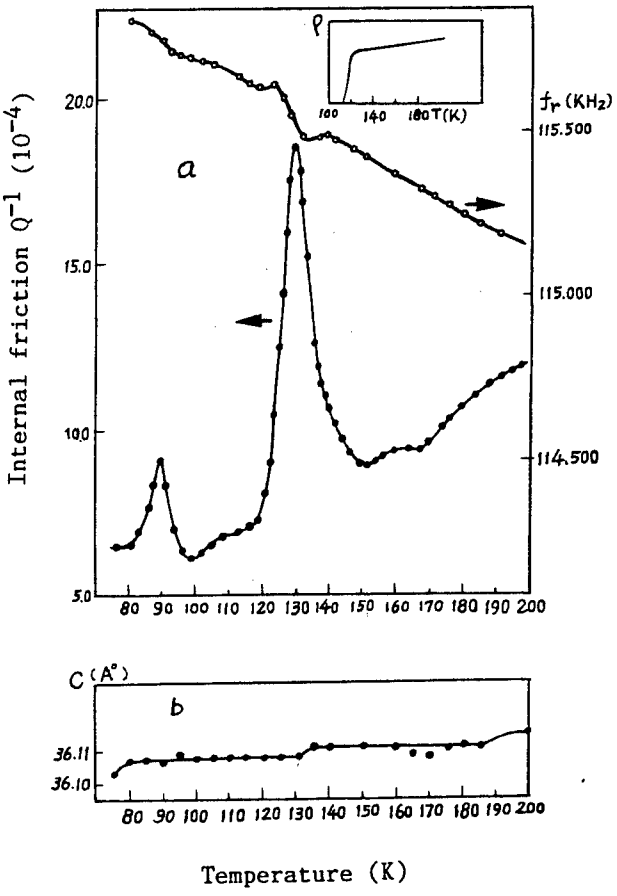

Fig.3 (a) The curves of internal friction Q^{-1} and resonant frequency fr versus temperature for Tl-Ca-Ba-Cu-O specimen. The inset is resistivity as a function of temperature. (b) Lattice parameter c as a function of temperature for the same specimen.

Besides the internal friction peak at 135K, there exists another smaller peak at about 90K as shown in fig.3(a), whose behavior is very similar to that of the 135K peak. It is speculated to be related

to a minor phase with lower Tc, which coexists with the 115K superconducting phase in the specimen.

Recently, S.Bhattacharya et al also found the evidence for phase transition at 120K-130K in YBCO by measuring the ultrasonic attenuation and velocity [6]. They considered the transition is of second order and the primary order parameter is possiblely rotation of the Cu-O complex in the a-b plane. In references [1] and [13], Y.Wang et al pointed out that the transition is of first order, the origin of lattice parameters jump on atomic scale is likely due to a rotation or distortion of oxygen octahedron which is similar to that in $LiNbO_3$ [16]. Now Bi-Sr-Ca-Cu-O , Tl-Ca-Ba-Cu-O and YBCO resemble each other in many respects, such as , layered perovskite structure, step-like-change in lattice parameters, internal friction peak above Tc and so on. It is reasonable to speculate that the mechanism of superconductivity for these systems is alike.

We would like to thank Jianguo Zhen, Zheng Yu and Xin Jin for providing specimens, Kesheng Wu and Yuping Zhu for help in experiments. This work was supported by National Science Fundation of China.

REFERENCES

[1] Y.Wang, H.Shen, J.Zhu, Z.Xu, M.Gu, Z.Niu and Z.Zhang, J.Phys.C 20, L665 (1987).
[2] H.Shen, Y.Wang, Z.Zhang and L.Sun, J.Phys.C20, L889(1987).
[3] X.Chen, L.Sun, Y.Wang, H.Shen and Z.Yu, J.Phys.C 21, 4063 (1988).
[4] X.Chen, Y.Wang and H.Shen, submitted to Phys.Stat.Sol.A (1988)
[5] G.Cannelli, R.Cantelli, F.Cordero, G.A.Costa, M.Ferreti and G.L.Olcese, Phys.Rev.B V.36, 8907 (1987).
[6] S.Bhattacharya, M.J.Higgins, D.C.Johnston, A.J.Jacobson, J.P.Stokes , D.P.Goshorn and J.T.Lewandowski, Phys.Rev.Lett.21,1181 (1988).
[7] L.Sun, Y.Wang, H.Shen and X.Chen, Phys.Rev.B38, 5114(1988)
[8] H.You, J.D.Axe, X.B.Kan, S.Hashimoto, S.C.Moss, J.Z.Liu, G.W.Crabtree and D.J.Lam, submitted to Phys.Rev.Lett. (1988).
[9] T.Laegreid, K.Fossheim, E.Sandvold and S.Julsrud, Nature V.336, 637 (1987).
[10] Y.Xu, S.He and Y.Guo, J. Wu Han Univ. (CHINA), No.4, 125 (1987)
[11] R.Ma, National Conference on High Tc Superconductor held in Baoji, CHINA, in April 3-7,1988.
[12] L.R.Testardi, in "Physical Acoustics", eds. by W.P.Mason and R.N.Thurston, V.10, P.193 (Academic Press,1973) and L.R.Testardi, Rev.Mod.Phys. 47, 637 (1975).
[13] Y.Wang, Invited talk on MRS Int. Meeting on Adv. Mat. (Tokyo, April, 1988) , to be published.
[14] Yasuhiko Syono, et al, to be published.

[15] Y.Wang, H.Shen, Z.Xu, Y.Zou, J.Zhu, Z.Zhang, Z.Yang, J.de Phys.42C, C5-1049 (1981).
[16] Y.wang, H.Shen, Z.Xu and H.Zhou, Ferroelectrics Letter,6,1 (1986)

Bi-BASED HIGH TEMPERATURE SUPERCONDUCTING SYSTEM

Hiroshi MAEDA, Yoshiaki TANAKA, Toshihisa ASANO, Masao FUKUTOMI, Hiroaki KUMAKURA, Daniel R,DIETDERICH, Yuji YOSHIDA, Hisashi SEKINE, Kazumasa TOGANO, Eiji YANAGISAWA*, Masanao MIMURA**, Kouichi NUMATA***, Junichi MACHIDA† and Kazunori JIKIHARA††
National Research Institute for Metals, Tsukuba Laboratories
1-2-1, Sengen, Tsukuba 305, Japan
* Asahi Glass Co. Ltd., Yokohama, Kanagawa 221
** Furukawa Electric. Co. Ltd., Yokohama, Kanagawa 220
*** Mitsubishi Heavy Industries, Ltd., Yokohama, Kanagawa
† Mitsui Mining & Smelting Co. Ltd., Ageo, Saitama 362
†† Sumitomo Heavy Industries, Ltd., Hiratsuka, Kanagawa 254

1. INTRODUCTION

The discovery of superconductivity in Bi-Sr-Ca-Cu-O system (BSCCO) with the critical temperature, T_c above 100 K has brought about a new phase in the research of high-T_c superconductors [1]. The BSCCO system has at least two superconducting compounds; one with a T_c of about 85 K (low-T_c phase) and the other of about 110 K (high-T_c phase). The two oxides can be expressed ideally by the general molecular formula $Bi_2Sr_2Ca_{n-1}Cu_nO_x$ ($x=2n+4+\delta$) with n=2 and 3, respectively. These crystal structures are similar, differing only in the number of CuO_2-Ca slabs inserted between double Bi-O layers.

The low-T_c phase is easily produced, while the formation of the high-T_c phase is difficult. One of the methods to enhance its formation is the addition of Pb [2]. The formation of the high-T_c phase is also enhanced in an atmosphere of reduced oxygen partial presssure, P_{O2} of about 1/13 [3]. For practical applications it is very important to investigate the superconducting properties, especially, the critical current density, J_c of Pb-doped BSCCO with the complete high-T_c phase. Furthermore, the application of a compound to a superconducting magnet requires the winding of tape or wire conductors with sufficient flexibility into solenoid.

In this report, we describe the preparation and superconducting properties of Pb-doped BSCCO pellet samples with high-density and high-preferred orientation, of thick films and also of some tapes and wires with high J_c.

2. EXPERIMENTAL PROCEDURES

Pb-doped BSCCO samples were mainly prepared by a conventional solid state reaction using high-purity powders of Bi_2O_3, PbO(or Pb_3O_4), $SrCO_3$, $CaCO_3$ and CuO. Disk-shaped pellets (20 mm in diameter and 1 mm in thickness) were sintered in the temperature range of 835-845 C mainly in a P_{O2} of 1/13 atm (sometimes in air). The pellets were pressed at room temperature during an interrupted sintering treatment. Using Pb-doped BSCCO powders, tapes and wires were prepared by a metal (Ag and Cu)-sheath technique and a doctor blade casting technique followed by the conventional process of rolling and sintering.

BSCCO films of above 1 μm in thickness were prepared by rf magnetron

sputtering and plasma spraying techniques. For these specimens, measurements of T_c and J_c were performed in magnetic fields using a standard four-probe resistive method. AC susceptibility was also measured at a frequency of 700 Hz. X-ray diffraction analysis, and scanning elctron microscopy (SEM) observation were carried out.

3. RESULTS AND DISCUSSION

3.1 Pellet sample

AC susceptibility measurements and X-ray diffraction patterns for Pb-doped samples show that the low-T_c phase exists for short sintering times and is converted into the high-T_c phase. Finally, the almost complete high-T_c phase can be obtained and the complete zero resistance is achieved at 110 K [4]. The sintering time can be reduced by one-fourth in a P_{O2} of 1/13 atm. The resistivity transition curves are changed in various magnetic fields in a similar manner with $YBa_2Cu_3O_7$(YBCO). The head of the transition curve is only slightly influenced by the field, while the tail of the curve shifts to lower temperature as the field is increased. From the mid-point of the transition curves the upper critical fields, H_{c2} are estimated to be 60 T at 77 K by a linear extrapolation and 140 T at 0 K using WHH theory of $H_{c2}(0) = -0.69T_c(dH_{c2}/dT)_{Tc}$.

J_c at 77 K in zero field, J_c(77K,0T) of Pb-free BSCCO is very small of an order of .1 A/cm^2. With the additon of Pb the J_c(77K,0T) is increased about 210 A/cm^2 [4]. The increase in J_c is mainly due to the increase in the volume fraction of the high-T_c phase. However, the J_c is less than the best value obtained for YBCO pellets. SEM observation shows that an as-sintered pellet sample has the isotropic cross-over growth of a thin planer crystal parallel to the c-plane and a lot of pores. Such a low density, about 60 % of the theoretical density and a low crystal preferred orientation is partially responsible for the low J_c in the BSCCO sustem. Since characteristic cleavage of the crystal occcurs between the Bi-O bi-layers along the c-plane it is possible to deform the pellet sample by compaction without any breakage of the high-T_c phase. For example, a sample is first sintered to form the almost high-T_c phase, then cooled to room temperature and compacted (pressed) uniaxially to about one-half in the thickness, and finally sintered again. The pressed sample is dense and highly textured with the c-plane laminated parallel to the pellet surface (perpendicular to the pressing direction). By this process a J_c(77K,0T) greater than 3500 A/cm^2 is achieved for the pellet with a nominal composition of $Bi_{0.8}Pb_{0.2}Sr_1Ca_{1.1}Cu_{1.6}O_x$. Furthermore, J_c tends to increase as the combined process of pressing and sintering is repeated. For a tape sample, which the combined process was repeated three times after Cu sheath was removed, we obtain a J_c(77K,0T) of 5000 A/cm^2 [5]. For compaction, of course, a cold isostatic press (CIP) treatment degrades J_c.

J_c is increased with increasing the final sintering time after pressing up to about 5 h at 835 °C and tends to decrease for further sintering time, mainly due to new isotropic crystal growth of the high-T_c phase. When a magnetic field is applied, J_c is reduced drastically in low fields up to 200 Oe, especially by one order in magnitude for the un-pressed sample with low J_c. This suggests that the superconducting link between grains is still very weak in the BSCCO system [6]. However, the degradation of J_c in field is

improved as the J_c(77K,0T) is increased. It is also found that J_c depends on the nominal composition, although at present we can not clear the optimum composition for J_c.

3.2 Wire and tape

Since grains of BSCCO can be easily deformed it is easy to fabricate the wires and tapes with a high density and a high preferred crystal orientation. Thin BSCCO ribbons with 30 μm thickness, which was prepared by the combined process of doctor blade casting, cold rolling (pressing) and sintering. A T_c of 107 K is achieved, and the highest J_c (77K,0T) obtained so far is about 1850 A/cm^2 for the ribbon with a nominal composition of $Bi_{0.7}Pb_{0.3}Sr_1Ca_1Cu_{1.8}O_x$. The ribbon has a sufficient flexibility to be bent about 30 mm diameter with no breakage even after the final sintering. The J_c shows no degradation after the bending. The ribbon has a high density of about 5.8 g/cm^3 and a high alignment of plate-like grains parallel to the ribbon surface.

An Ag sheathed BSCCO multifilamentary wire with 1330 filaments and a tape with 36 filaments were fabricated. Fine sintered powders with a nominal composition of $Bi_{0.8}Pb_{0.2}Sr_{0.8}Ca_1Cu_{1.4}O_x$ were packed in a Ag tube of 10 mm outer diameter (o.d.) and 6.7 mm inner diameter (i.d.), and cold worked. From the monofilamentary wire of 0.5 mm o.d., first a 70-filament wire, then a 70 x 19 = 1330 filament wire of 0.7 mm o.d. were fabricated, and finally sintered. Especially, for the fabrication of a 36-filament tape of 1.8 mm x 0.16 mm the combined process of cold rolling and sintering was repeated a few times. The 1330-filament wire shows a T_c of 105 K and the 36-filament tape shows a J_c(77K,0T) of 1050 A/cm^2. It is sure that the repetition of cold rolling (pressing) and sintering process has also a good effect on multifilamentary wires. A J_c of several thousands A/cm^2 will be obtained by the optimizing conditions of the present method.

3.3 films

We have prepared successfully superconducting BSCCO films by a new process based on rf magnetron sputtering [7]. An important characteristic of the new process lies in a specific substrate temperature control during deposition. For example, the substrate temperature was increased to as high as 800 °C for 10 to 30 min at an early stage of deposition, then gradually decreased and maintained in the temperature range between 700 °C and 740 °C for the rest of the deposition. A T_c of above 103 K is achieved with very high reproducibility when the film with about 1 um thickness is deposited on a MgO (100) substrate using a target of $Bi_{1.3}Sr_1Ca_1Cu_{1.5}O_x$ followed by annealing at 875 °C for 0.5 h. A partially melted underlayer is formed during the early stage of deposition. The underlayer plays a very important role in the formation of the films with a T_c of 100 K and above.

On the other hand, plasma spraying is one of the most useful methods for producing thick and large scale oxide films. Using fine sintered powders with a nominal composition of $Bi_{1.53}Pb_{0.48}Sr_{1.66}Ca_{1.18}Cu_{2.31}O_x$ thick films of about 150 μm in thickness were deposited on Ni substrate by plasma spraying. The coating of a YSZ underlayer of about 10 um in thickness is much effective to supress the diffusion between the substrate and the film. The as-sprayed films are amorphous and non-superconductive. After annealing at 840 °C for

about 90 h the films have a T_c of 107 K and J_c(77K,0T)'s of 10-30 A/cm^2.

4. Conclusion

A uniaxial pressing process during an interrupted sintering treatment is an effective method to improve J_c. By this process for Pb-doped BSCCO, a J_c(77K,0T) greater than 5000 A/cm^2 can be easily achieved, and the degradation of J_c in magnetic field can be greatly improved.

Thin ribbons with the high-T_c phase have been successfully prepared by the combined process of doctor blade casting, cold rolling and sintering. A J_c(77K,0T) of 1850 A/cm^2 is obtained. The ribbon is sufficiently flexible to be bent about 30 mm diameter even after the final sintering.

An Ag-sheathed BSCCO multifilamentary wire with 1330 filaments and a tape with 36 filaments have also been successfully fabricated. The 36-filament tape by the combination and repetition of cold rolling and sintering shows a J_c(77K,0T) of 1050 A/cm^2.

By a new process based on rf sputtering to form a partially melted underlayer BSCCO films with a T_c of above 100 K can be easily achieved, and also by plasma spraying thick films with the high-T_c phase is fabricated.

REFERENCES

1. H.Maeda, Y.Tanaka, M.Fukutomi and T.Asano : Jpn.J.Appl.Phys., 27(1988) L201.
2. M.Takano, J.Takeda, K.Oda, H.Kitaguchi, Y.Miura, Y.Tomii and H.Mazaki : Jpn.J.Appl.Phys., 27(1988) L1041.
3. U.Endo, S.Koyama and T.Kawai : Jpn.J.Appl.Phys., 27(1988) L1476.
4. E.Yanagisawa, D.R.Dietderich, H.Kumakura, K.Togano, H.Maeda and K.Takahashi : Jpn.J.Appl.Phys., 27(1988) L1460.
5. H.Sekine, K.Numata, K.Ogawa, K.Inoue and H.Maeda : submitted to Jpn.J.Appl.Phys.
6. H.Kumakura, K.Togano, K.Takahashi, E.Yanagisawa, M.Nakao, and H.Maeda : Jpn.J.Appl.Phys., 27(1988) L2059.
7. M.FUKUTOMI, J.MACHIDA, Y.TANAKA, T,ASANO, T.YAMAMOTO and H.MAEDA : Jpn.J.Appl.Phys.,27(1988) L1484.

PREPARATION AND PROPERTIES OF THE HIGH Tc Bi(2-x)PbxSr2Ca2Cu3Oy SUPERCONDUCTORS

LIN Wei, HONG Cangsheng , YANG Guowen , CHEN Jiping , JI Hong , WAN Yi
Changsha Research Institute of Mining & Metallurgy , P.R. of CHINA

1. INTRODUCTION

The discovery of the high Tc superconductors without rare-earth elements in Bi system[1] opens a new way to the high Tc superconductors. Although addition of a small amount of Pb may increase the percentage of high Tc phases in BSCCO system, it is difficult to produce satisfactory results without appropriate heat treatments[2], [3], [4]. It is , therefore, of great concern so far to further improve the superconducting properties of the superconductors in BSCCO system. In this paper the effect of the sintering at the temperature close to melting point on the critical parameters of the high Tc Bi(2-x)PbxSr2Ca2Cu3Oy superconductors is reported. The samples made under this sintering condition by nitrates co-decomposition(NCD) or solid reaction (SR) process were found to show a zero resistance temperature (Tco) of about 109 K.

2. EXPERIMENTAL

The samples were prepared according to the NCD & SR processes, respectively. The anatytically pure Bi2O3, PbO, SrCO3, CaCO3 & CuO were used as raw materials. In the case of NCD process, raw materials of nominal composition were dissolved in the dilute HNO3 solution, the resulting solution was boiled dry, followed by a calcination so as to decompose the nitrates into oxides, which were then ground into powders. In the case of SR process, the weighed raw materials should be intimately mixed by milling. Then these powders were pressed under 35-38x10^7 Pa into pellets of 12 mm diameter. The pellets were sintered in a tube electric furnace at a heating rate of 150-200°C/h, then furnace cooled at a similar rate. The sintering was carried out under the mixed atmosphere of Ar & O2 to keep a decreased partial pressure of O2. The exit rubber tube of the mixed gas was open through a water seal to the atmosphere.

The Tc measurement for the samples was performed by the standard four-lead method, and the critical current (Ic) was defined under a quench criterion of 1μV/cm. The differential thermal analysis(DTA) was carried out on some of the samples to determine their initial melting temperature. The crystal structure & phases were identified using X-ray diffraction, and the lattice parameters determined. The morphological observation was made with SEM , the chemical compositions of the samples were analysed with EPMA or XFA.

3. EXPERIMENTAL RESULTS AND DISCUSSIONS

The determination of the initial melting point. In order to assure the physical and

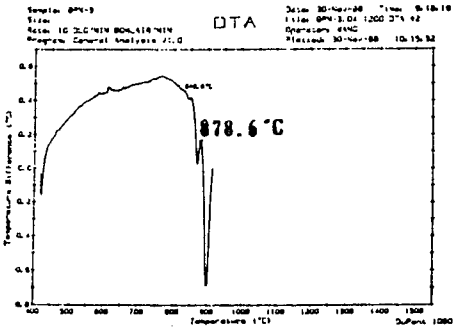

Fig. 1. DTA pattern of the sample by NCD

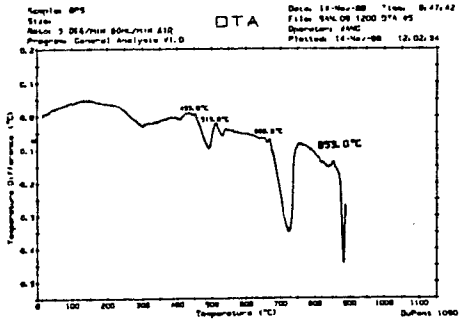

Fig. 2. DTA pattern of the sample by SR

chemical changes of different components occurring to a thorough degree during their sintering, and thus to obtain a dense and high Tc Bi(2-x)PbxSr2Ca2Cu3Oy superconductor, it is necessary to bring the sintering temperature and time under strict control. According to the results of DTA for the samples made by these two methodes, their initial melting points are given in fig.1 and fig.2 respectively. From the experimental results it is clear that under the flowing air of 80 ml/min the sintering temperature of more than 878.6 °C will lead to the melting of the NCD processed samples, and that for the SR processed samples under the same flowing atmosphere, even a temperature down to 853°C will lead to the melting. This can be explained by the higher surface activities of the SrO and CaO formed during the sintering of SrCO3 and CaCO3 used as raw materials for the preparation of SR processed samples.

Fig.3 & 4 show the effect of the sintering atmosphere on the initial melting point of Bi1.8Pb0.2Sr2Ca2Cu3Oy samples made by NCD process. The initial melting points of the samples were determined under the 10% O2 & Ar atmosphere. From the analysis on fig.1, 3 & 4 it can be seen that under the 20% O2 atmosphere, the initial melting point of the NCD samples is 878.6 °C, and under the 10% O2+Ar atmosphere 873.2°C, whereas under the Ar atmosphere only 797.3 °C, and that the initial melting point decreases with the decreasing partial pressure of O2. Therefore , the reduction in the partial pressure of oxygen in the sintering atmosphere can result in the decrease in the sintering tempreture.

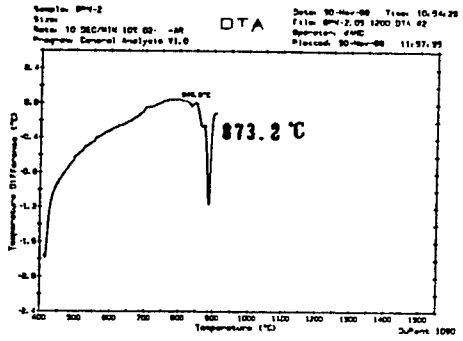

Fig.3. DTA pattern of the sample by NCD under 10% O2+Ar atmosphere

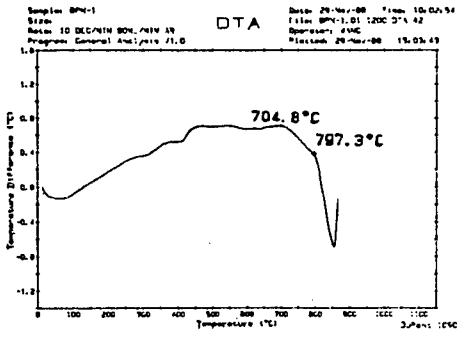

Fig.4. DTA pattern of the sample by NCD under Ar atmosphere

The effects of Pb on superconducting properties of Bi(2-x)PbxSr2Ca2Cu3Oy. The samples made by the two methods were investigated for the case of x=0.1, 0.2 & 0.3 respectively. Because of presintering at 800 °C for 20 h, the sintering condition were selected to be 865 °C for 70 h in air. The effect of Pb substitution on the Tc for

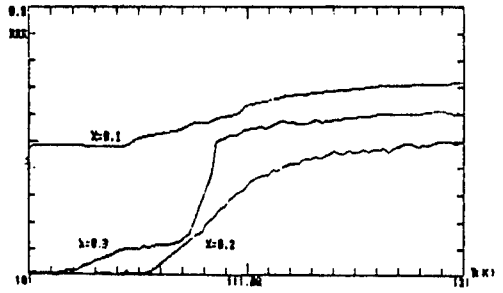

Fig.5. Temp. vs. res. curves of the sample by NCD with x=0.1, 0.2, 0.3

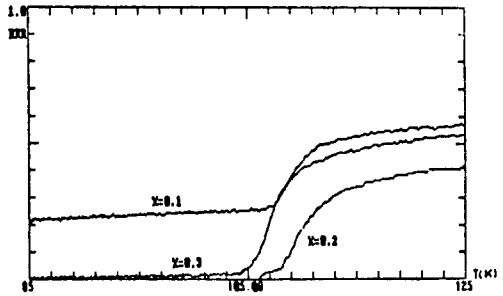

Fig.6. Temp. vs. res. curves of the sample by SR with x=0.1, 0.2, 0.3

the samples are showed in fig.5 and 6. The results showed that for the samples with x=0.1, whether they are made by NCD or by SR process, the zero resistance temperature was found to be very low (at least no superconducting at 77 K), in comparison with the Tco for the samples of x=0.2, which was found to be 106.3K for the NCD processed samples, and 105.5K for the SR processed samples respectively, and that for the samples with x=0.3 , Tco was 103.5K (NCD) and 103.4K (SR). To obtain an increased Tco, it is preferable to select the value of x to be 0.2.

The effect of sintering procedures and heat treatment conditions. Although the samples of x=0.2 showed a relatively high Tco, they suffered from a low Ic, one of three important parameters for evalution of superconductivity. The effects of the synthesis conditions were studied for the NCD samples of x=0.3 besides x=0.2. The results were given in Table 1. The experimental results of effect of the sintering condition showed

Table 1. Effect of sintering condition on the superconducting properties

X value (Pb content)	sintering atmosphere	presintering condition (°C/h)	sintering condition (°C/h) first	sintering condition (°C/h) second	Tco (K)	Ic for bulk sample (A) (77K, 0T)
0.2	10% O2	800 / 20	860/60		90.0	0.72
0.2	10% O2	800 / 20	860/60	870/20	103.8	
0.3	10% O2		860/60	870/20	103.5	2.25
0.3	10% O2	800 / 20	860/60	870/20	97.0	
0.3	10% O2		870/70		106.0	
0.3 *	10% O2		860/96		103.8	4.30
0.3 *	7% O2		840/84		103.5	4.20

* the samples have a nominal composition of Bi1.8Pb0.3Sr2Ca2Cu3Oy

that the direct sintering without presintering can lead to an increased Tco, and that the reasonably long sintering time is of advantage for an improvement of the superconducting properties. The reduction of the partial prossure of O2 and the decrease of the sintering temprerature can give also satisfactory results. This holds for the SR samples.

The preparation of the sample A under optimum condition. Based on the above experimental results the following sintering conditions are recommended for the samples with a nominal composition of Bi1.8Pb0.2Sr2Ca2Cu3Oy. The two step sintering was carried out under the 10%O2+Ar atmosphere. The first sintering happens at 865°C for 60 h, followed by the furnace cooling. Then the second sintering takes place at 870°C for 20 h, followed by the furnace cooling to 400°C before removal of the samples from the furnace. The Tc measurements showed that the zero resistance temperature is 108.3K

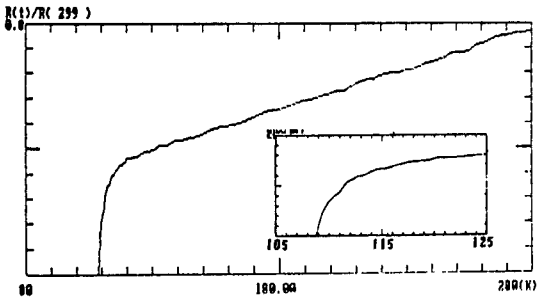

Fig.7. Temp. vs. res. curves of sample A

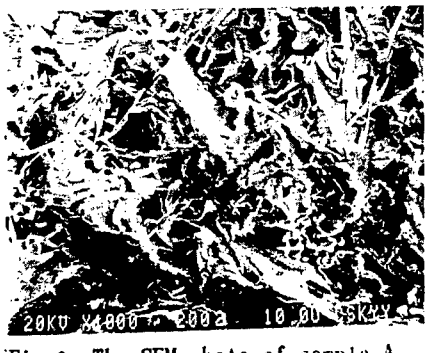

Fig.8. The SEM photo of sample A

(fig.7). The SEM photo of the sample A is showed in fig.8.
The dc Meissner effect measurement showed that the sample is biphasic with the 110 K phase dominating. Upper and lower limits of the superconducting volume fraction were observed to be 18.4% and 11.5% respectively at 77K and 20 Oe.

To observe the stability, sample A was subjected to a number of cooling & heating cycles. Then Tco was determined, and found to decrease with the increasing number of cooling and heating cycles, as showed in fig.9, after 10 cycles Tco fell from 108.8K down to 98.7K (the time between the first cycle and the last one being about 12 days), and to 96.5K after two months.

Because efforts were made to raise the proportion of high Tc phases by the partical substitution of Pb for Bi in the sample A with a nominal composition of Bi(2-x)PbxSr2Ca2Cu3Oy, and because both PbO and Bi2O3 have a lower melting points, the composition inhomogeneity may occur for a certain component during the sintering of the samples. The composition analysis was made for the different parts of the NCD samples. Table 2 gives the results of EPMA for the different parts of the samples. From table 2 it can be found that after sintering the different parts of sample have a significant difference in their composition, and the Pb content of samples considerably decreased. To further affirm the decrease in Pb content, XFA was performed for the Pb content. The results showed that after sintering the Pb content decresed by 31.5%.

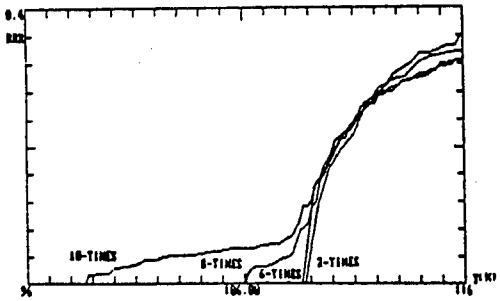

Fig.9. Temp. vs. res. curves of sample A with different cool-heat cycles

Table 2. The results of EPMA for the different parts of the sample

region to be detected	wt% Bi	Pb	Sr	Ca	Cu
surface	34.47	2.14	19.85	7.33	19.10
upper part*	33.47	3.45	19.60	5.39	20.94
middl part*	35.91	3.44	19.07	6.19	18.58
lower part*	35.63	2.08	19.73	6.39	19.18

* in the longitudinal section of sample

To investigate the effect of composition inhomogeneity on the superconducting properties, Tco was measured for the upper and under surface of samples (in relation to the samples position during sintering), and found to be 103.8K for the upper surface, and 100.3K for the under surface (fig.10). It seems that the further reduction of the partial pressure of oxygen and the sintering temperature may be favorable to the improvement of superconducting properties.

The sintering condition of high performance SR sample B. With the results of the sample A and of EPMA for the NCD samples in mind and according to the data provided in

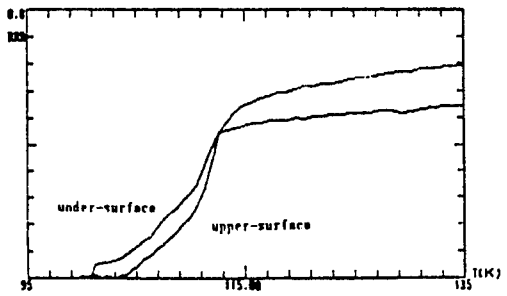

Fig.10. Temp. vs. res. curves of upper and under surface of sample

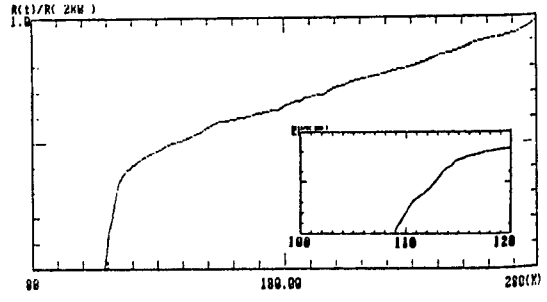
Fig.11. Temp. vs. res. curves of sample B

literature[4], the following conditions were selected for the sample B with a nominal composition of Bi1.85Pb0.35Sr2Ca2.07Cu3.06, 835 °C for 84 h under the 7%O2+Ar atmosphere, followed by furnace cooling down to 400°C before removal of samples from the furnace. Then the samples were subjected to XRD analysis and Tc measurements respectively. Tco was found to be 109 K(fig.11). The results of XRD analysis showed that a significant single-phase superconductivity appears in sample B, with the high Tc phase predominent over the sample (fig.12). "x" in the figure denotes the diffraction peaks for the low Tc phase. The lattice parameters were determined to be 5.42 Å for both a and b, and 37.26 Å for c.

It should be pointed out that our bulk samples have a low value of Ic. This is perhaps due to low densities for our samples, e.g. 2.9 g/cm^3 for the sample with an Ic of 0.7 A. Low proportion of superconducting phases may be another major factor leading to low Ic for our samples. For example, the percentage of superconducting phases was found to be about 15% in the sample of Ic=4.2 A.

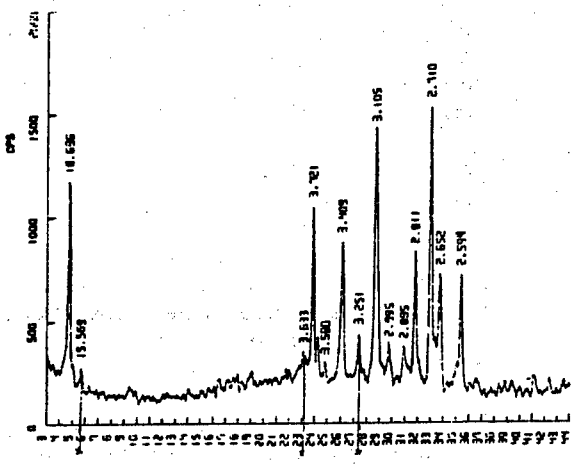

Fig.12. XD pattern of sample B

4. CONCLUSIONS

(1) The sintering at a tempra-ture approximating to the melting point is effective in improving the zero resistance temperature of BSCCO system. For example under this sintering condition, NCD samples showed a Tco=108.8K, and SR samples Tco=109K.

(2) The reduction of the partial pressure of oxygen and long sintering time at a lower temperature are favourable to the decrease of volatility of Pb during the sintering.

(3) The stability of the high Tc Bi(2-x)PbxSr2Ca2Cu3Oy superconductors remains to be a topic to be further studied.

ACKNOWLEGEMENT

The technical guidence by prof. FANG Junren at our institute, and the assistance by The Institute of Plasma Physics, Academia Sinica of China in determining the volume percentage of superconducting phases are greatly appreciated.

REFERENCES

[1] H.Maeda et al, JJAP 27(1988) 209
[2] Yutaka Yamada et al, JJAP 27(1988) 996
[3] Satoshi Royma et al, submitted to JJAP (1988)
[4] S.M.Green et al, submitted to PRL (1988)

CHEMICAL AND STRUCTURAL ASPECTS OF THE Bi,Pb-Sr-Ca-Cu-O SYSTEM

Mikio TAKANO

Institute for Chemical Research, Kyoto University, Uji 611, Japan

1. INTRODUCTION

The Bi-Sr-Ca-Cu-O (BSCCO) system is a rich system in which at least three superconducting phases have been found [1-3]. These have serial compositions expressed as $Bi_2Sr_2Ca_{m-1}Cu_mO_{2m+4}$ and are layered as //BiO/SrO/CuO_2/Ca/---/Ca/CuO_2/SrO/BiO// [4]. T_c increases as ~10K, ~80K, and ~110K for m=1, 2, and 3, respectively. Both the above compositions and structures are, however, considerably simplified in comparison with the real ones. The real compositions are nonstoichiometric with respect to both the cationic and anionic elements. And atomic positions in their structures are considerably shifted form their "ideal" positions so that each phase is featured by an incommensurate, one dimensional modulation.

As for the formation process, partial melting often plays the key role and, as a result, particle morphology, microstructure of sintered bodies, and even the kinds of phases formed are practically influenced.

Summarized here are some experimental results concerning the phase relation in this complex BSCCO system, effects of partial substitution of lead for bismuth on the formation and properties of the m=3 phase (the so-called high-T_c phase), and also a newly found phenomenon of magnetic suspension of a sintered pellet of the high-T_c phase which is not do due to the well-known pinning effect but due to the Meissner effect. These studies have been done in collaboration with active colleagues belonging to The National Defense Academy, Mie University, Kyoto University, Konan University, and Okayama University.

2. EXPERIMENTAL RESULTS AND DISCUSSION

Summarized in Fig. 1 are the phases formed in the BSCCO system by heating mixtures of Bi_2O_3, $SrCO_3$, $CaCO_3$, and CuO in air. The firing temperatures in parentheses were chosen so that melting did not occur as examined visually.

i) The Bi-Sr-Cu-O (BSCO) System

Four kinds of phases containing Bi, Sr, and Cu have been found in the BSCO system in contrast with the Bi-Ca-Cu-O system where we could not find any ternary oxide [5]. These are marked A, B, C, and D in Fig. 1. A stands for a solid solution expressed as $Bi_{2+x}Sr_{2-x}Cu_{1+\delta}O_y$ with $0.1 \leq x < 0.5$ and $0 < \delta < x/2$, while B stands for a compound, $Bi_{16}Sr_{17}Cu_7O_y$. It should be noted that $Bi_2Sr_2CuO_y$, the ideal m=1 phase, does not exist, but slight deviations toward Bi/Sr>1 and <1 stabilize the above phases. Structures and particle morphologies of A and B examined by X-ray diffraction (XRD) and scanning electron microscopy (SEM) are quite different. For example, particles of A are plate-like, while those of B are needle-like. The solid solution A, where the superconducting phase is included, crystallizes in the layered m=1 structure with pseudotetragonal cell parameters of $a=b\simeq 5.4$A and $c\simeq 24$A. The cell parameters vary so that a increases but c decreases with increasing x. The period, λ, of the one dimensional modulation along the b axis tends to decrease almost linearly from $\lambda/b \simeq 5.2$ at x=0.10 to $\simeq 4.2$ at x=0.50. Nominal Cu valences estimated independently from an oxygen content analysis and an iodometric titration are in good agreement to each

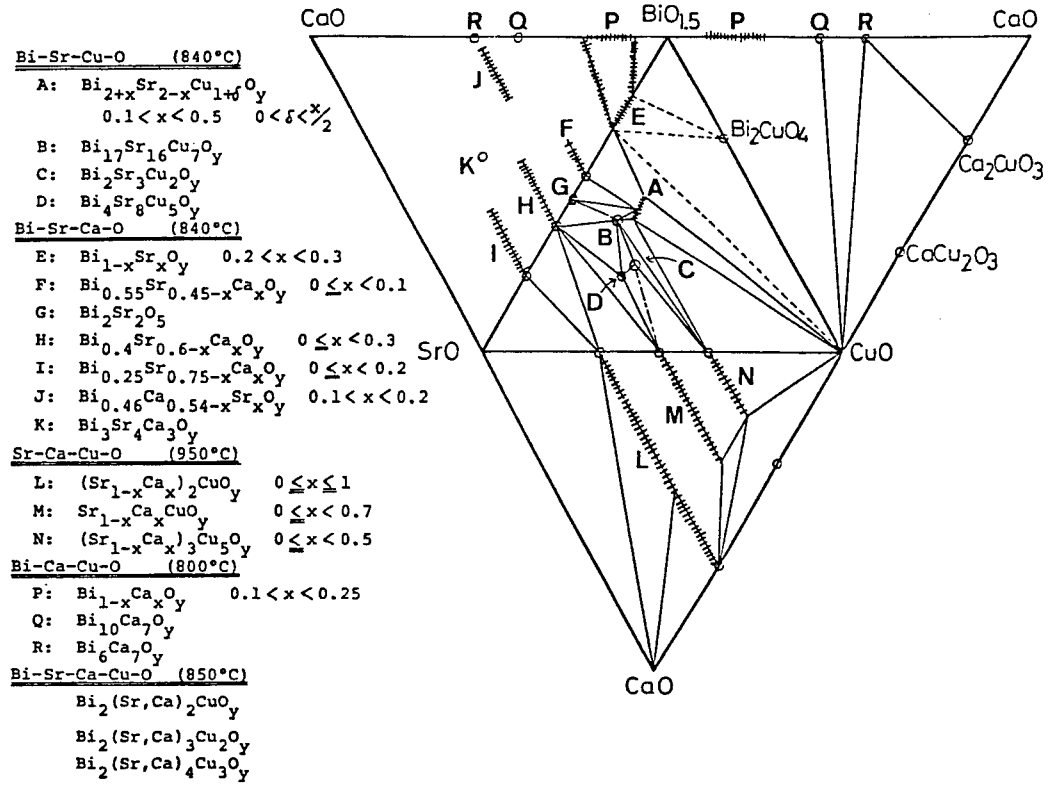

Bi-Sr-Cu-O (840°C)

A: $Bi_{2+x}Sr_{2-x}Cu_{1+\delta}O_y$ $0.1 < x < 0.5$ $0 < \delta < x/2$

B: $Bi_{17}Sr_{16}Cu_7O_y$

C: $Bi_2Sr_3Cu_2O_y$

D: $Bi_4Sr_8Cu_5O_y$

Bi-Sr-Ca-O (840°C)

E: $Bi_{1-x}Sr_xO_y$ $0.2 < x < 0.3$

F: $Bi_{0.55}Sr_{0.45-x}Ca_xO_y$ $0 \leq x < 0.1$

G: $Bi_2Sr_2O_5$

H: $Bi_{0.4}Sr_{0.6-x}Ca_xO_y$ $0 \leq x < 0.3$

I: $Bi_{0.25}Sr_{0.75-x}Ca_xO_y$ $0 \leq x < 0.2$

J: $Bi_{0.46}Ca_{0.54-x}Sr_xO_y$ $0.1 < x < 0.2$

K: $Bi_3Sr_4Ca_3O_y$

Sr-Ca-Cu-O (950°C)

L: $(Sr_{1-x}Ca_x)_2CuO_y$ $0 \leq x \leq 1$

M: $Sr_{1-x}Ca_xCuO_y$ $0 \leq x < 0.7$

N: $(Sr_{1-x}Ca_x)_3Cu_5O_y$ $0 \leq x < 0.5$

Bi-Ca-Cu-O (800°C)

P: $Bi_{1-x}Ca_xO_y$ $0.1 < x < 0.25$

Q: $Bi_{10}Ca_7O_y$

R: $Bi_6Ca_7O_y$

Bi-Sr-Ca-Cu-O (850°C)

$Bi_2(Sr,Ca)_2CuO_y$

$Bi_2(Sr,Ca)_3Cu_2O_y$

$Bi_2(Sr,Ca)_4Cu_3O_y$

Fig. 1. Phases formed in the Bi-Sr-Ca-Cu-O system and the relation between them.

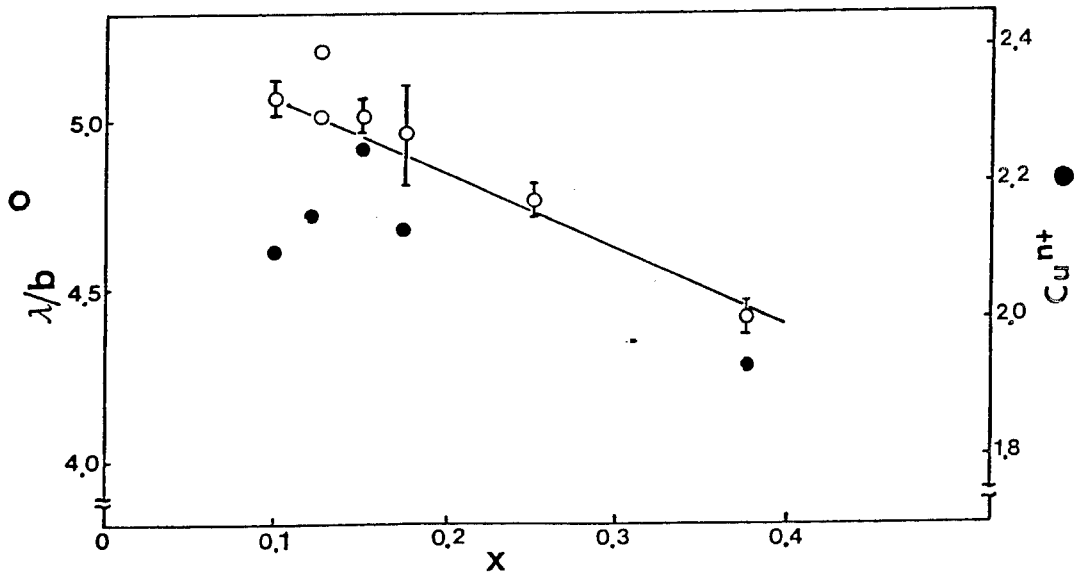

Fig. 2. Variations of the modulation period and the nominal Cu valence in solid solution A (see Fig. 1).

other, which are also plotted vs. x in Fig. 2. The valence shows a peak value of 2.25 at x=0.15, while it decreases to 2.10 at x=0.10 and 1.9 at x=0.50. It should be emphasized here that it is only x=0.10 that shows a well-defined superconducting transition as examined by measurements of electrical resistance and d.c. magnetization (T_c^{onset}=10K, T_c^{end}=7K). It is possible that a good deal of holes for x>0.10 tend to be trapped locally when the layers are modulated in shorter periods.

ii) The high-T_c (m=3) phase

It is now well-known that addition of lead to the Bi-Sr-Ca-Cu-O system drastically facilitates the formation of the high-T_c phase as typically shown in ref. 6. Lead has been found to induce a partial melting involving the m=2 phase and Ca_2PbO_4 which pre-exist, and the high-T_c phase seems to precipitate from the molten phase [7]. Lead substitutes at the bismuth sites, and the modulation is changed not only in its period along the b axis but also in symmetry [8]. And an investigation over a wide composition range has revealed that the new mode with $\lambda/b=8.7$ appears uniquely at Pb/Bi$\sim$1/5, while the new and the conventional ($\lambda/b\sim5$) modes are mixed at Pb/Bi$\sim$1/9 [9]. These findings clearly show that the lead-free and the Pb/Bi$\sim$1/5 phases should be considered as different phases. However, irrespective of these compositional and structural changes, T_c remains almost unaffected [9].

In our earliest paper [6], we suggested that the lead substitution might have increased the thermodynamical stability of the high-T_c phase. But this may be wrong as shown below. On annealing the high-T_c phase samples at 973K in air, a very interesting chemical reaction occurs. The electron diffraction pattern of the as-prepared sample (Fig. 3a) shows a modulation period of $\lambda/b=8.7$, while, after the annealing, only the conventional mode can be seen (Fig. 3c). This change can be understood, if

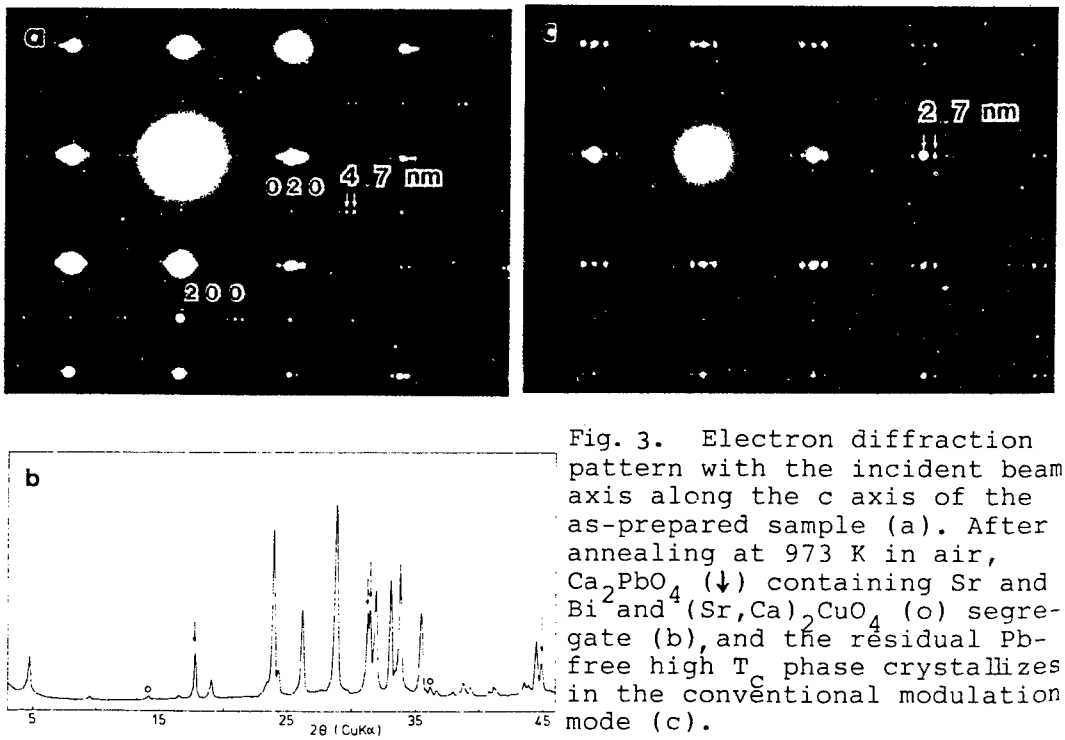

Fig. 3. Electron diffraction pattern with the incident beam axis along the c axis of the as-prepared sample (a). After annealing at 973 K in air, Ca_2PbO_4 (↓) containing Sr and Bi and $(Sr,Ca)_2CuO_4$ (o) segregate (b), and the residual Pb-free high T_c phase crystallizes in the conventional modulation mode (c).

one looks into the XRD pattern shown in Fig. 3b. A Ca_2PbO_4-like phase involving strontium and bismuth as found by an EPMA analysis and $(Sr,Ca)_2CuO_3$ segregates on annealing. However, the XRD peaks of the high-T_c phase remain sharp enough in comparison with those measured before the annealing. SEM observations also showed that the plate-like particles of the high-T_c phase remained intact expect that they carried fine particles of the segregated phases on their surfaces. Quite the same behavior was observed even at Pb/Bi_1/9. These results have strongly suggested that the lead-free high-T_c phase is more stable than the lead-substituted high-T_c phase. The most important role of lead has thus been considered as the induction of the partial melting.

Knowledge of the phase relation in the BSCCO system and of the effects of lead would be useful in finding a new, more advantageous reaction process that leads to microstructure of the high-T_c phase suitable for the purpose of technical applications.

iii) Magnetic Suspension due to the Meissner Effect

It is well-known that a superconducting specimen can be levitated on a magnet by the Meissner effect. If the specimen is provided with effective flux-pinning centers, it can be suspended under a magnet after a flux penetrating operation. Huang at al.[10] showed that a composite of YBCO and AgO having a strong pinning force floated below a cylindrical permanent magnet balancing with the gravity.

A sintered pellet of the above mentioned high-T_c phase has recently been found to be magnetically suspended [11]. It is very impressive to watch a pair of pellets floating above and below a magnet. However, the sample pellet is monophasic, and the magnetization curve plotted in Fig.4 shows that the pinning force is rather weak. The permanent magnet used is, on the other hand, not cylindrical but ring-shaped. Kitaguchi at al. [11] have invented a new magneto-balancing method to analyze the force exerted by the magnet and have concluded that the suspension is due to the Meissner effect rather than the pinning effect.

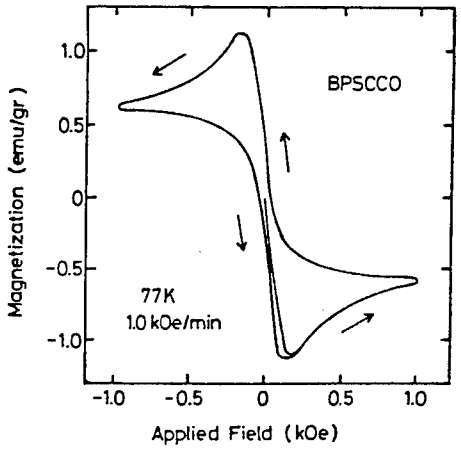

Fig. 4. Magnetization curve of a sintered pellet of the high-T_c phase at 77 K measured after cooling in zero-field. H_{max} = 1.0 kOe and dH/dt = 1.0 kOe/min.

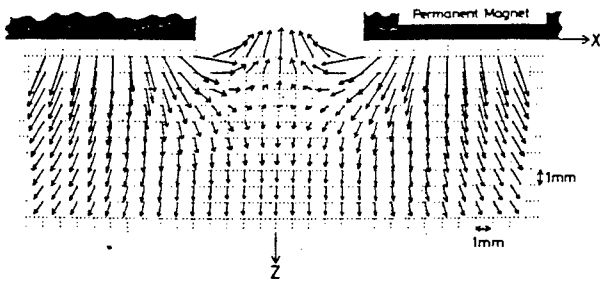

Fig. 5. Map of the magnetic field vector calculated for the ring-shaped permanent magnet (NEOMAX, 38 mm in outer-diameter, 10 mm in inner diameter, 7.2 mm in thickness, and Br = 11150 G).

Figure 5 illustrates the magnetic field map for the magnet used (NEOMAX,38mm in outer-diameter, 10mm in inner-diameter, 7.2mm in thickness,and Br=11150 G). It can be readily seen that a pair of ellipsoidal magnetic cavities are formed above and below the magnet. By moving the sample pellet through the magnet ring using the experimental system schematically shown in Fig.6, the force between the sample and the magnet was measured as a change in the magnet weight as a function of the distance between them. The experimental data are plotted in Fig. 7, where the Z axis passes vertically through the center of the magnetic ring. These are in good agreement with the magnitude of the force, F=Mz(H/ z), calculated using the data given in Figs.4 and 5. It is evident in the hysteresis seen in Fig. 7 that the weak flux pinning reduces the attractive force. We thus have concluded that the sample pellet is trapped in the magnetic hole owing to the Meissner effect. It should be noted here that a strong restoring force is exerted in the same way within the xy plane and, so, a pair of sample pellets do not drop but change their positions when the magnet is turned over.

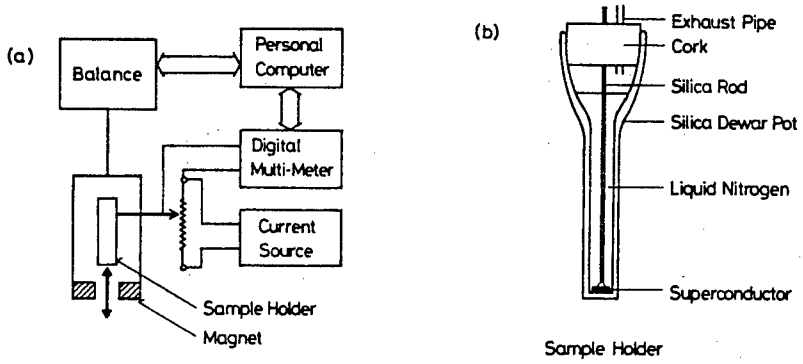

Fig. 6. System for the measurement of the magnetic force exerted upon the permanent magnet (a). The sample holder (b) was moto-driven through the magnet ring at about 2 mm/s.

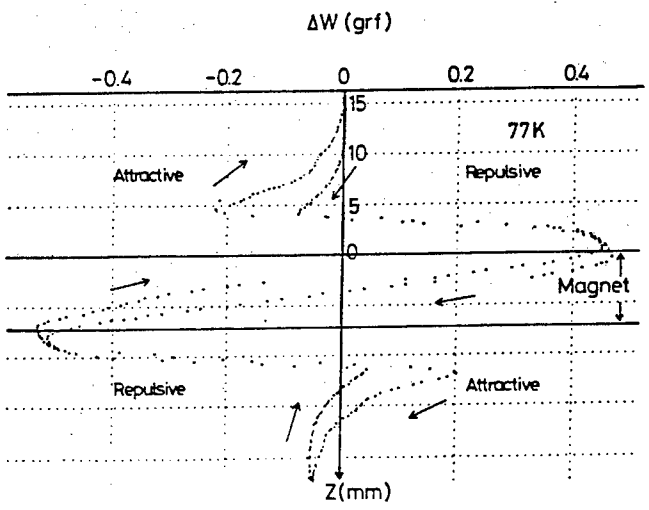

Fig. 7. Magnetic force measured as a function of the distance between the permanent magnet and the superconducting pellet.

REFERENCES

1) C. Michel, M. Hervieu, M. M. Borel, A. Grandin, F. Deslandes, J. Provost and B. Raveau, Z. Phys. B68 (1987) 421.
2) J. Akimitsu, A. Yamazaki, H. Sawa and H. Fujiki, Jpn. J. Appl. Phys. 27 (1988) L2080.
3) H. Maeda, T. Tanaka, M. Fukutomi and T. Asano, Jpn. J. Appl. Phys. 27 (1988) L209.
4) E. Takayama - Muromachi, Y. Uchida, Y. Matsui, M. Onoda and K. Kato, Jpn. Appl. Phys. 27 (1988) L556.
5) M. Takano, Y. Ikeda, J. Takada, K. Oda, H. Kitaguchi, Y. Miura, Y. Tomii and H. Mazaki, Proc. MRS Int. Meet. Adv. Mat., Tokyo, May 30 - June 3, 1988 (MRS, Pittsburg, 1988) and Y. Ikeda et al., to be submitted.
6) M. Takano, J. Takada, K. Oda, H. Kitaguchi, Y. Miura, Y. Ikeda, Y. Tomii and H. Mazaki, Jpn. J. Appl. Phys. 27 (1988) L1041.
7) T. Hatano, K. Aota, S. Ikeda, K. Nakamura and K. Ogawa, Jpn. J. Appl. Phys. 27 (1988) L2055.
8) S. Ikeda, K. Aota, T. Hatano and K. Ogawa, Jpn. J. Appl. Phys. 27 (1988) L2040.
9) Y. Ikeda, M. Takano, Z. Hiroi, K. Oda, H. Kitaguchi, J. Takada, O. Yamamot and H. Mazaki, Jpn. J. Appl. Phys. 27 (1988) L2067.
10) C. Y. Huang, Y. Shapira, E. J. McNiff, Jr., P. N. Peters, B. B. Schwartz, M. K. Wu, R. D. Shull and C. K. Chiang, Modern Phys. Lett. B2 (1988) 869.
11) H. Kitaguchi. J. Takada, K. Oda, A. Osaka, Y. Miura, Y. Tomii, H. Mazaki and M. Takano, Physica C, in press.

THE CRYSTAL STRUCTURES OF THE SUPERCONDUCTING PHASES IN THE TL-BA-CA-CU-O SYSTEM

Jing-kui LIANG, Yu-ling ZHANG, Jiu-qi HUANG, Si-shen XIE, Xiang-rong CHENG and Zhong-xian ZHAO
Institute of Physics, Chinese Academy of Sciences, Beijing

1. INTRODUCTION

After the discoveries of the high Tc superconductors in the R-Ba-Cu-O system (R-rare earth element) and in the Bi-Sr-Ca-Cu-O system [1-16], superconductor with Tc(0) above 120K was discovered in the Tl-Ba-Ca-Cu-O system [17-19]. In this article, we review the crystal structures of the superconducting phases in the Tl-Ba-Ca-Cu-O system determined by means of X-ray powder diffraction in our institute [20-27].

2. EXPERIMENTAL

The starting materials were analytical pure Tl_2O_3, BaO, CaO and CuO powder reagents. The appropriate amounts of them were mixed, ground and pressed into disc shape pellets. The pellets were sintered at 790 °C or 800 °C in air or in oxygen atmosphere for 8 h, and then cooled to room-temperature in the furnace. Some sample were annealed at 600 °C in air for 6 h. Thirty samples with different compositions were prepared.

The diffraction data were collected with Guinier-de Wolff monochromatic focusing camera (CoK_α radiation) and with Philips APD-10 auto-powder diffractometer (CuK_α radiation). Pure Si was used as internal standard.

3. EXPERIMENTAL RESULTS AND DISCUSSIONS

The results of the X-ray diffraction phase identification indicated that all samples were multi-phase in strict speaking. Apart from a small amount of other superconducting phases with different lattice constant c, CuO and $BaCuO_2$, most of the samples mainly contained one superconducting phase.

We had pointed out that there exist several superconducting phases and found that all of the phases with the planar distance d_1 of the first diffraction lines at 20.9Å, 18.7Å, 17.9Å, 15.9Å, 14.7Å, 12.7Å and 11.6Å may be superconducting phases (see reference [22]). Soon later, the above prediction had been confirmed by our work and others. Actually we found that the crystal structures of these superconducting phases are similar to each other; all of them belong to tetragonal system with same lattice constant a and different lattice constants c; the number of the stacking layers along Z axis is different and all of cations are arranged alternately at the positions of (0,0,z) and (1/2,1/2,z).

Tab.1 The lattice constants of $TlBa_2Ca_{n-1}Cu_nO_{2n+2.5}$ and $Tl_2Ba_2Ca_{n-1}Cu_nO_{2n+4}$

compound	$TlBa_2Ca_{n-1}Cu_nO_{2n+2.5}$				$Tl_2Ba_2Ca_{n-1}Cu_nO_{2n+4}$			
n	1	2	3	4	1	2	3	4
a(Å)	3.847	3.847	3.847	3.847	3.847	3.847	3.847	3.847
c(Å)	9.60	12.73	15.89	18.73	23.23	29.43	35.82	41.60
V($Å^3$)	142.1	188.4	235.2	277.2	343.8	435.6	530.1	615.7
(g/cm^3)	7.18	6.61	6.25	6.12	8.14	7.46	6.98	6.74

Tab.2 The atomic parameters of the crystal structures of $TlBa_2Ca_{n-1}Cu_nO_{2n+2.5}$ and $Tl_2Ba_2Ca_{n-1}Cu_nO_{2n+4}$ (n=1, 2, 3, 4)

n	ion	x	y	z	n	ion	x	y	z
1	1Cu	1/2	1/2	0	1	2Cu	1/2	1/2	0
	2Ba	0	0	0.201		4Ba	0	0	0.083
	1Tl	1/2	1/2	0.5		4Tl	0	0	0.297
	2O(1)	0	1/2	0		4O(1)	0	1/2	0
	2O(2)	1/2	1/2	0.210		4O(2)	0	0	0.410
	1O(3)	0	0	0.5		4O(3)	0	0	0.210
2	1Ca	0	0	0	2	2Ca	0	0	0
	2Ba	0	0	0.281		4Ba	0	0	0.115
	1Tl	1/2	1/2	0.5		4Tl	0	0	0.285
	2Cu	1/2	1/2	0.127		4Cu	0	0	0.450
	4O(1)	0	1/2	0.127		8O(1)	0	1/2	0.450
	2O(2)	1/2	1/2	0.281		4O(2)	0	0	0.200
	1O(3)	0	0	0.5		4O(3)	0	0	0.380
3	2Ca	0	0	0.100	3	4Ca	1/2	1/2	0.045
	2Ba	0	0	0.320		4Ba	0	0	0.145
	1Tl	1/2	1/2	0.5		4Tl	0	0	0.277
	1Cu(1)	1/2	1/2	0		2Cu(1)	1/2	1/2	0
	2Cu(2)	1/2	1/2	0.200		4Cu(2)	0	0	0.410
	2O(1)	0	1/2	0		4O(1)	0	1/2	0
	4O(2)	0	1/2	0.200		8O(2)	0	1/2	0.087
	2O(3)	1/2	1/2	0.325		4O(3)	0	0	0.350
	1O(4)	0	0	0.5		4O(4)	0	0	0.215
4	1Ca(1)	0	0	0	4	2Ca(1)	0	0	0
	2Ca(2)	0	0	0.166		4Ca(2)	0	0	0.076
	2Cu(1)	1/2	1/2	0.083		4Cu(1)	0	0	0.462
	2Cu(2)	1/2	1/2	0.250		4Cu(2)	0	0	0.386
	2Ba	0	0	0.353		4Ba	0	0	0.160
	1Tl	1/2	1/2	0.500		4Tl	0	0	0.274
	4O(1)	0	1/2	0.083		8O(1)	0	1/2	0.462
	4O(2)	0	1/2	0.250		8O(2)	0	1/2	0.386
	2O(3)	1/2	1/2	0.353		4O(3)	0	0	0.338
	1O(4)	0	0	0.500		4O(4)	0	0	0.220

According to the chemical compositions determined by electron energy spectrum analyses, the crystal structures of $Tl_2Ba_2CaCu_2O_8$ (2212) and $Tl_2Ba_2Ca_2Cu_3O_{10}$ (2223) (Other superconducting phases are also represented by symbols of the same

type) were determined by X-ray powder diffraction method [23,25]. They belong to body-centered tetragonal system. The arrangement order of layers along Z axis are as following: the Cu-O layer is adjacent to the Ca layer and the Ba-O layer; the Ba-O layer is adjacent to the Cu-O layer and the Tl-O layer; the Tl-O layer is adjacent to the Tl-O and the Ba-O layer; the Ca layer is adjacent to two Cu-O layer. The interlayer distances between two cation layers in different superconducting phases are approximately same. The interlayer distances of Ca-Cu, Cu-Ba, Ba-Tl and Tl-Tl are 1.47-1.61Å, 1.91-1.97Å, 2.86-2.79Å and 2.06-1.93Å respectively. Hence, according to the d_I value or the lattice constant c and the above mentioned relationships among cation arrangements, the ideal chemical formula can be deduced and the positions of cations can be determined roughly. The positions of oxygen anions can be determined according to the ionic interdistances, the coordination number and Pauling rule. And then the atomic parameters are refined according to the intensities of diffraction lines. The crystal structures of the other six superconducting phases in the Tl-Ba-Ca-Cu-O system were determined with this method. The lattice constants and atomic parameters are listed in Table 1, and Table 2. The crystal structures are shown in Fig. 1 and Fig. 2 (only c/2 period).From the figures, we can find out that all of cations are arranged alternately at the positions of (0,0,z) and (1/2,1/2,z)

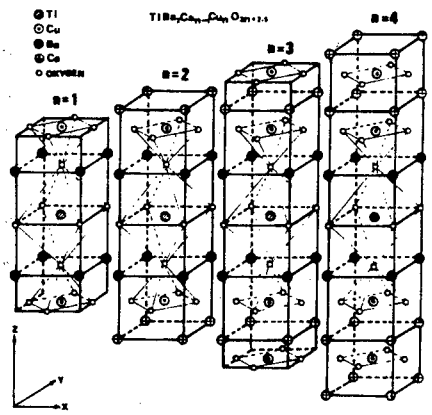

Fig.1 The crystal structures of $TlBa_2Ca_{n-1}Cu_nO_{2n+2.5}$

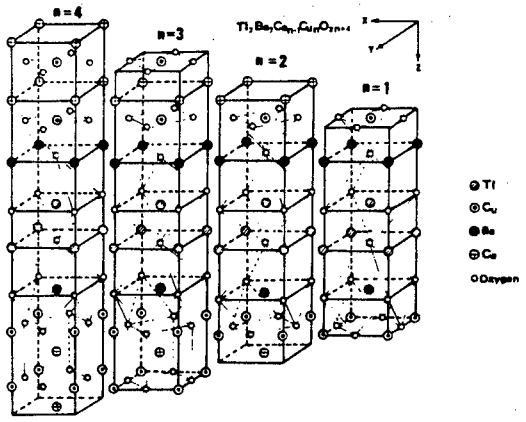

Fig.2 The crystal structures of $Tl_2Ba_2Ca_{n-1}Cu_nO_{2n+4}$

Under our synthetic conditions, samples which mainly contain (1212) or (1223) or (2212) or (2223) can be obtained. The zero resistance temperature of above mentioned superconducting phases are 75-90K (depending on the sintering condition,the existence of other phase), 110K, 100K and 120K respectively. Other four superconducting phases, (1201), (2201) (1234) and (2234) as minor phases coexist with other superconducting phases; but they are unambiguous exist. The low

angle diffraction lines of these eight superconducting phases in the Tl-Ba-Ca-Cu-O system are showed in Fig. 3. (CoK_α radiation) The intensity of diffraction line (001) of (1201) phase is very weak. The existence of this phase was discovered by TEM [28] and confirmed by x-ray diffraction lines.

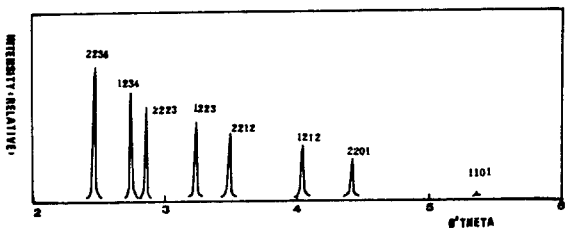

Fig. 3 The first diffraction line of the superconducting phases in the Tl-Ba-Ca-Cu-O system.

The crystal structures of the superconducting phases in the Tl-Ba-Ca-Cu-O system are divided into two types. The first type with single Tl-O layer belongs to primary tetragonal lattice (P4/mmm); its ideal chemical formula is $TlBa_2Ca_{n-1}Cu_nO_{2n+2.5}$. (n=1, 2, 3 and 4). The second type with double Tl-O layers belongs to body-centered tetragonal lattice (I4/mmm); its chemical formula is $Tl_2Ba_2Ca_{n-1}Cu_nO_{2n+4}$ (n=1, 2, 3 and 4). The crystal structures of these superconducting phases are closely related to each other. When a Tl-O layer is inserted into a primary tetragonal lattice, the d_t is increased by 2Å, there must be a displacement of (1/2,1/2) in X-Y plane between the two Tl-O layers in order to hold dense stack, the primary tetragonal lattice transfers into a body-centered tetragonal lattice and the lattice constant c is doubled. For single Tl-O intercalation or double Tl-O intercalation superconducting phases, the d_t is increased by 3.15Å when n is increased by 1.

From the point of view of the crystal structure, the crystal structure of the superconducting phases in the R-Ba-Cu-O system, the Bi-Sr-Ca-Cu-O system and the Tl-Ba-Ca-Cu-O system are composed of two units which are arranged along Z axis in a tetragonal lattice or a pseudo-tetragonal lattice. The two units are an intercalation (such as rare earth metals, Tl, Bi) and an oxygen-deficient pseudo-perovskite unit $M_{n\pm1}Cu_nO_{2n\pm1}$ (M is a alkali-earth atom and the atomic radius of which can be accord with the demand of perovaskite structure, such as Ba, Sr, Ca) In the R-Ba-Cu-O system, the number of M is n-1; while in the Bi-Sr-Ca-Cu-O system and in the Tl-Ba-Ca-Cu-O system, the number of M is n+1. The arrangement of cations in an oxygen-deficient pseudo-perovskite unit are listed in Table 3. The arrangement of cations in an oxygen-deficient pseudo-perovkite unit is the same in both a primary lattice and a body-centered tetragonal lattice.

In the Tl-Ba-Ca-Cu-O system, the crystal structures of the superconducting phases are quite similar to each other. The differences of the formation free energy of these superconducting phases are small. Under common synthesis conditions, several superconducting phases can be formed. It is possible that two different types of oxygen-deficient pseudo-

perovskite units can be stacked on both sides of a Tl-O layer. The intergrowth of two superconducting phases with lattice constant c 30Å and 36Å was observed under high resolution electronic microscope [29]. It is difficult to obtain single phase.

Table 3 The arrangements of cations along Z axis in the oxygen-deficient pseudo-perovskite unit $M_{n\pm1}Cu_nO_{2n\pm1}$

n	$M_{n+1}Cu_nO_{2n+1}$ (1)	
	Tl-Ba-Ca-Cu-O system (2)	Bi-Sr-Ca-Cu-O system (3)
1	Ba-Cu-Ba	Sr-Cu-Sr
2	Ba-Cu-Ca-Cu-Ba	Sr-Cu-Ca-Cu-Sr
3	Ba-Cu-Ca-Cu-Ca-Cu-Ba	Sr-Cu-Ca-Cu-Ca-Cu-Sr
4	Ba-Cu-Ca-Cu-Ca-Cu-Ca-Cu-Ba	--
n	$M_{n-1}Cu_nO_{2n-1}$ (1)	
	La-Ba-Cu-O system	Y(R)-Ba-Cu-O system
1	Cu (4)	-
2	-	-
3	Cu-Ba-Cu-Ba-Cu (5)	Cu-Ba-Cu-Ba-Cu (5)

Note: (1) M can be one kind of alkali-earth metal or more than one kind.

(2) The superconducting phases containing single Tl-O intercalation and double Tl-O intercalation layers are obtained.

(3) The superconducting phases containing double Bi-O are obtained, (but the superconducting phase containing single Bi-O layer is not obtained).

(4) When n=1, only the superconducting phase containing double La-O intercalation is obtained (K_2NiF_4 type structure).

(5) When n=3, only the superconducting phases with single intercalation Y (La or other rare earth element) are obtained.

The Tc of the superconductor increase with the number of Cu-O layers, which play important role in high Tc superconductivity. P. Haldear et al [30] pointed out that the lg(Tc) is proportional to 1/f, in which $f=(nC_{Cu}+C_{Tl})I/c$, C_{Cu}=3.1Å, C_{Tl}=2Å, I=1 (for single Tl-O intercalation), 2 (for double Tl-O intercalation), in the Tl-Ba-Ca-Cu-O system and in Bi-Sr-Ca-Cu-O system. When 1/f is extrapolated to 1/f=1, i.e. the oxide contained no intercalation but only oxygen-deficient pseudo-perovskite unit, Tc will reach 185K. As a matter of fact, the oxide which does not contain intercalation is non-superconductor. So, we believe that intercalation is indispensable to high Tc superconductor, the Tc relates not only to the number of Cu-O layer but also to the number of layers in a intercalation and the property of intercalation. The thicker the intercalation, the higher Tc. The Tc of superconducting phase contained double Tl-O layer is 10-20K higher the Tc of the superconducting phase with only single Tl-O layer. Under the condition that the crystal structures are same, the Tc of superconducting phase in Tl-Ba-Ca-Cu-O system is about 20K higher than that of the superconducting phase in Bi-Sr-Ca-Cu-O system. The main ways to increase Tc is to

improve the sintering condition, to increase the layers in oxygen-deficient pseudo-perovskite unit, to improve the property of intercalation and to increase the number of layer in the intercalation.

4. CONCLUSIONS

Eight superconducting phases were determined by X-ray powder diffraction method. The lattice constant a of the eight superconducting phases are same, while the lattice constants c of these superconducting phases are different. These superconducting phases are divided into two types. One type has only single Tl-O layer; it belongs to primary tetragonal lattice with space group P4/mmm; its ideal chemical formula is $TlBa_2Ca_{n-1}Cu_nO_{2n+2.5}$ (n=1,2,3,4). Another type contains double Tl-O layer; it belongs to body-centered tetragonal lattice with space group I4/mmm; its chemical formula is $Tl_2Ba_2Ca_{n-1}Cu_nO_{2n+4}$ (n=1,2,3,4). The relationship between the crystal structure and the superconductivity was discussed. The precise atomic parameters of the crystal structures, especially the atomic parameters of oxygen anions, can not be obtained until a single phase sample or single crystal is obtained.

REFERENCES

1. J.G. Bednorz and K.A. Muller, Z. Phys. B, 64(1986)189
2. M.K.Wu et al., Phys. Rev. Lett.,58(1987)908
3. Z.X.Zhao et al., Kexue Tongbao, 32(1987)661
4. P.H.Hor et al., Phys. Rev. Lett. 58(1987)1891
5. J.Cava et al., Phys. Rev. Lett., 58(1987)1676
6. W.I.F.David et al., Nature, 327(1987)310
7. J.D. Jorgensen et al., Phys. Rev. B, 36(1987)3608
8. Y.Le Page et al., Phys. Rev. B, 36(1987)3617
9. C.Michel et al., Z. Phys. B, 68(1987)421
10. H.Maeda et al., J. Appl. Phys., 27(1988)L209
11. C.W.Chu et al., Phys. Rev. Lett., 60(1988)941
12. Kazumasa Togano et al., Jpn. J. Appl. Phys. 27(1988)L323
13. R.M.Hazen et al., Phys. Rev. Lett. 60(1988)1174
14. S.S.Xie et al., Solid State Commun., 66(1988)1211
15. M.A. Subramanian et al., Science, 239(1988)1015
16. J.K.Liang et al., Modern Physics Lett. B, 2(1988)483
17. Z.Z. Sheng et al., Phys. Rev. Lett., 60(1988)937
18. Z.Z. Sheng and A.M. Hermann, Nature, 332(1988),55 and 138
19. Y.L.Zhang et al., Supercond. Sci. and Technol., 1(1988)92
20. J. K. Liang et al., Scientia Sinica, vol. 31, No. 12(1988)
21. J. K. Liang et al., Physica C 156(1988)616
22. J. K. Liang et al., Modern Phys. Lett. B, 2(1988)673
23. J. K. Liang et al., J. Phys. D, 21(1988)1031
24. J. K. Liang et al., Z. Phys. B (in press)
25. J. K. Liang et al., Physica Status Solidi (a) (in press)
26. J. K. Liang et al., Modern Phys. Lett. B (to be published)
27. J. Q. Huang et al., Modern Phys. Lett. B (to be published)
28. Y. Liu et al., J. Phys. C, 21(1988)L1039
29. K. K. Fung et al., Phys. Rev B (to be published)
30. P. Haldar et al., submitted to Science (preprint)

SYNTHESIS AND SUPERCONDUCTIVITY OF HIGH MULTI-CuO-LAYER $TlBa_2Ca_{n-1}Cu_nO_{2n+3}$ COMPOUNDS

Hideo IHARA, Ryouji SUGISE,* Takehiko SHIMOMURA,** Masayuki HIRABAYASI, Norio TERADA, Masatosi JO, Kunihiko HAYASHI and Madoka TOKUMOTO
Electrotechnical Laboratory, Umezono, Tsukuba, Ibaraki 305 Japan,*Ube Industries Ltd. Ube Yamaguchi 755 Japan, **Unitika R & D center, Uji Kyoto 611 Japan.

Abstract

The preparation process, lattice structure and superconducting properties of a new $TlBa_2Ca_{n-1}Cu_nO_{2n+3}$ superconductor family were studied. In the sample preparation process, phase transformation from $Tl_2Ba_2Ca_2Cu_3O_{10}$ (2223) to $TlBa_2Ca_3Cu_4O_{11}$ (1234) phase through $TlBa_2Ca_2Cu_3O_9$ (1223) phase was observed. The $TlBa_2Ca_4Cu_5O_{13}$ (1245) phase was prepared in a similar way from 2223 through 1234 phase.

The single Tl-O layered compounds have a simple tetragonal phase of the space group of P4/mmm. Electron diffraction patterns and lattice images from a high resolution TEM have confirmed that these compounds have an oxygen-deficient layered-perovskite structure. Their c-lattice constants follow the c-axis rule of linear relations of $c = 6.3 + 3.2\ n$ Å (n = the multiplicity of CuO layers). These compounds have Tc values of 50, 91, 117, 122 and 115 K for n=1, 2, 3, 4 and 5, respectively. The 1234 phase showed the highest Tc value in the $TlBa_2Ca_{n-1}Cu_nO_{2n+3}$ superconductor family.

1. Introduction

Search for new high-Tc superconductors is of great importance from both scientific and technological standpoints. Increasing the Tc value is a principal objective in materials design of oxide superconductors. For this purpose we have many empirical rules concerned with crystal structure, composition and electronic structure . One of the promising rules is the relationship between Tc value and the number of Cu-O layers derived from the layered perovskite compounds of $Tl_2Ba_2Ca_{n-1}Cu_nO_{2n+4}$ and $Bi_2Sr_2Ca_{n-1}Cu_nO_{2n+4}$.[1-3] If we can prepare a new superconducting compound with four or five Cu-O layers for example, the Tc value is expected to be higher than that of the $Tl_2Ba_2Ca_2Cu_3O_{10}$ (2223) phase[4].

Another purpose of materials design for Tl compounds is the reduction of Tl content, because of its toxicity and shortage in natural resources. The reduction seems to be possible, since Tl is thought to be merely a structural stabilizer and has no important direct role in superconductivity. Therefore the double Tl-O layers can be reduced to the single Tl-O layer. The increase in the number of Cu-O layers leads to a decrease in Tl content. Thus we intended to prepare a new superconductor with four or five Cu-O layers in single Tl-O layer compounds and also in double Tl-O layers compounds.[5]

In this work, we have synthesized new $TlBa_2Ca_3Cu_4O_{11}$ (1234) and $TlBa_2Ca_4Cu_5O_{13}$ (1245) superconductors with T_c of 122.1 and 117 K, respectively. The lattice structure of these compounds were determined by x-ray and electron diffraction and high resolution TEM (transmission electron microscope) measurements .

The idea of synthesis of single Tl-O layer compound is based on a condensation and polymerization reaction as in polymer science. At first, a double Tl-O layered compound with a small number of Cu-O layers is synthesized. Then the number of CuO layers is increased by evaporating the Tl component. Furthermore one of the two Tl-O layers of the double unit is evaporated to obtain the single Tl-O layer compound. A part of the single Tl-O layers is eliminated to further increase the multiplicity of Cu-O layers.

2. Experimental

The samples were prepared by firing the mixed powders of Tl_2O_3, CaO_2, BaO_2 and CuO with nominal compositions of $Tl_4Ba_2Ca_3Cu_4O_y$, $Tl_2Ba_2Ca_5Cu_6O_y$ and $Tl_{2.5}Ba_2Ca_4Cu_5O_y$ for 1234, 1245 and 2234 phases, respectively. The mixed powders of starting materials were pressed into pellets of diameter 10 mm and thickness 1mm under a pressure of 2000 kg/cm^2.

The pellets were fired at 885 ~ 890 °C for about 30 ~ 60 min in flowing oxygen gas. The firing time was determined by measuring the weight of the sample to know the quantity of evaporated Tl_2O_3. Then the samples were cooled in air to room temperature by taking them out of the furnace. The structure was determined by x-ray diffraction (XRD) with a Cu target, electron diffraction and high resolution TEM techniques.

3. Results and Discussion

The sample preparation process was monitored by weighing the sample pellets for sintering time as shown in Fig. 1 [6]. The decrease of the pellet weight is caused by the evaporation of Tl element. The X-ray powder diffraction patterns shows the 2223, 1223 and 1234 phases in Fig. 2. The characteristic peaks at 2 =5.0°, 5.6° and 4.6°, show the reflections from (002) plane of the 2223 plane, and (001) plane of the 1223 phase and (001) plane of the 1234 phase, respectively. The 2223 phase appeared after sintering for 15 min, then the 1223 phase came out with the decrease of peak intensity of the 2223 phase at 20 min. After 35 min sintering 2223 phase disappeared and 1223 phase becomes prominent. Father prolonged sintering the 1234 phase formed and increased in volume with disappearance of 1223 phase.

The mechanism of the phase transformation is not clear at present stage. In those phase transformation, two processes; order-disorder reconstruction process or intercalation process are possible. During these phase transformations the required Ca and Cu ions seem to be supplied from an amorphous phase coexisted with the crystal phase. The excess Ba ions seem to be excluded outside of the crystal phase. These facts are suggested by existence of amorphous phase from TEM observation and by easy formation of $BaCO_3$ after leaving the sample in air.

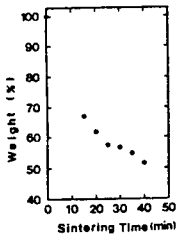

Fig. 1 Weight % ($W_{sintered}/W_{initial}$) of the sample pellet vs sintering time

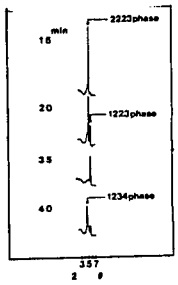

Fig. 2 Change of the x-ray diffraction patterns with sintering time.

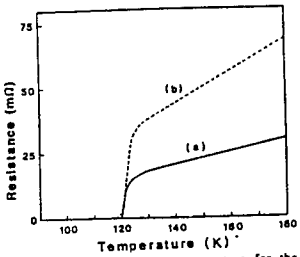

Fig. 3 Resistance versus temperature for the $TlBa_2Ca_3Cu_4O_{11}$ sample.

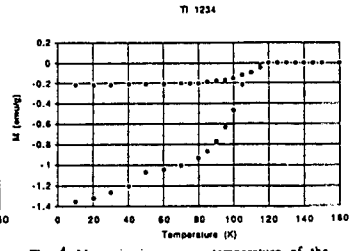

Fig. 4 Magnetization versus temperature of the $TlBa_2Ca_3Cu_4O_{11}$ (1234) sample under 100 Gauss.

a. $TlBa_2Ca_3Cu_4O_{11}$ (1234)

Figure 3 shows the temperature dependence of the resistance for the present low-Tl sample with 1234 phase. The T_{co}, T_c and T_{ce} values are 123.6, 121.9 and 120.6 K, respectively[5]. Magnetization measurement of Fig. 4 showed the onset temperature of superconducting transition at 122.0 K, which corresponds to the resistively measured Tc value. The amplitude of the Meissner signal in the 1234 phase sample is comparable to that in a well prepared $YBa_2Cu_3O_{7-y}$ superconductor[10] which indicates the bulk nature of superconductivity over 50 volume % of the 1234 phase.

The x-ray diffraction pattern shows a tetragonal structure with the lattice constants of a = b = 3.85 Å and c = 19.1 Å for the 1234 phase[5]. The phase is completely different from the previously reported 2212 and 2223 phases.[2, 7] The samples with the starting composition of $Tl_4Ba_2Ca_3Cu_4O_y$ have formed almost the single 1234 phase except for a small amount 2223, 2212 and amorphous phases. A trace of $BaCuO_2$ and amorphous phase was detected by the electron probe micro-analysis. Most of the peaks were identified only by the Miller indices of the 1234 phase.[5]

The composition of the tetragonal phase was determined as $TlBa_2Ca_3Cu_4O_{11}$ (1234) within an experimental error of 10 %. The result leads to the conclusion that the phase has single Tl-O layer and four Cu-O layers.

The electron diffraction pattern of [010] zone shows the simple tetragonal structure with the lattice constant of a=3.9 Å and c=19 Å as shown in Fig. 5.[7] A modulation with a period of (006) along the (00*l*) direction is obviously observed, which corresponds to the lattice parameter of 3.2 Å. The lattice image of Fig. 5 shows the periodic light and dark bands along

the c-axis. The image can be interpreted as a projected charge density of the crystal atoms. The period of a colinear dark spot lines separated by a wide light band is 19 Å. The light band corresponds to the light atoms of Cu and Ca, and the dark band to heavy atoms of Tl and Ba. Three colinear thick dark lines in the dark band along the a-axis are attributed to the single Tl layer and double Ba layers on both sides of the Tl layer. Seven colinear dark lines in the light band are attributed to the four Cu-layers and three Ca-layers stacking alternatively. The image of the Ca atom is smaller than that of the Cu atom because of the lack of d-electrons in the Ca atom. Each dark colinear line along the a-axis is assigned to each component atom as shown in Fig. 5.

The distance between Tl layers is 19 Å, which is consistent with the result of c=19.1 Å from the XRD measurement. The average space between the Cu layers in the lattice image corresponds to 3.2 Å, which is equal to the distance evaluated from the (006) periodic modulation in the (h0*l*) diffraction pattern. Then the space between the Tl and Cu layers is estimated as 4.75 Å. Each of the component atoms has the common distance of 3.9 Å along a-axis, which is consistent with the lattice constant of a=3.85 Å.

From these results, we can derive the simple tetragonal lattice structure of the 1234 phase as shown in Fig. 6. The unit cell consists of five-fold simple tetragonal sub-cells. Three-fold sub-cells in the middle part are composed of Cu and Ca atoms, of which the sub-lattice parameter along the c-axis is 3.2 Å. The sub-lattice parameter c (marked with c_1) is consistent with the length of 3.2 Å which corresponds to the period for periodic (006) modulation in the (h0*l*) diffraction pattern. The room between Cu-O layers is too small to be occupied by oxygen ions. Then oxygen vacancies are formed in the Ca layers of this 1234 phase as shown in Fig. 7 (b). Thus the 1234 phase is an oxygen deficient layered perovskite.[5, 8] On the other hand, both top and bottom tetragonal sub-cells are composed of Tl, Ba and Cu atoms, of which the sub-lattice parameter along the c-axis (marked with c_2) is estimated as 4.75 Å. From the lattice image , we can evaluate the distances between the Tl and Ba layers and between the Ba and Cu layers as 2.75 Å and 2.0 Å, respectively. The oxygen content of the 1234 phase is evaluated as 2n+3=11 from the lattice structure. The oxygen content is near to the observed value of 11.5 $\pm$ 1 by an inert gas fusion and non-dispersive IR method.

The primitive tetragonal lattice of Fig. 6 have the space group of P4/mmm.[8] The space group is the same as that of tetragonal $YBa_2Cu_3O_6$.[9] The observed lattice parameter c is consistent with the c-axis rule of c = 6.3+3.2n =19.1 Å (n=4) for the single Tl-O layer compound $TlBa_2Ca_{n-1}Cu_nO_{2n+3}$. [5] This c-axis rule can be derived from the c_1 and c_2 lattice parameters as c = (n-1) c_1 + 2 c_2

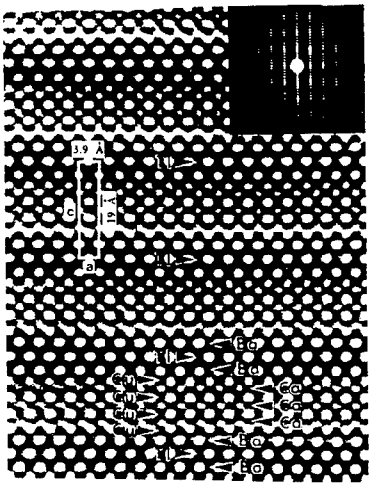

Fig. 5 The electron diffraction pattern and the lattice image of [010] zone of the 1234 crystal with the lattice constants of a = 3.9 Å and c = 19 Å.

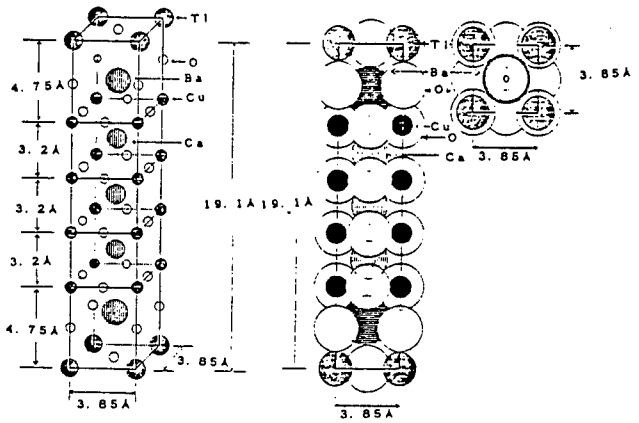

Fig. 6 (a) : The lattice structure of the 1234 crystal with the space group of P4/mmm and the lattice constants of a=b=3.85 Å and c=19.1 Å. (b) : Packing model of component ions of the 1234 crystal using realistic ion radius.

b. $TlBa_2Ca_4Cu_5O_{13}$ (1245)

Figure 7 shows the temperature dependence of the resistance for the 1245 phase sample. The resistive curve shows two-step drops as shown in earlier mixed phase Bi-Sr-Ca-Cu-O sample.[3] The high temperature drop shows a T_c value of 117 K, and the low temperature drop a T_c value of 108 K. The T_c at 117 K is attributed to the 1245 phase and the T_c at 108 K to the 1256 phase. The 1256 phase is sometimes observed in the lattice images from the high resolution TEM for the 1245 sample as an intergrowth phase. Another possibility, however, is not necessarily excluded. The high T_c might be attributed to the 1234 phase and the low T_c to the 1245 phase, because the 1234 phase usually has a wide range of Tc value (117 ~ 122 K). The 1234 phase was sometimes observed in the lattice images of the 1245 sample, though the 1234 phase was not detected in the x-ray diffraction pattern. At any rate the results lead to the fact that the 1245 phase has not shown a higher Tc value than the 1234 phase.

Figure 8 shows magnetization versus temperature for the 1245 phase sample measured at a field of 10 Gauss. The magnetization had a tendency to saturate above 10 Gauss. The magnetization curve shows the starting drop point of 117 K. The point corresponds to the resistively measured Tc value. Even though the amplitude of the Meissner signal is small in comparison with the 1234 phase by about a factor of 20, the Tc of 117 K is attributed to a bulk superconductor from the major 1245 phase and not from other minor 1256 nor 1234 phases in consideration of a smaller applied field by a factor 10 than in Fig. 4.

The x-ray diffraction pattern of the 1245 sample shows a tetragonal structure with the lattice constants of a = b = 3.85 Å and c = 22.2 Å. The result leads to the fact that the phase has single Tl-O layer and five Cu-O layers. The electron diffraction pattern and the lattice image viewed along [010] for the 1245 phase. The electron diffraction pattern of [010] zone gives the simple tetragonal structure with the lattice constant of a=3.9 Å and c=22 Å. From these results, we can derive the simple tetragonal lattice structure of the 1245 phase by adding CuO and Ca layers to the 1234 crystal lattice in Fig. 6 .

The oxygen content of the 1245 phase is evaluated as 2n+3=13 from the lattice structure. The oxygen content is near to the observed value of 13 $\pm$ 1. The observed c-lattice parameter is consistent with the c-axis rule of c = 6.3+3.2n = 22.3 Å (n=5) for the single Tl-O layer compound $TlBa_2Ca_{n-1}Cu_nO_{2n+3}$.[8]

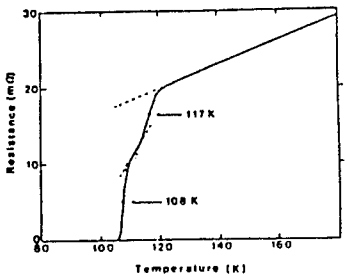

Fig. 7 Resistance versus temperature of the samples of $TlBa_2Ca_4Cu_5O_{13}$ (1245) phase.

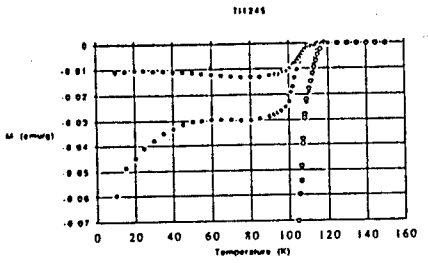

Fig. 8 Magnetization versus temperature of the 1245 sample under 10 Gauss.

4. Discussion

The new superconductor family of $TlBa_2Ca_{n-1}Cu_nO_{2n+3}$ (n=1 ~ 5) have shown c lattice constants of 9.4, 12.6, 15.9, 19.1 and 22.2 Å and counter to Tc values of 50, 91, 116, 122 and 117 K for n=1, 2, 3, 4 and 5, respectively . The Tc values follow the empirical formula of Tc= 121n exp (-n/4) as a function of n. Their lattice constants followed well the c-axis rule of c = 6.3+3.2n for the single Tl-O layer compound. The calculated and experimental lattice constants c are in good agreement within 0.1 Å. The highest Tc value was obtained for the n=4 phase. The average valence (z) of Cu ion in this $TlBa_2Ca_{n-1}Cu_nO_{2n+3}$ family is expressed as z = 2 + 1/n.[5] The structure with four Cu-O layers in a unit cell is responsible for the highest T_c value. This result would be explained by an average valence of the Cu ion of +2.25, or a Cu^{3+} ion concentration of 25 % .

The new high-Tc superconductors of single Tl-O layer compounds have less than half the Tl content of the previous 2223 phase. They are very important in science and technology, because of their new composition and structure, very high Tc and reduced thallium content.

The family of $Tl_2Ba_2Ca_{n-1}Cu_nO_{2n+4}$ (n=1 ~ 4) has been prepared and their lattice constants followed well the c-axis rule of c = 2(8.2+3.2n) for the double Tl-O layer compound. They have shown the c lattice constants of 23.2 , 29.3 , 35.6 and 42.0 Å and the Tc values of 80 K, 110 K, 127 K and 115 K for n=1, 2, 3 and 4, respectively as shown in Fig. 9 a 10. The Tc values follow the emperical formula of Tc= 115n exp (-n/3). The calculated and experimental lattice constants c are in good agreement. The highest Tc value was obtained for the n=3 sample. This result would be explained by the density of states at the Fermi level or proper carrier concentration. The density of states at the Fermi level would increase with number of CuO layers (n) upto a certain n, propably 3 or 4. The stoichiometric double Tl-O layer compound $Tl_2Ba_2Ca_{n-1}Cu_nO_{2n+4}$ has always divalent Cu^{2+} ions in contrast to single Tl-O compound $Tl_1Ba_2Ca_{n-1}Cu_nO_{2n+3}$ in which the averge valence (z) of Cu ion is expressed as z = 2 + 1/n.. Tl vacancies or their occupation by Cu or Ca ions are thought to contribute to the formation of higher valence Cu^{3+} ions. This is consistent with Tl deficient concentration in the high-Tc samples of double Tl-O layered compounds.

In summary, the new $TlBa_2Ca_3Cu_4O_{11}$ (1234) and $TlBa_2Ca_4Cu_5O_{13}$ (1245) superconductors with single Tl-O layer and four or five Cu-O layers have been designed and synthesized. They have T_c values of 122.1 and 117.0 K. Both phases have a simple tetragonal structure with the lattice constants of c=19.1 and 22.3 Å and the lattice constant of a=b=3.846 and 3.848 Å, respectively. The high-resolution electron microscopic measurement gave the simple tetragonal diffraction patterns, and the lattice images of the oxygen-deficient layered-perovskite structure with a single Tl-O layer alternating with four or five Cu-O layers. Their c-lattice constants follow the c-axis rule of c=6.3+3.2n [Å]. Their space group is P4/mmm. The phases have a large superconductor family of $TlBa_2Ca_{n-1}Cu_nO_{2n+3}$ (n=1, 2, 3, 4, 5, ----). Their Tc values follow some emperical fomulae and they are strongly related to the valence of Cu ion.

New high Tc oxide superconductor $Tl_2Ba_2Ca_3Cu_4O_{12}$ (2234) with double Tl-O layer and four Cu-O layers has a body-centered tetragonal structure with the lattice constant of a=b=3.85 Å and c=42.0 Å and its space group is I4/mmm. The lattice constant c follows well the c-axis rule of c = 2(8.2+3.2n) for the double Tl-O layer compound. The Tc value of its superconductor was 117 K, unexpectedly lower than the 127 K of the three Cu-O layer 2223 compound.

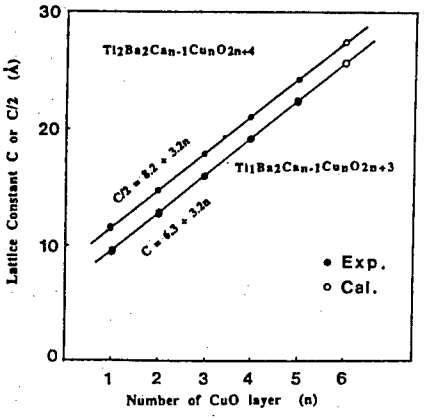

Fig. 9 The lattice constants c or c/2 versus the number of Cu-O layer for the $TlBa_2Ca_{n-1}Cu_nO_{2n+3}$ or $Tl_2Ba_2Ca_{n-1}Cu_nO_{2n+4}$ compounds, respectively. The lines are c=6.3+3.2n and c/2=8.2+3.2n. The filled circles are experimental ones and the open circles are calculated ones.

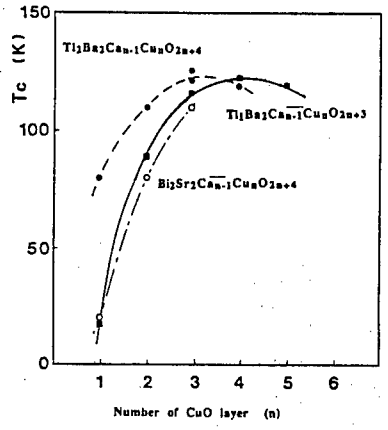

Fig. 10 Tc values versus the number (n) of Cu-O layers of $TlBa_2Ca_{n-1}Cu_nO_{2n+3}$ compounds compared with $Tl_2Ba_2Ca_{n-1}Cu_nO_{2n+4}$ and $Bi_2Sr_2Ca_{n-1}Cu_nO_{2n+4}$ compounds.

The authors gratefully acknowledge Messrs. T. Oosuna and K. Ibe for electron microscope measurement at JEOL.

References

[1] S. kondoh, Y. Ando, M. Onoda and M. Sato, Solid State Comm. , 65 1329 (1988).
[2] Z. Z. Sheng & A. M. Hermann, Nature 332, 55 (1988); R. M. Hazen, L. W. Finger, R. J. Angel, C. T. Prewitt, N. L. Ross, C. G. Hadidiacos, P. J. Heaney, D. R. Veblen, Z. Z. Sheng, A. Elali, A. M. Hermann, Phys. Rev. Letter. 60 1657 (1988).
[3] H. Maeda, Y. Tanaka, M. Fukutomi, T. Asano, Jpn. J. Appl. Phys. 27 209 1988.
[4] J. M. Wheatley, T. C. Hsu, P. W. Anderson, Nature 333 121 (1988).
[5] H. Ihara, R. Sugise, M. Hirabayashi, N. Terada, M. Jo, A. Negishi, M. Tokumoto, Y. Kimura, T. Shimomura, Nature 334 510 (1988). : H. Ihara, M. Hirabayashi, N. Terada, M. Jo, K. Hayasi, A. Negishi, M. Tokumoto, H. Oyanagi, R. Sugise, T. Shimomura and S. Ohasi, Proc. MRS Intern. Meeting on Advanced Materials (May 1988, Tokyo); IEEE Magn. MAG25 No.3 (1989).
[6] R. Sugise, M. Hirabayashi, N. Terada, M. Jo, T. Shimomura and H. Ihara; Jpn. J. Appl. Phys. 27 L1709 (1988).
[7] M. A. Subramanian, J. C. Calabrese, C. C. Torardi, J. Gopalakrishnan, T. R. Askew, R. B. Flippen, K. J. Morryssey, U. Chowdhry, A. W. Leight, Nature 332 420 (1988).
[8] H. Ihara, M. Hirabayashi, R. Sugise, N. Terada, M. Jo, K. Hayashi, M. Tokumoto, T. Shimomura and S. Ohashi, (in print Phys. Rev. B 38 No16 (1988)).
[9] J. D. Jorgensen, M. A. Beno, D. G. Hinks, L. Soderholm, K. J. Volin, R. L. Hitterman, J. D. Grace, Ivan K. Schuller, C. U. Segre, K. Zhang, M. S. Kleefisch, Phys. Rev. B 36 3608 (1987).
[10] M. Tokumoto, H. Ihara, T. Matsubara, M. Hirabayashi, N. Terada, H. Oyanagi, K. Murata, Y. Kimura, Jpn. J. Appl. Phys. 26 1565 (1987).

SINGLE CRYSTAL GROWTH AND CHARACTERIZATION OF BI2SR2CACU2O8

YAN Yifeng, CHU Xi, K.K.FUNG, YANG Qiansheng and Z.X. ZHAO
Institute of Physics, Chinese Academy of Sciences, Beijing

1. INTRODUCTION

Michel et al. described superconductivity at a temperature of 22K in the Bi-Sr-Cu-O system [1] and Maeda et al. observed superconductivity up to 105K in the multiphase Bi-Sr-Ca-Cu-O (BCSCO) system[2] . This has been confirmed by several groups[3,4]. It has been found that there are two layered phases responsible for the superconductivities. The phase responsible for 85 K superconductivity has commonly been identified to be the Bi2Sr2CaCu2O8 compound with an orthorhombic structure of a=5.41, b=5.42, c=30.78 Å respectively[7]. There is an incommensurate structure along b-axis which has been found [7] .The another phase which responsible for superconductivity at 110 K also has been identified to the Bi2Sr2CaCu2O8 compound with an orthorhombic structure of a=5.41, b=5.42 and c=36.82 Å, respectively[5]. All of the works metioned above were based on baulk samples. To futher study other physical properties of this superconducting system and understand the mechenism of high-Tc superconductivity, it is very important to growth large and high quality superconducting single crystals. In this paper we report the preparation of large and high quality plate-like single crystals with self-flux method and present the study of the crystals by X-ray procession technique and electron diffraction.

2. EXPERIMENTAL

Single crystals were grown by a self-flux method. The raw materials were prepared by first grounding high purity reagents of $CaCO_3$, $Sr(NO_3)_2$, Bi_2O_3 and CuO according to the formula of Bi:Sr:Ca:Cu=2:2:1:2 in a ball milling and put into a Al_2O_3 crucible. The mixture was calcined in a resistant furnace at a temperature of 865 °C and held for 7 hrs. The sintered powder was regrounded and put into the Al_2O_3 crucible which was then put back into the resistant furnace. The powder material was melt at 1025°C and soaked for 16 hrs at this temperature. After this, it was cooled down to 925°C at the rate of 80°C/hr and held for 8 hrs, then slowly cooled to 835 °C at rate of 1 °C/hr, and finally down to room temperature at the rate of 10°C/hr. No post annealing treatments were performed. In the final products, many plate-like single crystals are randomly stacked. The crystals are of irregular shape, have dark metallic luster, with typical dimenssions of 5 x 6 x 0.5 mm^3 (see fig.1), but some largest ones can be with dimmensions of 10 x 14 x 1 mm^3

3. EXPERIMENTAL RESULTS AND DISCUSSIONS

The resistivity of the single crystal was directly measured by a standard four-probe technique. By using high

quality silver paste, four gold wires with diameter of 0.05mm as the electrodes, were adapted on the surfaces of the crystal. The A.C magnetic susceptibility was detected by mutual

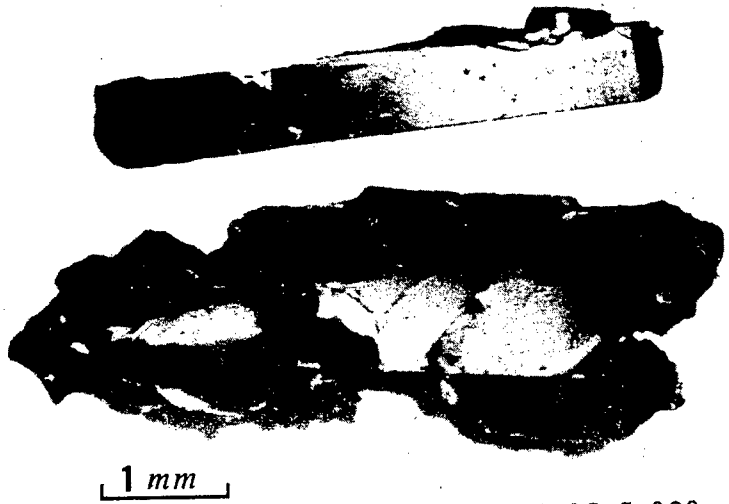

Fig.1 Optical photograph of Bi2Sr2CaCu2O8 single crystals

inductance method. Fig.2a show the result of resistivity measurement in a single crystal. The resistivity of the crystal at room temperature is 300 mΩ.cm. The superconductivity occurs at a temperature of 88 K and rearches zero resistivity at 85.8 K. It is obvious that a sharp diamagnetic drop occurs at around 84 K in the crystal from the A.C. magnetic measurement (see fig.2b).

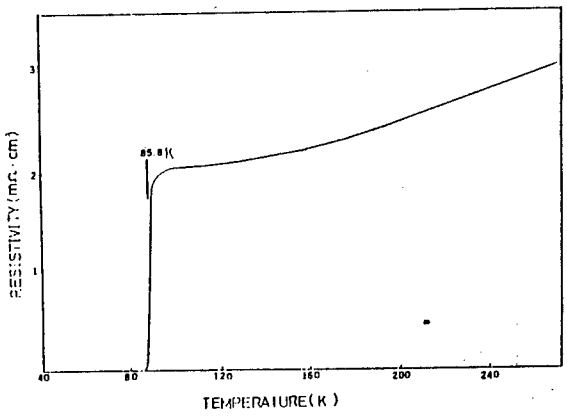

Fig.2a Temperature dependence of resistivity for the Bi2Sr2CaCu2O8 single Crystal.

X-ray procession photographs taken with filtered Mo-K radiation show that the a-,b-axes of the structure are parallel to the crystal plate and c-axis perpendicular to it. Figure 3 shows a first level procession photograph taken along

the c-axis. Satelite spots due to the modulation have been found to be along the b-axis. Procession photographs also

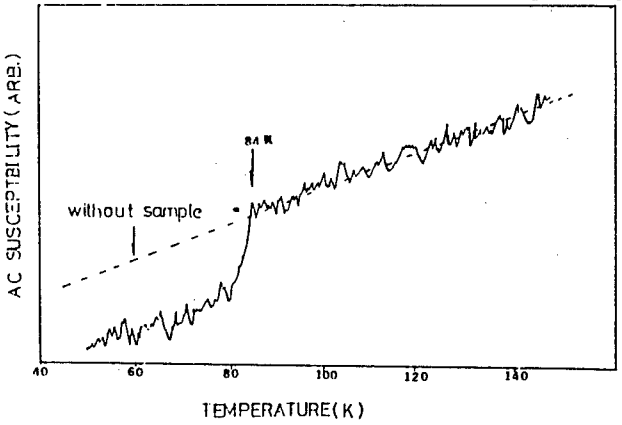

Fig.2b Temperature dependence of A.C magenization for the Bi2Sr2CaCu2O8 single crystal.

indicate a F-centered basic lattice with a=5.41, b=5.42 and c=30.78 Å respectively[14]. The determination of the composition of the crystal was done on a Philips 505 scanning microscope equipped with a fully computerised EDAX analysis system. Exciting voltage of 25kv was chosen for the experiment. A standard sample with the stoichometry of Bi:Sr:Ca:Cu =1:1:1:2

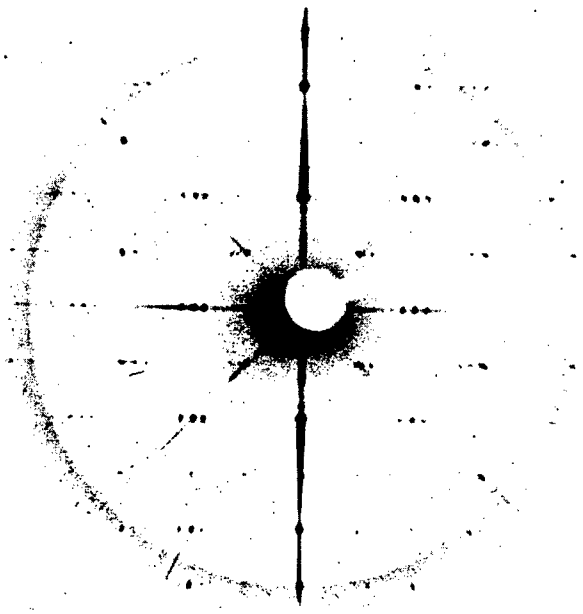

Fig.3 First level X-ray procession photograph at [001] for Bi2Sr2CaCu2O8 single Crystal.

was utilized to calibrate the experimental data. The composition of the single crystal is very close to $Bi_2Sr_2CaCu_3O_8$ and homogeneous through the sample.

Specimens for transmission electron microscopy in a Philips EM420 electron microscope were prepared by repeatedly cleaving the single crystal using cellotape into very thin

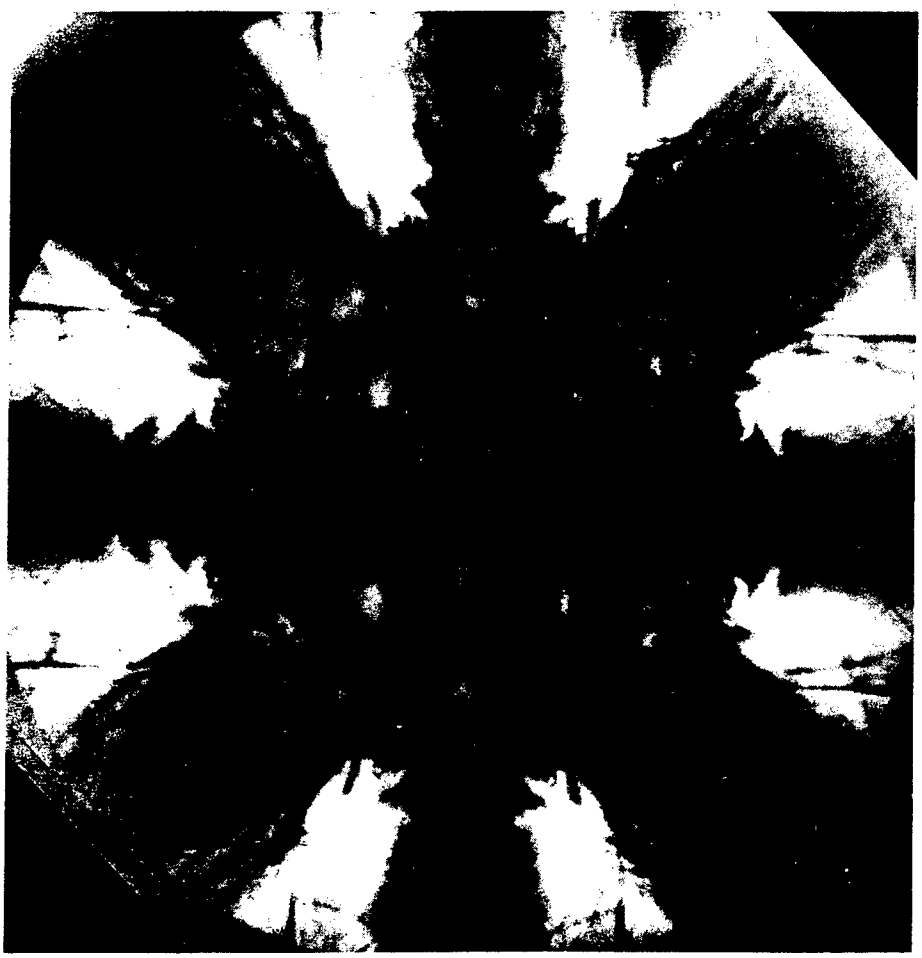

Fig.4 [001] Tanaka pattern showing 2mm symmetry

flakes. Specimens with extensive areas of uniform thickness and few dislocations were easily obtained. This should be compared with specimens from powdered compounds prepared by crushing the powder particles into minute particles. Defects, especially dislocations are necessarily induced by this processure. The quality of the cleaved specimens can be judged from the large angle convergent beam electron diffraction Tanaka pattern shown in Fig. 4 [8]. This is a [001] Tanaka pattern obtained from an area of about 3 um. The symmetry of the pattern is 2mm, the mirror planes being the a and b planes. The c plane is also a mirror plane. This is deduced from the (220) dark field pattern which shows clearly the presence of a twofold axis. The point group of the basic lattice is there-

fore mmm. The space group of Bi2Sr2CaCu2O8 is Fmmm, It should be pointed out that the crystals often contain growth faults, a common feature in layered compounds. [001] convergent beam electron diffraction patterns from such faulted crystals show a reduced symmetry of m, with the mirror plane being the a plane. The b mirror plane is lost.

4. CONCLUSIONS

From the view point of crystal growth, the slowly cooling rate (about 1 °C/hr.) is necessary for the growth of Bi2Sr2Ca-Cu2O8 single crystals because the long c-axis limited the growing rate of the crystals. In comparson to the crystals which grown at the cooling rate of 5 °C /hr from 925°C to 825°C [10], the dimensions of the crystals, which grown at the cooling rate of 1 °C /hr from 925 °C to 825°C at this experiment, become larger and the quality has also been improved. However, it is not to say the slower the cooling rate is, the better the crystals are, because the Bi_2O_3 compound very easy separates out around the melt point just as we have observed in some experiments [5] .

Acknowledgements

We thank Prof. C.Z. Li, Z.H. Mai for helpful discussions. Dr. D.N. Zheng, J.H. Wang assistance for the measurement of superconductivity and Prof. G.Z. Yang for encouragement.

REFERENCE

[1] C.Michel, M.Heriveu, M.M.Borel, A. Grandin,F.Deslandes, Ja. Provost and B. Raveau, Zeit. Phys. B68, 421(1987)

[2] H.Maeda,.Tanaka, M.Fukutomi and T.Asano, Jpn..Appl.Phys. 27, (1988).

[3] C.W.Chu, J.Bechtold, L.Gao, P.H.Hor, Z.J.Huang,R..Meng, Y.Y.Sun, Y.Q.wang and Y.Y.Xue, Phys. Rev. Lett. Vol.60, 941(1988).

[4] J.M.Tarascon, Y.Lepage, P.Barboux, B.G.Bagley, L.H.Greene, W.R.Mckinnon, G.W.Hull, M.Giroud and D.M.Hwang, Phys.Rev. B 37, 9382(1988)

[5] Y.F. Yan et al. (unpublished)

[6] Y.F. Yan, C.Z. Li, J.H. Wang, Y.C. Chang, Q.S. Yang et al., Modern Phys.lett.B, Vol.2, No. 2(1988) 571-575.

[7] X. Chu, Z.H.Mai, Y.F. Yan, et al. to be published in Modern Phys. Lett. B

[8] M. Tanaka, JEOL News 16E. No 3, 1978.

IN-SITU GROWTH OF YBCO SINGLE-CRYSTAL FILMS AT LOW TEMPERATURE

Yoshichika BANDO*, Takahito TERASHIMA*, Kenji IIJIMA**, Kazunuki YAMAMOTO**, Kazuto HIRATA**, Jun TAKADA**

* Institute for Chemical Research, Kyoto University, Uji, Kyoto-fu 611, Japan

** Research Institute for Production Development, Shimogamo, Sakyo-ku, Kyoto 606, Japan

1. INTRODUCTION

High-quality single-crystal thin films of high-T_c oxide superconductor would play an important role for the elucidation of the nature of the oxide superconductor as well as the device applications. Recent efforts have been directed toward the in-situ growth of a high-T_c phase at low temperatures, because it may give the superconducting films with a perfect surface and a complete interface suitable for electronic device application. The in-situ growth of the YBCO thin films has been mainly achieved by evaporation techniques, including electron-beam heated coevaporation [1,2] and pulse excimer laser evaporation [3,4].

One of the crucial parameters in forming the YBCO crystal by evaporation is the relatively high oxygen pressure. The equilibrium oxygen partial pressure over the Cu_2O-CuO mixture is the highest among the metal-oxygen systems. For the YBCO crystal formation, the oxygen pressure as high as 10^{-2} Torr may be at least required above 500°C. The high oxygen pressure is the most crucial condition for deposition of YBCO using electron-beam evaporation, because it makes generally a deposition rate decrease rapidly. Therefore, it is necessary for the in-situ growth of YBCO by evaporation to keep the oxygen pressure at the substrate locally above 10^{-2} Torr and the background oxygen pressure below 10^{-4} Torr. At first, Cornell University group [1] succeeded in preparing crystalline films at low temperatures under the local oxygen pressure of 10^{-3} Torr by in-situ process, but epitaxial films have not been obtained yet. Next, we have reported the in-situ growth of YBCO single-crystal films above 600°C which exhibit a T_c of 90K [2], and a J_c of 4×10^6 A/cm^2 at 77K [5]. Recently, many groups have attempted in-situ growth of the high-T_c phase by coevaporation method using atomic or activated oxygen in the place of molecular oxygen [6-10]. On the other hand, the oxygen partial pressure of 10^{-1} Torr in pulsed excimer laser evaporation has been chosen. And the single-crystal films with a high-T_c of 93K have been epitaxially grown on the $SrTiO_3$(100) at 650°C.

2. EXPERIMENTAL

We have realized the local oxygen pressure of 10^{-2}~10^{-1} Torr at a substrate by flowing oxygen gas near by it and achieved low temperature growth of YBCO single-crystal films by activated reactive evaporation (ARE). Figure 1 shows the ARE system [11]. The YBCO films were prepared by coevaporation of metals from three separate sources. During deposition, the background pressure in the chamber is around 10^{-5} Torr. The ARE process involves the introduction of oxygen plasma by RF oscillation (13.56MHz) at application of 100 watt which may activated the oxidation of copper. The film growth rate was typically 4A/s and the substrate temperatures were kept at around 600°C.

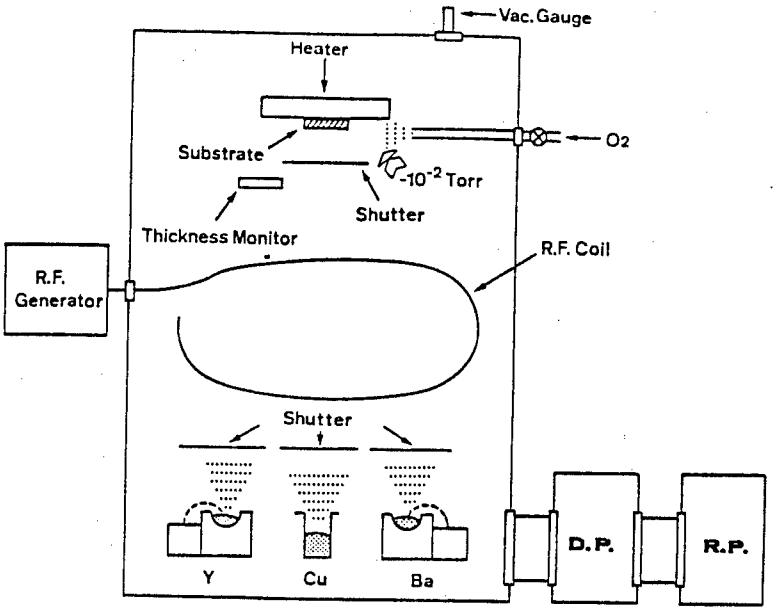

Fig. 1 Deposition system

3. EXPERIMENTAL RESULTS AND DISCUSSIONS

Structural properties of the film deposited on a $SrTiO_3$(100) were examined by means of X-ray diffraction, RHEED, LEED and TEM. The films grown on a (100) face of $SrTiO_3$ exhibited the monophasic YBCO with c-axis perpendicular to the film surface. A 1000 Å thick film with a T_c(R=0) of 89K has an orthorhombic structure and the two domains with a- and b- axes parallel to the in-plane <100>$SrTiO_3$ direction [12]. Typical transport properties are $\rho(T_c$ onset)=60 $\mu\Omega\cdot$cm and $\rho(300)/\rho(95K)$=3.4. The resistive transition is T_c(R=0)=90K, and the critical current density (J_c) is 4×10^6 A/cm^2 at 77K.

The high-quality single-crystal thin films have been obtained by epitaxial growth at relatively low temperatures using ARE process. Generally speaking, it is to be expected that initial growth of epitaxial film will occur in a layer-by-layer manner, when crystalline quality of the film is good. The initial growth of YBCO film was observed by in-situ RHEED patterns. Figure 2 shows the change of RHEED patterns along the <100>$SrTiO_3$ azimuth during growth of YBCO at 650°C. The pattern of a $SrTiO_3$ substrate sputtered by Ar ions at 650°C exhibits streaks with low background, indicating a well-crystallized and smooth surface. The values indicated in Fig. 2 were the thickness monitored by a quartz oscillating sensor located near the substrate. The one atomic layer of YBCO crystal corresponds to a thickness of about 2Å along the c-axis. The pattern at an initial stage of 3Å in thickness is the streaks sharper than that of the substrate. The sharp streaks in the patterns continue until 200Å. This suggests that the growth of YBCO occurs in a layer-by-layer growth manner, resulting in formation of an atomically smooth surface. Extra faint streaks in the middle of the strong YBCO streaks in Fig. 2 were also observed in the pattern along the <110>$SrTiO_3$ azimuth. After the oxidation of the film, the extra-streaks disappeared. It suggested that the (2x2) superstructure originate from an oxygen vacancy ordering.

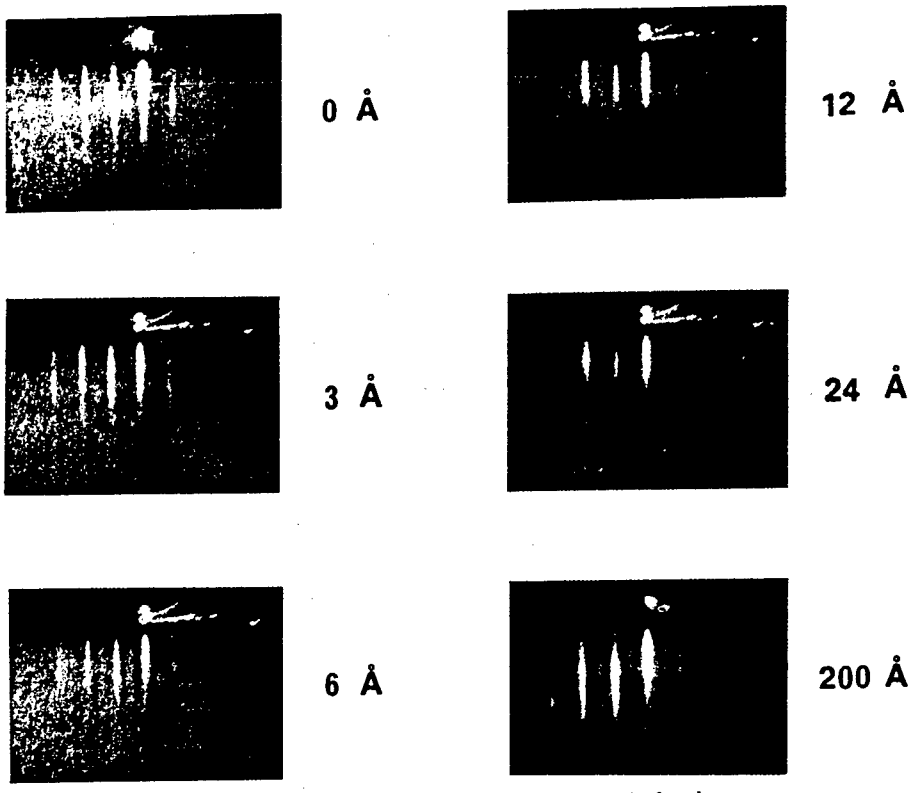

Fig. 2 In-situ RHEED patterns observed during growth of YBCO on $SrTiO_3$(100)

A 100Å thick film showed T_c (R=0) at 82K, indicating that the film was uniform in thickness and continuous, and no interaction between the substrate and YBCO film occurred.

An Auger electron spectroscopy for an as-grown film exposed to air has revealed no trace of contaminants except Y, Ba, Cu and O. In many cases, the peak due to carbon appeared but the carbon contaminant could be removed by heating the sample in an oxygen atmosphere. We have observed a sharp LEED pattern of (1x1) with a low background which guarantees a good crystalline order at the outermost surface of a (001)-oriented film [13]. The surface quality of our films seems to be suitable for the surface-sensitive measurements such as electron tunneling and angular resolved ultraviolet photoemission spectroscopy (ARUPS).

In the Ag/AlO_x (60Å thick)/ (001)YBCO tunnel junctions, a single set of the peaks appears in dI/dV-V curve for tunneling along the c-axis, as shown in Fig. 3 [14]. The energy gap Δ(44K)=10~12meV and the coupling constant $2\Delta/kT_c$=2.5~3.2 were obtained. The value of the coupling constant depend greatly on the estimation of T_c. The highest T_c will be estimated by a resistivity measurement, but the T_c of tunneling surface should be measured from a temperature dependence of gap parameter. The peaks in the dI/dV-V curve could be observed clearly below 50K but it is now difficult to estimate exactly T_c of the YBCO film surface from the temperature dependence of the peaks.

The electronic energy-band properties of YBCO were investigated by ARUPS with synchrotron radiation as the light source by Sakisaka et al. [13]. ARUPS data of our films reveal a clear Fermi edge and dispersive

nature of the valence bands, indicating the validity of the band concept for the YBCO.

5. CONCLUSION

We have in-situ prepared the high-T_c superconducting oxide thin films at low temperatures by ARE method. The YBCO single-crystal films exhibited the superior superconducting properties such as a T_c of 90K and a J_c (at 77K) of $4x10^6$ a/cm^2. It was demonstrated by in-situ RHEED that the initial growth of YBCO crystal at 650°C occurred in the layer-by-layer manner. The perfect film surface was obtained in the (001) oriented films by in-situ growth at low temperatures, as be demonstrated by the UPS, LEED and AES measurements. Electric measurement of the NIS junction along the c-axis revealed the gap energy of 11 meV at 4.4K.

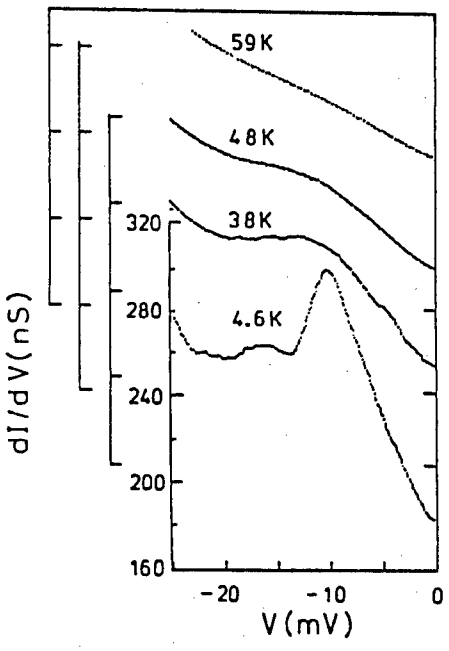

Fig. 3 Differential conductances (dI/dV) as a function of applied voltage at various temperatures, where YBCO(001)/$SrTiO_3$(100) has T_c= 87K with ΔT_c=4K

REFERENCES

1) D.K. Lanthrop, S.E. Russek and R.A. Buhrman, Appl. Phys. Lett., 51, 1554 (1987).
2) T. Terashima, K. Iijima, K. Yamamoto, Y. Bando and H. Mazaki, Jpn. J. Appl. Phys., 27, L91 (1988).
3) X.D. Wu, A. Inam, T. Venkatesan, C.C. Chang, E.W. Chase, P. Barboux, J.M. Tarascon and B. Wilkens, Appl. Phys. Lett., 52, 754 (1988).
4) B. Roas, L. Schultz and G. Endres, to be published in Appl. Phys. Lett.
5) Y. Bando, T. Terashima, K. Iijima, K. Yamamoto, J. Takada, K. Hirata and H. Mazaki, Extended abstract of the 20th (1988 International) Conference on Solid State Devices and Materials, Tokyo, Japan, p.419, (1988).
6) K. Moriwaki, Y. Enomoto, S. Kubo and T. Murakami, to be published in Jpn. J. Appl. Phys.
7) J. Kwo, M. Hong, D.J. Trevor, R.M. Fleming, A.E. White, R.C. Farrow, A.R. Kortan and K.T. Short, to be published in Appl. Phys. Lett.
8) R.J. Spah, H.F. Hess, H.L. Stormer, A.E. White and K.T, Short, Appl. Phys. Lett., 53, 441 (1988).
9) N. Missert, R. Hammond, J.E. Mooji, V. Matijasevic, P. Rosenthal, T.H. Geballe, A. Kapitulnik, M.R. Beasly, S.S. Laterman, C. Lu, E. Garivin, R. Barton, preprint.
10) R.M. Silver, A.B. Berezin, M. Wendman and A.L. DeLozanne, Appl. Phys. Lett., 52, 2174 (1988).
11) T. Terashima, K. Iijima, K. Yamamoto, J. Takada, K. Hirata, H. Mazaki and Y. Bando, J. Cryst. Growth (1988).

12) K. Kamigaki, H. Terauchi, T. Terashima, K. Iijima, K. Yamamoto, K. Hirata and Y. Bando, Jpn. J. Appl. Phys., 27, L1899 (1988).
13) Y. Sakisaka, T. Kameda, T. Maruyama, M. Onchi, H. Kato, Y. Aiura, H. Yanashima, T. Terashima, Y. Bando, K. Iijima, K. Yamamoto and K. Hirata, submitted in Phys. Res.
14) J. Takada, H. Mazaki, T. Terashima, K. Iijima, K. Yamamoto, K. Hirata and Y. Bando, Extended abstract of the 20th (1988 International) Conference on Solid State Devices and Materials, Tokyo, Japan, p.455, (1988).

GROWTH OF HIGH Tc SUPERCONDUCTING THIN FILMS BY MBE

Junming ZHOU , Zhimin ZHOU , Xiaobing MEI and Yong LU
Institute of Physics, Chinese Academy of Sciences, Beijing

1.INTRODUCTION

Molecular beam epitaxy is one of the efficient techniques for preparing multilayer thin films. Recently, with the breakthrough of High Tc superconducting materials MBE technique has been used to prepare High Tc superconducting thin films in several laboratories [1]. In contrast with other thin film techniques there are certain advantages of MBE technique as following:

(1) In situ RHEED dynamic observation of thin film growth processes can be used to adjust the growth parameters, serve to grow the single crystal thin film , which is useful for investigating the superconductivity mechanism.

(2) Multi-chambers interconnection provides the way, for future semiconductor-superconductor hybrid integration.

(3) Sample transfer air lock of MBE system allows us exchanging substrates without breaking vacuum. Therefore it overcomes the moisture of source materials and the escape of poisonous materials from the system.

2.EXPERIMENTAL

The experiments were taken in home made MBE system, which was used to prepare III-V compond semiconductor superlattice. Except thoroughly cleaning, a ultrasonic oxygen nozzle was mounted on the position of one of five beam sources flange and the oxygen beam directly collimate the substrate in order to enhance the oxidization efficiency and remain the high vacuum out of substrate in the growth chamber. Four different elements or oxides can be load into four crucibles with separated shutters, and the four substrates can be put on the sample roller simultaneously. The pump system of growth chamber consists of ion pump and titanium sublimation pump and entry chamber is roughly pumped by turbomolecular pump and maintained by ion pump.

The beam source assembly is the conventional design, in which the crucible is made of PBN , and the heater Ta foil. In practice the PBN crucible has been proved to bear high temperature for evaporating enough beam intensity of yttrium and worked stably. The capacity of crucible is 10-20ml, which prepares films about 100 times, if there is no accident. The manipulator equiped with heater of 800 C has five degrees of freedom, in order to satisfy sample exchang with sample roller and adjastment of sample position for RHEED observation.

For epitaxy of III-V compond materials beam sources shroud should be cooled by liquid nitrogen, but we found that liquid nitrogen or water cooling can not make big diffrence for preparing high Tc superconducting thin films. However when water cooling is used, the thermal equilibrium

time must last more than three hours before growth, in order to stabilize the distribution of temperature gradient in diffrent region of the shroud, otherwise the first run gives the diffrent result from other runs in the same day even-though the same parameters are used.

3.EXPERIMENTAL RESULTS AND DISCUSSIONS

(1) YBaCuO

The pure metals were used as the source materials and co-evaporated to form alloy thin films. The X-ray luminescence analysis provided the evidence for adjusting temperatures of the different beam sources, then the stoichiometrical composition of 1:2:3 for superconducting phase was obtained. The deposition rate was about 0.4 A/s. The thin film taken from the vacuum system was dark blue, smooth, shiny and dense. Because of the metal deposition thin film was not suitable to expose to air for long time, the thinkness of the film was measured after oxidization. According to the different deposition times, the thinknesses were from 2500 A to 7000 A.

The co-evaporation of all metals for preparing YBaCu without using oxygen nozzle made the thin film so dense,that the post-oxidization procedure could not be directly adopted that of the sputtering film or electron-gun oxide deposition thin film . The longer low temperature pretreatment was used the better result obtained. The samples pretreated at 200-300 C for two hours first, then kept at 600 C for 6-11 hours and at 750 C for 1-2 hours, finaly treated at high temperature (870-900 C). In the whole procedure the sample was in the fluent highly pure oxygen flux of 0.7 liter/min. Fig.1 showed the R-T curves of the samples No. 0116-1, 0118-1 and 0120-1, which were grown in the same condition and treated by the diffrent procedures and transition characterestics were different as well. No.0116-1 sample was kept at 600 C for 9 hours, then reached up to 870C directly. The temperature of zero resistance of No. 0116-1 sample was 46.8 K. The two samples of No. 0118-1 and 0120-1 were kept at 600 C for 10 hours and treated at 750 C for 1 and 1.5 hours respectively, then at high temperature. Their temperatures of zero resistance were 72 k and 77.4 K respectively.

AES analysis gave that percentage of the oxygen atoms in the 0118-1 and 0120-1 samples were 44.3% and 48.9%. The better sample, the higher oxygen composition, but oxygen percentage was still lower than superconducting thin films prepared by other diffrent methods. It showed that the samples prepared by MBE were shortage of oxygen in common. It might be attributed to rather dense alloy films.

Fig.2 showed AES depth profile of the sample of 6000 A thinkness (0128-1A, 70.8 K for zero resistance). X axis was the sputtering time and y axis intensities of the Auger peaks of the diffrent components of the films. The total depth was 2400 A. The result implied that depth profiles of components of all the elements were uniform except surface layer and showed that the beam fluxes were stable during

growth.

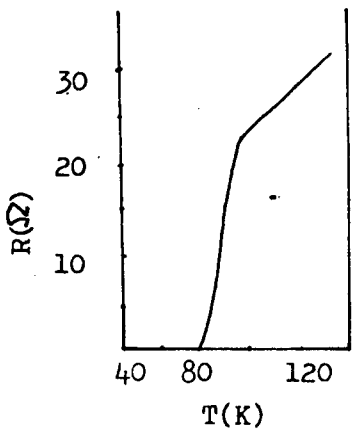

Fig.1A. R-T curve of the sample of No. 0120-1

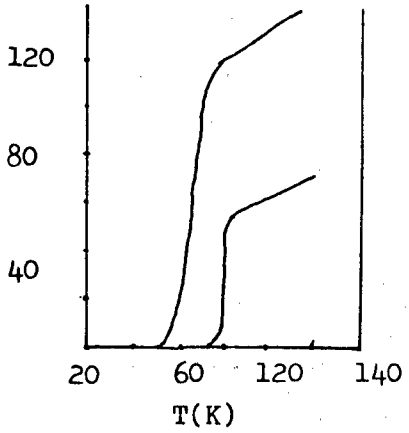

Fig.1B. R-T curve of the sample of No. 0116-1 and 0118-1

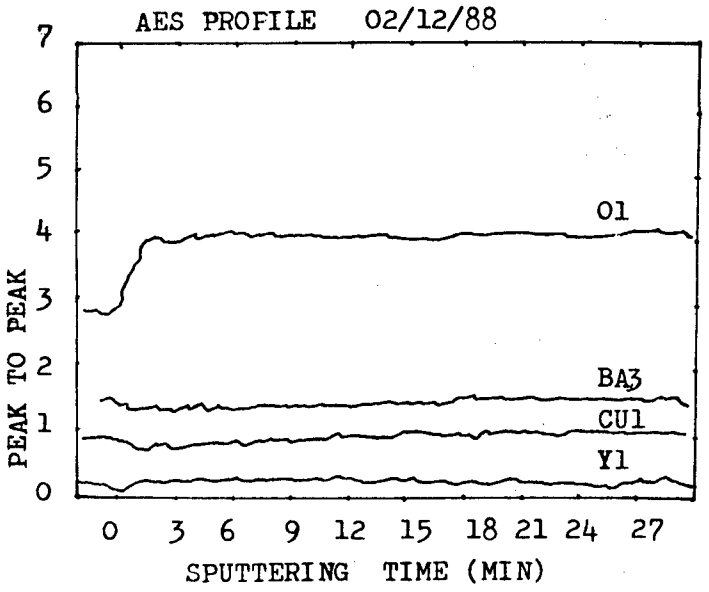

Fig.2 The 0128-1A sample's AES spectrum shows AES peak valves of every element of TBaCuO via the sputtering time

The TEM photograph (x 5400) in Fig.3 allow to be seen the larger area of connected domain of the superconducting film prepared by MBE and that means the film was rather dense.

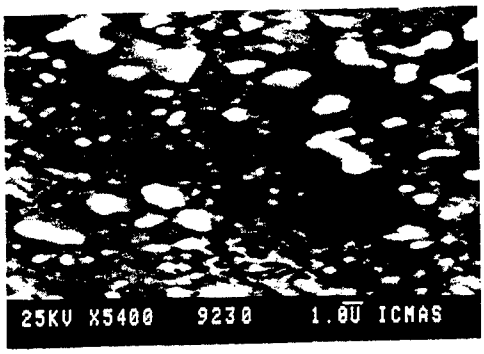

Fig.3 TEM photograph of 0206-1 sample (5400 x)

(2) TlBaCaCuO

Recently the materials of non-rare earth system have promoted scientist's interest. The bulk materials of Tl-Ca-Ba-Cu-O compound with zero resistance above 100 K have been reported [2] and the thin film of this compound obtained certain developing, but the poison is the obstacle to prepare it widely. The problem could be relaxed by using MBE technique, because the sample exchange air look prevent poisonous materials from escaping.

In comparison with yttrium, the melting point of thallium is much lower, there is no difficult to prepare the stoichiometrical TlBaCaCu Thin film by the conventional MBE technique.But the problem is that the TlBaCaCu thin film can not be oxidized for long time at high temperature, because thallium is much more volatile than yttrium, or thallium should be evaporated at all before forming superconducting phase. That is why in situ oxidization of Tl compounds during deposition is much more important than that of yttrium compounds. In order to enhance the oxidization effect, higher oxygen flux, lower growth rate, higher substrate temperature should be used.

The experimental results showed that in the condition of existance of the oxygen flux, thallium could be oxidized significantly even the substrate was not heated, and copper could be oxidized only at higher substrate temperature. But with increasing the substrate temperature the sticking confficience of thallium on the substrate decreases rapidly.

The goal,we want achieve is that to grow single crystal high Tc superconducting thin film by MBE technique without post oxidization. In order to obtain the single crystal thin film , the higher substrate temperature should be the necessary condition. If the sticking coefficience of thallium was so low at this substrate temperature, the new growth technology for enhancing the thallium sticking coeffience should be investigated, otherwise reality will be troubled with too much consumption of thallium.

4. CONCLUSION

The YBaCu alloy thin film, deposited by resistance heating method have been prepared stoichiometrically. After appreciate post-oxidization treatment, the YBaCuO superconducting thin film with zero resistance of 77 K has been obtained. The superconducting of the thin film, deposited without oxygen, strongly depends on the post-oxidization procedure. TEM analysis showed that the the film was dense and its connection domains were large, but there was existed the problem of shortage of oxygen.

The possibility of MBE preparation of TlBaCaCuO superconducting thin film was investigated. We found that in situ oxidization was rather important stage. The very low substrate temperature (room temperature) made the oxidization efficiency of copper deposition low. Increase of substrate temperature was useful for copper oxidization and formation superconducting phase, but decrease the sticking coefficience of thallium on the substrate rapidly. Therefore search a suitable epitaxy technology is the key for keeping a appreciate thallium sticking coefficience on substrate.

REFERENCES

[1] C.Webb, S-L.Weng, J.N.Eckstein, N.Missert, K.Char, D.G.Schlom, E.S.Hellman, M.R.Beasley, A. Kapitulnik and J.S.Harris, Jr. Appl. phys. lett. 51 (1987) 1191
[2] Z.Z.Sheng et al, Phys. Rev. Lett. 60 (1988) 937

SYNTHESIS AND CHARACTERIZATION OF ARTIFICIALLY LAYERED Bi-Sr-Ca-Cu OXIDE FILMS

Junichi SATO*, Masatsugu KAISE, Shozo IKEDA, Keikichi NAKAMURA, Keiichi OGAWA
NATIONAL RESEARCH INSTITUTE FOR METALS, 1-2-1 SENGEN TSUKUBA 305, JAPAN
*HITACHI CABLE LTD, 3-1-1 SUKEGAWACHO HITACHI 317, JAPAN

1.INTRODUCTION

Soon after the discovery of multiphase oxide superconductors in the Bi-Sr-Ca-Cu-O system [1], it was realized that these phases can be distinguished by the number of $CuCaO_2$ perovskite layers sandwitched by two $BiSrO_{5/2}$layers [2]. Frequent observations of many phases having different numbers of $CuCaO_2$ layers, ie $Bi_2Sr_2Ca_nCu_{n+1}O_x$ (n=0-4) [3] suggest that the free energy of these phases has no sharp minimum against the number of $CaCuO_2$ layers. In contrast to the difficulty of obtaining a single phase by the conventional solid state reaction, it becomes recently clear that the multilayer deposition technique is one of the most promising methods to obtain a single phase having the desired layer thickness [4 and 5]. We have attempted to synthesize films with n=0 to 4 using the two target multilayer deposition technique. We shall report some new results on the structure and superconducting property of these films.

2.EXPERIMENTAL

The deposition technique used was two target reactive dc and rf magnetron sputtering. Targets were metallic Bi (dc) and sintered oxide Sr-Ca-Cu-O (rf) with a cationic ratio 2:2:2 in the above order. The reactive gas was Ar-10%O_2 which was blown directly to the substrate through oxygen nozzles. The total pressure during the sputtering measured in the vicinity of the targets was 1 to 1.2 Pa. The substrate was cleaved (001) MgO and the substrate temperature (Ts) was varied from RT to 700°C. The modulation wave length Λ was adjusted by changing the sequential deposition time for each layer, typically 5W x 9s for the Bi-O layer and 140W x 16 to 36s for the Sr-Ca-Cu-O layer; the sequence was repeated 100 times to obtain a multilayered film. To see the effect of annealing ,the films were posted-annealed in air at 660, 730, 810, 850 and 870°C for 1 to 3 h. The resultant films were characterized by the conventional θ-2θ Cu Kα X-ray diffraction (XRD), and by taking EDAX analysis, high resolution SEM images (HRSEM) and high resolution transmission electron micrographs. The electrical resistivity was measured by the conventional four probe method.

3.RESULTS AND DISCUSSION

In order to obtain a desired modulation wavelength Λ of a multilayered film deposited at a given substrate temperature, we have kept the deposition time for the Bi-O layer constant and varied that for the Sr-Ca-Cu-O layer. When the $Sr_2Ca_2Cu_2$ oxide target alone was sputtered on to the substrate kept at room temperature, the composition became approximately 1:1:1, ie Cu/(Ca+Sr)=0.5. When the Bi and oxide targets were sputtered alternately to form a multilayered film, the composition of the film, ie Cu/(Ca+Sr) was found to depend significantly on the amount of Bi

in the film. Figure 1 shows such a relation observed in the films deposited at various substrate temperatures. The Sr to Ca ratio in the films was almost independent of the sputtering conditions and was found to be around 0.8. The thick line in the figure shows a relation between the Cu/(Sr+Ca) ratio and Bi concentration calculated from the ideal composition $Bi_2Sr_2Ca_nCu_{n+1}O_x$. The observed dependence of the Cu/(Sr+Ca) on the Bi concentration (and consequently on Λ) tells us that the sticking coefficient of each component is not only the function of the substrate temperature but also of the relative concentration of each component. Any deviation from the ideal composition, ie n=0,1,2$\cdots$, indicates the presence of chemical disorder in the present film.

Figure 2 shows the X-ray diffraction patterns of the multilayered films deposited at Ts=650°C. The index 2,2,n,(n+1) in the figure shows that the produced film was attempted to simulate to $Bi_2Sr_2Ca_nCu_{n+1}O_x$ (n=0-4). All the diffraction lines can be assigned to (00ℓ). Those patterns for n=0 to 3 are nearly similar to the recently published results [4] except for the fact that the present patterns show no significant peaks arising from impurity phases such as CuO. Since the diffraction peaks observed at $2\theta = 29°$ (Figure 2) arise from a single unit of stacking, the present as-deposited multilayered film must be crystalline.

The HRSEM image shows that the surface of the present multilayered film is smooth indeed and neither grain boundaries nor precipitates are found in the figure. The smooth surface is in contrast with that of the films sputtered from a single composite target of Bi-Sr-Ca-Cu oxide onto the same substrate kept at 650°C, in which many fine grains were found to grow. The resistivity vs temperature curve of the as-deposited multilayered film was characteristic of semiconducter, unexpectedly from the layered superconducting perovskite structure. When the film was annealed above 810°C, it became superconducting except for the film of the shortest Λ, ie the one simulated to 2201.

Figure 3 shows a high resolution transmission electron micrograph of

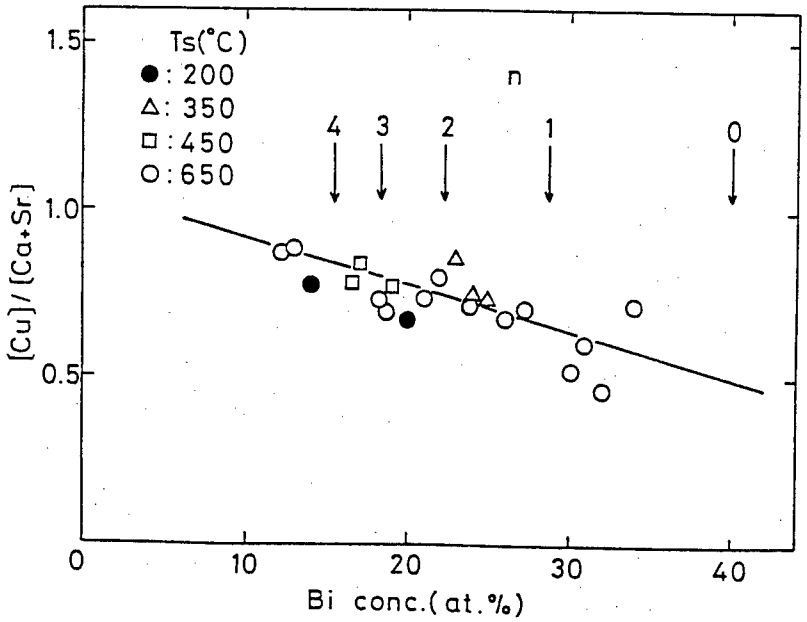

Figure 1 The molar ratio Cu/(Ca+Sr) vs Bi concentration (atomic fraction of cationic ions) in as-deposited multilayered films.

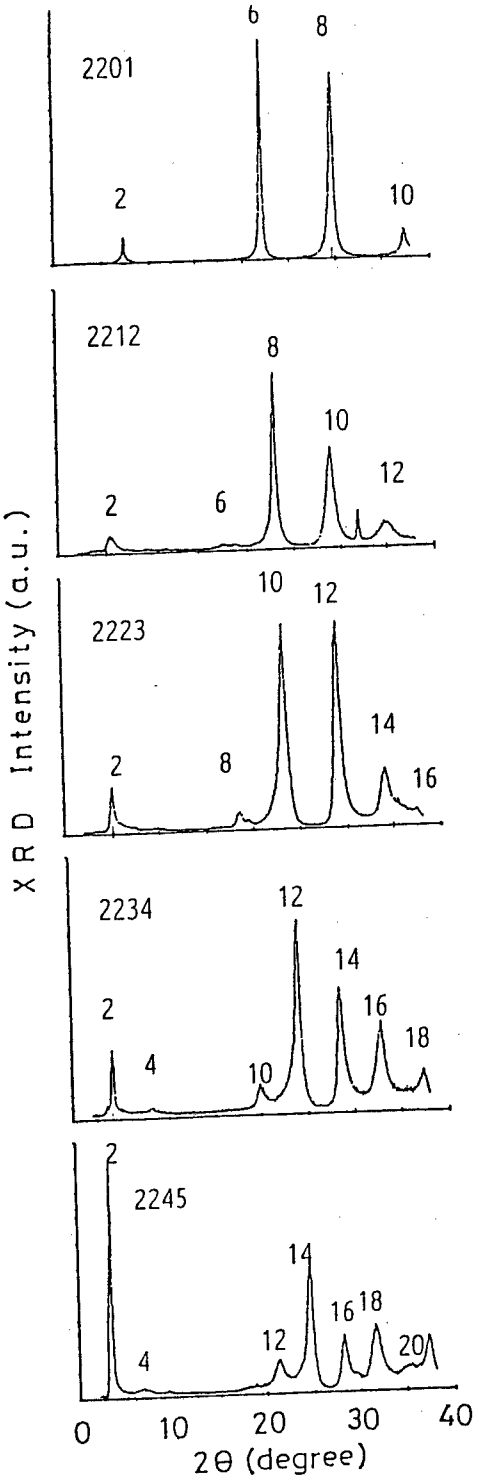

Figure 2 X-ray (Cu Kα) diffraction pattern of the as-deposited multilayered films (Ts=650°C), simulated to the 2201, 2212, 2223, 2234 and 2245 phases, respectively. The integer ℓ marked on the diffraction lines represents the index ℓ of the diffraction line arising from (00ℓ) planes.

the cross section of the multilayered 2234 film which was annealed for 1 h at 810°C. Well developed layered structures are clearly seen in the figure. The lattice constant c is evaluated to be 43 Å which is in agreement with the expectation from the 2234 composition. In some portions of the figure the characteristic strain field modulation is also observed.

The X-ray and HRSEM studies, however, showed that the major phase 2234 decomposed into the 2212 and 2201 phases on the surface of the multilayered 2234 film when annealed for 1 h at 850°C. More detailed studies on the thermal stability will be reported in the conference.

4. SUMMARY

The Bi-O/Sr-Ca-Cu-O multilayered films have been synthesized using two target reactive magnetron sputtering. The modulation wave length Λ (c/2 of the crystal) was found to be controlled by varying the deposition time for one layer unit of Sr-Ca-Cu-O while keeping that for Bi-O constant. The resultant films have smooth surface, Λ ranging from 12 to 26 Å and atomic arrangements close to those of the crystalline Bi-Sr-Ca-Cu-O system.

Main parts of this report were based on the paper to appear in Jpn. J.Appl. Phys. Letter. A substantial part of this work was reported in the ISTEC workshop on superconductivity held at Ooiso from Feb.1 to 3, 1989.

Figure 3 The high resolution transmission electron micrograph of the cross section for the multilayered 2234 film.

REFERENCES

[1] H.Maeda,Y.Tanaka,M.Fukutomi and T.Asano, Jpn.J.Appl.Phys.27(1988)L209.
[2] R.M.Hazen,L.W.Finger,R.J.Angel,C.T.Prewitt,N.L.Ross,C.C.Hadidiacos, P.J.Heaney,D.R.Veblen,Z.Z.Sheng,A.El Ali, A.M.Herman, Phys.Rev.Lett.60(1988)1657.
[3] S.Ikeda,H.Ichinose,T.Kimura,T.Matsumoto,H.Maeda,Y.Ishida and K.Ogawa, Jpn.J.Appl.Phys.27(1988)L999.
[4] H.Adachi,S.Kohiki,K.Setsune,T.Mitsuya and K.Wasa, Jpn.J.Appl.Phys.27(1988)L1883.
[5] J.Sato,M.Kaise,K.Nakamura and K.Ogawa, to be published in Proceeding of the Conference on the Science and Technology of Thin Film Superconductors; Colorado Springs (Nov.14-17th,1988).

PREPARATION OF YBaCuO THIN FILMS BY MAGNETRON SPUTTERING WITH IN-SITU PLASMA OXIDATION

YANG Senzu* , LI Yuan* , SUN Zhijian* , JI Zhengming* , WU Peiheng* , ZHANG Shiyan** and LIU Hanmo***
*Department of Information Physics, Nanjing University
**Department of Physics, Nanjing University
***Center of Materials Analysis, Nanjing University

1.INTRODUCTION

Since the discovery of high-temperature superconductive oxides [1,2,3], several techniques of depositing films have been reported including sputtering, electron beam deposition, and laser deposition [4,5,6,7,8,9,10]. Usually, to make films superconducting it is essential to anneal them at high temperature (~900°C). Besides, the composition of an as-sputtered film deviates from that of the sintered target. High temperature annealing and composition diviation affect film's morphology and crystal structure. Thus, a low temperature process is indispensable [11,12]. Furthermore, selecting an appropriate distance and position between target and substrate is also important.

This paper reports that superconducting films can be obtained without post annealing. A sintered target with the $Y_1Ba_2Cu_3O_{7-\delta}$ composition is used with substrate temperature ranging from 600°C to 650°C. Film thickness is 5000Å after sputtering for about 3 hours. The zero resistance temperature of the film is 82K. The X-ray diffraction pattern of the Y-Ba-Cu-O thin film indicates that c-axis is highly oriented, perpendicular to the film plane. The SEM photograph indicates that grains are of submicron size.

2.EXPERIMENTAL

Thin films are prepared by rf magnetron sputtering, using a sintered target with the $Y_1Ba_2Cu_3O_{7-\delta}$ composition at substrate temperature ranging from 600°C to 650°C. The substrates are $SrTiO_3$ and ZrO_2 single crystals with (100) face. Sputtering is carried out in mixture gas with 30% oxygen. Film thickness is 5000Å after sputtering for about 3 hours. After sputtering, the YBCO films are plasma oxidized for 80 minutes which is performed in situ with Va=300V, Ia=10-20MA. During plasma oxidation the substrates are kept at 480°C - 550°C , while the pressure of oxygen is increased to about 1 Torr. After plasma oxidation, substrates are no longer heated. The YBCO films are stored in chamber with O_2 at 1 atmospheric pressure for more than 8 hours.

Ag pads are evaporated onto the film through a metal mask. Then copper wires are bonded to the Ag pads to measure the film resistivity.

3.RESULTS AND DISCUSSIONS

Films fabricated by magnetron sputtering and plasma oxidation look very smooth and mirror like. Figure 1(a) and 1(b) show respectively the trails of substrate and thin film surface drawn on "α step 200". Roughness of thin film is 105Å.

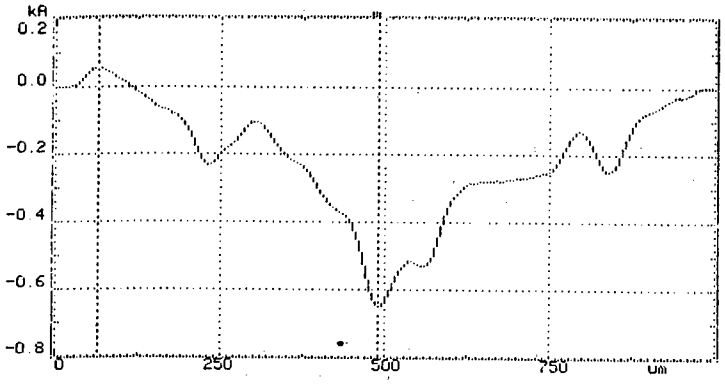

Fig.1(a) Trail of substrate surface

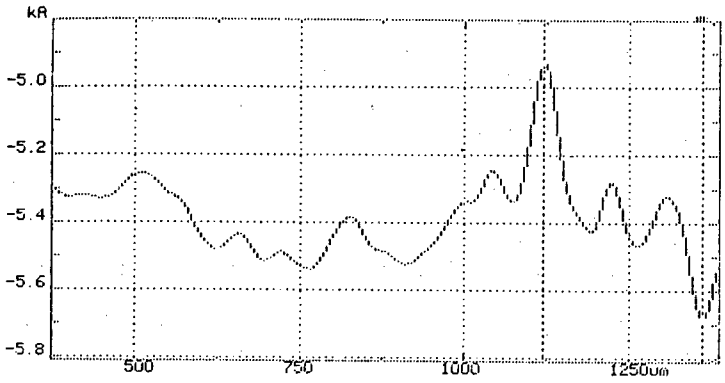

Fig.1(b) Trail of thin film surface

The films show quite sharp transition with zero resistance temperature at 82K (Fig.2).

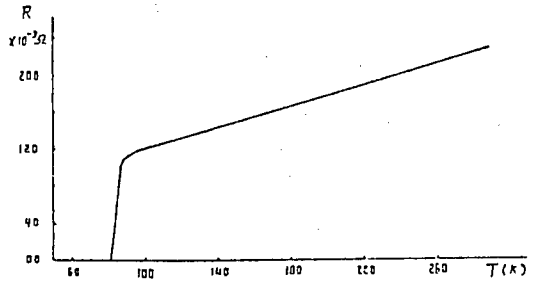

Fig.2 Temperature dependence of resistance for Y-Ba-Cu-O thin film

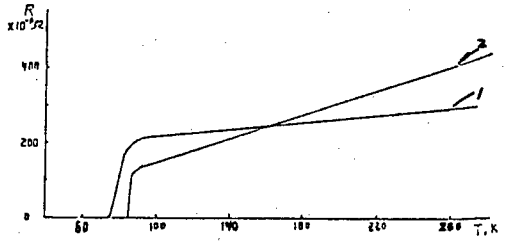

Fig.3 (1) Without plasma oxidation
(2) Plasma oxidized film

And for plasma oxidized film the resistance before transition drops more steeply than that of those films fabricated without plasma oxidation (Fig.3).

The X-ray diffraction patterns of a YBCO thin film (~5000Å) show only (00L) reflections (Fig.4). This indicates that the thin film consists of YBCO whose (00L) planes are paralled to the substrate surface.

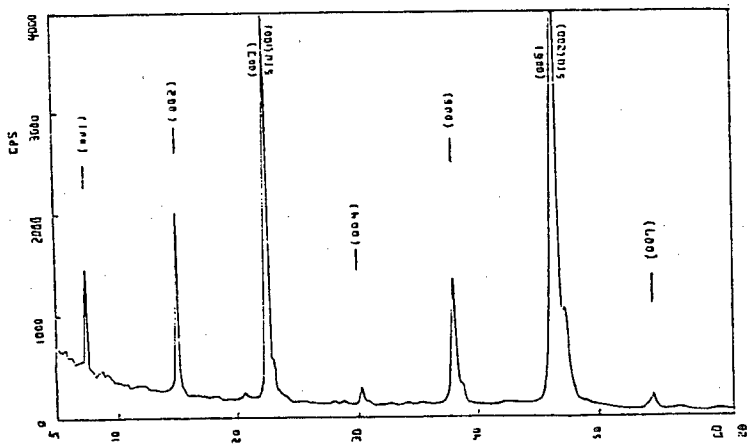

Fig.4 X-ray diffraction pattern for an YBCO thin film on a SrTiO (100) substrate

SEM photographs of the thin film of YBCO fabricated by magnetron sputtering with plasma oxidation process is shown in Fig.5. This is typical grain structure. It also indicateds that grains are submicron size. The critical current density of the thin film is about $1x10^4$ A/cm at 77K. Fig.6 shows, for film sputteded without plasma oxidation, the characteristic structure of the coalescence of column type crystallines. The critical current density is $Jc=4x10^2$ A/cm [13].

Fig.5 SEM photograph of a YBCO thin film sputtered in $Ar+O_2$ (30%) at substrate temperature of 600-650°C, and plasma oxidized afterwards

Fig.6 SEM photograph of a YBCO thin film sputtered at a substrate temperature of 250°C and post annealed in O_2 flow at 900°C for 15 minutes and 450°C for 4 hours

In order to obtain uniform films we have found in our system, substrates should be arranged in a circle whose center is the projection of target center and whose radius R is smaller than 1.5cm. In such a way the deviation of film composition can be made the smallest possible (Table I).

Table I: Film composition vs substrate positioning (target composition Y:Ba:Cu=1:2:3)

R (cm)	0	1.0	1.5	2.5	3.0
Y:Ba:Cu	1:1.8:2.7	1:2.1:3.2	1:1.5:2.4	1:1.2:2.2	1:0.2:0.4

The distance between target and substrate also influences the film composition. In our system the optimum is found to be 2.2cm.

4.CONCLUSION

During rf-magnetron sputtering, the substrate temperature should be carefully chosen so that the quality of the fabricated thin film can be improved. To our experience, a temperature between 600°C and 650°C seems a good choice.

In-situ plasma oxidation of the thin film can be completed in two steps. After sputtering, the substrate temperature is kept at 480 - 550°C, while oxygen pressure is increased to 1 torr. This step ususlly should take 80 minutes. Then the film is held in the chamber for more than 8 hours with O_2 at 1 atmospheric pressure and substrate no longer heated.

X-ray diffraction shows that the film is highly oriented with c-axis perpendicular to the substrate, and SEM indicates a morphology better than that of a film fabricated not using in-situ oxidation.

REFERENCES

[1] J.G.Bednorz and K.A.Muller, Z.Phys. B64, 189 (1986)
[2] M.K.Wu et al, Phys.Rev.Lett. 58, 908 (1987)
[3] Z.X.Zhao et al, Kexue Tongbao No.6 (1987)
[4] B.R.Zhao et al, Chineae Phys. Lett. 4, No.6 (1987)
[5] Z.R.Bao et al, Kexue Tongbao 32, No.17 (1987)
[6] Zheng Jia-qi et al, Proceeding of the Bejing International Workshop on High Temperature Superconductivity, Bejing, China, 29 June-1 July (1987)
[7] M.Tonouchi et al, Jan.J.Apl.Phys. 26, L1642 (1987)
[8] M.Gorvitch and A.T.Fiory, Appl.Phys.Lett. 51, 1027 (1987)
[9] C.Webb et al, Appl.Phys.Lett. 51, 1191 (1987)
[10] J.Narayan et al, Appl.Phys.Lett. 51, 1845 (1987)
[11] T.Miura et al, FED HiTcSc-ED WORKSHOP, June 2-4 (1988), 75-80
[12] T.Kobayashi et al, MRS International Meeting on Advanced Materials, Tokyo, May (1988)
[13] Li Yuan et al, ACTA PHYSICA TEMPERATURAE HOMILIS SINICA Vol.9, No.4 (1988)

HIGH Jc SUPERCONDUCTING THIN FILM

H.ITOZAKI, S.TANAKA, K.HIGAKI, K.HARADA, S.YAZU and K.TADA
Sumitomo Electric Industries Ltd.
1-1 1-Chome Koyakita Itami 664 JAPAN

1.INTRODUCTION

After the discovery of high Tc superconducting materials(1,2), many studies have been done in the field of thin film. Because high Tc superconducting thin film has big potential in electronics, such as sensors(3) or high speed devices(4). The authors have obtained high Jc superconducting thin films of LnBaCuO(Ln:Ho,Y,Er), BiSrCaCuO and TlBaCaCuO. Here we will report the preparation conditions of these high Jc superconducting thin films and their properties.

2.EXPERIMENTAL

Films have been prepared by rf magnetron sputtering with a single target. The target was prepared by sintering mixed power of Ln_2O_3, $BaCO_3$, CaO, Bi_2O_3, Tl_2O_3 and CuO for each system as the composition listed in Table 1. A substrate was MgO single crystal. The glow discharge was radio-frequency exited (13.56 MHz) under 80% Ar and 20% oxygen atmosphere. The substrates were heated at 350 to 800°C. The films were annealed at 800 to 950°C. In the case of TlBaCaCuO films, the substrate temperature were kept at 350 ° C and the films were annealed in a sealed tube containing Tl_2O_3, because of a high vapor pressure of Tl compound. The temperature dependence of the film resistivity and the critical current densities were measured by a four-prove method in a cryostat. For these measurements, an annealed thin film was etched with a diluted HCl (0.5 vol%) solution to form a narrow region with an area of about 20 um in length and 20 um in width. The structure and morphology were analyzed by X-ray diffraction (XRD), reflection high-energy electron diffraction (RHEED), scanning electron microscopy (SEM).

3.EXPERIMENTAL RESULTS AND DISCUSSIONS

3-1 LnBaCuO Thin Film

We have investigated epitaxial growth of HoBaCuO thin film as a function of substrate temperature and post annealing temperature. The results are schematically drawn in Fig.1(5). This diagram is divided into four regions of film crystallinity; amorphous, partially crystallized, poly-crystal and epitaxial growth regions. The epitaxial film can be obtained by the deposition with the substrate temperature of more than 600°C.

We have gotten a high Jc single crystal thin film of LnBaCuO (Ln:Ho,Er,Y) by optimizing the sputtering and post annealing conditions(6,7). Deposition rate was about 2-5nm/min The film was post annealed at 920°C. Fig. 2 shows a X-ray diffraction pattern of the HoBaCuO thin film. As only strong (00n) peaks exist in the chart, (001) planes grown parallel to the (001) of the substrate surface. Fig. 3 shows the RHEED pattern of this film. The streak patterns indicate that a or b axis are

aligned perfectly and the surface is extremely smooth. Fig. 4 shows the morphology of this film observed by a high resolution SEM. Its surface roughness is less than 5nm. Therefore, we obtained the mostly perfect single crystal HoBaCuO thin film.

The temperature dependence of resistivity of HoBaCuO thin film is shown in Fig.5. Superconducting transition temperature of zero resistance is 84K and the transition width (10-90%) is 0.4K. Temperature dependence of critical current density of LnBaCuO (Ln:Ho, Y, Er) thin films is shown in Fig. 6. More than 3 MA/cm2 is obtained for each films at 77.3K. Magnetic field dependence of critical current densities of the HoBaCuO thin film is shown in Fig.7. The Jc sustained more than 1.5 MA/cm2 at 1 tesla. This value is considerably high compared with the reported values for sintered polycrystalline materials(8).

Table 1 Preparation condition of superconducting thin films

	LnBaCuO	BiSrCaCuO	TlBaCaCuO
METHOD	RF MAGNETRON SPUTTERING		
SUBSTRATE	MAGNESIA SINGLE CRYSTAL		
DEPOSITION CONDITION			
TARGET	Ln:Ba:Cu =1:2.2:3.4	Bi:Sr:Ca:Cu. =1.4:1:1:1.5	Tl:Ba:Ca:Cu =0.7:2:2:3
GAS	Ar+O_2(20%)	Ar+O_2(20%)	Ar+O_2(20%)
GAS PRESSURE	0.05Torr	0.02Torr	0.05Torr
SUB. TEMP.	750 °C	600-800 °C	350 °C
THICKNESS	700nm	200nm	700nm
POST ANNEAL			
TEMP. ATMOSPHERE	850-950 °C (O_2)/(1atm)	800-900 °C (O_2)/(1atm)	850-900 °C (O_2+Tl)/(1atm)

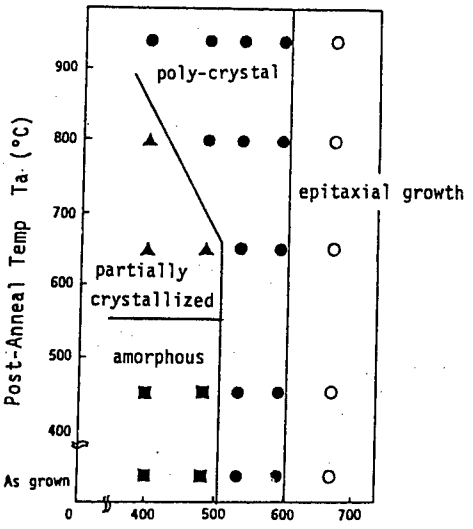

Fig.1 Substrate temperature and post-annealed temperature dependence of film crystallinity

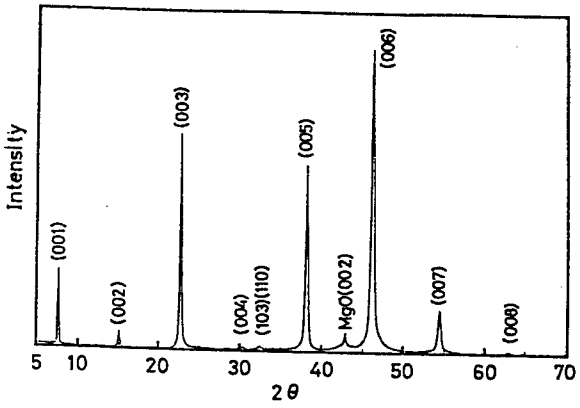

Fig.2 X-ray diffraction pattern of HoBaCuO thin film

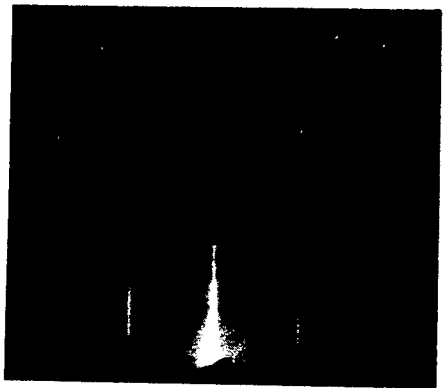

Fig.3 RHEED pattern of HoBaCuO thin film

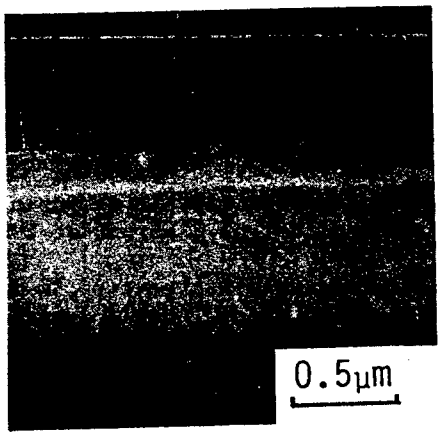

Fig.4 Morphology of HoBaCuO thin film

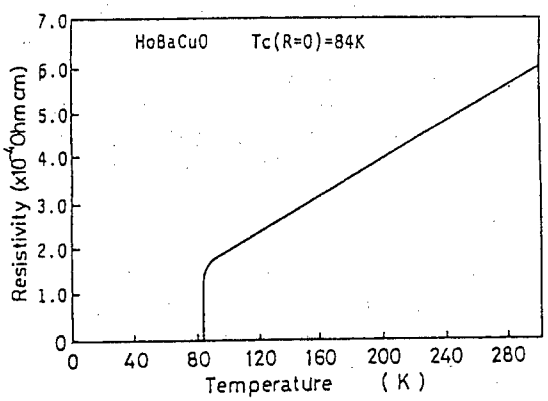

Fig.5 Temperature dependence of resistivity for HoBaCuO thin film

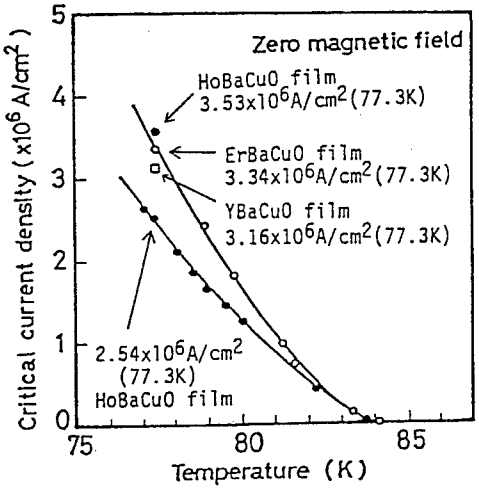

Fig.6 Temperature dependence of Jc for Y, Er or Ho based thin films

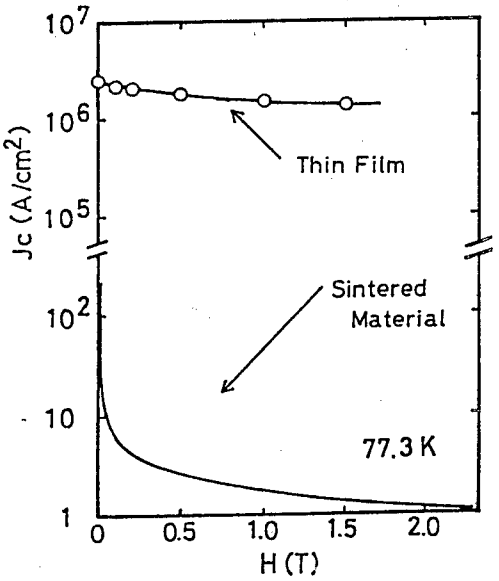

Fig.7 Magnetic field dependence of Jc for HoBaCuO thin film

3-2 BiSrCaCuO Thin Film

A BiSrCaCuO thin film was also prepared by the rf magnetron sputtering with single target(9). Preparation conditions are listed in Table 1. X-ray diffraction pattern of BiSrCaCuO thin film is shown Fig.8. It indicates that the film is c-axis textured and is composed of a single 2223 high Tc phase with c=37.2A. As RHEED pattern shows fine rings, this thin film is c-axis textured poly-crystalline.

Temperature dependence of critical current densities is shown in Fig.9. One film has the Jc of 1.9 MA/cm2 at 77.3K and that of 21MA/cm2 at 40K. The another film has 3.4 MA/cm2 at 77.3K.

Magnetic field dependence of critical current density at 77.3K was also investigated. As the applied magnetic field increases, the Jc decreases as shown in Fig. 10. The degradation of Jc depends on the direction of the applied field to the substrate and to the direction of the current flow. If the current flows parallel to the magnetic field, no Lorentz force comes out and Jc should not be affected by the magnetic field. But Fig. 10 shows that the degradation in this case has been occurred. This indicates that the film has many obstacles for the current to flow and the actual current passes in the zigzag way. Therefore the magnetic flax gets force and the degradation of the Jc occurs. As this film is polycrystalline, many grain boundaries might act as these obstacles. In the other cases where the current and the magnetic field are perpendicular to each other, the degradation is larger than above case. Comparing the two cases (b) and (c) in the fig. 10, degradation of (c) is larger than that of (b). Magnetic flux which are parallel to the surface are pinned stronger than those which are perpendicular to the surface. The magnetic flux might be pinned at grain boundaries or stacking faults, which are mainly located parallel to the surface. Jc becomes 0.26 MA/cm2 under the magnetic field of even 0.5 tesla at 77.3K. This degradation is much larger than that of HoBaCuO thin film which can sustain more than 1.5 MA/cm2 under the magnetic field of 1 tesla.

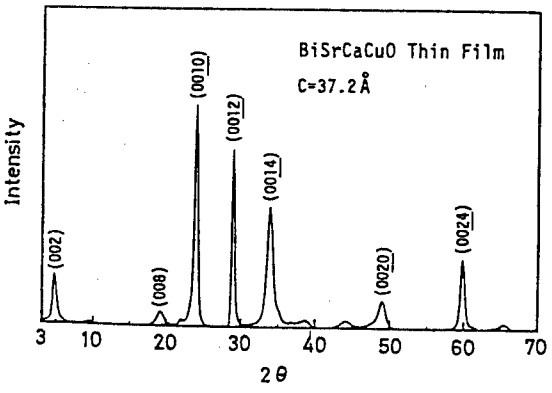

Fig.8 X-ray diffraction of BiSrCaCuO thin film

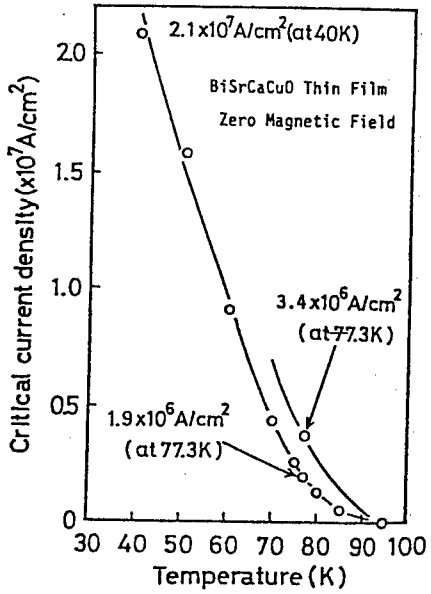

Fig.9 Temperature dependence of Jc for BiSrCaCuO

3-3 TlBaCaCuO Thin FIlm

TlBaCaCuO thin film was also prepared by the sputtering(10). As thallium is volatile, the film is deposited without heating the substrate. This film was post-annealed around 900°C in oxygen and thallium vapor. X-ray patterns of the as deposited film and the post annealed film are shown in Fig.11. The as deposited film is amorphous, and the post annealed film is c-axis textured polycrystalline. The superconducting transition of zero

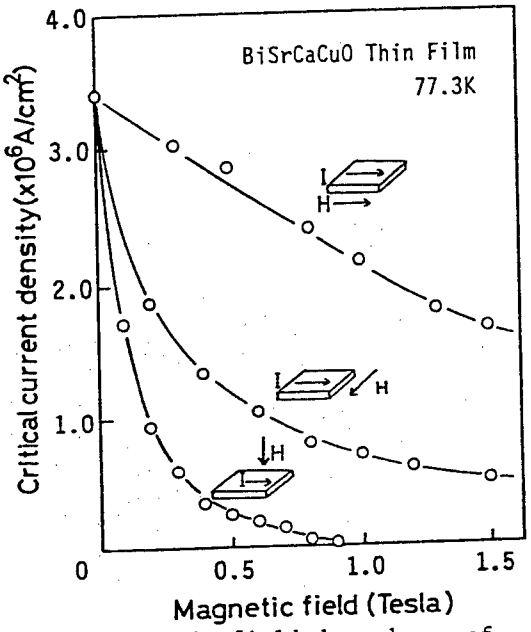

FiG.10 Magnetic field dependence of critical current density for BiSrCaCuO thin film

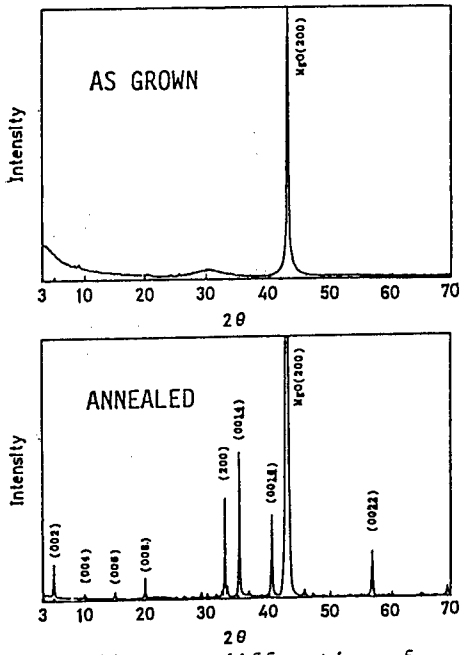

Fig.11 X-ray diffraction of TlBaCaCuO thin film

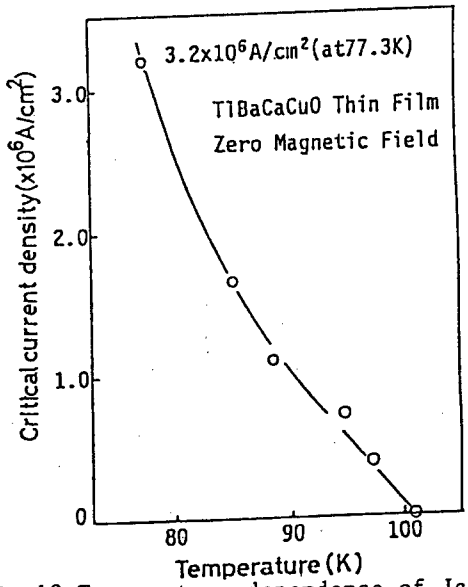

Fig.12 Temperature dependence of Jc for TlBaCaCuO thin film

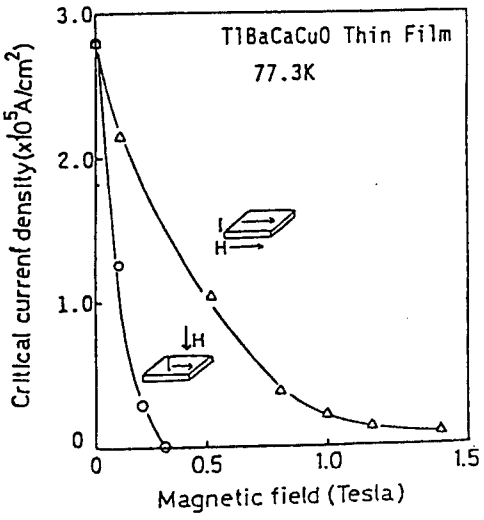

Fig.13 Magnetic field dependence of Jc for TlBaCaCuO thin film

resistance of this film is 115K. We also obtained a 2212 phase TlBaCaCuO thin film, whose Tc was 102K. The temperature dependence of Jc of this 2212 phase film is shown in Fig.12. The Jc of 3.2 MA/cm2 was obtained at 77.3K under zero magnetic field. Applied magnetic field strongly suppress the critical current densities(Fig. 13). We found many tiny pores in the surface of the film which is probably caused by evaporation of Tl compound. These defects of the film and the grain boundaries will be the cause of rapid degradation of the critical current density by the applied magnetic field.

4 CONCLUSION

Experimental results are summarized in Table 2. We obtained high Jc superconducting LnBaCuO (Ln: Ho,Er,Y), BiSrCaCuO and TlBaCaCuO thin films. These films have more than 3MA/cm2 at 77.3K under zero magnetic field. Applied magnetic field strongly suppress the Jc in poly-crystalline BiSrCaCuO and TlBaCaCuO films compared with in the case of single crystal LnBaCuO film.

Table 2 Characteristics of high Jc superconducting thin film

	HoBaCuO	BiSrCaCuO	TlBaCaCuO
Tc(R=0)	90K	105K	115K
Jc(77.3K)	$3.5X10^6A/cm^2$	$3.4X10^6A/cm^2$	$3.2X10^6A/cm^2$
CRYSTALINITY	SINGLE	POLY	POLY
MOPHOLOGY	FLAT	ROUGH	ROUGH
Jc UNDER MAG. FIELD	$1.5X10^6A/cm^2$ (at 1.0T)	$2.6X10^5A/cm^2$ (at 0.5T)	$1.2X10^5A/cm^2$ (at 0.1T)

REFERENCES

1)J.G.Bednorz and Muller,Z.Phys.B64,189(1986).
2)M.K.Wu,J.R.Ashburn,C.W.Chu,Phys.Rev.Lett.58,908(1987).
3)Y.Enomoto,T.Murakami and M.Suzuki,in Proc.5th.Int.Workshop on Future Electron Devices,Miyagi-Zao,June 1988,p325.
4)S.Takada,in Proc.5th.Int.Workshop on Future Electron Devices, Miyagi-Zao,June 1988,p305.
5)S.Tanaka and H.Itozaki,Jpn.J.Appl.Phys.to be submitted.
6)S.Tanaka and H.Itozaki,Jpn.J.Appl.Phys.27,L622(1988).
7)H.Itozaki,S.Tanaka,K.Higaki,and S.Yazu, Physica C153-155, 1155 (1988).
8)J.W.Ekin,Adv.Ceram.Mater.2,586(1987).
9)H.Itozaki,K.Higaki,K.Harada,S.Tanaka,N.Fujimori and S.Yazu,in Proc.1st. Int. Symp. on Superconductivity,Nagoya,Japan,August 1988.
10)S.Yazu,in Proc.Ist Int Symp.on Superconductivity,Nagoya,Japan, August 1988.

THE PRESENT SITUATION AND PROBLEM OF HIGH Tc SQUIDS

Ushio KAWABE,
Central Research Laboratory
Kokubunji, Tokyo 185

Many new superconductors with high critical temperatures above liquid nitrogen temperature[1-4] have been discovered. Although high Tc SQUIDs[5-8] have been fabricated with the new superconductors, we can not yet draw their merit because they belong to the typical type II superconductor. The present situation of this research field is still at the basic stage of searching for new materials and inquiring into their properties. It is not too much to say that there is not yet a new superconductor bearable for their application to high Tc SQUIDs.

From the experimental results on two dc-SQUIDs fabricated with a typical $YBa_2Cu_3O_x$ thin film of new superconductors and with a typical niobium thin film of ordinary superconductors[6], it was shown that the output voltage of the $YBa_2Cu_3O_x$ thin film SQUID is about one tenth smaller than that of the Nb thin film SQUID, and that the $YBa_2Cu_3O_x$ thin film SQUID is about 1000 times noisier than the Nb thin film SQUID. This means that the present $YBa_2Cu_3O_x$ thin film SQUID can detect big magnetic signals from a human heart with dificulty, but that it can not detect faint magnetic signals from a human brain. However, the Nb thin film SQUID has to be operated in liquid helium, but the $YBa_2Cu_3O_x$ thin film SQUID can be operated simply in liquid nitrogen. This is convenient for practical use.

The IBM group has recently fabricated a single-layered dc-SQUID with the TlBaCaCuO thin film having the transition temperature of 105K, obtained a considerably large output voltage across the SQUID, and drasitically improved the 1/f noise near 10 Hz[9]. This improvement is due to the superconducting critical temperature being high (not enough, but considerably) to operate the SQUID at liquid nitogen temperature. For biomedical applications, however, a noise energy of 10^{-30} JHz^{-1} down to 1 Hz is required[10], and so the TlBaCaCuO thin film dc-SQUID is still of no practical use.

Most of thin film dc-SQUIDs[5-9] are fabricated, on both side of the square hole, with two weak links which are constructed of many Josephson junctions naturally formed between grain boundaries. Each grain boundary is thought to have each superconducting critical temperature. The superconducting current and the resistance of the weak links are a function of a temperature, and so they are easily affected by thermal fluctiuation and further by Aslamazov-Larkin's fluctuation especially near the transition temperature. Also any new superconductors have the far larger G-L parameter depending on the crystal anisotropy

than that of ordinary metal superconductors. This means that the new superconductor has a tiny lower critical field, at which magnetic flux begin to enter into the body in the form of an Abrikosov's array of quantized vortex lines, and that a transport current running from bank to bank across the SQUID produes a Lorentz force on the flux lines tending to make them move either from link to hole or from hole to link unless there is a strong pinning force against it. The pinning force diminishes with increasing the operating temperature. The hysteresis and the flux shift have already been observed also in the magnetic flux -.SQUID output voltage curves of thin film dc-SQUIDs[5-9]. It is an intrinsic problem for various SQUID noise factors that the operation temperature is high.The SQUIDs described above are a single-layered SQUID without a flux transformer. Practical SQUID magnetometers need a flux transformer composed of a relatively large superconducting pick-up loop coupled to the input coil. It is very important to fabricate a tri-layered structure SQUID with the flux transformer. However, the insulator and buffer materials for the tri-layered structure are coated on the YBaCuO ground film and then the superconducting critical temperature of the ground film is degrated because of film stress[8]. This is one of the present problems for fabricating the tri-layered structure SQUID.

In order to get out of these Tantalus' difficulties, it will be a clue how to treat the new superconductor and how to improve the material quality.

REFERENCES

1) J. G. Bednortz and K. A. Muller: Z. Phys. B26, 189(1986)
2) M. K. Wu, J. R. Absburn, C. J. Torng, P. H. Hor, P. L. Meng, L. Gao, Z. J. Huarg, Y. Q. Wang, and C. W. Chu:Phys. Rev. Lett. 58, 908(1987)
3) H. Maeda, Y. Tanaka, M. Fukutomi and T. Asano:Jpn Appl. Phys. , L209(1988)
4) Z. Z. Sheng, A. M. Hermann, A. Elali, C. Almason, J. Estrada, T. Datta and R. J. Matson:Phys. Rev. Lett. 60, 937(1988)
5)R. H. Koch, C. P. Umbach, G. J. Clark, P. Chaudari, and R. B. Laibowitz :Appl. Phys. Lett. 51, 200(1987)
6) H. Nakane, Y. Tarutani, T. Nishino, H. Yamada and U. Kawabe :Jpn J. Appl. Phys. 26, L1925(1987)
7) Y. Tarutani, H. Nakane, T. Yamashita, T. Aida and U. Kawabe :Int'l.Meeting on Advanced Materials, May 30-June 3, 1988, Sunshine City , Tokyo, Jpn.
8) J. Clarke: FED HiTcSc-ED WORKSHOP, June 2-4, 1988, Miyagi-Zao, Jpn.
9) R. H. Koch et. al: Fall Meeting on Materials Research Society, Nov. 28-Dec.3, 1988, Boston, Ma.
10) J. Clarke: Nature 333, 29(1988)

INVESTIGATION OF YBaCuO THIN FILMS AND DEVICES

Guang-Cheng XIONG, Shi-guang WANG, Shou-Zheng WANG, Guang-Ji CUI,
Xiang-Hui ZENG, Hua-Ming Jiang, and Yuan-Dong DAI
Department of Physics & Institute of Solid State Physics
Peking University, Beijing 100871, P.R. China

1. INTRODUCTION

Since the discovery of high T_c superconducting ceramics, intensive researches have been carried out to develop potential applications. Josephson effects and quantum interference phenomena have been observed in the devices fabricated with these materials[1-7]. The investigation of the noise of high T_c SQUID has revealed that the noise originated from the magnetic flux creeping in the thin films[8]. In order to produce excellent thin film devices, epitaxial film specimens were prepared[9-11], and various technique were developed for the patterning of devices[3-5,12].

In this report, we present our results on the preparation of high T_c $YBa_2Cu_3O_{7-x}$ thin films, the patterning technique, and the properties of thin films dc SQUID's.

2. PREPARATION OF THIN FILMS

Many techniques, such as dc and rf magnetron sputterings, multilayer deposition and coevaporation by electron beam guns, spin on from liquid precusors, have been employed to produce thin films of YBaCuO in our University. So far, we have succeeded in preparation of high T_c thin films, with zero resistance above liquid nitrogen temperature, by using the multilayer deposition and dc magnetron sputtering.

The multilayer deposition technique has been discussed previously [10]. Briefly, the Y_2O_3, BaO (sintered $BaCO_3$) and Cu placed in three crucibles were evaporated alternately by an electron gun. Sapphire, polycrystalline YSZ, single crystal $SrTiO_3$ were used as substrates, which were kept at 200°C during deposition. Post annealing was required to form the single phase $YBa_2Cu_3O_{7-x}$. The films on the $SrTiO_3$ normally have an epitaxial feature with a-axis perpendicular to the substrates, while those on YSZ are c-axis texture. The film thicknesses were ranging from 0.5-1 um. Zero resistance temperature up to 85 K could be achieved, while the critical current density was rather low, typically $5X10^2$ A/cm^2 at liquid nitrogen temperature.

The sputtering films were prepared in a dc magnetron sputtering system with a planer superconducting target [11]. During a deposition the substrate temperature was kept at about 790°C. After an in situ annealing at 400°C for 30 min. in pure oxygen atmosphere, the films have smooth and shiny surfaces. The argon pressure was $1X10^{-1}$ Torr in the sputtering chamber. The oxygen partial pressure was $1X10^{-2}$ Torr. Atypical sputtering condition was 110V and 200mA

with the sputtering rate of 30 A/min. X-ray diffraction patterns of the films indicated that the films on (100) $SrTiO_3$ epitaxially grew with c-axis perpendicular to the substrate surface. The Zero resistance temperature of the films are greater than 88 K. The critical current density in a 1700 Å films is $3X10^5$ A/cm² at 78 K.

3. PATTERNING TECHNIQUE AND MEASUREMENT SYSTEM

We patterned the thin film devices by chemical wet etching employing $HCl-H_3PO_4$ mixture as an etchant [12]. It was found that the ratio 1:1:1 between H_2O-HCl(37%)-H_3PO_4(85%) at 50°C was the best for our YBaCuO thin films. The photoresist Shiepley 1470 was used as the etching mask, which was found to be safe to the superconductivity of $YBa_2Cu_3O_{7-x}$ films. The conventional photolithographic procedure was carried out to define the pattern desired. Figure 1 shows the resistances of a sputtering film before and after etching process, in which two constrictions of 8 um was patterned, as a function of temperature. It shows that the T_c decreases about one degree after pattering. Since the sputtering films were more compact and homogeneous, they were easy to be patterned than the multilayer deposited films. The devices had clearer edge, and the side-etching was much less serious than those of the multilayer deposited films.

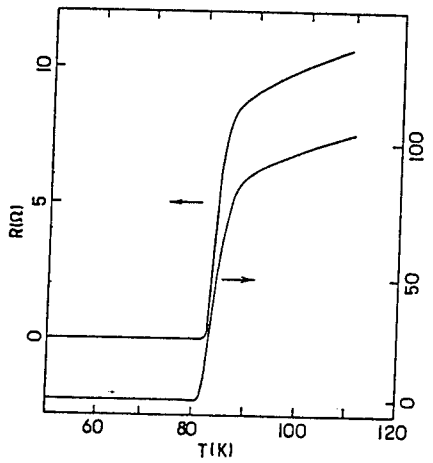

Figure 1 Resistances of a sputtering $YBa_2Cu_3O_{7-x}$ thin film, before (upper) and after (lower) etching process, as a function of temperature.

The dc SQUID was formed by a superconducting slab with two parallel constrictions. The length was twenty micrometers, and the width was ranging from a few to twenty micrometers, which should be design in accordance with the critical current density of the films. The area enclosed by the loop was 40X40 um².

Four copper pads were deposited before photolithography, and the leads were connected to samples with indium soldering or silver paste, through which we applied the bias current , I_B, and detected the voltage across the SQUID, V. The voltage was taken down by an X-

Y recorder. The samples were mounted in a copper block attached to the end of a german silver tube, which could be slide up and down in a dewar. This enabled us to perform our measurements from room temperature down to 4 kelvin, by adjusting the distance between the thermal block and the liquid helium surface. The temperature of the block was monitored by carbon or platinum resistive thermometer. A magnetic field was applied via a 5-turned coil with a diameter of 5 mm. The coil was mounted on the block and 1 mm from the SQUID. The field coefficient in the center of the SQUID loop was estimated to be 1×10^{-3} T/A.

A superconducting $YBa_2Cu_3O_{7-x}$ can was used to screen the earth and the low frequency magnetic field [6].

4. RESULTS AND DISCUSSION

We have fabricated dc SQUID both from the multilayer deposited and the dc sputtered thin films. The sample, shown in Figure 1, had an Ic of 2 mA at the liquid nitrogen temperature, since the sputtering films had an very high critical current density. This value was two orders of magnitudes larger than the designed Ic for our dc SQUID. Since the temperature was only a few degrees from T_c, we could not reduce the critical current by increasing the working temperature, which would drive the device into the fluctuation regime, resulting in a drastic rising of noise level. Therefore it was very difficult to observe the quantum interference effect in this sample.

For the devices fabricated with multilayer deposited films, the Ic's were normally lower. The devices manifested dc and ac Josephson effects, and had a bridge-type current-voltage characteristics, and the temperature dependence of critical current was Ic $(1-T/T_c)^{3/2}$. This is attributed to be the properties of the granular structure of thin films, which demonstrated the same temperature dependence as well. It also explain why Josephson effect could be observed in constrictions which have a dimension much larger than the GL coherence length for this material.

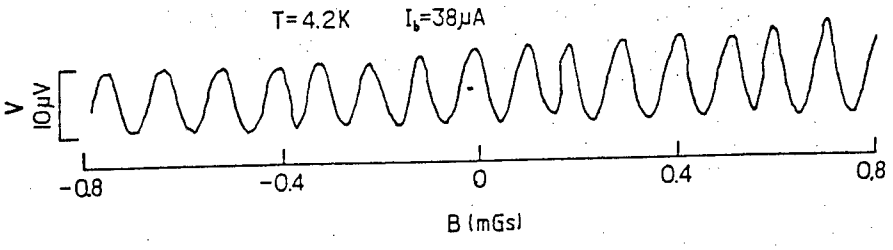

Fig. 2 Output voltage of a dc SQUID as a function of magnetic field applied.

Figure 2 shows a typical output voltage across the SQUID as a function of the applied magnetic field in the SQUID loop. One sees that the period is $1.1X10^{-7}$ T. According to the micrograph of the sample, the constriction was 14um in width and area enclosed by the loop was $(46um)^2=2.1x10^{-9}$ m^2. But the area inferred from the period measured was $2x10^{-8}$ m^2, being an order of magnitude larger than the geometrical area determined by SEM. We attribute this discrepancy to the so-called "flux focusing" effect, which was also observed in the high T_c SQUID by Koch *et al* [4], and the penetration of magnetic field in bridges region. Since the large superconducting pads screen the magnetic field from the pad center and increases the field near the pad edges, where the SQUID is located. The flux enclosed was increased by a factor of 5. when the temperature below 40 K. The penetration of flux in the bridges region due to porous film could lead to an effect area larger than the geometrical area. This may increase the flux by 80%, if we take the area enclosed the central lines of the bridges. The sum of the two effects would give rise to a discrepancy of an order of a magnitude in the applied flux.

One sees that the oscillatory output voltage has a rather good periodicity. It extended to 15 period without notable attenuation. However, we also found the noise might smear the "triangle wave" when the temperature increased. Nevertheless, from the $V-I_B$ curve, one would justify that it is possible to carry out the lock-in operation in the white noise region.

5. SUMMARY

The superconducting devices have been fabricated with YBaCuO thin films, patterned by using wet etching technique. The superconducting quantum interference effect has been observed in the devices made of multilayer deposited films. Due to the technical difficulty, we chose to make a bridge-typed dc SQUID. It is generally believed that the tunnel junction devices are more robust and have a wider temperature range of optimum operation than the bridge-typed one. However, owing to the simplicity of fabrication, the bridge-typed devices has been adapted in many past commercial applications. Moreover, the wet etching method developed in our lab, having only a minor degradation on the superconductivity of YBaCuO thin films, makes such fabrication technique much easier.

It is known that the noise of high T_c SQUID originates mainly from the flux creeping in the superconducting films. The improvement of film quality is one of the key factors for high performance thin films devices. The successful preparation of high j_c thin films has made a further step towards the the application of this materials. The problem we are facing is to fabricate proper weak links in the sputtering films. The research is going on, and the further results will be reported at the symposium.

REFERENCES

[1] The Superconducting Electronics Research Group and High T_c Superconducting Materials Research Group, Journal of Nanjing University (Natural Sciences), 23 227, 1987.

[2] G.J.Cui, X.F.Meng, S.G.Wang, K.Shao, H.M.Jiang, Y.D.Dai, Y.Zhang, R.P.Peng, Z.L.Bao, F.R.Wang, S.Z.Wang, Z.Y.Ye, C.Y.Li, K.Wu, and D.L.Yin, Solid State Commun. **64** 321, 1987.

[3] A.Enokihara, H.Higashino, K.Setsune, T.Mitsuyu, and K.Wasa, Jpn. J. Appl. Phys. **27** L1521, 1988.

[4] R.H.Koch, C.P.Umbach, G.Clark, P.Chaudhari, and R,B.Laibowitz, Appl. Phys. Lett. **51** 200, 1987.

[5] S.G.Wang, G.J.Cui, Y.D.Dai, H.M.Jiang, X.H.Zeng, J.Z. Li, Z.L.Bao, S.Z.Wang, C.Y.Li, and D.L.Yin, to appear in *Proc. ASC'88*, IEEE Trans. on Magn. MAG-25, 1989.

[6] G.J.Cui, S.G.Wang, H.M.Jiang, J.Z.Li, C.Y.Li, C.D.Lin, R.Z.Liu, Q.L.Zheng, Y.S.Fu, and W.C. Qiao, to appear in *Proc. ASC'88*, IEEE Trans. on Magn. MAG-25, 1989.

[7] M. Matsuda and S.Kuriki, Appl. Phys. Lett. **53** 621, 1988.

[8] M.J.Farrari, M.Johnson, F.C.Wellstood, J.Clarke, P.A.Rosenthal, R.H.Hammond, and M.R.Beasley, Appl. Phys. Lett. **53** 695, 1988.

[9] F.B.Laibowitz, R.H.Koch, P.Chaudhari, and R.J.Gambino, Phys. Rev. B35 8821, 1987.

[10] S.Z.Wang Z.L.Bao, S.L.Wang, G.Li, Z.Y.Ye, C.Y.Li, and D.Yin, to appear in *Proc. ASC'88*, IEEE Trans. on Magn. MAG-25, 1989.

[11] G.C.Xiong, S.Z.Wang *et al*, to be published.

[12] K.Shao, C.H.Cao, H.Zhu, H.Y.Shen, J.T.Liu, S.G.Wang, G.J.Cui, Y.D.Dai, Y.Zhang, H.M.Jiang, T.Y.Yang, J.Z.Li, X.W.Wu, Z.L.Bao, S.Z.Wang, C.Y.Li, and D.L.Yin, Mod. Phys. Lett. B1 375, 1988.

FABRICATION AND PATTERNING OF Bi(Pb)SrCaCuO THIN FILMS

Ienari IGUCHI, Yoko KANKE, Zhongmin WEN
Institute of Materials Science, University of Tsukuba,
Tsukuba, Ibaraki-ken 305

1. INTRODUCTION

The thin film fabrication utilizing high-T_c oxide superconductors is quite important for device applications. The fabrication of BiSrCaCuO thin films has been reported using various technique such as magnetron sputtering [1-3], electron beam evaporation[4], chemical vapor evaporation [5] etc.. However, only several groups reported the successful fabrication of thin films above 100K probably because of the complicated nature of BiSrCaCuO compounds.

In this presentation, we report the fabrication of Bi(Pb) SrCaCuO thin films above 100K by rf magnetron sputtering and the patterning of these films into a dc SQUID or a tunnel junction by wet etching and/or dry etching process.

2. THIN FILM - EXPERIMENTAL

The sputtering of Bi(Pb)SrCaCuO thin film was performed using a target containing a small amount of Pb. The powdered target was prepared by calcining a mixture of Bi_2O_3, PbO, $SrCO_3$ $CaCO_3$ and CuO with the appropriate composition ratio at 800°C for 10h. The target size was 94mm in diameter and the distance between the target and the substrate was 45mm.

Among many targets tested, $Bi_{1.2}Pb_{0.06}Sr_{1.0}Ca_{1.0}Cu_{1.6}O_y$ yielded the best results for the growth of a high-T_c phase. We used a polished (100) MgO single-crystal substrate of 0.5mm thick. The sputtering gas was pure argon of the pressure 2 Pa. The film growth rate was about 30Å/min.

We investigated the growth of a high-T_c phase under different substrate temperatures and annealing conditions. The substrate temperature was varied from 300°C to 710°C. The annealing process was done in air. Note that the annealing in pure oxygen gas yielded worse results. The film resistivity was measured with the conventional four probe technique by changing the polarity of current. The non-annealed films exhibited an amorphous or some crystal structure different from the BiSrCaCuO superstructure and were nonsuperconducting. As shown later, it was found that the substrate temperature around 700°C and the annealing temperature at 886°C were one of optimum conditions for the growth of a high-T_c phase.

3. THIN FILM - RESULTS

Figure 1 shows the resistivity vs temperature curves for Bi(Pb)SrCaCuO thin films fabricated using targets with differ-

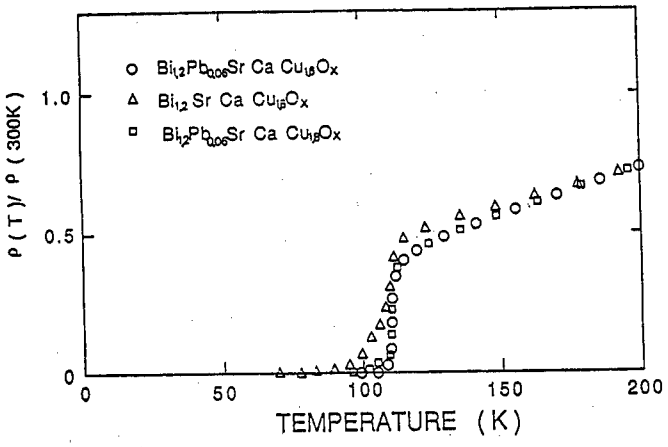

Fig. 1 Resistivity vs temperature curves of thin films fabricated using targets with different atomic composition.

ent composition when the substrate temperature was 700°C and the annealing temperature was 886°C. It should be noted that the film without Pb doping exhibited a long-tailing behavior in the transition region. Those films with Pb doping exhibited a sharp transition and had a T_C of 100K or above.

Figure 2 shows the resistivity vs temperature curves for thin films annealed at three different temperatures when the substrate temperature was fixed at 700°C. The superconducting properties were quite sensitive to the annealing temperature and the thin films of T_C above 100K were only fabricated at 886°C. The T_C of Fig. 2 was 104K. The X-ray diffraction pattern showed only the presence of a low-T_C phase for the 875°C annealed sample and the presence of very small peaks of a high-T_C phase for the 890°C annealed sample. Note that ρ(300K) was 67.7μΩcm, 14.3μΩcm and 217μΩcm for 875°C, 886°C and 890°C

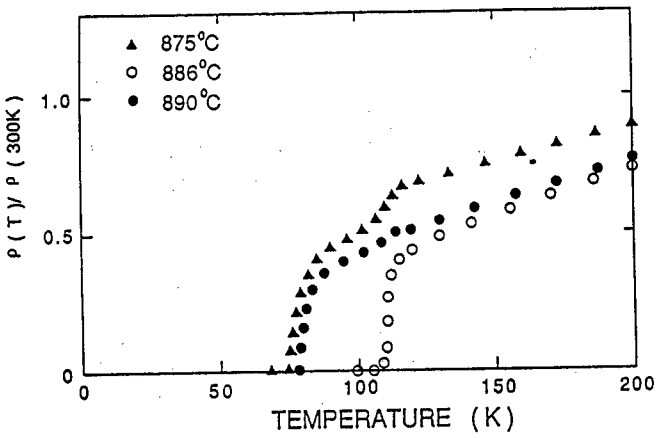

Fig. 2 Resistivity vs temperature curves of thin films fabricated at different annealing temperature when the substrate temperature was 700°C.

samples respectively.

The EPMA analysis led to the atomic composition ratio Bi:Pb:Sr:Ca:Cu = 2.53:0.005:1.99:1.07:1.96 for the film annealed at 886°C. The observed composition ratio was far from the (2223) phase but closer to the (2212) phase probably because of mixed phase nature of materials. Note that a very small amount of Pb was detected, although the X-ray diffraction pattern exhibited the high-T_c and low-T_c phases of Bi oxide superconductors only. The role of Pb is not clear, nevertheless it may play an important role for the growth of a high-T_c phase implicitly.

The critical current of thin films was measured by a transport current technique. Figure 3 shows the temperature dependence of the critical current density for the 104K film. It was $3 \times 10^4 A/cm^2$ and $1.2 \times 10^3 A/cm^2$ at 77K, indicating that the electric transport was limited by the grain boundaries typical for polycrystal materials. A step-like behavior at about 80K was observed, directly reflecting the mixed phase nature of the fabricated film.

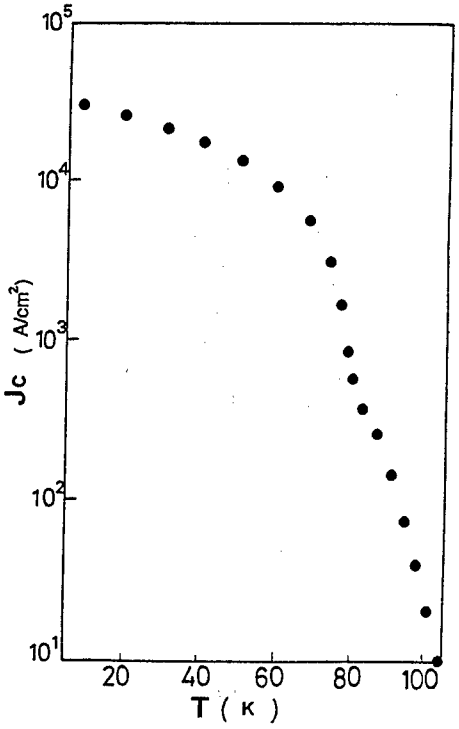

Fig. 3 Temperature dependence of critical current density of Bi(Pb)SrCaCuO film.

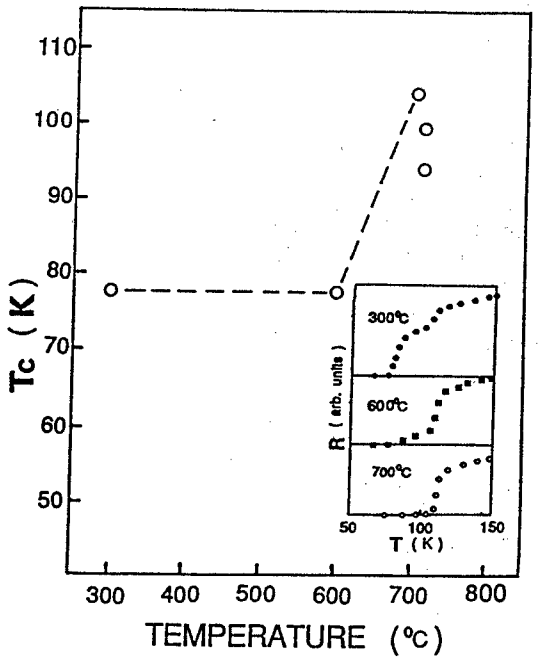

Fig. 4 T_c vs substrate temperature when the annealing temperature was fixed at 886°C. The insertion shows the resistivity vs temperature curves at different substrate temperatures.

The dependence of superconducting transition temperature of films on the substrate temperature was investigated by changing the substrate temperature from 300°C to 710°C with the annealing temperature fixed at 886°C. Although the presence of a high-T_c phase was recognized more or less in the X-ray diffraction patterns for all samples, the growth of a high-T_c phase was found to be enhanced around 700°C.

Figure 4 shows the measured T_c vs substrate temperature. The insertion shows the resistivity vs temperature curves at different substrate temperatures. It is understood that the optimum condition for realization of a high-T_c film above 100K lies in the narrow substrate temperature range around 700°C.

4. PATTERNING

Using the Bi(Pb)SrCaCuO thin films fabricated above, we performed the patterning of thin films into a dc SQUID pattern or a tunnel junction by wet etching or dry etching process. For the wet etching process, the phosphoric acid (H_3PO_4) was used, whereas, for the dry etching process, the ECR argon plasma was used. In the photolithography, a positive type photoresist (AZ-1450) was also used. The wet etching process yielded rather poor results for patterning which contained microshorts or cutoff of lines. On the other hand, the dry etching process yielded good results for micro-patterning at least down to 5μm. The etching rate was, however, found to be quite slow (25nm/min).

In order to overcome this problem, we took the process by first introducing the dry etching process to some extent, then after by performing the wet etching process. Figure 5 shows the photograph of a dc SQUID pattern thus made. The junction width was about 10 μm. A tunnel junction was formed first by patterning a Bi(Pb)SrCaCuO stripline of about 0.5mm wide, then depositing a counter electrode(Pb) strip by a mechanical mask.

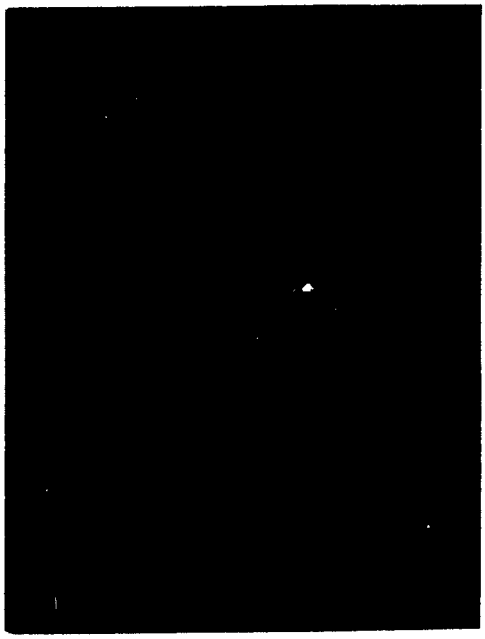

Fig. 5 The photograph of a dc SQUID pattern.

5. CONCLUSIONS

We have reported the fabrication of Bi(Pb)SrCaCuO thin films by rf magnetron sputtering under various heat treatments and the patterning of these films into a dc SQUID or a tunnel junction. The optimum condition for fabrication of thin films above 100K was found to lie in the very narrow range of both substrate and annealing temperatures. The films fabricated using the target with Pb doping had better quality than those without Pb doping in our experiment. The patterning of Bi oxide films was done by both wet etching and dry etching processes. The dry etching process appeared to be more convenient for micropatterning, but the etching rate was very slow. The combination of dry and wet etching processes led to some optimum result from the viewpoint of the micropatterning and the etching rate.

ACKNOWLEDGEMENTS

The authors are very grateful to Dr. S. Takada, Dr. H. Akoh and members of their group in Electrotechnical Laboratory for kindly providing us their ECR plasma facilities.

REFERENCES

[1] S. Hatta, Y. Ichikami, K. Hirochi, K. Setsune, H. Adachi and K. Wasa: Jpn. J. Appl. Phys. 27 (1988) L855.
[2] M. Fukutomi, J. Machida, Y. Tanaka, T. Asano, T. Yamamoto and H. Maeda: Jpn. J. Appl. Phys. 27 (1988) L1484.
[3] Z. Wen, Y. Kanke and I. Iguchi: Physica C156 (1988) 817.
[4] T. Yoshitake, T. Satoh, Y. Kubo and H. Igarashi: Jpn. J. Appl. Phys. 27 (1988) L1262.
[5] M. Ihara and T. Kimura: Proceeding of the 1988 Applied Superconductivity Conference (San Franscisco).

MAGNETIC PROPERTIES OF THE HIGH Tc SUPERCONDUCTORS

Yuan-Dong DAI, Guo LU, Chin LIN, Chong-De WEI, Kai-Xuan CHEN, Ya-Qin ZHOU, Qing-Rong FENG, Yun-Xi SUN, Zun-Xiao LIU, Zi-Zhao GAN
Department of Physics, Peking University, Beijing

1. INTRODUCTION

Following the discoverey of 30-40 K superconductor LaBaCuO by Muller and Bednortz [1], several liquid nitrogen temperature superconductors have been discovered [2-5]. These high T_c superconductors are not ideal type-II superconductors. They exhibit typical granular superconductivity. Critical current of sintered sample is greatly limited by the granular behavior. Granular superconductors exhibit various physical behavior at low field [6-8]. On the other hand, flux pinning plays an important role in the application at high field and large current. Magnetic properties at low and high fields have attracted much attention [9-12].We have investigated magnetic properties and critical currents of the high T_c superconductors at different field. The results are reported and discussed briefly.

2. EXPERIMENTAL

YBaCuO and Bi(Pb)SrCaCuO samples were prepared by solid state reactions. Appropriate starting materials of YBaCuO were sintered at 930° C for 72 hours, pulverized and pressed into pellets, sintered at 910° C for 48 hours, annealed at 700° C for 24 hours, cooled down to room temperature in the furnace. Nominal composition $Bi_{1.7}Pb_{0.3}Sr_2Ca_2Cu_3O_x$ were sintered at 800° C for 48 hours. The pellets were sintered at 860° C for 100 hours, cooled down to room temperature in the furnace. The process was carried out in air.

Low field susceptibility was measured by LDJ 8500 vibrating sample magnetometer. High field magnetic loop was measured by a moving sample magnetometer. Magnetic critical current was calculated by Bean model. The dimensions of the sample for DC magnetic measurements were $2*2*5$ mm^3. AC susceptibility was measured by a mutual inductance bridge. Real part (χ') and imaginary part (χ'') of the suaceptibility were picked up by a two phase lock-in amplifier. Transport critical current was measured directly by four lead with Ag paste. The contact resistance was about 10 milliohm.

3. EXPERIMENTAL RESULTS AND DISCUSSIONS

3.1 Low field susceptibility

Fig. 1 shows the magnetization curve of YBaCuO at low field. It is similar to that described by YAN [6]. When $H<H_{J1}$, magnetization is proportional to the field and reversible. With increasing field, magnetization deviates from the linear dependence at $H=H_{J1}$. When $H_{J1}<H<H_{J2}$, magnetization is irreversible and remanent magnetization appears. Remanent magnetization is essentially saturated at $H=H_{J2}$. When $H>H_{J2}$, magnetization is proportional to the field again.

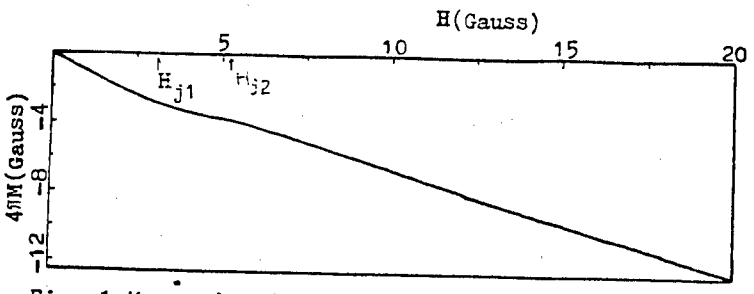

Fig. 1 Magnetization curve of YBaCuO at low field.

We estimated the effective penetrating depth (λ_J) by Rosenball [13] and Tinkham [14] theory about granular superconductivity.

$$H_{J1} = (4\pi/10)\,\lambda_J J_{jc} \qquad (1)$$

where J_{jc} is the transport critical current of the bulk sample. In our experiments, H_{J1} = 3 - 4 Oe, J_{jc} = 130 - 250 A. λ_J was estimated to be 10^{-2} cm.

Furthermore,

$$\lambda_J = (c\Phi_0/8\pi^2 a J_{jc})^{1/2} \qquad (2)$$

where Φ_0 is flux quantum hc/2e, a is the dimension of superconducting area. Deduced value of a was tens Å. The actural value of J_{jc} was larger than the measured one due to the self-field effect of the measuring current. Therefore, a might be hundreds Å. It was much smaller than the dimension of grains, indicating that many weak links existed in the grains.

The diamagnetization at $H>H_{J2}$ resulted from the Meissner effect of grains. The percentage of superconducting area in the sample was estimated from $4\pi\chi_m$ at $H>H_{J2}$, where χ_m was the susceptibility corrected for demagnetic field. Considering the voids in the sample, the mass percentage of superconducting area (F) was approximately estimated to be $4\pi\chi_m/P$, where P was the filling coefficient. The Landon penetrating depth was neglected in the estimation. The maximum value of F was 0.8 - 0.9 for YBaCuO in our experiments. The actural value was lower than it because some shielding effects still existed even in carefully prepared samples. One reason for this phenomenon was that many grains were not superconducting. Another was that there were many weak links penetrated by flux or nonsuperconducting areas in grains. The estimation for superconducting areas was in agreement with that suggested from the dimension of the superconducting area.

We measured remanent magnetization for different samples. It was essentially saturated at a critical field H_{J2}. The larger the nonsuperconducting areas were (the lower the $4\pi\chi_m$ was), the larger the saturation remanent was.

3.2 AC susceptibility

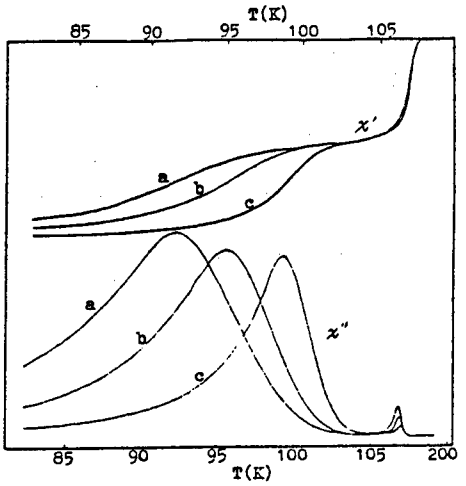

Fig. 2 Complex susceptibilities of $Bi_{1.7}Sr_{0.3}Ca_2Cu_3O_x$

a. H=1.63 Oe,
b. H=0.81 Oe,
c. H=0.16 Oe.

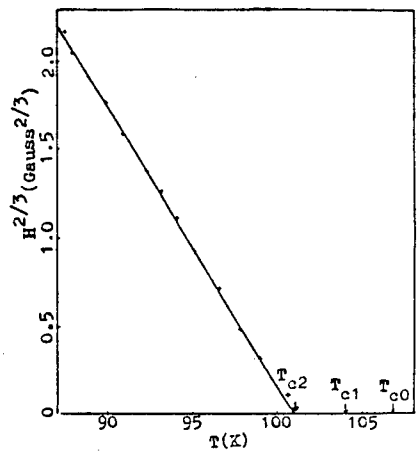

Fig. 3 Variation in T_{c2} with the amplitude of AC field.

Fig. 2 shows AC susceptibility of the Pb-substitued 2223 single phase BiSrCaCuO sample. Similar to that reported by Mazaki et al [7-8] in YBaCuO and BiSrCaCuO, there are two peaks in imaginary part. The high temperature peak is due to the superconducting transition of grains themself. The low temperature peak is due to the superconducting transition of weak links between grains. When AC field increased, the peak for weak links shifted to low temperature. Our results, as shown in Fig. 3, showed that $1-T_{c2}(H)/T_{c2}(0)$ is proportional to $H^{2/3}$, where H is the amplitude of AC field, $T_{c2}(H)$ is the temperature corresponding to the low temperature peak. Extrapolated value of $T_{c2}(0)$ was 101.1 K. Superconducting transition temperature of grains (T_{c0}) was 106.8 K. On the other hand, we measured resistivity of the sample. T_{c1}, at which resistivity equals to zero, was 104.0 K. The difference between $T_{c2}(0)$ and T_{c1} was 2.9 K. Dubson [15] measured current-voltage characteristics of YBaCuO near superconducting-normal transition, and suggested that due to the granular superconductivity, there were two transition temperatures, zero resistance

temperature T_{c1} and zero dissipating temperature T_{c2}. When $T_{c2}<T<T_{c1}$, the resistance of the sample equals to zero but the sample can not carry current (critical current equals to zero). Our susceptibility measurements confirmed this suggestion and demonstrated that when a field was applied, zero dissipating temperature T_{c2} decreased linearly with $H^{2/3}$. In fact, this behavior is quasi de Almeida-Thouless relationship describing the boundary between reversible and irreversible magnetization in granular superconductor. Our experiments showed that there were three critical temperatures at zero field in granular superconductor, superconducting transition temperature of the grains T_{c0}, zero resistance temperature T_{c1}, and zero dissipating temperature T_{c2}.

We also investigated AC susceptibility of YBaCuO. Similar results were obtained. The links between grains are stronger in YBaCuO than those in BiSrCaCuO. The difference between zero dissipating temperature $T_{c2}(0)$ (91.8 K) and zero resistance temperature T_{c1} (91.9 K) was very small. We could not distinguish between T_{c0} and T_{c1} in experiments.

3.3 Magnetic current J_c

The capacity to get through current at high field is very important for the application of superconductor at high field. Usually, Bean model is used to determine magnetic current from magnetic loop at high field. We systematically measured magnetic loops of YBaCuO, $LaBa_{1.5}Ca_{0.5}Cu_3O_{7-x}$, Bi- and Tl-superconductors. Experiments showed the magnetic current of YBaCuO maintains some value at high temperature (77 K). The magnetic loops of $LaBa_{1.5}Ca_{0.5}Cu_3O_{7-x}$ were similar to those of YBaCuO. Although the magnetic current of Bi- and Tl-superconductors was comparable with that of YBaCuO at low temperature (4.2 K). With increasing temperature, magnetization became negative at both increasing and decreasing fields, similar to that in ideal type-II superconductor. Magnetic currents of various high T_c oxide superconductors are shown in Fig. 4. The flux pinning in Bi- and Tl-superconductors is very weak at high temperature. The stronger flux pinning in YBaCuO and LaBaCuO is perhaps due to the twin boundary, oxygen deficiency or/and oxygen disorder in the Cu-O plane. These areas form flux pinning centers. Oxygen concentration varies little in Bi- and Tl-superconductors. There is no such pinning center.

The value of J_c, shown in Fig. 4, was calculated by Bean model $J_c=30\ \Delta M/d$, where d was the dimension of the sample (about 2 mm). Our experiments [11] and Tompson [9] showed that magnetic current essentially limited in the interior of superconducting grains. Weak links between grains had been broken at high field. The actual value of magnetic current in superconducting grains was at least larger by two orders of magnitude than calculated value.

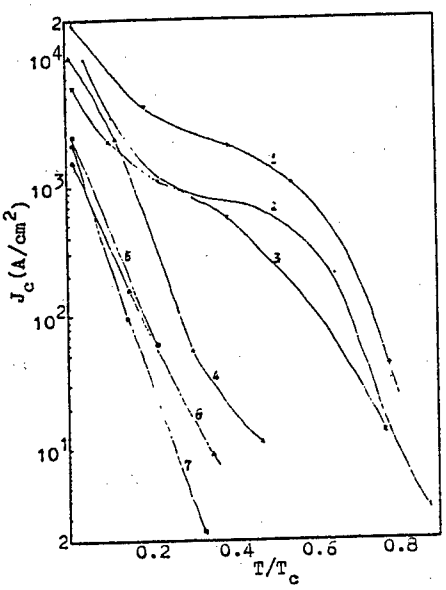

Fig. 4 Temperature dependence of magnetic current, H=4 T.
1. $YBa_2Cu_{2.7}Ag_{0.3}O_{7-x}$,
2. $YBa_2Cu_3O_{7-x}$,
3. $LaBa_{1.5}Ca_{0.5}Cu_3O_{7-x}$,
4. $Tl_2Ba_2Ca_2Cu_3O_{10}$,
5. $Bi_2Sr_2CaCu_2O_8$,
6. $Tl_2Ba_2CaCu_2O_8$,
7. $Bi_2Sr_2Ca_2Cu_3O_{10}$.

The addition of Ag in YBaCuO enhances flux pinning. We measured magnetic loops of $YBa_2Cu_{2.9}Ag_{0.1}O_{7-x}$ and $YBa_2Cu_{2.7}Ag_{0.3}O_{7-x}$. J_c increased markedly, indicating the marked enhancement of flux pinning.

4. CONCLUSIONS

Low field susceptibilities were analyzed by granular superconductivity theory. The results showed that there were many weak links in the superconducting grains. The grains were divided into many small superconducting domains with dimensions of hundreds to a thousand Å. AC susceptibility measurements demonstrated that there were three superconducting transition temperatures. The temperature corresponding to the low temperature peak in varied linearly with $H^{2/3}$. Magnetic loops and magnetic currents at high field were investigated systematically. The results showed that flux pinning in the Bi- and Tl-superconductors was very weak at high temperature. Substitution of Ag for Cu in YBaCuO could enhance flux pinning.

We wish to thank Prof. Dao-Le YIN and Prof. Shou-Sheng YAN for valuable discussions. We are grateful to Ke WU, Jian LAN, Li-Xin XUE, and Guo-Zhong LI for experiments.

REFERENCES

[1] J.G.Bednorz and K.A.Muller, Z.Phys., B64, 189(1986).
[2] M.K.Wu, J.R.Ashbum, C.J.Tomg, P.H.Hor, R.L.Meng, L.Gao, Z.J.Huang, Y.Q.Wang, and C.W.Chu, Phys. Rev. Lett., 58, 908(1987).
[3] C.X.Zhao et al., Kexue Tonbao (Chinese), 32, 412(1987).

[4] Z.Z.Sheng, A.M.Hermann, A.ElAli,C.Almasan, J.Estrada, T.Datta, a
R.J.Matson, Phys. Rev. Lett., 60, 937(1987).
[5] H.Maeda, Y.Tanaka, M.Fukutomi, and T.Asano., Jpn. J. Appl. Phys., 2
L209(1988).
[6] Hong ZHANG, Shou-Sheng YAN, Wen-Bin ZHANG, Zhao-Hui SHEN, Yun-Xi SU
Guo-Zhong LI, and Ke WU, Solid State Commun., 62, 1183(1988).
[7] Hiromasa Mazaki, Mikio Takano, Yaswnori Ikeda, Yoshichika Bando, Ryo
Kanno, Yasuo Takeda, and Osamu Yamamoto, Jpn. J. Appl. Phys., 2
L1749(1987).
[8] Takekazu Ishida and Hiromasa Mazaki, Jpn. J. Appl. Phys., 27,
L531(1988).
[9] J. R. Tompson, D. K. Christen, S. T. Sekula, J. Brynested, and Y. C
Kim, preprint.
[10] Mitsuru Vehara, Yuji Asada, Kircshi Maeda, and Keiichi Ogama,
preprint.
[11] Y.D.Dai, C.Lin, W.B.Zhang, S.Q.Feng, X.Zhu, C.D.Wei, Z.X.Liu, Y.X.Su
J.Lan, G.Z.Li, K.Wu, K.X.Chen, D.L.Yin, and Z.Z.Gan, to be publishe
in Proceedings of High Temperature Superconductivity, Singapore, June
1988.
[12] Chongde Wei, Chin Lin, Zhaohui Shen, Zunxiao Liu, Jian Lan, Ke W
Lixin Xie, Yuandong Dai, Zizhao Gan, to be published in Internationa
J. Modern Phys..
[13] J.Rosenblatt, Rev. De Phys. Appl., 9, 217(1974).
[14] M.Tinklam, C.J.Lobb, to be published in Solid State Physics, 42.
[15] M. A. Dubson, S. T. Herkert, J. J. Calabrese, D. C. Harris, B. R
Patter, and J. C. Garland, Phys. Rev. Lett., 60, 1061(1988).

PRACTICAL PROPERTIES AND WIRE FABRICAION PROCESSES OF HIGH-T_c OXIDE SUPERCONDUCTORS

Kazumasa TOGANO*, Hiroaki KUMAKURA*, Daniel R. DIETDERICH*, Hiroshi MAEDA*, Eiji YANAGISAWA** and Masanao MIMURA***
* National Research Institute for Metals, Tsukuba, Ibaraki 305
** Asahi Glass Co. Ltd., Yokohama, Kanagawa 221
*** Furukawa Elec. Co. Ltd., Yokohama, Kanagawa 220

1. INTRODUCTION

The discovery of high-T_c oxide superconductors, especially of the Y-Ba-Cu-O[1], Bi-Sr-Ca-Cu-O[2] and Tl-Ba-Ca-Cu-O[3] compounds, which show superconductivity above liquid nitrogen temperature, has had great impact not only on basic physics but also on the field of superconductivity applications. To utilize superconducting materials in magnet requires that their tape or wire conductors have sufficient flexibility to be wound into a solenoid. However, the high-T_c oxide compounds are intrinsically brittle just like intermetallic compound superconductors, and hence special techniques must be developed for making flexible tape or wire conductors.

Another requirement for practical wire or tape conductors is that they should have sufficiently high transport critical current density J_c even in applied magnetic fields. However, the J_c for oxide superconducting materials prepared by the conventional sintering method still remains very low compared to the level of practical application. In particular, the J_c drastically decreases with increasing the applied magnetic field. One of the factors limiting the J_c of the polycrystalline materials is anisotropy in J_c as well as in upper critical field H_{c2}. In addition to these anisotropy factors, there are two other important factors that determine the J_c of the oxide superconductors. One is weak links at grain boundaries and the other is flux pinning.

In this paper, we present the results of attempting to fabricate Bi(Pb)-Sr-Ca-Cu-O tapes with flexibility by powder technique through doctor blading[4] or cold working of Ag-sheathed oxide powder[5]. The tapes show a significant improvement of transport J_c compared to the bulk specimen. Some experimental evidences for achieving the improvement in intergrain coupling in the tape are also presented.

2. EXPERIMENTAL

The appropriate amounts of Bi_2O_3, Pb_3O_4, $SrCO_3$, $CaCO_3$ and CuO powders were mixed, calcined and heat treated at 845°C for 120h to form high-T_c phase of the Bi-Sr-Ca-Cu-O system. This was milled into a fine powder for subsequent processing. Organic formulation consisting of solvent, binder and dispersant was then added and again milled together. The resulting slurry was cast under a doctor blade into a green tape of 50-150 μm thickness on the carrier sheet. Ribbon samples, typically 3mm in width and 100mm in length, were cut from the tape and heat treated at 500°C for 1h. The ribbon was then sandwiched between stainless steel sheets and cold

rolled together. A small reduction of total cross sectional area results in an effective densification of the oxide ribbon. The ribbon was then subjected to a final heat treatment of sintering.

Tape conductors have also been prepared by conventional fabrication methods of powder using Ag-sheath. The oxide powder of Bi(Pb)-Sr-Ca-Cu-O was prepared by mixing the appropriate amounts of reagents and calcination at 800°C for 12h. The powder was then packed into a Ag-tube and cold worked to a tape of 0.5mm in thickness by swaging and rolling. The tape was then cut into 3cm length and the short samples were then subjected to the combination process of sintering and intermediate cold rolling.

3.RESULTS AND DISCUSSION

The addition of the rolling process was found to greatly improve the packing density, producing a highly oriented grain structure in both of the doctor blade processed (DBP) and Ag-sheathed tapes. Figure 1 shows the back-scattered electron image of the longitudinal cross section at the center of the Ag-sheathed tape, showing that the high-T_c plate-like grains are aligned in parallel direction to the tape surface, i.e., c-axis alignment perpendicular to the surface. Such a structure of dense alignment of the plate-like grains greatly improves the flexibility of the tape, especially for the DBP-tape. The DBP-tape after the final sintering can be bent elastically into a small diameter of about 30mm without any breakage. Figure 2 shows the DBP-tape bent on a 38mm-diameter bobbin.

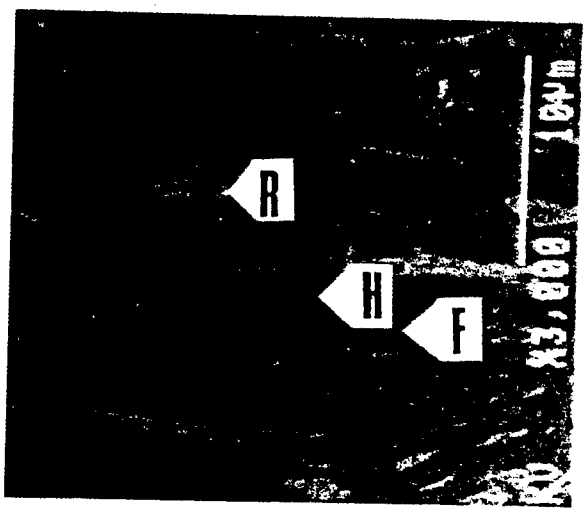

Fig. 1 BSE image of the longitudinal cross-section at the center of the Ag-sheathed tape prepared by adding intermediate cold rolling during sintering process. H, F and R denote the high-T_c phase, Bi-free phase and Bi-rich phase, respectively.

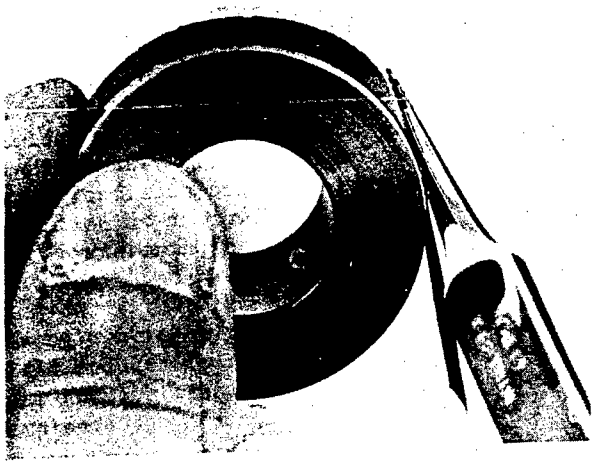

Fig. 2 Doctor blade processed Bi(Pb)-Sr-Ca-Cu-O tape bent on a 38mm-diameter bobbin after the final sintering.

The inclusion of the intermediate rolling process was also found to greatly improve the superconducting properties of the tape. Figure 3 shows the J_c at 77K and 0T of the Ag-sheathed tape. The tape was initially sintered at 835°C for 80h and then subjected to the combination process of sintering at 835°C and cold rolling, and the J_c is plotted as a function of total sintering time. The highest J_c is 3050A/cm^2. Similar improvement of J_c was also obtained for the DBP-tape. The DBP-tape processed without rolling has a T_c of 97K and a poor J_c of less than 10A/cm^2 at 77K and 0T. However, by the addition of the rolling process, T_c above 100K and J_c in excess of 1000A/cm^2 were easily obtained. The highest J_c obtained so far is 2050A/cm^2.

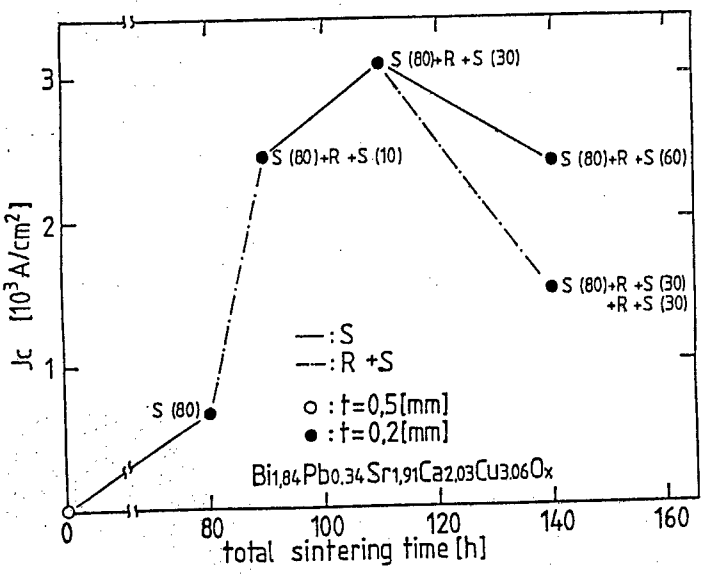

Fig. 3 J_c of the Ag-sheathed tape as a function of the total sintering time. S(t) denotes the sintering and its time, and R denotes the rolling process.

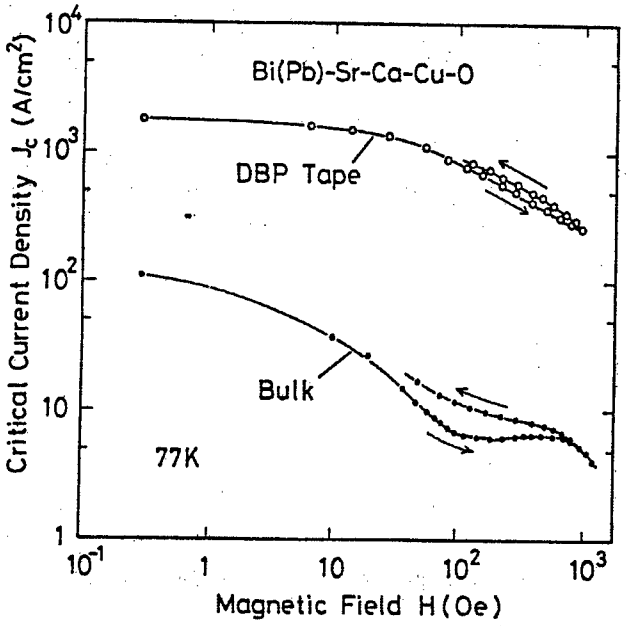

Fig. 4 J_c-H curve for doctor blade processed tape. The result for bulk sample prepared by conventional sintering process is shown for comparison.

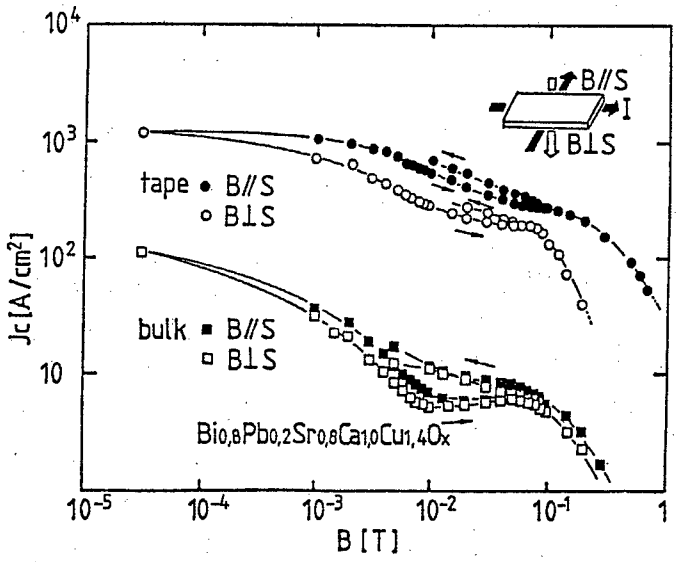

Fig. 5 J_c-H curve for the Ag-sheathed tape. The result for bulk sample prepared by conventional sintering process is shown for comparison.

Figures 4 and 5 show the J_c's of the SDP and Ag-sheathed tapes as a function of magnetic field. J_c-H curves of a bulk sample prepared by the conventionl sintering are also shown in the figure. J_c of the tape is much larger than that of the sintered bulk sample at entire magnetic fields. Especially, J_c degradation with increasing magnetic field is significantly decreased for the tape. This improved J_c property in magnetic fields suggests that the coupling of grains along the current direction is improved in the tape. Both of the tape and bulk samples show hysteresis in the J_c-H curve as shown in Figs. 4 and 5. Similar hysteresis was also reported for sintered Y-Ba-Cu-O[6]. It is considered that the hysteresis is attributed to the grain boundaries having weak coupling nature which was affected by the local magnetic field induced by the large shielding current. It should be also noticed that the hysteresis is also reduced in the tapes than in the bulk samples.

This improvement in coupling nature was also confirmed by the A.C. susceptibility measurement[7]. Figure 6 shows the χ' vs. temperature curves for the DBP tape, when the A.C. magnetic field was applied perpendicular(Fig. 6(a)) and parallel(Fig. 6(b)) to the tape surface. The data for bulk sample is also shown for the comparison. Both the tape and bulk samples showed a two step transition in χ'vs. temperature curve in large A.C. field amplitude , higher and lower temperature transitions corresponding to the intragrain and intergrain

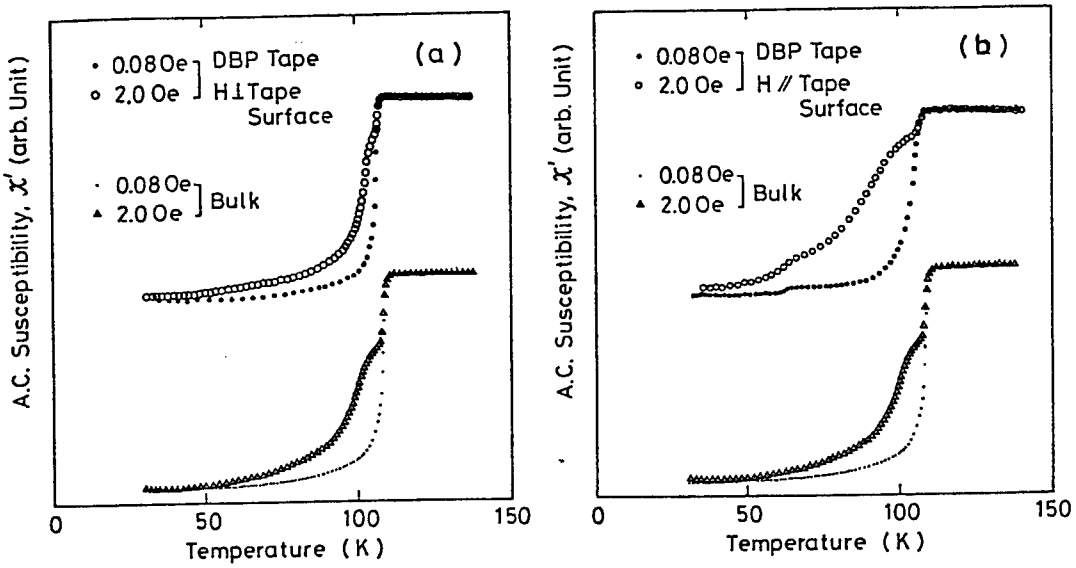

Fig. 6 χ'-T curves measured at 700 Hz with A.C. field amplitudes of 0.08 and 2.0 Oe for doctor blade processes Bi(Pb)-Sr-Ca-Cu-O tape, when the A.C. field is applied perpendicular (a) and parallel (b) to the tape surface. The results for the bulk sample are also shown for comparison.

superconductivities, respectively. However, the curve for the tape shows a strong dependence on the field direction, i.e., the lower temperature transition is much smaller in the field perpendicular to the tape surface, while it becomes much larger in the parallel field compared to those of the bulk sample. This result indicates that the current transfer between the grains is much improved only in the direction parallel to the tape surface.

4.CONCLUSIONS

Highly oriented grain structure in which the grains are aligned in such a way to maximize the intergrain electronic coupling has been obtained for the Bi(Pb)-Sr-Ca-Cu-O tapes prepared by the modified doctor blading and Ag-sheathing techniques. This structure results in a significantly improved transport J_c-H characterisistics for the tape. The tape processed by the modified doctor blading shows a sufficient flexibility to be bent into a small diameter of about 30mm.

REFERENCES

1. M.K.Wu, J.R.Ashburn, C.J.Torng, P.H.Hor, R.L.Meng, L.Gao, Z.J.Huang, Y.Q.Wang and C.W.Chu, Phys. Rev. Lett., 58, 908(1987).
2. H.Maeda, Y.Tanaka, M.Fukutomi and T.Asano, Jpn. J. Appl. Phys., 27, L209(1988).
3. Z.Z.Sheng and A.M.Hermann, Nature, 332, 138(1988).
4. K.Togano, H.Kumakura, H.Maeda, E.Yanagisawa, N.Irisawa, J.Shimoyama and T.Morimoto, Jpn. J. Appl. Phys, 28, L278(1989).
5. M.Mimura, H.Kumakura, K.Togano and H.Maeda, submitted to Appl. Phys. Lett.
6. K.Noto, H.Morita, K.Watanabe, T.Murakami, Y.Koyanagi, I.Yoshii, I.Sato, H.Sugawara, N.Kobayashi, H.Fujimori and Y.Muto, Physica 148B, 239(1987).
7. H.Kumakura, K.Togano, H.Maeda, E.Yanagisawa and T.Morimoto, to appear in Jpn. J. Appl. Phys. 28(no.2), (1989).

$YBa_2Cu_3O_y$ SUPERCONDUCTORS PREPARED WITH DIFFERENT PROCESSES AND THEIR CHARACTERISTICS

WU Xiaozu, WANG Jingrong, TANG Xiede, LIU Fengsheng,
WU Suihua, YE Yongcai, ZHOU Lian
Northwest Institute for Non-ferrous Metal Research
(Originally called Baoji Institute for Non-ferrous Metal Research)
P.O. Box 71, Baoji, Shaanxi, China

1.INTRODUCTION

To put YBCO materials with 90 K Tc into practical uses has been being the eager goal of industries and scientists since this exciting superconductor was discovered[1,2]. Jcg of 10^5-10^6 A/cm^2 for the superconducting YBCO grains has been found[3,4], but the transport Jct of YBCO polycrystalline superconductors is much less than this value due to "weak-link" nature between grains[5,3,7] according to many researchers[5,6]. In order to enhance Jct and put into practice, a lot of new methods, such as Melt-Textured Growth (MTG)[8,9] and Metal Sheathed Working Process[10], came out so as to get an approach to the goal of improving weak-link and fabricating practical materials.

In this paper, some experimental results of technical and superconducting properties for these new processes and an ordinary solid phase powder sintering process developed in our Institute have been presented.

2.EXPERIMENTAL

The studied samples were prepared by the following processes:

(1)Ordinary solid-phase powder sintering. The samples were prepared with mixed powders or chemical co-precipitation powders.

(2)Metal sheathed working. The mixed powders were sufficiantly pulverized in a suitable metal tube and worked to tapes or wires, then heat-treated into superconductors.

(3)Preform-melting. The tape or wire preforms fabricated by the above second process were melted in a H_2-O_2 flame and cooled into wires, them given an additional heat treatment afterwards.

The **Jc** values of all the samples were measured by a standard four-probe technique at a criterion of 1 μv/cm at 77 K.

3. RESULTS AND DISCUSSION

(1) Solid phase powder sintering

The Jc effects of main technical parameters, such as the starting powder purity, the bulk density, the sintering temperature and sintering time, as well as the sintering cycles, have been studied. No obvious difference has been found for the bulk materials prepared with different powder purities of 2N and 5N. The typical Tc is about 92 K, and Jc is

600 - 607.5 A/cm^2 (0 T, 77 K) for the samples those area of cross-sections being about 1 mm^2.

Bulk density ρ-critical current density Jc. Jc increases with ρ, but Jc has a peak near 90% of theoretic density due to the poorer oxygen soaking ability when the density is quite high.

Sintering temperature and time - Jc. The range of sintering temperature and time are 900-940°C and 20-50 h, respectively. Higher Jc can be got at higher temperature for shorter time, or at lower temperature for longer time. Jc will decrease greatly when the sintering temperature is below 900°C, related to a large amount of micro-cracks. Jc is the highest when sintered at 900-920°C, because there are not excessively large grains basically but homogeneous micro-structure of fine equi-axial grains.

Usually, Jc can be enhanced by increasing the cycles of milling and sintering. but it is not effective if the material is homogeneous enough because the effect of the cycles is to improve the homogenity of micro-coposition.

The effects of annealing on Tc and Jc. It is found that there will be two resistive transitions under unfit annealing, as shown in Fig.1. For the first transition, the Tc_1, onset is 94-96 K, and for the second transition, the Tc_2 is 90-92 K. It is shown in Fig. 2 that a single transition is obtainable by annealed at an optimal temperature, its Tc_{onset} = 95.6 K, Tc_0 =92.5 K. This variation of superconductivity might be due to the effect of ordered oxygen vacancies. The highest transport Jc of 1513 A/cm^2 at 77 K and zero field has been obtained for the sample with a cross-section area of 0.14 mm^2 after systematic studies of processes.

(2) Metal sheathed working process

The wire (tape) samples have been produced with the Powder-in-Tube process, this is, the YBCO powders were sheathed in a metal tube, then the composite tube was worked and sintered to form wire or tape samples. The effects of different metal sheaths, the YBCO powder preparation, the composite working, and the final sintering heat-treatments on the technology and superconductivity have been investigated. The results indicate the following factors are favourable for composite working: using Ag as the sheath, working under the multiple compressive stress, deforming in a slow speed. Jc of the final material turns higher if the preformed powder are denser. The final heat-treatments (sintering and annealing) are very important for the improvement of superconducting properties of wires (tapes). Under the same condition, the grains are easier to grow for the metal sheathed working process than the normal solid phase sintering process, so Jc is smaller. Jc of 600 A/cm^2 (0 T, 77 K) can be reached for the wires (tapea) by choosing reasonable technics.

(3) Preform-wire melting process

Melting process, aimed to increase the density of material and improve the growth of grains, held out great hopes of enhancing Jc. In this work, the Jc effects of melting technics, especially, the final sintering and annealing treatments have been studied on the preformed wires prepared by powder-in-tube process. From the SEM pictures (Fig. 3), it is seen that the material after melting is much denser than normal sintered material, but the polycrystalline structure is still disorder. Because the material

melted at 1050-1250°C is polyphase, it must be heat-treated to form single phase superconductors. The final heat-treating temperature is obviously lower than that of powder-sintering, so Jc tends to be higher in a reasonable cooling rate. From the experimental results in this work, it is shown that the bulk material prepared by this kind of melting is still polycrystalline aggregate on the whole, although it turns denser and tends to texture locally. It is quite difficult to get real texture-growth by melt-process on technique, so that Jc is not easy to be enhanced to a practical level since the weak-link nature couldn't be solved thoroughly. At present, Jc of 660 A/cm^2 (0 T, 77 K) can be reached for the wires fabricated with a stable process.

(4) Jc characteristics for the materials by the three different processes

After measuring the Jc values of many samples, it is found that the Jc values are obviously affected by S, the area of cross-section of samples, as shown in Fig. 4. The data on one solid bar indicate the Jc values of the same sample but with different area. A theoretically approximate Jc-S dependence has been drawn as shown as the dashing line in Fig.4 and it has the following expression:

$$Jc = A \exp\left(-B\sqrt{S} + CS^{-1}\right) \qquad (1)$$

here A,B, and C are constants. It shows good agreement with the experimental pattern from Fig.4. The same rule can be seen for the wires and tapes by metal-sheathed working process, as well as the wires by melting process, as shown in Fig.5. The size effect of Jc can be explained from the effect of self-magnetic field of sample transport current due to its low critical magnetic field and its poor heat conductivity[11].

From the same Jc characteristics of different samples prepared by the three processes, it turns out that there are no important differences in nature for the materials by the different processes, this is, the weak-link nature resulting in low Jc has not been improved basically, so that Jc is limited in an order of 10^3 A/cm^2 (0 T, 77K) for the bulk samples.

4.CONCLUSIONS

(1)The main methods to enhance Jc of YBCO superconductors prepared by the three processes mentioned above are: to prepare the powders carefully and finely so as to ensure the homogenity of micro-composition, the accurate stoichiometry, the reasonable microstructure, and fine equi-axial grains in the materials; to improve the oxygen soaking ability while the density increasing; to choose reasonable annealing temperature and time so as to get a bulk material with a microstructure of highly ordered oxygen vacancies.

(2)The size-effect of Jc exists in all the samples prepared by the three processes and has the approximate expression of $Jc \propto A \exp(-B\sqrt{S}+CS^{-1})$, here S is the area of cross-section of sample, A,B, and C are three constants.

(3)All the samples have the same microstructure of polycrystalline without obvious textured orientation and improvement of weak-link feature, so Jc is limited to a level of 10^3 A/cm^2(0 T, 77K).

REFERENCES

1.Z.X.Zhao, et al, KEXUE TONGBAO, 3 (1987)
2.C.W.Chu, et al, Phys. Rev. Lett., 58, 405 (1987)
3.M.Suenaga, et al, In High Temp. Superco. MRS, Vol, EA-11, 247 (1987)
4.J.M.Ekin, et al, J.Appl. Phys., June 26 (1987)
5.J.M.Ekin, et al, in HTS, M.R.S., Pittsburgn, EA-11, 223 (1987)
6.R.J.Cava, et al, Phys. Rev. Lett., 58, 1676 (1987)
7.D.C.Larbalestier, et al, Submitted to J.Appl. Phys.
8.S.Jin, et al, Appl. Phys. Lett., 5, No.24, 2074 (1988)
9.S.Jin, et al, Phys. Rev. B, 37, No. 13 (1988)
10.R.Beyers, et al, Appl. Phys. Lett., 51, No.8 614-616 (1987)
11.J.R.Wang, et al, Proceeding of ICEC 12, Southampton, UK (1988)
12.X.D.Tang, et al, Proceeding of ICMC 88', Shenyang, China (1988)

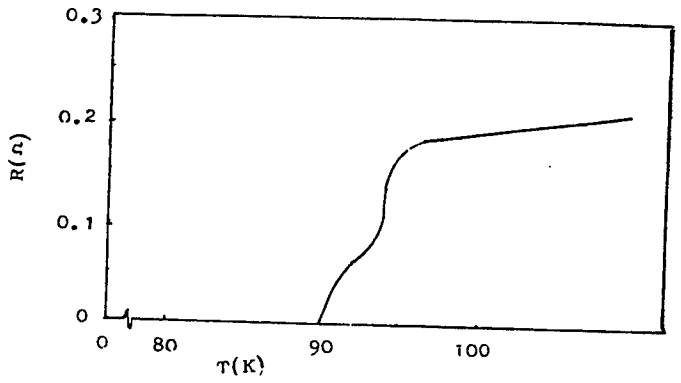

Fig.1. R-T curve with the two transitions for a bulk YBCO sample.

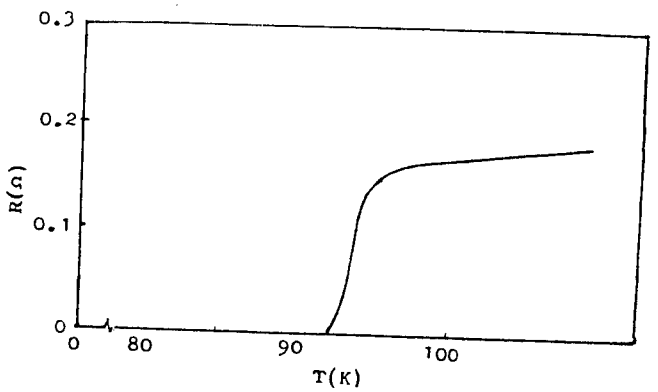

Fig.2. R-T curve with the mono-transition for a bulk YBCO sample.

(a)

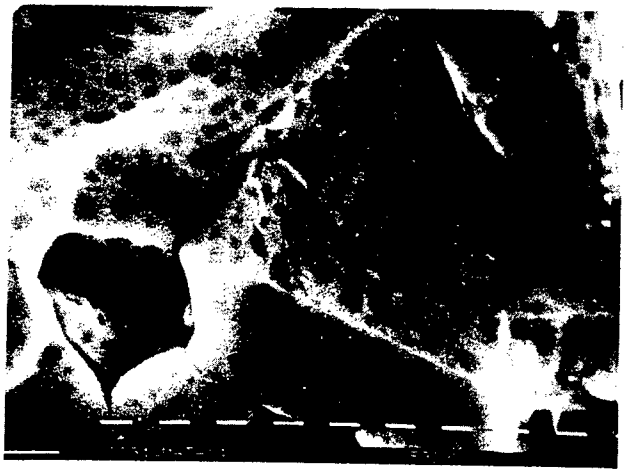

(b)

} Scanning electron micrographs for the samples by powder-sintering process (a) and melting process (b).

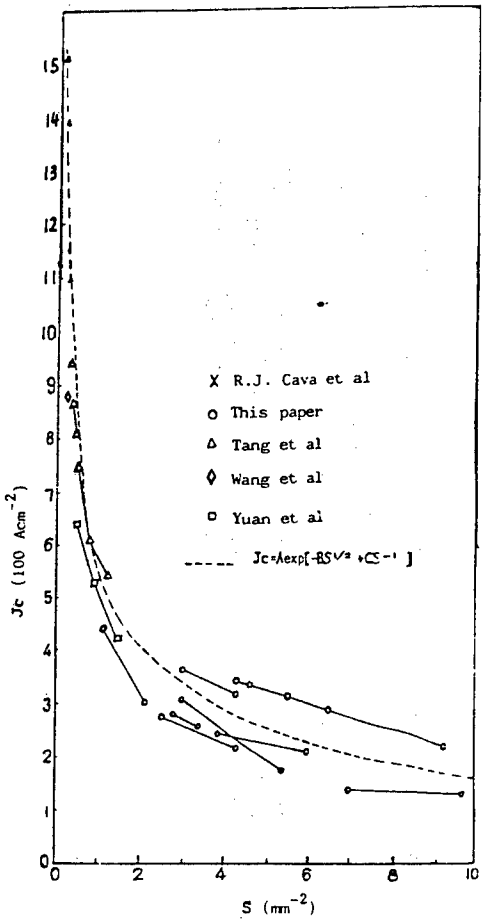

Fig.4 The dimensional effect on Jc and the comparasion with the theoretic curve. The data on a bar are for the same sample but different cross-sections.

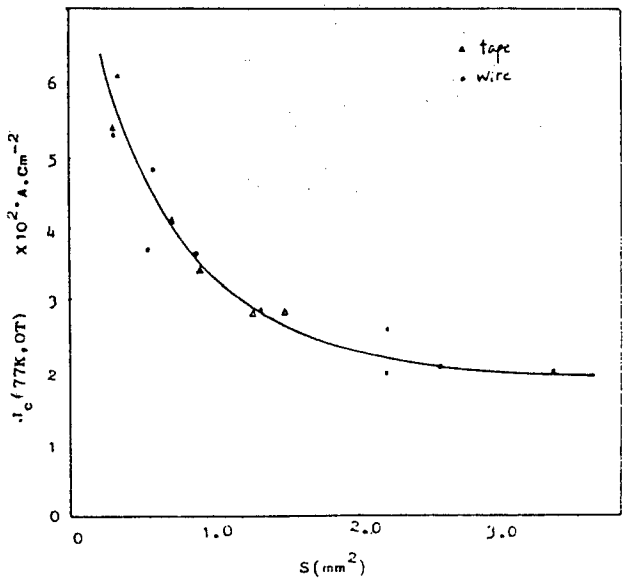

Fig.5 Jc effect of cross-section area for the wires (tapes) prepared with metal sheathed working process.

The Magnetic Shielding Properties of an YBCO Superconducting Cylindrical Tube with One End Closed

Y.J.Qian, J.W.Qiu, and Z.M.Tang

Department of Physics, Fudan University, Shanghai, China

J.R.Wang, J.P.Li, P.F.Xu, and X.K.Teng

The Baoji Institute for Nonferrous Metal Research, Baoji, China

Abstract

An YBCO superconducting magnetic shielding tube was developed and a shielding coefficient of 10^5 as well as a capability of maximum shielding field of 40 $x10^{-4}$ Tesla was obtained with the device.

PACS index 74.60.-w

The oxide superconductors with transition temperature higher than liquid nitrogen boil point (77K) offer attractive advantages for a wide variety of both small and large scale applications. Since the obstacle related to the low critical current density of existing oxide superconductors, the small scale applications may firstly come to realization. The devices depending on the Josephson effect, such as DC and RF-SQUIDS operated at 77K, seems to be greatly promised. In fact, several prototype RF-SQUIDS has already been constructed and have shown very promising performance[1,2]. The magnetic shielding devices at liquid nitrogen temperature will be needed when these sensitive devices come to practical applications. Oxide superconductors themself can be naturally considered as ideal shielding materials at 77K. We have previously studied the magnetic shielding properties of an YBCO hollow cylinder with both ends open. It was found that a value of 8×10^{-4} Tesla of DC field could be shielded by that cylinder[3]. According to our knowledge learned from other investigations[4], a value of 5 to 10 $\times 10^{-4}$ Tesla was the typical value of external magnetic field which could be shielded by most oxide superconducting shielding devices. In this paper we report a remarkable progress in this subject. A shielding capability of 40 $\times 10^{-4}$ Tesla of DC field was obtained with an YBCO shielding device currently made.

The new device was made from $Y_1Ba_2Cu_3O_{7-x}$ compound which was worked out on the basis of a systematic study of the ordinary powder sintering process for a series of bulk samples[5]. The stoichmetric

Y:Ba:Cu=1:2:3 mixture of Y_2O_3 (99.95%), BaO(97%) and CuO(99%) was well pulverized and packed into a crucible, followed by a firing in air at 900°C for 24 hours and then furnace cooled down to room temperature. After two cycles of milling and sintering, the resulted homogeneous powders of 150 g were formed into a cylindrical tube of 16 mm i.d. and 140 mm in length with one end closed by the socalled isostatic pressing technique. Then the tube was carefully machined down to the final size of 23 mm o.d. with leaving the inner diameter as it was. The resulted tube was then heat-treated in a quarts fur nace at a temperature of 900°C for 36 hours, then cooled down to 500°C and maintained at this temperature for 24 hours. Both the heat-treatment and the cooling were processed in the flowing pure oxigen. A slightly shrink of the oxide tube was found after the sintering and annealling process. Pieces of small sample were cut out from the resulted tube for the characterization of superconducting properties with leaving the tube length of 102 mm. A typical I-V curve measured with the standard four-probe technique is shown in Fig.1. A direct transport critical current density of 262 A/cm² was deduced from this measurement. It is noteworth to point out that the transport critical current depends on the cross sectional area of the sample being measured [6]. The value of 262 A/cm² for the present sample of cross sectional area of 3.33 cm² can be converted to an equivalent value of 700 to 800 A/cm² if the cross sectional area of the sample is 1 mm². It was found that the material is quite stable proved by both the magnetization and transport measurement during a period of several

months. The same value of the transport critical current and the same shape of the magnetization curve were obtained after 20 days and 5 months of the initial measurements respectively.

For the magnetic shielding test, the tube was placed inside a copper wire solenoid which produces the DC field. The field probe was placed inside the oxide tube. Since the lack of DC field probe at 77K, we have recalibrated a commercial Hall probe(Oxford Instrument, Model 5200) at the liquid nitrogen temperature. The external field was scanned up and down with a current scanner. The internal field Hi as a function of the applied field He at 77K is shown in Fig.2. The arrows and numbers in the figure indicate the directions of the field scanning. During the initial increase in the applied field, Hi is indetectable within the detection limits of the field probe ($.01 \times 10^{-4}$ T) provided He is smaller than a certain value which we defined as a threshold field Ha for this particular tube. Hi starts to increase rapidly when Ha is reached. In the succedent scannings Hi follows a hysteresis loop which together with the record of the initial scanning is very similar with the properties of a type-II superconducting hollow cylinder [7] . Based on the Bean model [8] and the assumption of

$$|Jc(r)|=Jc(T)Bo/[|B(r)|+Bo] \qquad (1)$$

as well as the approximation of Ha >> Hc1, one is able to deduce the following equations for describing two branches of the hysteresis loop in the first sector respectively

$$Hi/Bo=[(1+He/Bo)^2+Ic(T)/Bo] \qquad (2)$$

$$Hi/Bo=[(1+He/Bo)^2-Ic(T)/Bo] \qquad (3)$$

The solid circes in Fig.2 were calculated from equ.(2) and (3)

with an assumed parameter Ic(T)/Bo of 10^4. It is not suprising that the calculated points do not fit the experimental curve well as the approximations taken in this simple model. In fact, it is well known that rather than a function of temperature only, the critical current drops drasticaly at weak field range (10×10^{-4} T). The value of Ha observed in this measurement is comparable with Hc1 too[9]. We are going to analyse the results on a more sophiscated model with cxpecting to deduce more information of the oxide compound, such as Hc1 and Bo. At present we may conclude that the shielding mechanism of the current device belongs to the screen current one and a 40×10^{-4} Tesla of DC field can be effectively shielded with the present tube. A same order of constant field can be held inside this cylindrical tube too depending on the operation procedure or application purposes.

To confirm this conclusion, the AC weak-signal modulation technique was used to measure the variation of the internal field Hi. Actually, the AC method measures the slope of the curve of Hi versus He and gives much high resolution with the use of lock-in amplifier. According to the AC measurement, there was no variations of 10^{-7} Tesla in the internal field at the range of the applied field less than the threshold field Ha. Therefore, a coefficient defined by He/Hi as high as 10^5 for this particular device is obtained. The AC measurement showed also several interesting phenomena which are believed to be connected with the special features of the oxide superconductor, i.e. the granularity and the short coherence length. These phenomena are being analyzed. The inner diameter of this cylindrical tube was originally

capability of 40 $x10^{-4}$ Tesla DC field has been obtained. The present device, certainly, is useful for some application, such as 77K SQUID.

References

1. J.E.Zimmerman, J.A.Beall, M.W.Cromar, and R.H.Ono
   Appl.Phys.Lett.51,617 (1987)
2. J.W.Qiu, X.F.Chang, Y.J.Qian, B.C.Miao, and Z.M.Tang
   Submitted to Chinese Jour of Low Temperature Phsics
3. Y.J.Qian, J.W.Qiu, J.R.Wang, J.P.Li, P.F.Xu, and X.K.Teng
   to appear in Cryogenics (Proceedings of ICEC 12)
4. In completing this work, we were aware of several reports given on the use of magnetic shielding made from 123 material at the Applied Superconductivity Conference in San Francisco. But we have no the details of them yet. An only publication, we are able to mention, is 'Z.Chai et.al in the Proceedings of the Chinese National Conference on High Tc Superconductivity April, 1988 (Baoji, China) P.518 (in chinese)'
5. J.R.Wang, J.P.Li, P.K.Xu,K.G.Wang, S.Q.Wang, and L.Zhou
   to appear in Cryogenics (Proceedings of ICEC 12)
7. J.B.Kim, C.F.Hempstead, and A.R.Strnad
   J.Appl.Phys. 34, 3226 (1963)
8. C.P.Bean and J.D.Livingston
   Phys.Rew.Lett. 12, 14 (1964)
9. T.R.Dinger, T.K.Worthington, W.J.Gallagher, R.L.Sandstorm
   Phys.Rew.Lett. 58, 2687 (1987)
10. J.W.Thomasson and D.M.Ginsberg
    Rew.Sci.Instrum. 47, 387 (1976)

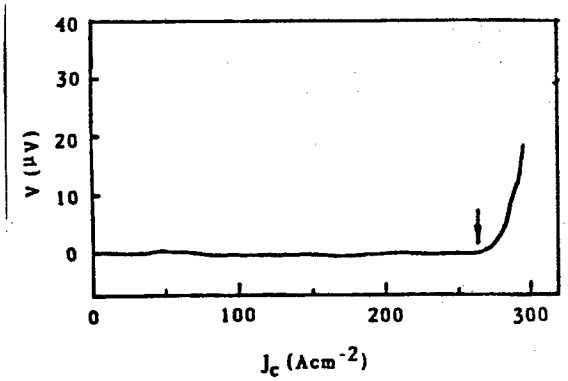

Fig.1 I-V characteristic measured at 77K and in the earth field for a sample cut from the YBCO tube.

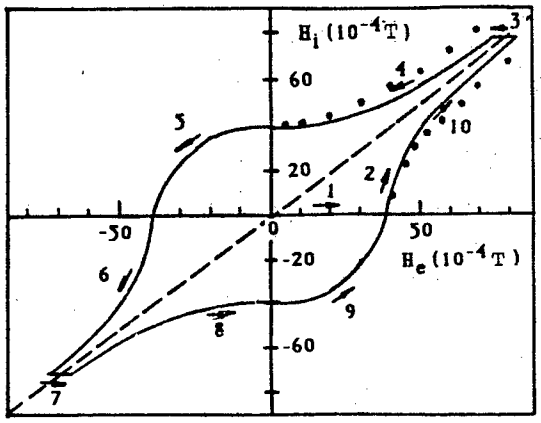

Fig.2 The recorded internal field as a function of the external field at 77K. The solid circles present the calculated points (see in text).

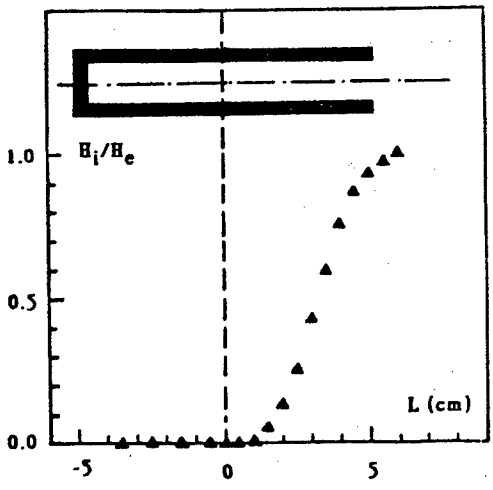

Fig.3 The field distribution inside theYBCO tube. Hi, He and L are the internal and external field as well as the distance from the axis center of the tube, respectively.

- END -

NTIS
ATTN: PROCESS 103
5285 PORT ROYAL RD
SPRINGFIELD, VA 22161

22161

Foreign Broadcast Information Service (FBIS) and Joint Publications Research Service (JPRS) publications contain political, economic, military, and sociological news, commentary, and other information, as well as scientific and technical data and reports. All information has been obtained from foreign radio and television broadcasts, news agency transmissions, newspapers, books, and periodicals. Items generally are processed from the first or best available source; it should not be inferred that they have been disseminated only in the medium, in the language, or to the area indicated. Items from foreign language sources are translated; those from English-language sources are transcribed, with personal and place names rendered in accordance with FBIS transliteration style.

Headlines, editorial reports, and material enclosed in brackets [ ] are supplied by FBIS/JPRS. Processing indicators such as [Text] or [Excerpts] in the first line of each item indicate how the information was processed from the original. Unfamiliar names rendered phonetically are enclosed in parentheses. Words or names preceded by a question mark and enclosed in parentheses were not clear from the original source but have been supplied as appropriate to the context. Other unattributed parenthetical notes within the body of an item originate with the source. Times within items are as given by the source. Passages in boldface or italics are as published.

SUBSCRIPTION/PROCUREMENT INFORMATION

The FBIS DAILY REPORT contains current news and information and is published Monday through Friday in eight volumes: China, East Europe, Soviet Union, East Asia, Near East & South Asia, Sub-Saharan Africa, Latin America, and West Europe. Supplements to the DAILY REPORTs may also be available periodically and will be distributed to regular DAILY REPORT subscribers. JPRS publications, which include approximately 50 regional, worldwide, and topical reports, generally contain less time-sensitive information and are published periodically.

Current DAILY REPORTs and JPRS publications are listed in *Government Reports Announcements* issued semimonthly by the National Technical Information Service (NTIS), 5285 Port Royal Road, Springfield, Virginia 22161 and the *Monthly Catalog of U.S. Government Publications* issued by the Superintendent of Documents, U.S. Government Printing Office, Washington, D.C. 20402.

The public may subscribe to either hardcover or microfiche versions of the DAILY REPORTs and JPRS publications through NTIS at the above address or by calling (703) 487-4630. Subscription rates will be provided by NTIS upon request. Subscriptions are available outside the United States from NTIS or appointed foreign dealers. New subscribers should expect a 30-day delay in receipt of the first issue.

U.S. Government offices may obtain subscriptions to the DAILY REPORTs or JPRS publications (hardcover or microfiche) at no charge through their sponsoring organizations. For additional information or assistance, call FBIS, (202) 338-6735,or write to P.O. Box 2604, Washington, D.C. 20013. Department of Defense consumers are required to submit requests through appropriate command validation channels to DIA, RTS-2C, Washington, D.C. 20301. (Telephone: (202) 373-3771, Autovon: 243-3771.)

Back issues or single copies of the DAILY REPORTs and JPRS publications are not available. Both the DAILY REPORTs and the JPRS publications are on file for public reference at the Library of Congress and at many Federal Depository Libraries. Reference copies may also be seen at many public and university libraries throughout the United States.